

NASA-CR-176119 DE85-
017588

DOE/CS/54209-28
(DE85017588)

Energy
CONSERVATION

NASA-CR-176119 DE85-
017588

19850026021

EVALUATION OF HALF WAVE INDUCTION MOTOR DRIVE FOR USE IN PASSENGER VEHICLES

Final Report

By
R. G. Hoft
A. Kawamura
A. Goodarzi
G. Q. Yang
C. L. Erickson

LIBRARY COPY

MAR 14 1985

TECHNICAL INFORMATION CENTER
LIBRARY, NASA
HAMPTON, VIRGINIA

March 21, 1985

Work Performed Under Contract No. AI01-78CS54209

University of Missouri-Columbia
Columbia, Missouri

Technical Information Center
Office of Scientific and Technical Information
United States Department of Energy



NF01772



DISCLAIMER

This report was prepared as an account of work sponsored by an agency of the United States Government. Neither the United States Government nor any agency thereof, nor any of their employees, makes any warranty, express or implied, or assumes any legal liability or responsibility for the accuracy, completeness, or usefulness of any information, apparatus, product, or process disclosed, or represents that its use would not infringe privately owned rights. Reference herein to any specific commercial product, process, or service by trade name, trademark, manufacturer, or otherwise does not necessarily constitute or imply its endorsement, recommendation, or favoring by the United States Government or any agency thereof. The views and opinions of authors expressed herein do not necessarily state or reflect those of the United States Government or any agency thereof.

This report has been reproduced directly from the best available copy

Available from the National Technical Information Service, U S Department of Commerce, Springfield, Virginia 22161

Price Printed Copy A11
Microfiche A01

Codes are used for pricing all publications. The code is determined by the number of pages in the publication. Information pertaining to the pricing codes can be found in the current issues of the following publications, which are generally available in most libraries: *Energy Research Abstracts (ERA)*, *Government Reports Announcements and Index (GRA and I)*, *Scientific and Technical Abstract Reports (STAR)*, and publication NTIS-PR-360 available from NTIS at the above address.

DOE/CS/54209-28

(JPL-9950-1039)

(DE85017588)

Distribution Category UC-96

EVALUATION OF HALF WAVE INDUCTION MOTOR DRIVE
FOR USE IN PASSENGER VEHICLES

FINAL REPORT

by

R. G. Hoft, A. Kawamura, A. Goodarzi,
G. Q. Yang and C. L. Erickson

March 21, 1985

for

JPL Contract Number 956728

Department of Electrical and Computer Engineering
University of Missouri-Columbia
Columbia, Missouri 65211

1085-34334 #

TABLE OF CONTENTS

| | Page |
|--|------|
| 1.0 ABSTRACT..... | 2 |
| 2.0 EXECUTIVE SUMMARY..... | 3 |
| 3.0 TWO-PHASE BIFILAR INDUCTION MOTOR/INVERTER SYSTEM | 6 |
| 3.1 SPECIFICATIONS..... | 6 |
| 3.2 SYSTEM DESCRIPTION | 9 |
| 3.2.1 CIRCUIT CONFIGURATION AND OPERATION | 9 |
| 3.2.2 PWM CONTROL OF INVERTER..... | 13 |
| 3.3 MOTOR DESIGN..... | 15 |
| 3.3.1 OPERATING POINTS..... | 15 |
| 3.3.2 NATURE OF INDUCTION MOTOR..... | 15 |
| 3.3.3 MOTOR DESIGN PROCEDURE..... | 16 |
| 3.3.4 COMPUTER-AIDED DESIGN..... | 22 |
| 3.3.5 EFFICIENCY..... | 31 |
| 3.4 INVERTER DESIGN..... | 32 |
| 3.4.1 SWITCHING DEVICE REQUIREMENTS..... | 32 |
| 3.4.2 POWER CIRCUIT..... | 33 |
| 3.4.3 TRANSIENT VOLTAGE..... | 34 |
| 3.4.4 CONTROL CIRCUIT..... | 35 |
| 4.0 FINAL DESIGN AND EXPECTED PERFORMANCE OF TWO-PHASE BIFILAR INDUCTION MOTOR/INVERTER SYSTEM.. | 35 |
| 4.1 MACHINE DATA..... | 35 |
| 4.2 INVERTER DATA..... | 36 |
| 4.3 INVERTER/MOTOR PERFORMANCE..... | 36 |
| 4.4 SYSTEM SCHEMATIC DIAGRAM..... | 38 |
| 5.0 COMPARISON OF TWO-PHASE BIFILAR AND THREE PHASE BRIDGE INVERTER/MOTOR SYSTEMS..... | 40 |
| 5.1 ADVANTAGES AND DISADVANTAGES OF TWO-PHASE SYSTEM..... | 40 |
| 5.2 SIMULATION RESULTS..... | 42 |
| 5.3 PERFORMANCE FUNCTION COMPARISON..... | 49 |
| 6.0 CONCLUSIONS..... | 50 |
| APPENDIX A MOTOR SPECIFICATIONS PROVIDED BY JPL | 52 |
| APPENDIX B ALTERNATIVE INVERTER-MOTOR CONFIGURATIONS | 62 |
| APPENDIX C IDEALIZED COMPARISON OF TWO-PHASE AND THREE-PHASE INVERTERS | 65 |
| APPENDIX D DETAILED DESIGN OF TWO-PHASE BIFILAR INDUCTION MACHINE | 73 |
| APPENDIX E MOTOR TRANSIENT TEMPERATURE RISE | 97 |
| APPENDIX F DETAILED INVERTER DESIGN | 104 |
| APPENDIX G SIMULATION RESULTS | 130 |
| APPENDIX H DERIVATION OF INDUCTION MOTOR D-Q EQUATIONS IN STATIONARY REFERENCE FRAME..... | 208 |

1.0 ABSTRACT

This report describes research performed at the University of Missouri-Columbia to devise and design a lower cost inverter-induction motor drive for electrical propulsion of passenger vehicles. A two-phase inverter-motor system is recommended. It is predicted to provide comparable vehicle performance, improved reliability and nearly a 10% cost advantage for a high production vehicle because of the reduction in total parts count, decreased total rating of the power semiconductor switches and somewhat simpler control hardware compared to the conventional three-phase bridge inverter-motor drive system. The major disadvantages of the two-phase inverter-motor drive are that the two-phase motor is larger and more expensive than a three-phase machine, the design of snubbers for the power switches is difficult because motor lead and bifilar winding leakage inductances produce higher transient voltages, and the torque pulsations are relatively large because of the necessity to limit the inverter switching frequency to achieve high efficiency.

The conclusions of this research are based on analyses and simulations. An actual model of the two-phase system must be constructed and evaluated to prove the advantages claimed for the proposed system. The most challenging engineering design task will be to design the inverter, motor and snubber circuits to minimize transient voltages with high system efficiency.

2.0 EXECUTIVE SUMMARY

This report describes research performed at the University of Missouri-Columbia to devise a lower cost induction motor drive for use in electrical propulsion of passenger vehicles. The work was done during the period from January through August of 1984 in two phases.

Phase I - Concept and Feasibility Study

(January-May)

Phase II - Detailed Design and Performance Analysis

(June-August)

As a result of Phase I, three preferred candidate systems were identified.

- A. Half Wave Three-Phase Inverter-Motor (three power switches, three pairs of bifilar wound stator windings)
- B. Four Switch Three-Phase Inverter-Motor (four power switches - two legs of conventional three-phase inverter, conventional three-phase machine, motor line returned to center-tap of dc source)
- C. Two-Phase Inverter-Motor (four power switches, two pairs of bifilar wound stator windings)

After a detailed analysis of the candidate systems at the beginning of Phase II, the two phase inverter-motor was selected as the lowest cost approach to meet the electrical passenger vehicle system requirements.

Detailed analyses and digital computer simulations were carried out to design the inverter circuit and the two-phase induction motor required. The two-phase system has the following advantages over the conventional three-phase inverter-motor drive:

1. The number of power semiconductor switching devices is reduced from six to four.
2. The current rating of each power switch is 65% of that required for each switch in the equivalent three-phase system.
3. The total number of components is estimated to be about 70% of the number required for the three-phase circuit. This also implies higher reliability and lower manufacturing assembly cost.
4. The motor transient temperature rise is reduced due to the increased volume of copper.
5. Somewhat simpler control hardware is possible because of the common emitter circuit so that isolation is not required in the base drive circuits.
6. The total system cost is estimated to be about 90% of that for the three-phase system.

The overall efficiency is almost the same for the two-phase system and the three-phase system - approximately 91% at the 12kw, 80% speed operating condition.

The major disadvantages of the two-phase approach are increased motor size and cost, more difficult snubber design for transient voltage suppression, and greater torque pulsations.

For a high production electric passenger vehicle, the two-phase inverter-motor system developed on this research should provide significant cost advantages for the electric vehicle application when compared to the conventional three-phase bridge inverter-induction motor drive. It is important to note that the conclusions of this research are based on analysis and simulations. An actual model of the two-phase system must be constructed and evaluated to prove the advantages claimed for the proposed inverter-motor system. The most challenging engineering task will be to design the inverter, motor and snubber circuits to minimize transient voltages while retaining high system efficiency.

3.0 TWO-PHASE BIFILAR INDUCTION MOTOR/INVERTER SYSTEM

3.1 Specifications

The inverter-motor drive system requirements are defined by the contractual motor specifications in Appendix A. These system requirements are as follows:

Inverter input:

240V battery

Motor output:

a. Shaft power output

- 1) 30kW for 1 hour with 20% duty cycle at maximum speed
- 2) 60kW for 3 minutes with 30% duty cycle at 80% of maximum speed
- 3) 16kW for 3 minutes with 30% duty cycle at 10% of maximum speed

b. Maximum motor speed between 8,000 and 16,000 rpm

c. Two or four pole motor, totally enclosed, convection cooled with 40°C maximum ambient air and 4000 hours operating life at 80% of maximum speed with 12kW output

Fig. 1 is a graphical representation of the motor requirements. It illustrates one method of satisfying the specifications. However, later in this section, an alternate motor design is described which results in a reduction in motor size and weight below that implied by

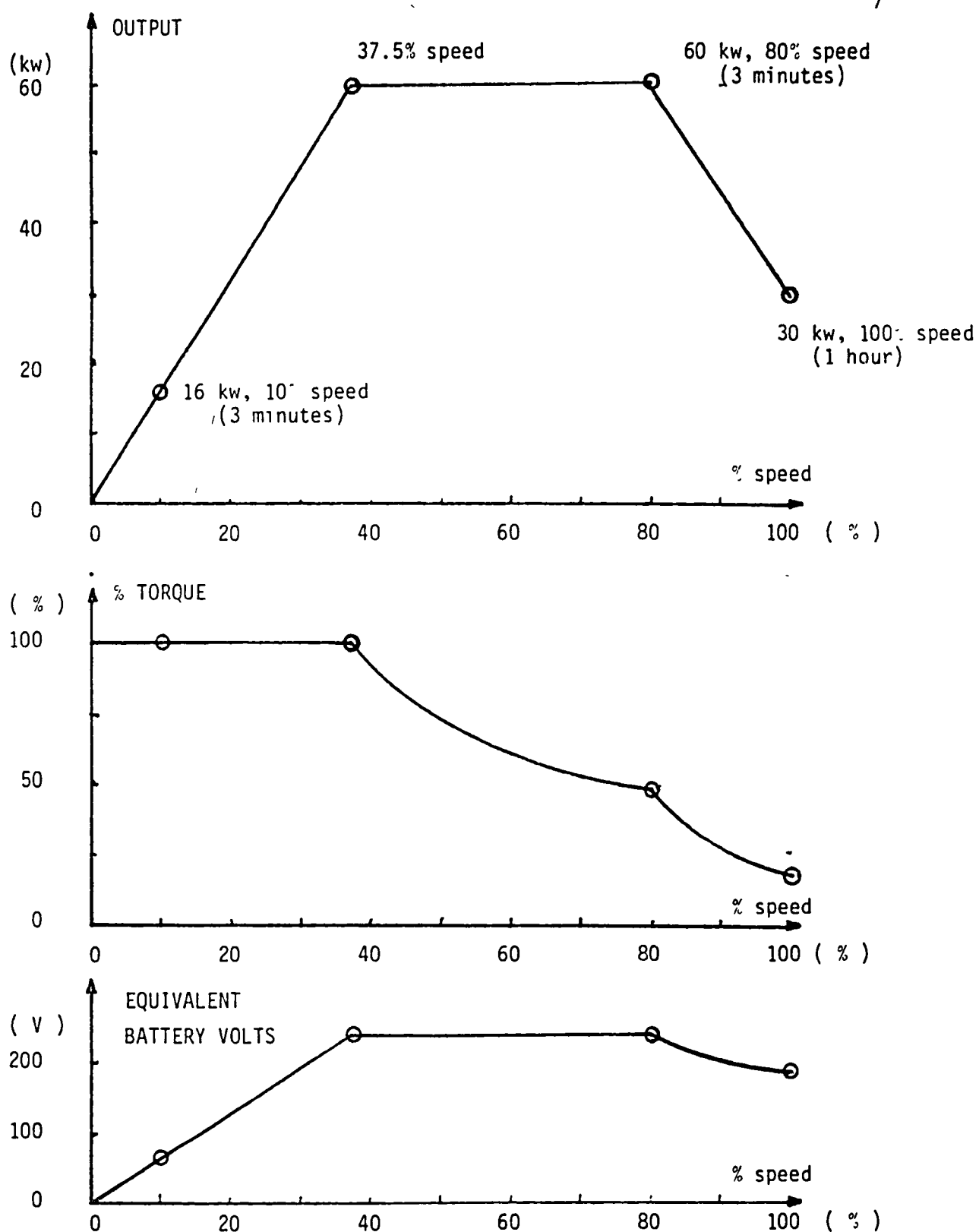


Fig. 1 Graphical Representation of Motor Requirements

Fig. 1. For Fig. 1, it is assumed that a constant volts/Hz is applied to the motor from zero speed to 37.5% speed. In this range the air-gap flux is essentially constant, implying a constant torque capability and a linearly increasing output power with speed. At 37.5% speed, the maximum voltage available is required, and so the motor voltage is assumed constant from 37.5% speed to 80% speed. It should be noted that whenever the equivalent battery voltage is less than 240V, it is assumed that PWM control of converter output voltage is used to provide this voltage reduction. Since the output power requirement is only 30kW at 100% speed, it is possible to reduce the motor applied voltage from 80% to 100% speed. The capability implied by Fig. 1 would meet the specification requirements since the three specified operating points lie on the power vs. speed curve, which defines the power capability at each speed.

The inverter-motor system also is to be designed to minimize the function

$$F = \text{Cost} + 10 \times \text{Weight} - 120 \times \text{Efficiency} \quad (1)$$

where each of the parameters on the right side of this relationship is for the total inverter and motor system expressed as follows:

Cost = retail cost in dollars

Weight = total weight in kilograms

Efficiency = % efficiency at 80% of maximum motor speed with 12kW output

As a result of this research, a two-phase inverter/motor drive is proposed. The remainder of this report describes the system design to meet the specifications. In addition, the report explains why the system proposed is considered the preferred induction motor approach for this application.

3.2 System Description

3.2.1 Circuit Configuration and Operation

During the first phase of the research, several alternative inverter-induction motor combinations were considered. The following preferred candidate systems were selected for more detailed analyses:

- A. Half-wave inverter driven three-phase bifilar wound induction motor (Appendix B, Fig. B-1).
- B. Four switch inverter driven three-phase induction motor (Appendix B, Fig. B-2).
- C. Two-phase inverter driven induction motor with two pairs of bifilar wound stator windings as shown in Fig. 2.

As a result of an evaluation of each of these systems, including simulations to determine the peak current in the power switches at the 60kW - 80% speed operating point, the two-phase approach shown in Fig. 2 was selected. It has two significant advantages compared to the alternative candidate systems: (1) the lowest total power switch rating (the power switch peak current times its peak voltage times the

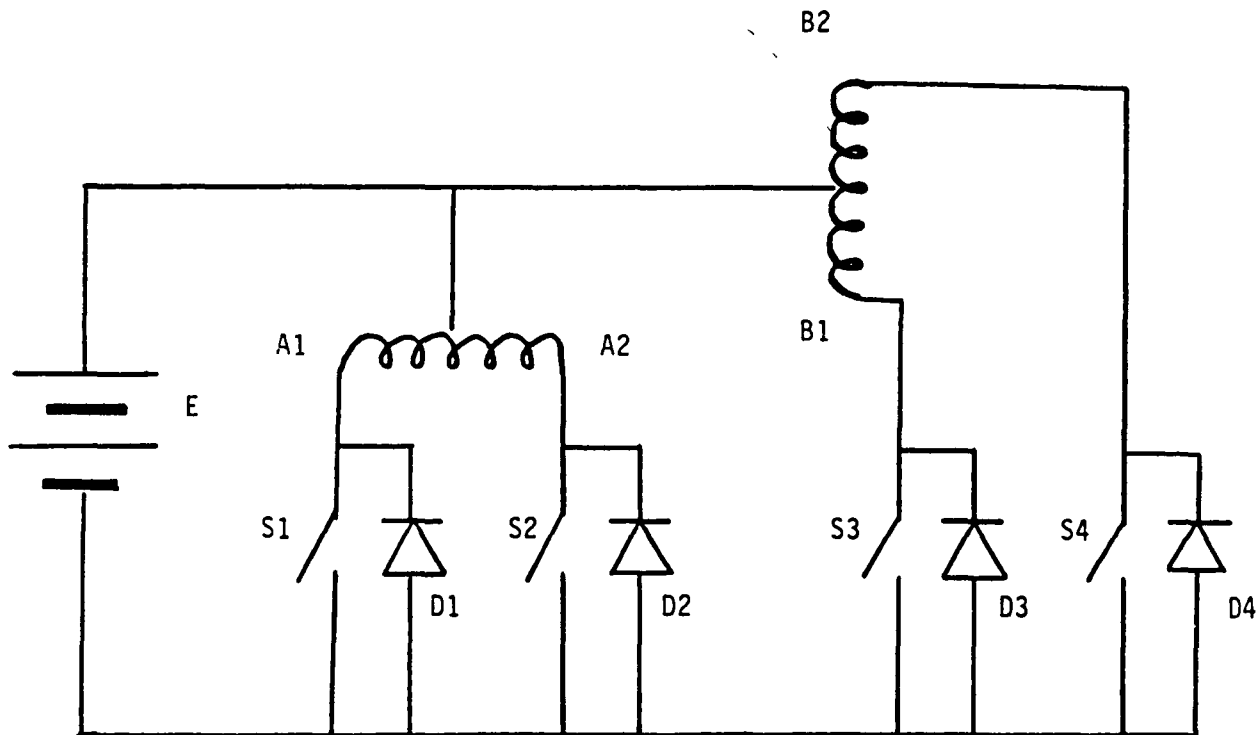


Fig. 2 Two-phase Bifilar Induction Motor/Inverter

number of switches required); (2) it is one of the two alternatives (Fig. B-1-b is the other) which may be arranged to have a common emitter connection with transistor switches or common cathodes if thyristors are used. This second advantage makes it possible to simplify the control hardware since gate or base drive isolation is not required. The primary disadvantages of the scheme in Fig. 2 are that the motor size and weight is increased by 10%-20% compared with the three-phase bridge system (Fig. B-3), the power switch snubber design is more difficult since line and bifilar winding leakage inductances produce additional transient voltages, and there are relatively large torque pulsations because of the necessity to limit the inverter switching frequency to achieve high efficiency. Appendix C contains an idealized comparative analysis of the two-phase and three-phase inverter arrangements.

The two-phase bifilar induction motor has only two stator phases, each of which includes a pair of tightly magnetically coupled coils. Fig. 2 shows the circuit configuration. Fig. 3 is an alternate circuit. However, Fig. 2 is the preferred approach since it simplifies the control hardware as mentioned previously. With transistor switches, all emitters are common, and all cathodes are common with thyristor switches. Thus, isolation is not required for the base drive or gate drive circuits.

Four switching devices and four free-wheeling diodes are required in the circuit of Fig. 2. The center-taps of

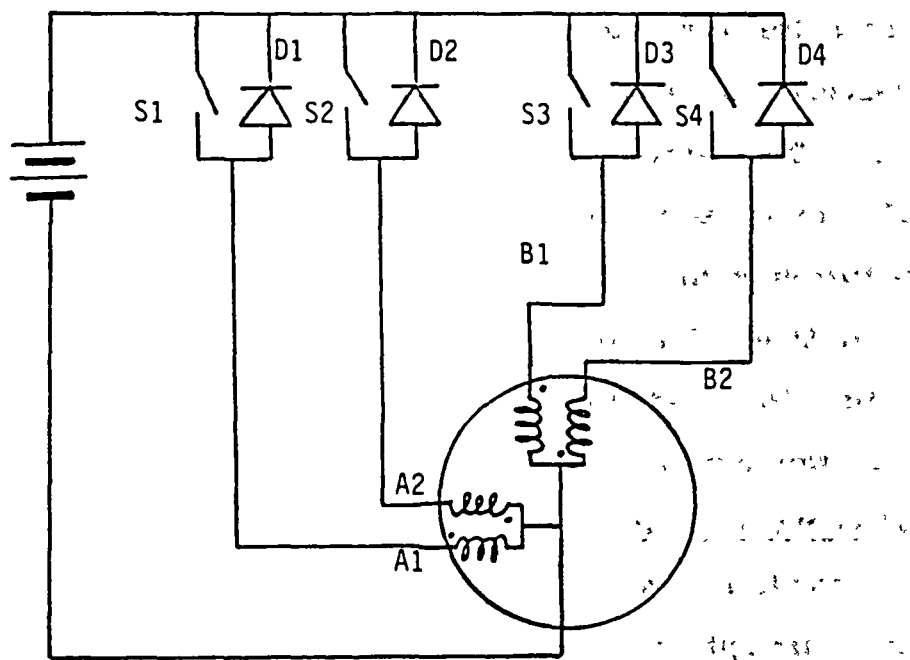


Fig. 3 Alternate configuration for Two-phase Bifilar
Induction Motor/Inverter

the stator windings are connected to the positive side of the battery. The operation of the inverter is as follows. Suppose switch S1 is closed, and current is flowing from the battery through stator winding A1. When S1 is opened and S2 is closed, the current through stator winding A1 is transferred to the bifilar winding A2. As a result, free-wheeling diode D2 conducts, and the stored energy in the winding returns to the battery. After this diode current reduces to zero, the current starts to flow through switch S2. The current in stator windings B1 and B2 is controlled in a similar manner. However, the conduction intervals for switches S3 and S4 are displaced 90 electrical degrees from those for S1 and S2. Controlling the two-phase currents in this fashion, a rotating magnetic flux is produced in the machine.

3.2.2 PWM Control of Inverter

PWM control is employed in the inverter system so that the current through the stator windings can be shaped to the optimum waveform. In the light load case, the current is shaped to approach a sinusoidal waveform as shown in Fig. 4-a. The switching pattern is controlled such that the stator current always stays within a given band from the sinusoidal function. With heavy load, a current waveform approaching a square wave is delivered to the motor to provide maximum power with minimum peak motor current as shown in Fig. 4-b.

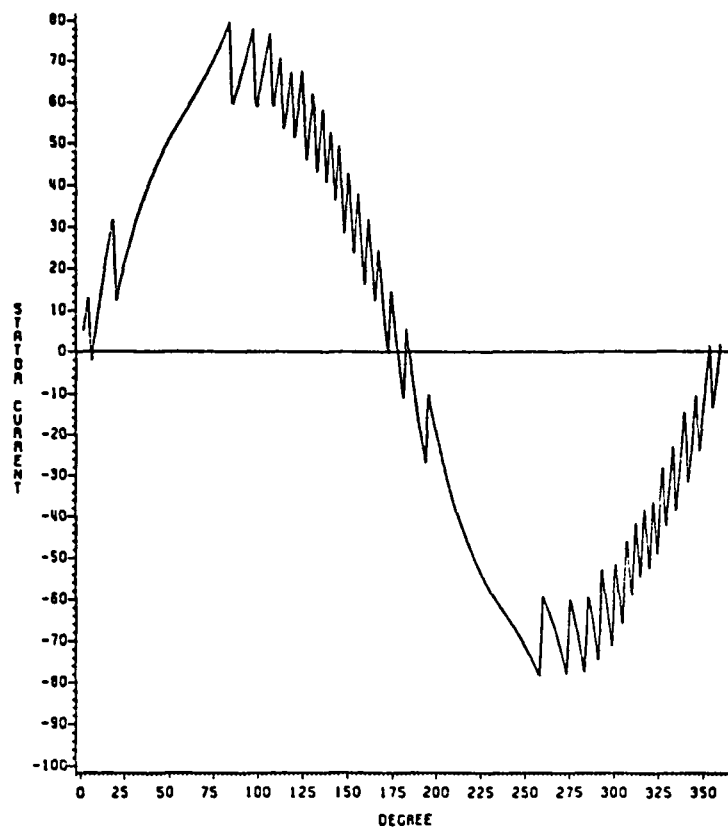


Fig. 4-a Current waveform for light load

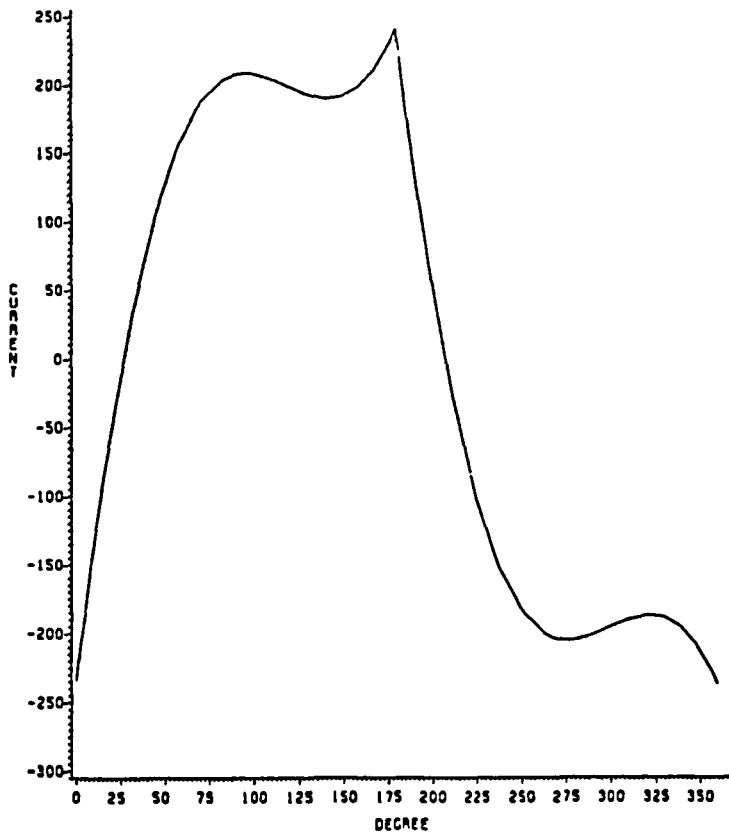


Fig. 4-b Current waveform for heavy load

With a microprocessor controller, it is also possible to control the PWM voltage waveform and the applied frequency to maximize efficiency at the 80% speed, 12 kW operating point. This might be accomplished by storing the required control program in memory, or possibly by an on-line efficiency optimization technique.

3.3 Motor Design

3.3.1 Operating Points

As indicated in section 3.1, three specific operating points are required.

16kW output at 10% speed (3 minutes, 30% duty)

60kW output at 80% speed (3 minutes, 30% duty)

30 kW output at 100% speed (1 hour, 20% duty)

The two-phase bifilar induction motor proposed must satisfy the operating conditions at each of these points.

3.3.2 Nature of Induction Motor

The polyphase induction motor maximum power output as a function of inverter frequency is given by

$$P_{\max} = C_1 \frac{(V)}{f}^2 f \quad (2)$$

where

$$C_1 \triangleq \text{constant} = \frac{3P}{8\pi L_{1r}}$$

$P \triangleq$ number of poles

$L_{1r} \triangleq$ rotor leakage inductance

$V \triangleq$ rms value of stator voltage

$f \triangleq$ source frequency

When an induction motor is connected to an inverter, a similar maximum output is achieved, neglecting the effects of harmonics. Since the output voltage and frequency of the inverter may be adjusted, the maximum output power given by (2) can be changed, depending on the speed control strategy. If V/f is maintained constant over the low frequency range, the maximum power is proportional to the frequency (or rotor speed). After maximum stator voltage V is reached, the maximum power decreases proportional to $1/f$ since V is constant and f increases. In Fig. 5, generalized curves for the maximum power P_{max} , rated power P_R , stator current I_p , stator voltage V , and slip frequency f_s are plotted as a function of rotor speed.

The rated output power as a function of slip frequency f_{SR} , which may change at different source frequencies, is

$$P_R = C_2 \left(\frac{V}{f}\right)^2 f f_{SR} \quad (3)$$

where

$$C_2 \stackrel{\Delta}{=} \text{constant} = \frac{3P}{2R_2}$$

$$R_2 \stackrel{\Delta}{=} \text{rotor resistance}$$

$$f_{SR} \stackrel{\Delta}{=} \text{rated slip frequency at different source frequencies}$$

3.3.3 Motor Design Procedure

For these discussions, the following variables are defined:

— Peak output power; Corresponding peak stator current; Corresponding peak stator voltage and slip frequency f_{smax}

- - - Rated output power; Corresponding rated current; Corresponding rated stator voltage and rated slip frequency f_{SR}

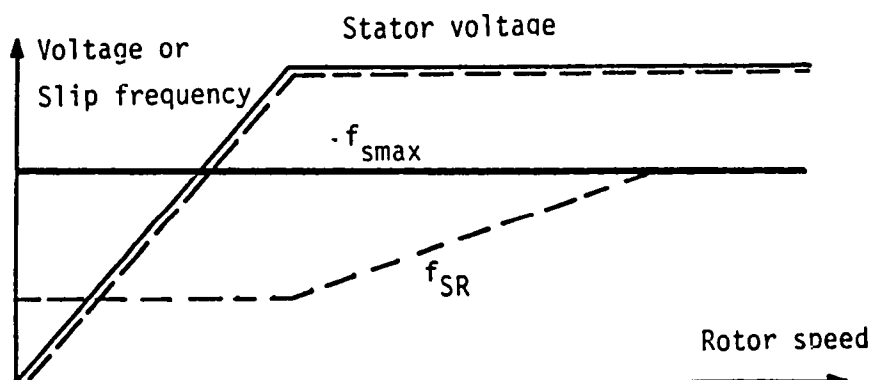
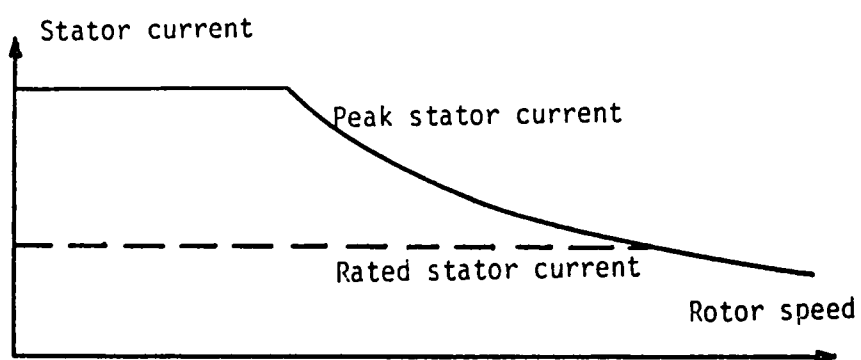
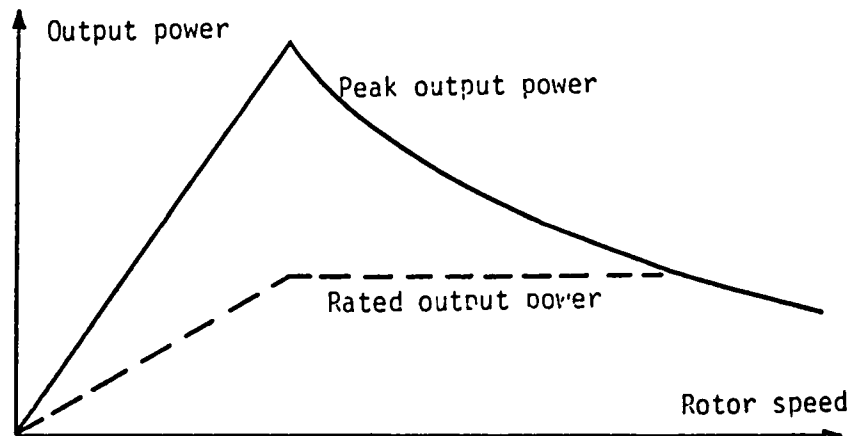


Fig. 5 Generalized motor characteristics

Base frequency f_B \triangleq the design frequency for the motor (the frequency when V reaches a maximum)

Base output P_B \triangleq the rated output at the base frequency

Base current I_B \triangleq the current which produces rated output at the base frequency

Base voltage V_B \triangleq the motor voltage at base frequency

Peak output power P_p \triangleq the maximum output power at f_B

Peak current I_p \triangleq the current which achieves P_p

There is a simple relation between these variables:

$$\frac{P_p}{P_B} = \frac{I_p}{I_B} = \frac{f_{smax}}{f_{SR}} \quad \text{at } f_B \quad (4)$$

where f_{smax} is the maximum slip frequency which produces P_p at f_B

Fig. 6 shows three possible motor designs. One possible design to satisfy the specifications is shown by the B curves in Fig. 6, where the maximum power output is 16kW at 10% speed and 60kW at 80% speed. However, this is not the optimum motor design, because the peak current is

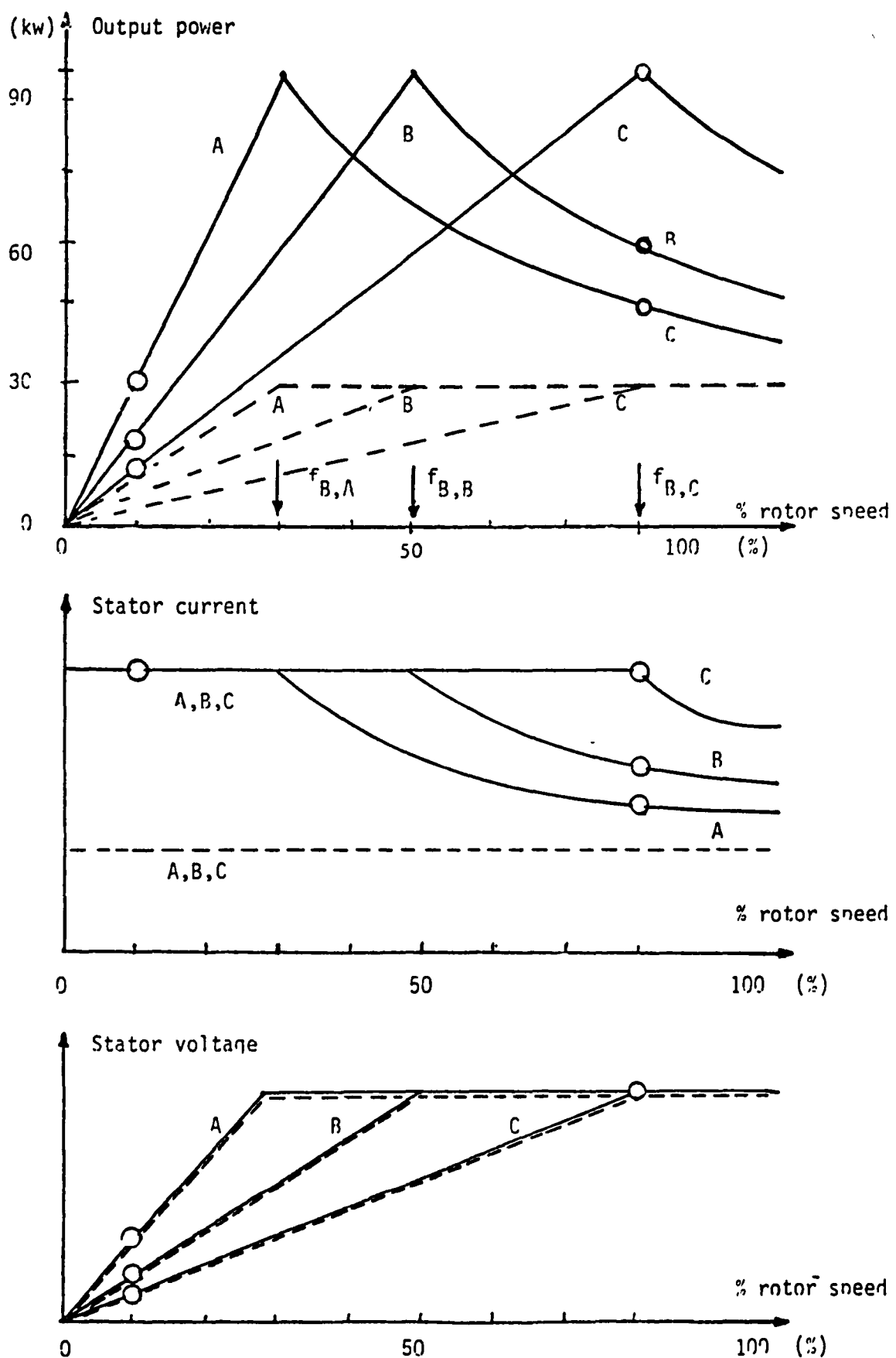


Fig. 6 Three-phase possible machine designs

excessive at low speed and the motor weight is not a minimum. It is very important to have minimum peak current since the power switch device ratings are determined by the maximum current through the devices. The peak current can be reduced for a given output power by lowering the base frequency, but this increases the size of the machine. Therefore, the base frequency should be increased, resulting in a smaller machine. Then, the voltage should be increased at low frequency to saturate or overexcite the machine. This permits higher power output with reduced peak current and minimum motor size and weight. The optimum machine design should have nearly equal peak currents at 10% speed.

Constant V/f operation means nearly constant air-gap flux. Thus, by increasing the V/f ratio, oversaturated air-gap flux can be achieved. Since output power is proportional to the product of air-gap flux and rotor current, larger air-gap flux helps to decrease the rotor current, and as a result, lower stator current can deliver the same output power. This mechanism is shown in Fig. 7. Case I on this figure corresponds to case B on Fig. 6. In the digital simulation program, this saturation effect can be easily checked by sensing the magnetizing current. Thus, by a trial and error method, oversaturation of air-gap flux is simulated, and stator current can be reduced until the allowable saturation flux is reached.

Also, when the motor is operated at the overloaded output, the temperature rise due to the greater loss is a

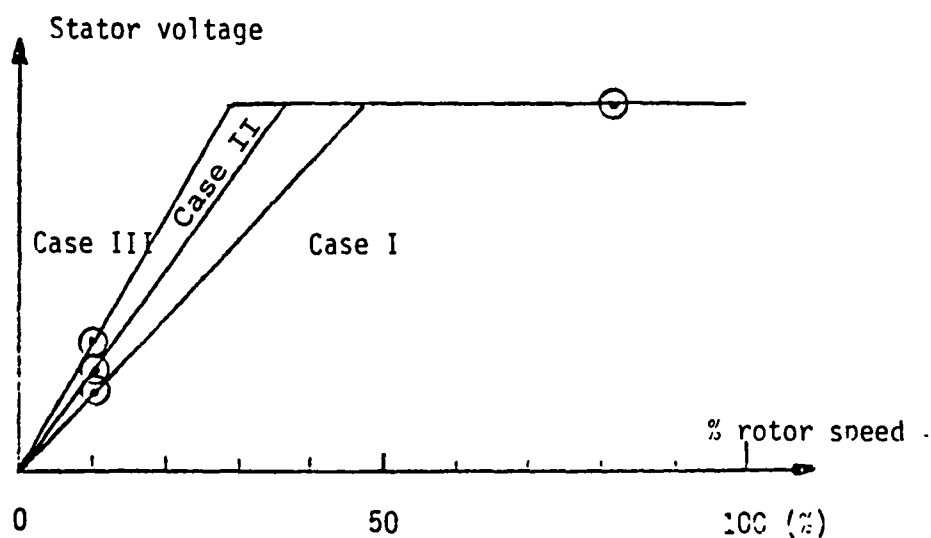
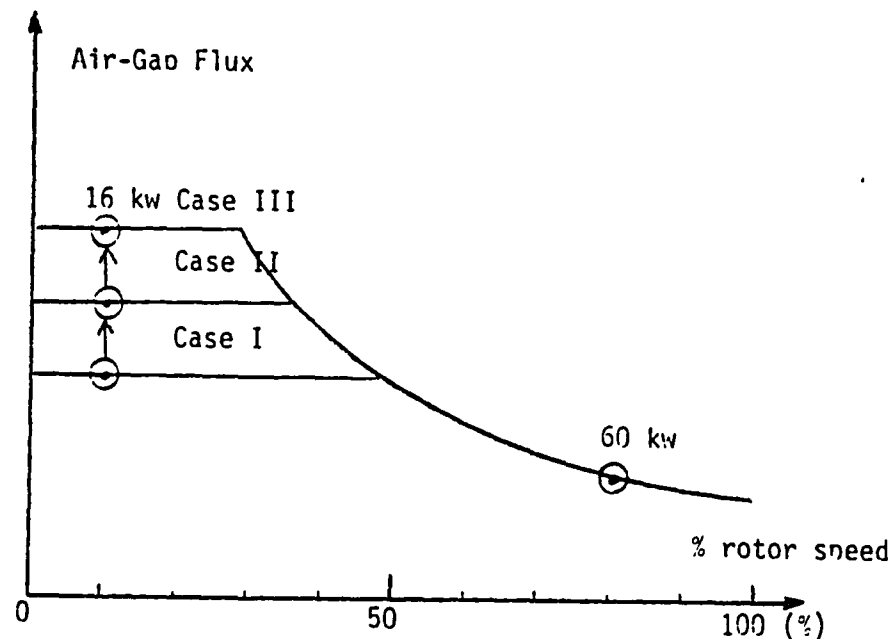


Fig. 7 Mechanism of air-gap flux saturation

very important factor for machine design. In summary, the induction motor design is optimized when the following conditions are satisfied:

1. 60kW output is designed to be maximum output power at 80% speed.
2. 16kW output at 10% speed is achieved by over-saturation of air-gap flux so that the peak current is almost the same as that for 60kW at 80% speed.
3. 30kW output is equal to the rated output at 100% speed.
4. The temperature rise at the overload condition is within an allowable range.
5. The weight of the motor is minimized.

3.3.4 Computer-Aided Design

The design of the two-phase induction motor involves four steps. A flow chart is given in Fig. 8.

Step 1: Choose the Base Operating Point

Since a machine can be almost uniquely designed at a base operating point (base frequency, base voltage and base output power), the base point should be selected carefully so that the designed machine is the optimum one satisfying all required operating conditions. Usually one must come back to Step 1 after checking the given conditions in Step 3.

Maximum frequency and pole number

For a given power rating, the size and the weight of an ac machine decrease as the rated frequency increases. On

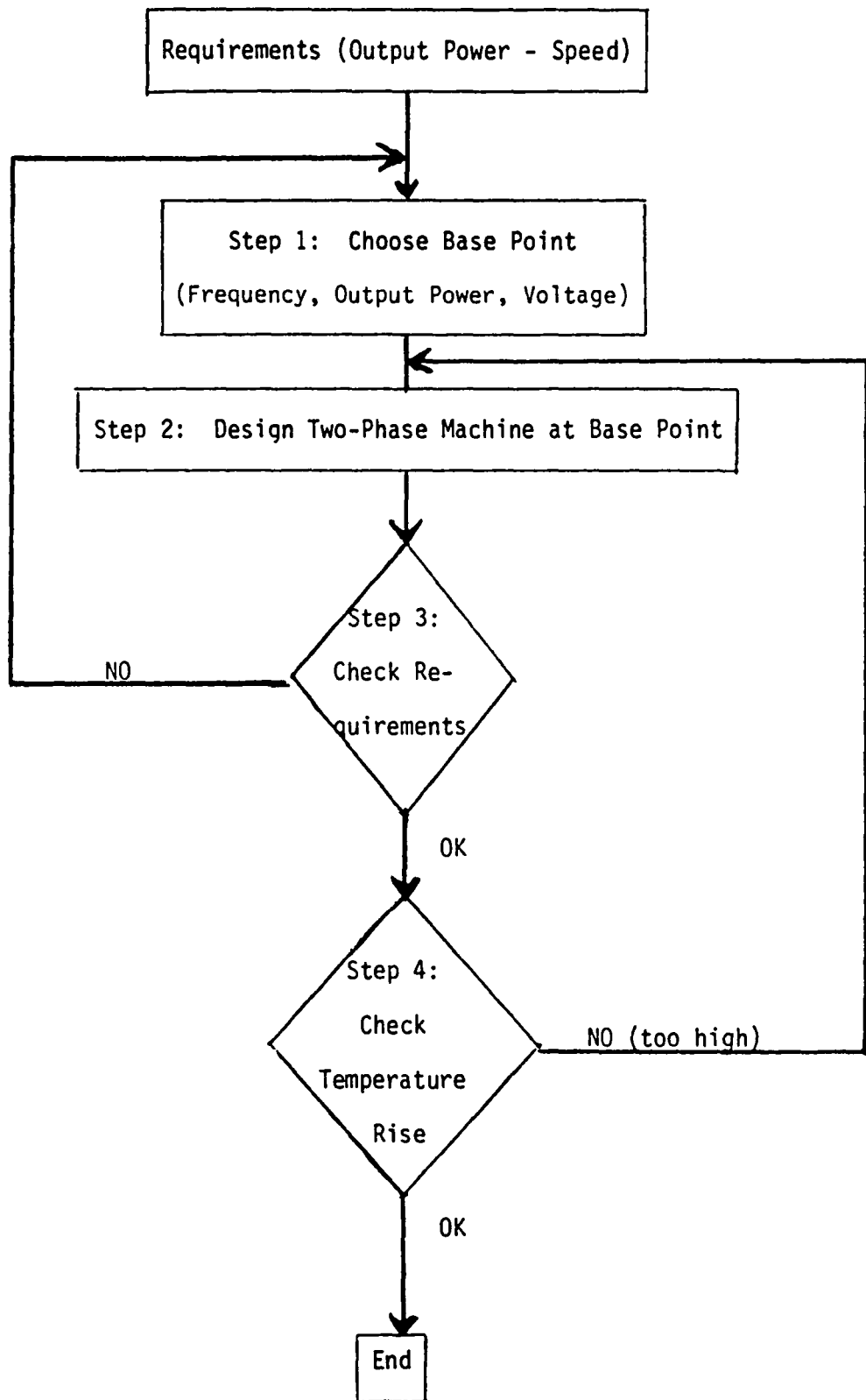


Fig. 8 Design flow chart

the contrary, the iron loss increases at high frequency, and the mechanical bearings become very expensive at high rotor speeds. A rotor maximum speed of 12,000 rpm is chosen because this is believed to provide a reasonable practical trade-off between losses, weight and bearing cost. For a given power rating and maximum speed, as the pole number increases, the maximum ac source frequency increases, which causes greater iron loss and switching loss. Thus, a two-pole machine is chosen, which sets the maximum ac source frequency at 200Hz.

Base voltage, base frequency and base output power

The base operating condition to establish the motor design is chosen as the 30kW output, 40% speed point shown in Fig. 9. The base voltage is selected as follows. With the PWM technique, the peak value of the fundamental component of the output voltage can change from zero to a maximum of $(4/\pi)(V_{DC})$, where V_{DC} is the battery voltage of 240V. The motor is designed such that the applied voltage as a function of speed changes as shown in Fig. 10. The V/Hz (Volts/ Hertz) is constant from zero to 40% speed. From 40% to 80% speed, the V/Hz is reduced with speed as the voltage is linearly increased to a maximum of 306V peak at 80% speed. Then the voltage is fixed at the maximum value from 80% speed to 100% speea. A base voltage of 241V peak at 40% speed is chosen by an iterative technique. Since, roughly speaking, the induction motor output power is proportional to the square of the applied voltage and inversely proportional to the applied frequency ($P \propto V^2/f$),

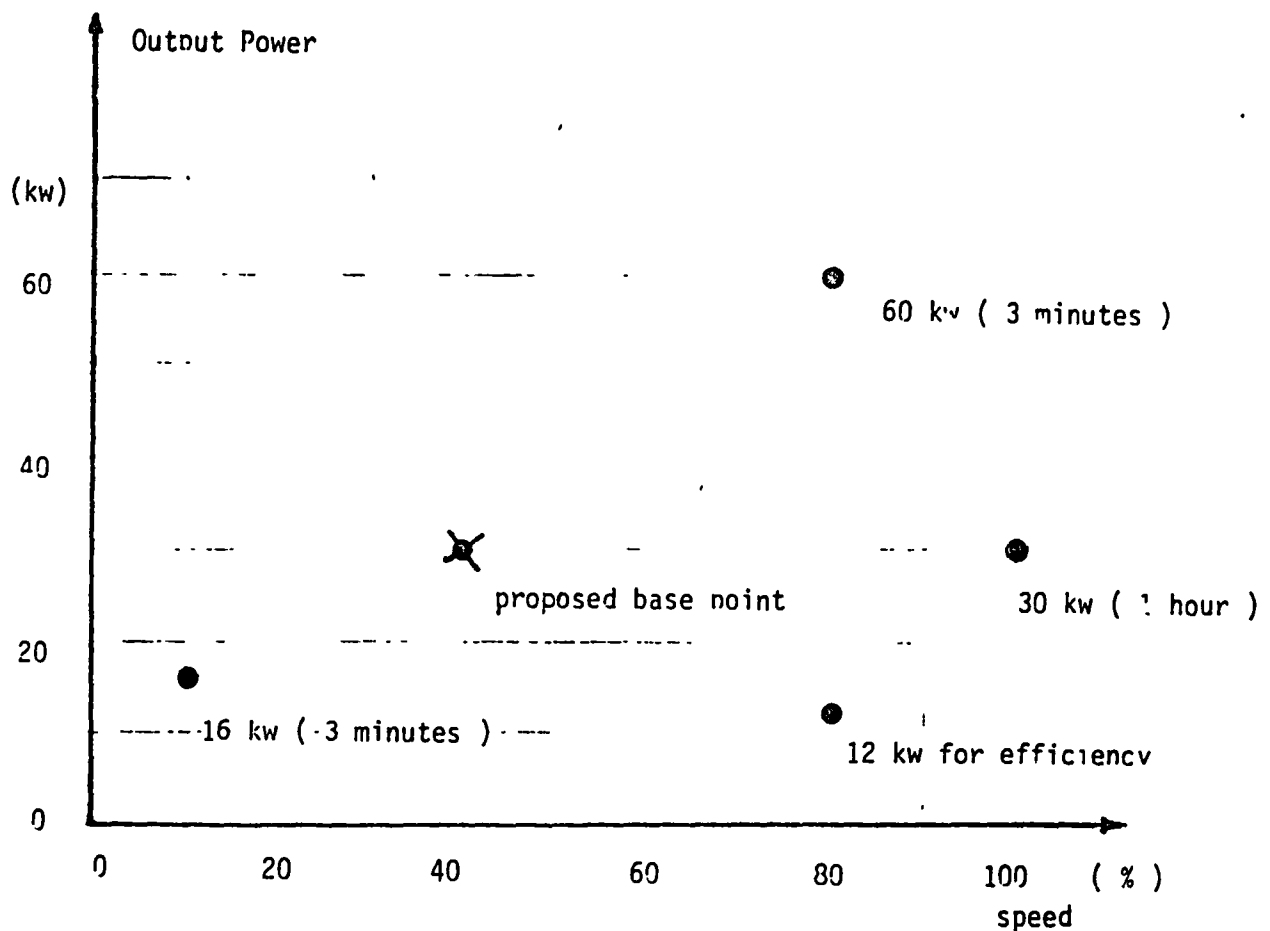


Fig. 9 Output power-speed requirement

Note: ● are specification operating points.

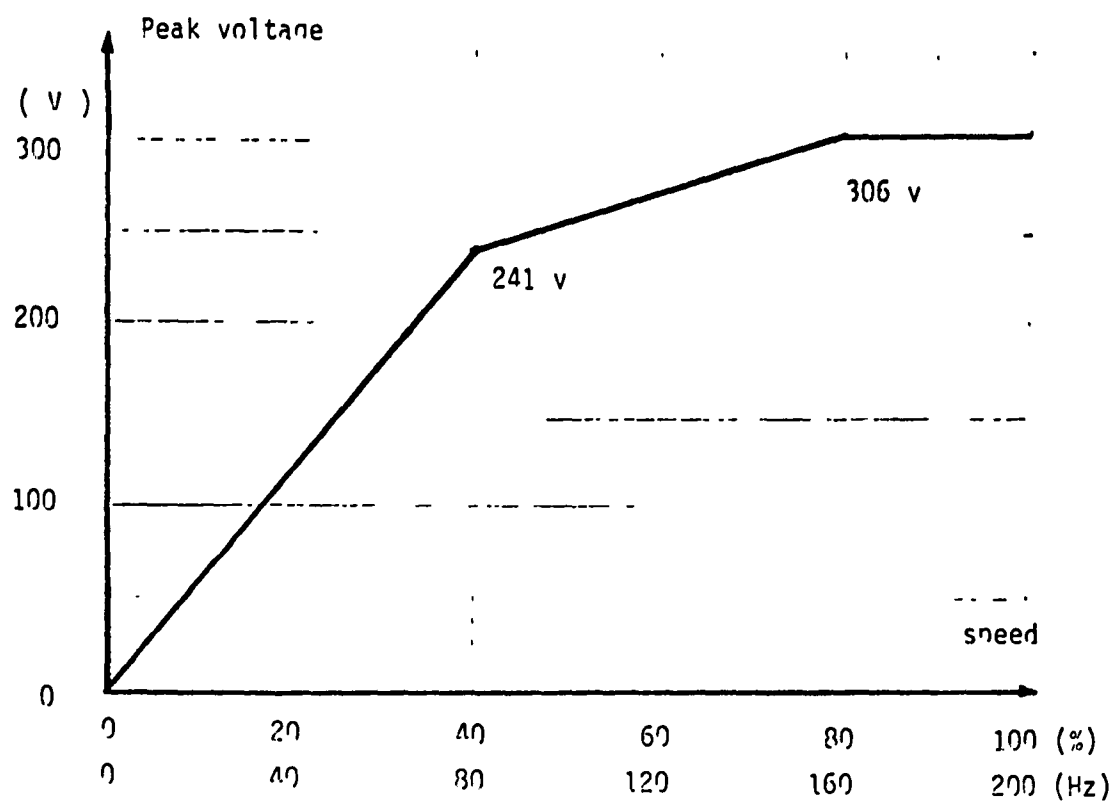


Fig. 10 Motor fundamental peak voltage vs. speed
or frequency for proposed base point

the proposed voltage variation in Fig. 10 implies that the rated output power at different speeds is

7.5kW at 10% speed

30kW at 40% speed

38kW at 80% speed

30kW at 100% speed

The 16kW, 10% speed point requires about twice the rated output power that would be delivered with the low speed range constant V/Hz of 241V/80Hz. (This implies approximately 60V at 10% speed, or 20Hz.) Thus, the motor voltage must be increased above 60V at 10% speed to provide 16kW. When the voltage is increased at a given frequency, the air-gap flux increases, which drives the machine further into saturation. This may result in excessive motor current due to the reduction of the magnetizing reactance. Thus, the motor voltage required for maximum power at 10% speed must be high enough to drive the machine into saturation without excessive current. However, if the V/Hz is too high at 10% speed, it will be too low at 80% speed because the maximum voltage available with a 240V source will be reached at a lower speed. A low V/Hz at 80% speed will mean that the 60kW output cannot be achieved.

Step 2: Design the Machine at the Base Operating Point

The detailed design of the induction motor, both in mechanical and electrical characteristics, is included in Appendix D. When the base operating point is given, the

machine is essentially uniquely defined. The final design is determined in Appendix D after several iterative trials. The resulting machine parameters are as follows:

| | | |
|---------------------------|----------|-------------------------------------|
| External diameter | D_o | 11.5 inches |
| Internal diameter | D | 5.75 inches |
| Rotor length | L | 6.3 inches |
| Weight | W | ≈ 190 lb (≈ 86 kg) |
| Stator resistance | R_s | 0.0274Ω |
| Rotor resistance | R_r | 0.0213Ω |
| Magnetizing inductance | L_m | 13.86mH |
| Stator leakage inductance | L_{ls} | 0.25mH |
| Rotor leakage inductance | L_{lr} | 0.27mH |

Step 3: Check the Output Power by Simulations,

Considering Saturation Effects

Since the machine is designed for the base operating point, the maximum output power should be checked by digital simulations, including the saturation effect of the air-gap flux. Appendix G describes the detailed simulations.

Fig. 11 shows the simulation results for the output power-speed relations at 10%, 40%, 80% and 100% speed of the finally designed motor, when the stator current is limited to 245A peak. All of the specified operating points are satisfied. At the maximum power output of each curve, the current is almost a square wave since this current waveform results in more power output than with sinusoidal current for the same peak current. At the 16kW, 10% speed point, the greatest saturation of the magnetic core occurs. The

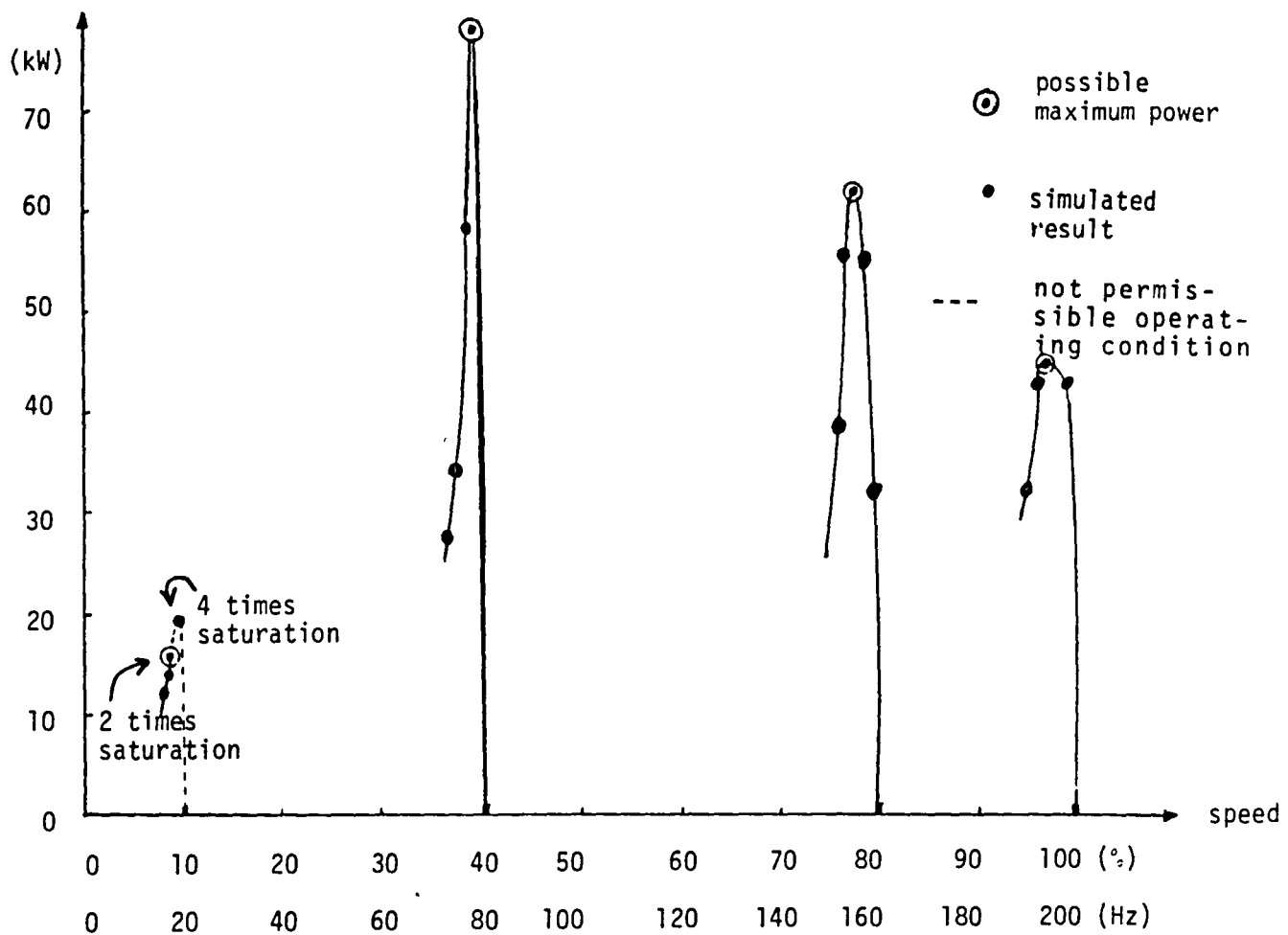


Fig. 11 Output power-speed curves of two-phase motor from simulations.
(Peak current limited to 245 A)

saturation effect of the core is implemented in the simulation study by changing the magnetizing and leakage inductances of the machine. If the magnetizing current exceeds the allowable limit, then the magnetizing and leakage inductances are replaced with adjusted values, which are calculated from the B-H curve. This modification is easily implemented in Step 2. If the magnetizing current still exceeds the allowable limit, which occurs for very low slip frequency, then this is not considered a permissible operating condition.

At the 60kW output, 80% speed operating point, under-saturation of the core occurs because the voltage is not high enough to produce rated flux. In this case, when the magnetizing current in the simulation is below the allowable limit, the magnetizing and leakage inductances are recalculated in Step 2 using the B-H curve.

Step 4: Check the Temperature Rise

Most of the heat generated in the machine comes from the copper loss, which is proportional to stator resistance times the square of the current. According to the simulation results, the rms currents at the given operating points are as follows:

- 1) 16kW at 10% speed (3 mins., 30% duty) $I_{1\text{rms}} = 200\text{A}$
- 2) 60kW at 80% speed (3 mins., 30% duty) $I_{1\text{rms}} = 175\text{A}$
- 3) 30kW at 100% speed (1 hour) $I_{1\text{rms}} = 115\text{A}$

Assuming a conventional rotor fan type construction, the air flow is reduced at lower rotor speeds so that the worst-case cooling condition is the 10% speed point. If the

iron and mechanical losses are considered negligible, then the highest transient temperature rise occurs for the 16kW, 10% speed operating point. Since this condition continues for three minutes with a 30% duty cycle, the load pattern is assumed to be 16kW for three minutes, followed by no output for seven minutes, repeated several times. The temperature rise is estimated by solving the heat balance differential equations (Appendix E). The estimated temperature rise is 50 °C. The bifilar windings help to reduce the temperature rise because of the increased volume of copper. The temperature rise is higher if the same heat loss is generated in a smaller volume of copper.

In the calculation of the temperature rise, the most pessimistic conditions are considered. First, static air is assumed for the heat dissipation. Next, the heat transfer to the core and frame is neglected. Thus, the actual temperature rise should be somewhat less than 50°C.

3.3.5 Efficiency

In accordance with the JPL specifications, the most important operating point from the standpoint of efficiency is the 12kW, 80% speed point. The theoretical approach to optimize the efficiency of an induction machine implies that the magnetizing current should be equal to the rotor current.* But, since the V/Hz is reduced at the 80% speed

* T. W. Jian, N. L. Schmitz, D. W. Novotny, "Characteristic Induction Motor Slip Values for Variable Voltage Part Load Performance Optimization," IEEE PAS, Jan. 1983, pp. 38-46.

point, the magnetizing current does not reach the optimized value because of the undersaturation of the air-gap flux. Thus, the best that is possible is to make the magnetizing current its maximum value and to control the current to get 12kW output at 80% speed. Simulation results, performed by an iterative method changing the slip frequency and the amplitude of the sinusoidal motor current, give 98.6% efficiency at a slip frequency of 1.16Hz (0.725% slip). The current and output power are shown in Appendix G. The pulsating power is +65%. These simulations neglect the iron loss, stray loss, and mechanical losses. If these losses are included, the efficiency is expected to be about 95%.

3.4 Inverter Design

3.4.1 Switching Device Requirements

In Step 3 of the design procedure in the previous section, three given output power-speed operating points were checked by simulations. The maximum peak current through the stator winding is 245A when either 16kW at 10% speed or 60kW at 80% speed is required. Since the forward blocking voltage of the device is two times 240V, the total VI rating of the devices for the two-phase inverter will be $(240 \times 2 \times 245) \times 4 = 470\text{kVA}$.

From the viewpoint of the power dissipation in the switching devices, 16kW output at 10% speed produces the maximum switching loss. From the simulations, the switching frequency is 3.4kHz at 16kW, 10% speed, and 160Hz at 60kW, 80% speed.

In summary, the switching device requirements are

Peak current = 245 A

RMS current = 200.5A

Maximum switching frequency = 3.4kHz

Peak voltage (not including transients) = 480V

3.4.2 Power Circuit

As a result of a study of the available transistor and thyristor devices to meet the switching requirements for this application, MG300M1FK1 Toshiba power transistors are recommended. These transistors have 1000V blocking capability, 300A dc rating and 1.6kW maximum power dissipation capability. Thus, this Toshiba transistor provides a nominal dc voltage safety factor of $1000/480 = 2.08$ and an rms current safety factor of $300 \times \sqrt{2} = 2.12$. (Note: This does not include the transient voltages across the transistors. The transient voltages are discussed in the next section.)

The two-phase inverter requires four power switch modules, each of which includes a Darlington power transistor, a freewheeling diode, a snubber circuit and a base drive. However, only one heat sink is required since the MG300M1FK1 transistor is an isolated package. Also, no base drive isolation is necessary for the circuit of Fig. 2 with common emitters.

The two-phase and three-phase inverter circuits both can deliver power to the motor load or take power from the source. This is accomplished by the proper control of the inverter switching instants relative to the ac voltage generated by the load machine, which produces a negative

slip. Appendix G.5 gives simulation results for regenerative operation.

The detailed inverter design is described in Appendix F.

3.4.3 Transient Voltage

The two-phase system does present a more difficult snubber design problem because of the leakage inductances that will be present in the bifilar windings and because of the inductances in the motor leads from the inverter to the motor. It will be necessary to use special techniques to minimize the motor lead inductance, such as using parallel closely spaced flat conductors between the inverter and the motor or packaging the inverter essentially on the motor housing.

The amplitude of the voltage spike primarily depends on the equivalent leakage inductance of the bifilar winding and the lead inductance between the inverter and motor. The energy stored in these inductances must be dissipated in the snubbers. Based on estimated practical values of total leakage and lead inductance, the voltage spike phenomena can be simulated by the digital computer, as shown in Appendix F. However, a precise design of the snubbers required can be accomplished only through experiment with an actual model of the inverter.

As shown in Appendix F, the peak transistor voltage is about 900V with 4 μ H total lead and leakage inductance. However, if the inductance is reduced to 1 μ H, the peak transistor voltage is approximately 600V. This would reduce the

transistor voltage safety factor from 2.08 (as given in the previous section) to about 1.6, which is still a quite reasonable voltage safety factor.

3.4.4 Control Circuit

A microprocessor controller will be used, which consists of an MPU, ROM, RAM, timer, I/O port and current sensors which can provide a variety of speed and torque controls. In either case using PWM, the speed or torque controller generates the frequency and amplitude commands for the stator current. This current is regulated so as to stay within a hysteresis band of the reference command by PWM control of the inverter. Also, the switching frequency is monitored and limited to less than 3.4kHz. The maximum fundamental inverter frequency command is 200Hz.

The use of the microprocessor permits the implementation of very sophisticated controls to provide optimal efficiency at any operating point and protection of the drive system.

4.0 FINAL DESIGN AND EXPECTED PERFORMANCE OF A TWO-PHASE INVERTER/BIFILAR INDUCTION MOTOR SYSTEM

4.1 Machine Data

| | |
|-------------------|---------------------------------------|
| External diameter | $D_o = 11.5$ inches |
| Internal diameter | $D = 5.75$ inches |
| Rotor length | $L = 6.3$ inches |
| Weight | $W \approx 190$ lb (≈ 86 kg) |
| Output rating | 30kW |
| Number of phases | 2 |
| Base frequency | 80Hz |

| | |
|---------------------------|-----------------------|
| Maximum speed | 12,000 RPM |
| Base voltage (rms) | 170V |
| Base current (rms) | 110A |
| Stator resistance | $R_s = 0.0274 \Omega$ |
| Rotor resistance | $R_r = 0.0213 \Omega$ |
| Magnetizing inductance | $L_m = 13.86mH$ |
| Stator leakage inductance | $L_{ls} = 0.25mH$ |
| Rotor leakage inductance | $L_{lr} = 0.27mH$ |

4.2 Inverter Data

| | |
|------------------------------------|--|
| Power switching devices | (4) Toshiba MG300M1FK1 Transistors |
| Input voltage | 240V |
| Output voltage | 240V (peak or rms) |
| Output current | 245A peak; 200A rms |
| kVA rating | 96kVA |
| kW rating | 60kW |
| Maximum output frequency | 200Hz |
| Maximum switching frequency | 3.4kHz |
| Estimated efficiency | |
| at 12kW, 80% speed operating point | 95.4% |

4.3 Inverter/Motor Performance

The digital computer simulations described in Appendix G provide the following performance data at the specified operating points:

16.4kW output at 10% speed

Slip frequency = 1.7Hz (slip = 8.50%)

Switching frequency = 3.4kHz

Stator peak current= 245A*

Stator rms current = 200A

Pulsating torque = ±20%

60.5kW output at 80% speed

Slip frequency = 3.2Hz (slip = 2%)

Switching frequency = 160Hz

Stator peak current = 245A**

Stator rms current = 175A

Pulsating torque = ±30%

13.1kW output at 80% speed

Slip frequency = 1.16 Hz (slip = 0.725%)

Switching frequency = 1.6 kHz

Stator peak current = 103A***

Stator rms current = 53.2A

Pulsating torque = ±65%

*The current is a PWM controlled wave form with a square wave envelope 205±40A.

**The inverter voltage is a square wave producing an unmodulated current waveform.

***The current is a PWM controlled sinusoidal waveform with an envelope of ± 38A.

Motor efficiency (only with copper loss) = 98.6%

Motor efficiency (with 3.4% iron and stray mechanical loss) = 95.2%

Inverter efficiency (with snubber, on-state and switching loss) = 95.4%

Total efficiency = 91%

4.4 System Schematic Diagram

The complete schematic diagram of the inverter/motor drive system is shown in Fig. 12.

As mentioned previously, transient voltages are produced by lead inductances and leakage inductances due to imperfect coupling between the bifilar motor windings. With the input capacitor connected across the inverter dc bus very close to the inverter transistors and motor windings, the dc lead inductance is minimized. Snubber circuits are included to suppress voltage transients due to the imperfect coupling between bifilar windings and the inductance of the leads between the inverter transistors and motor windings. This also implies that the inverter transistors must be mounted very close to the motor.

The design of the snubbers is discussed in Appendix F. However, the precise snubber configuration can be determined only through experimentation with an actual model of the inverter. A final optimum arrangement may include varistors and additional capacitors.

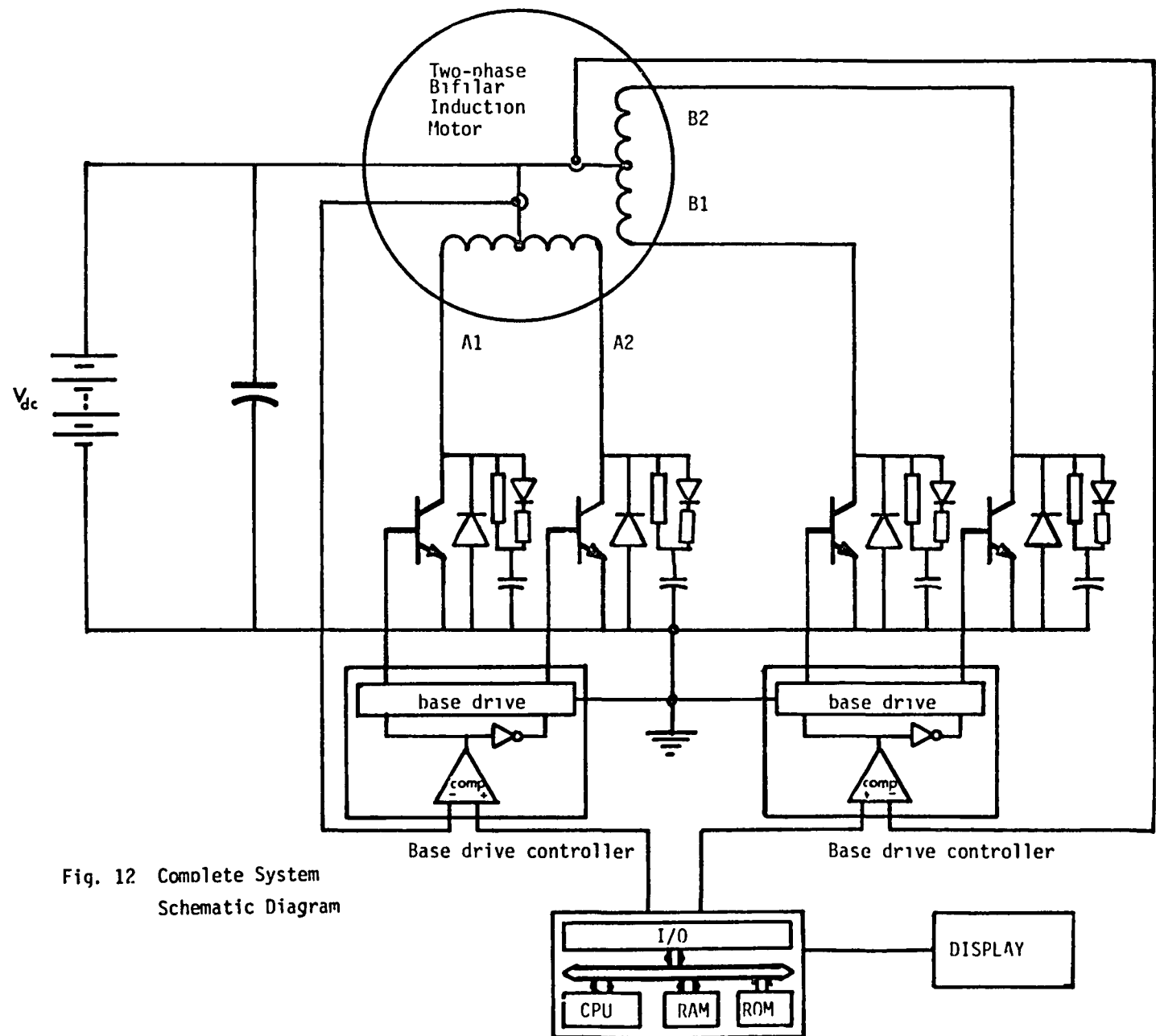


Fig. 12 Complete System Schematic Diagram

The base drive circuits are critical for reliable power transistor operation with minimum switching loss. Current sensors are required to detect each motor winding current for the PWM controlled current operations as well as for overcurrent protection. Sophisticated control strategies can be implemented in the microprocessor software.

5.0 COMPARISON OF TWO-PHASE BIFILAR AND THREE-PHASE BRIDGE INVERTER MOTOR SYSTEMS

5.1 Advantages and Disadvantages of Two-Phase System

Advantages

- A. The number of power switching devices is reduced from six to four.
- B. The current rating of each power switch is 65% of the value required for the three-phase bridge inverter (Fig. B-3). This has been verified by simulation as shown in Table II of the next section.
- C. The total number of components is estimated to be about 70% of the number required for the three-phase system. Since four transistor switches are used instead of six as in the three-phase bridge inverter, this would imply about two-thirds as many components. However, some circuits are not repeated for each switch and the snubbers are more complex for the two-phase inverter. The component count reduction also implies higher reliability and lower manufacturing assembly cost.

- D. The motor transient temperature rise is reduced due to the increased volume of copper.
- E. The control hardware is somewhat simpler due to the common emitter arrangements so that isolation is not required in the base drive circuits.
- F. The total component cost for the two-phase system is estimated to be about 90% of that for the three-phase system. This cost reduction cannot be proven until prototype equipments are manufactured. The cost will be reduced because of the reduced total number of components, the elimination of the need for base drive circuit isolation, and the reduced peak current in the transistor switches. However, the cost will be greater because of the higher peak transistor voltages required, the need for very effective snubbers to minimize transient voltages, the requirement for a somewhat larger motor than for three-phase, and the necessity to minimize motor bifilar winding leakage inductances and lead inductances in the inverter current switching paths. It is presently estimated that these tradeoffs will result in reducing the two-phase system cost to about 90% of that for a three-phase inverter/motor drive.

Disadvantages

- A. The size, weight and cost of the two-phase motor is greater than for the three-phase machine. It

is estimated that an equivalent three-phase motor would have 85% of the weight and 90% of the cost of the two-phase bifilar machine.

- B. The design of the snubbers for the power switches is more difficult since motor lead inductances and bifilar winding leakage inductances produce additional transient voltages.
- C. The torque pulsations are relatively large because of the necessity to limit the inverter switching frequency to achieve high efficiency.

5.2 Simulation Results

Digital simulations to compare the two-phase and three-phase systems are presented in Appendix G. Table I lists the parameters used for the simulations. The results of these simulations are summarized in Tables I and II.

Fig. 13-a shows the stator voltage and current per phase, and Fig. 13-b shows the instantaneous output power for the two-phase machine. Fig. 13-c and Fig. 13-d show the corresponding variables for the three-phase machine.

The output power or torque pulsations are greatest for the two-phase system at the 60kW operating point since a square wave voltage is supplied from the two-phase inverter. However, at the 12kW operating point, with sinusoidal current control, the torque pulsations of the two-phase system are nearly as large because the inverter switching frequency must be limited to achieve high efficiency.

Table I Machine Parameters

| <u>Bifilar Two-Phase Induction Motor</u> (at 160Hz) | <u>Three-Phase Induction Motor</u> (at 320Hz) |
|--|--|
| $R_s = 0.0274$ | $R_s = 0.00578$ |
| $R_r' = 0.0213$ | $R_r' = 0.0038$ |
| $L_{1s} = 2.94 \times 10^{-4} H$ | $L_{1s} = 5.95 \times 10^{-5} H$ |
| $L_{1r} = 3.23 \times 10^{-4} H$ | $L_{1r} = 7.0 \times 10^{-5} H$ |
| $L_m = 26.8 \times 10^{-3} H$ | $L_m = 3.32 \times 10^{-3} H$ |
| Weight=86kg | Weight=73kg |

Note: A four pole three-phase motor was used for this comparison because more commercial data was available to us on this type of machine. However, we believe a two pole three-phase machine is somewhat preferable.

Table II Comparison of Two-Phase and Three-Phase Inverter-Motor System

Case I: 80% speed, 60kW output (for peak current comparison)

Two-Phase Induction Motor

Peak current $I_p = 245A$

rms current $I_{rms} = 175.8A$

slip = 2.0%

$P_{out} = 60.5kW$

frequency = 160.0Hz

Three-Phase Induction Motor

Peak current $I_p = 375A$

rms current $I_{rms} = 243A$

slip = 1.25%

$P_{out} = 60.2kW$

frequency = 329.8Hz

Case II: 80% speed, 12kW output (for efficiency comparison)

Two-Phase Induction Motor

Peak current $I_p = 103A$

rms current $I_{rms} = 53.2A$

slip = 0.725%

$P_{out} = 13.1kW$

frequency = 160Hz

efficiency (only copper loss)=98.6%

Three-Phase Induction Motor

Peak current $I_p = 105A$

rms current $I_{rms} = 66A$

slip = 0.8%

$P_{out} = 12.5kW$

frequency = 329.8Hz

efficiency (only copper loss)=98.9%

VOLTAGE & CURRENT (80% S,60KW,MOTOR OPERATION)

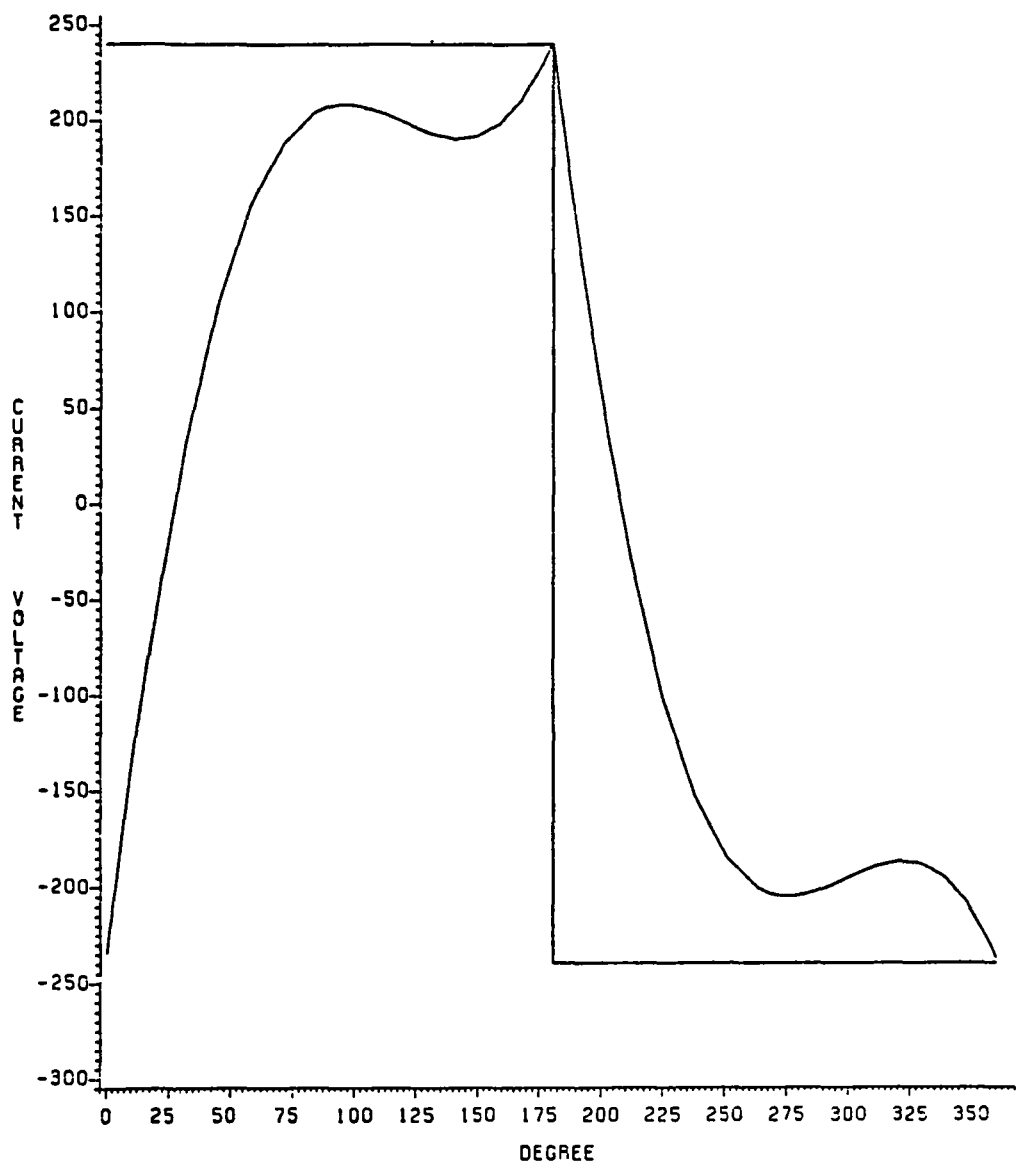


Fig. 13-a Two-phase

OUTPUT POWER (80% S, 60KW, MOTOR OPERATION)

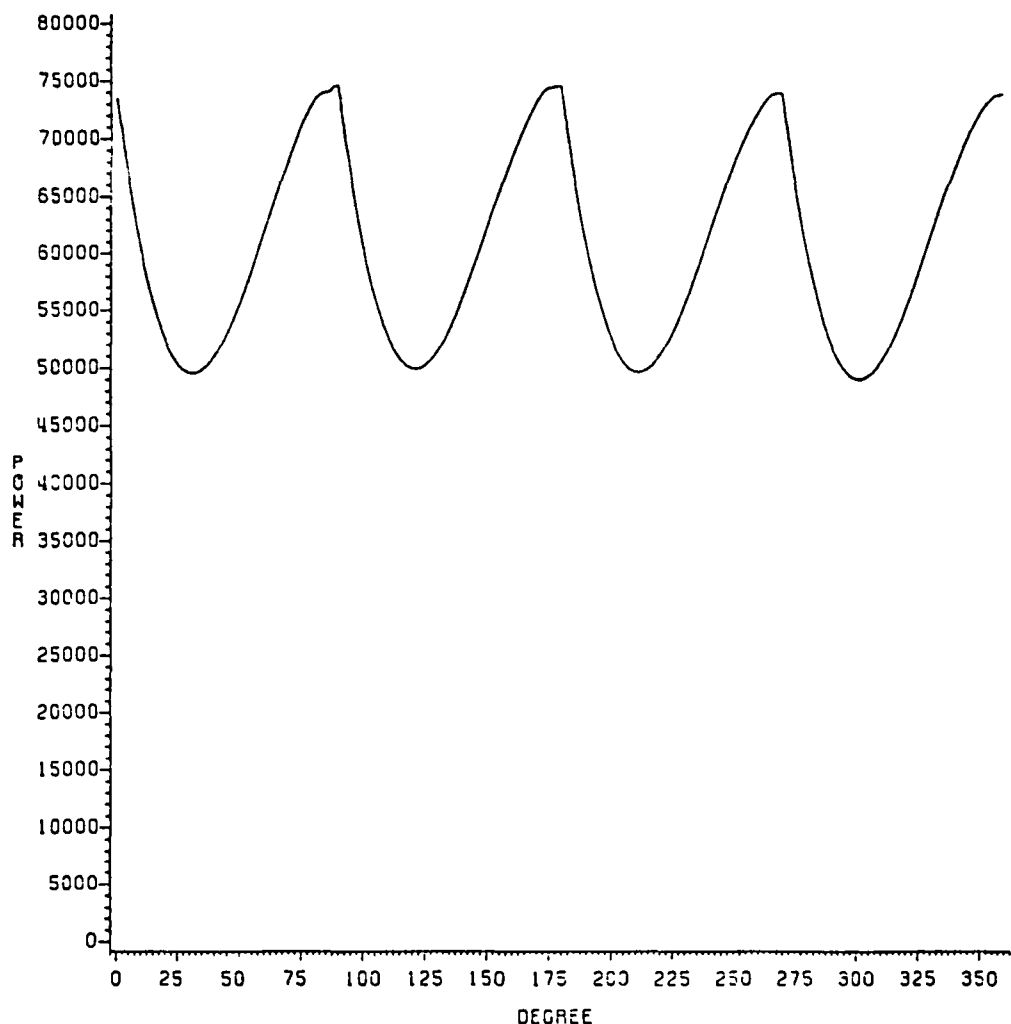


Fig. 13-b Two-phase

VOLTAGE & CURRENT (80% SPEED,MOTOR OPERATION)

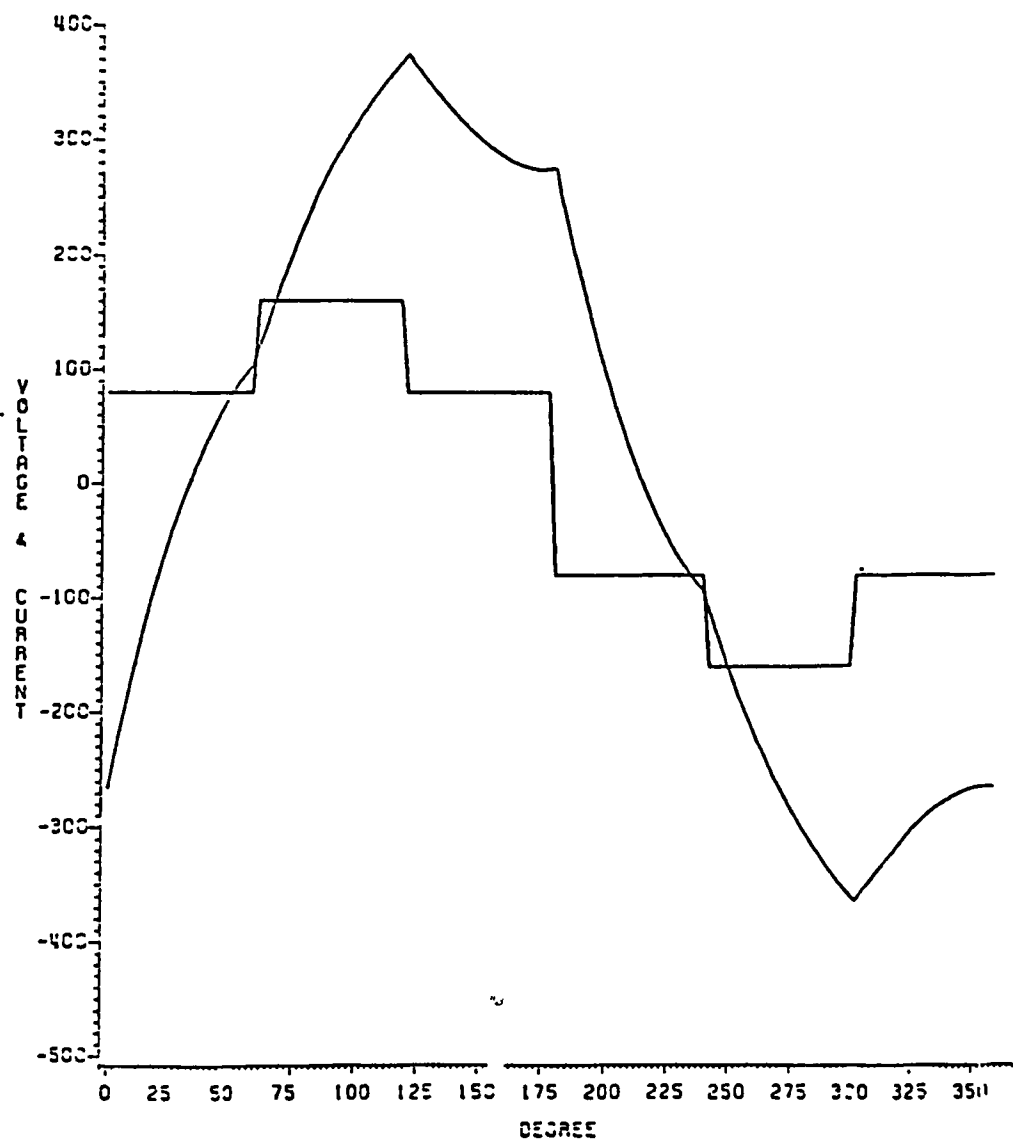


Fig. 13-c Three-phase

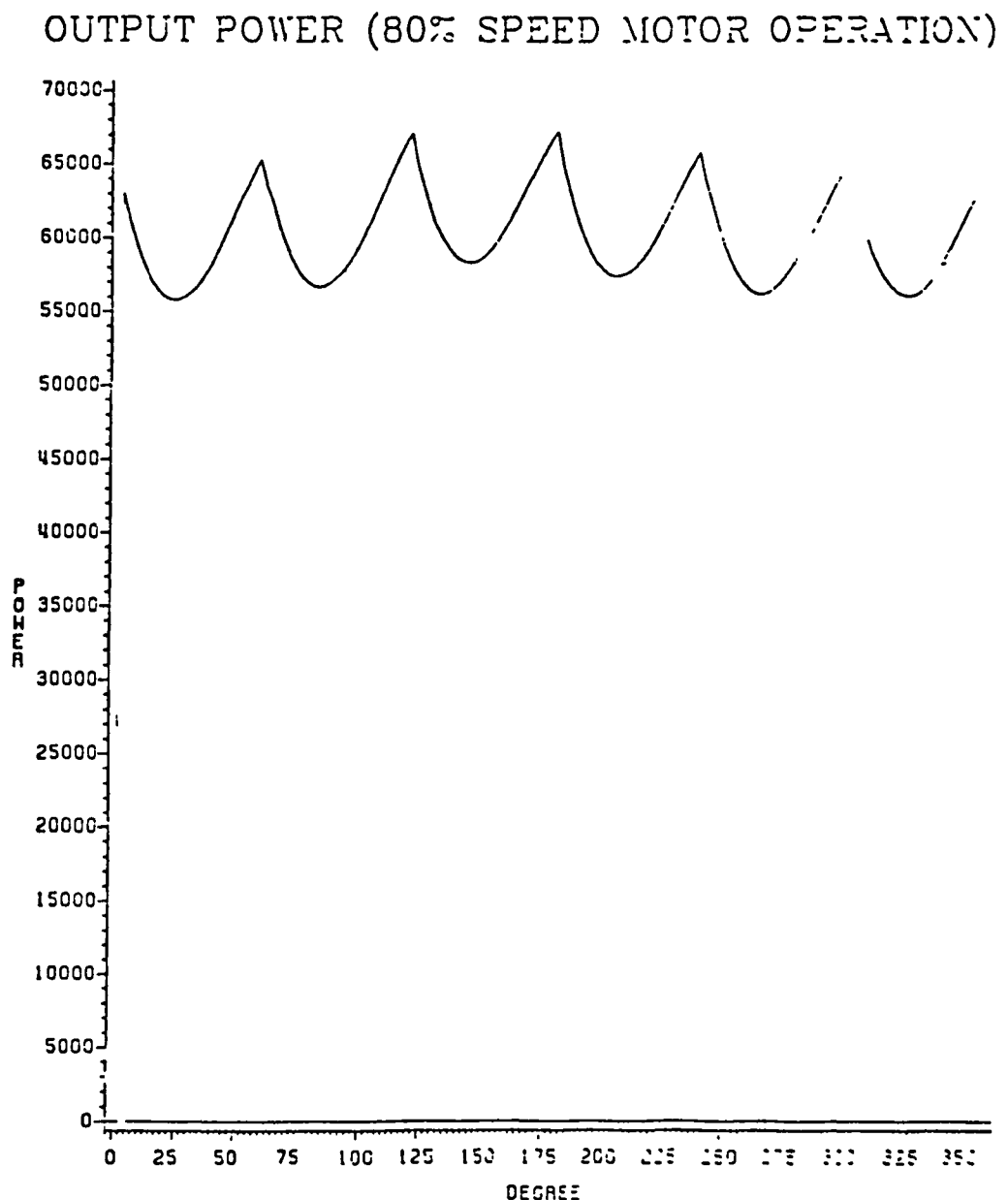


Fig. 13-d Three-phase

5.3 Performance Function Comparison

Machine: The following data are used

| | | |
|----|---|--------|
| 1) | Cost of two-phase machine | \$360* |
| | Cost of three-phase machine | \$325* |
| 2) | Weight of two-phase machine | 86kg |
| | Weight of three-phase machine | 73kg |
| 3) | Efficiency at 12kW, 80% speed | |
| | Two-phase machine | 95% |
| | Three-phase machine | 95% |
| 4) | Performance function F (F=C + 10W - 120E) | |
| | Two-phase machine | -10.1K |
| | Three-phase machine | -10.3K |

Inverter: The following data are used

| | | |
|----|--|--------|
| 1) | Estimated manufacturing cost of two-phase inverter | \$1000 |
| | Estimated manufacturing cost of three-phase inverter | \$1200 |
| 2) | The weight and efficiency of the two-phase and three-phase inverters are estimated to be essentially the same. | |
| 3) | Performance function (neglecting the weight and efficiency terms) | |
| | Two-phase inverter | \$1000 |
| | Three-phase inverter | \$1200 |

*These are best judgment estimates assuming at least 10,000 units/year.

Inverter-Motor System: (Including only the parameters in the Performance Function which are different.)

Two-phase system \$360+\$1000+\$10X86=\$2220

Three-phase system \$325+\$1200+\$10X73=\$2255

Thus, the two-phase system has only a very slight advantage over the three-phase system based on the Performance Function.

6.0 CONCLUSIONS

The proposed two-phase inverter-motor drive has the following advantages over the traditional three-phase bridge inverter-motor system:

1. The number of power semiconductor switching devices is reduced from six to four.
2. The current rating of each power switch is 65% of that required for each switch in the equivalent three-phase system.
3. The total number of components is estimated to be about 70% of the number required for the three-phase system. This also implies higher reliability and lower manufacturing assembly cost.
4. The motor transient temperature rise is reduced due to the increased volume of copper.
5. Somewhat simpler control hardware is possible because of the common emitter circuit so that isolation is not required in the base drive circuits.

6. The total component cost is estimated to be about 90% of that for the three-phase system.

The overall efficiency of the two systems is about the same and the Performance Function in the JPL Specifications is also nearly equal for the two-phase and three-phase systems.

The major disadvantages of the two-phase system are:

1. The weight and cost of the two-phase machine are greater. It is estimated that the three-phase machine would have 85% of the weight and 90% of the cost of the two-phase bifilar machine.
2. The snubber requirements for the inverter power transistors are much more severe for the two-phase inverter since motor lead inductances and bifilar winding leakage inductance produce additional transient voltages.
3. The torque pulsations are relatively large because of the necessity to limit the inverter switching frequency to achieve high efficiency.

For a high production electric passenger vehicle, the two-phase inverter-motor system developed on this research should provide significant cost advantages for the electric vehicle application when compared to the conventional three-phase bridge inverter-induction motor drive. It is important to note that the conclusions of this research are based on analysis and simulations. An actual model of the two-phase system must be constructed and evaluated to prove the advantages claimed for the proposed inverter-motor system. The most challenging engineering task will be to design the inverter, motor and snubber circuits to minimize transient voltages while retaining high system efficiency.

APPENDIX A

MOTOR SPECIFICATIONS PROVIDED BY JPL

EXHIBIT I**Induction Motor Specification**

The following is a specification for an ac induction motor to be used in conjunction with a Pulse Width Modulated (PWM) Inverter and a 240 volt battery for propulsion of electric vehicles using a fixed ratio gear reduction.

I. BACKGROUND

Numerous traction drives have been developed using inverter driven induction motors. In all cases the inverter converts dc battery power into three-phase power of controlled frequency and voltage. While control algorithms vary, with all schemes, the electrical frequency is maintained close to the mechanical frequency and the voltage to frequency ratio is maintained below a critical maximum (lest magnetic saturation occur).

Compared with dc systems, such ac drives are advantageous in that inherent four quadrant performance is achieved, motor cost is greatly reduced, motor weight and losses are approximately halved while motor maintenance is virtually eliminated. Until recently, however, these advantages were offset by cost, weight, and inefficiency problems of the inverter.

II. SYSTEM DESIGN PHILOSOPHY

With traction drives, where PWM inverters provide the ac power, the usual constraints of voltage and frequency are nonexistent. Accordingly, the requirement for producing torque under high slip conditions is deleted, and thus the

need for compromise between "starting characteristics" versus "running efficiency" is eliminated. Accordingly, traction type machines are designed for maximum efficiency with minimal rotor resistance.

For each torque-speed point of operation, a range of excitation voltage-slip frequency values may be used; however, only one value of voltage and slip frequency produces optimal efficiency. With modern inverter technology it is possible to control both voltage and frequency such that optimal system efficiencies prevail over the entire torque speed plane. From experience it has been found that the optimal solution corresponds to maintenance of a constant slip frequency with the excitation voltage per Hertz varying roughly as the square root of the torque. Since selection of the inverter control parameters is flexible, it follows that the appropriate optimization sequence is:

1. Design optimized motor.
2. Characterize this motor.
3. Design appropriate inverter control algorithm.

The above philosophy is embodied in the attached specification.

With traction systems, cost, weight, and efficiency parameters are of key importance. In order to meaningfully optimize these parameters, relationships must be established between these parameters. From JPL studies it has been found that for passenger vehicles the "cost of weight" is

approximately \$10/kg and the value of efficiency is approximately \$120/. Accordingly, for both the motor and the inverter, the total cost, C^1 , to be minimized is:

$$C^1 = C + 10W - 120E \quad (1)$$

where C is the retail dollar cost

W is the weight in kg

E is the efficiency in %

Since efficiency is primarily important in terms of range and since maximum range is under freeway conditions, E is defined under the speed and power conditions associated with freeway driving (55 mph, 12 kW shaft output).

A totally enclosed convective cooled design is recommended since:

1. Expected heat loss is low as motor efficiency will be in the range of 92% to 95%.
2. Duration of operation is limited by the battery storage capability. (With 150 km of driving, heat produced by motor will be less than 1.2 kWh.)
3. With open design, dirt particles may cause stator winding damage.

III. DISCUSSION OF SPECIFICATIONS

1. Voltage

The nominal battery voltage is 240 V dc. This corresponds to a maximum inverter output voltage of 165 V

rms (sine modulation) and 185 V rms (six-step mode). The inverter will control to lower voltages in accordance with the control algorithm.

2. Power Output

Since the bidder shall determine actual speeds and torques, specifications are presented in terms of shaft output power and fraction of maximum speed. (The gear reduction ratio and inverter control constants will be determined after establishing the motor.)

2a. Power at Maximum Speed

This specification establishes one hour thermal and torque breakdown capability of handling the rated power at full speed. Since efficiency and breakdown torque both improve with decreasing speed, it follows that this power level can be maintained for all speeds above base speed.

2b. Power at 10% Maximum Speed

This specification establishes the torque breakdown capability below base speed and corresponds to vehicle acceleration.

2c. Power at 80% Maximum Speed

This specification establishes the torque breakdown capability at 0.8 N_{max} (55 mph) and corresponds to vehicle acceleration at this speed.

3. Maximum Speed

As maximum speed is increased, cost and weight decrease. Accordingly, moderately high speeds are desirable - consistent with mechanical and windage limits. With previous efforts, maximum speeds between 9,000 and 20,000 rpm have been used. The actual maximum speed selected will be on the basis of Equation 1.

4. Number of Poles

As the number of poles is increased, the conductor losses generally drop while the magnetic losses increase. (The inverter switching losses are proportional to frequency and, therefore, proportional to pole number; this impact is, however, small and will be neglected.) The optimum pole number will be determined on the basis of Equation 1.

5. Weighting Function (See Equation 1)

This function relates cost and efficiency to the retail price of the motor. The motor is to be designed such that the value of this function is minimized. The efficiency is defined at 0.8 N_{max} and 12 kW shaft output. Excitation for this point of operation will be the optimal efficiency voltage (probably less than 185 V rms). The corresponding slip frequency will be noted.

6. Efficiency and Power Factor

Efficiency and power factor are defined under "optimal conditions" where the excitation voltage is such that the

resulting slip frequency matches that associated with optimal efficiency at 0.8 N_{max} , 12 kW. Since excitation voltage is limited to 185 V rms, slip frequencies higher than optimal will prevail for some combinations of high torque and high speed. Efficiency and power factor are to be specified for at least five torque and five rpm values.

IV. EXPECTED RANGES OF PARAMETER VALUES

Based on JPL studies, the following ranges of parameters are expected for an optimized machine:

| | |
|---|------------------------|
| 1. Weight | 65 to 95 kg |
| 2. Frame Size | 10" to 12" |
| 3. Pole Number | 2 or 4 |
| 4. Maximum Speed (N_{max}) | 8,000 to 16,000 rpm |
| 5. Base Speed | 0.35 to 0.45 N_{max} |
| 6. Optimal Slip Frequency | 1 to 2 Hz |
| 7. Efficiency at 0.8 N_{max} , 12 kW | 92% to 95% |
| 8. Power Factor for 7. | 85% to 90% |

Induction Motor Specification

1. Input line voltage, maximum rms: 185 V
(will be varied as required for speed and torque control)
2. Power output:

| | |
|---|-------|
| 1 hr. (20% duty) at maximum speed (N_{max}) | 30 kW |
| 3 min. (30% duty) at 0.8 N_{max} | 60 kW |
| 3 min. (30% duty) at 0.1 N_{max} | 16 kW |
3. Speed, N_{max} , between 8,000-16,000 rpm
(to be selected by contractor)
4. Number of poles: two or four
(to be selected by contractor)
5. Weighting function F to be minimum:

$$F = \text{cost} + 10(\text{weight}) - 120(\text{efficiency})$$

where

 - cost is retail cost in \$
 - weight is in kg
 - efficiency is in % measured at 0.8 N_{max} , 12 kW
shaft power with optimal voltage excitation
6. Construction: totally enclosed.
7. Cooling: convection air, maximum ambient 40 C.
8. Life: 4000 hours at full load.

In presenting the quotation the bidder shall:

Describe the selected design.

Specify the size and weight.

Specify the torque breakdown profile over the whole range of speed (either graphically or in tabular form).

Specify efficiency and power factor versus speed and torque for optimal excitation.

T. W. Macie

9/23/83

APPENDIX B**ALTERNATIVE INVERTER/INDUCTION MOTOR CONFIGURATIONS**

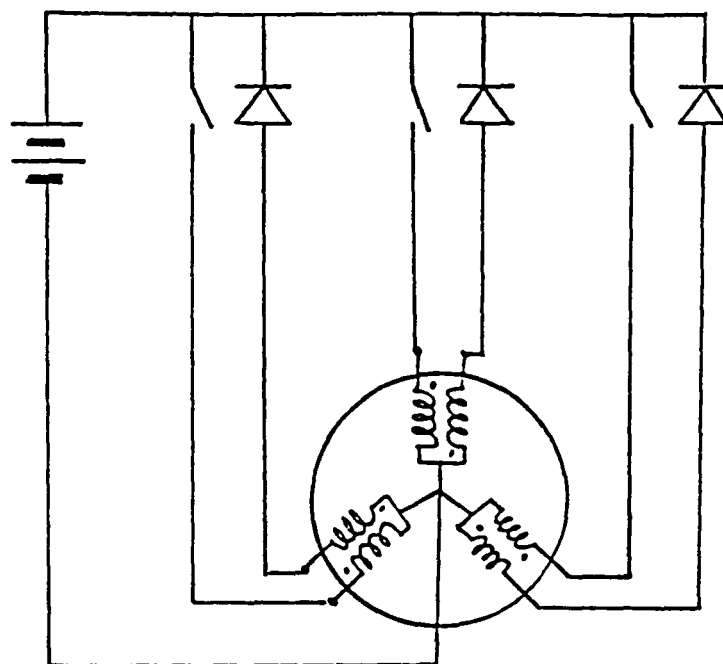


Fig. B-1-a Half-wave inverter driven three-phase
bifilar induction motor

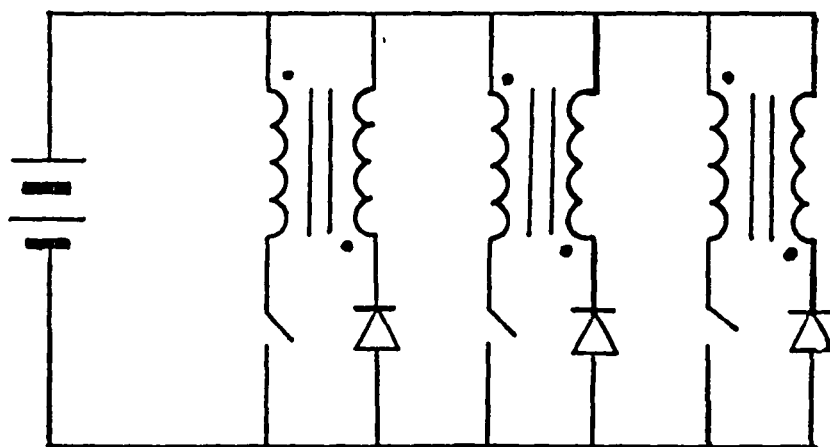


Fig. B-1-b Alternative arrangement for half-wave inverter
driven three-phase motor

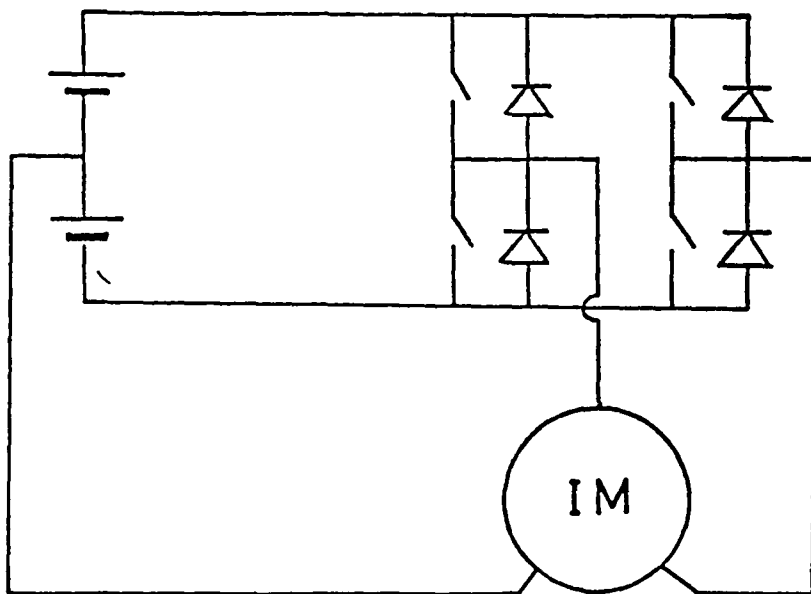


Fig. B-2 Four-switch inverter driven three-phase induction motor

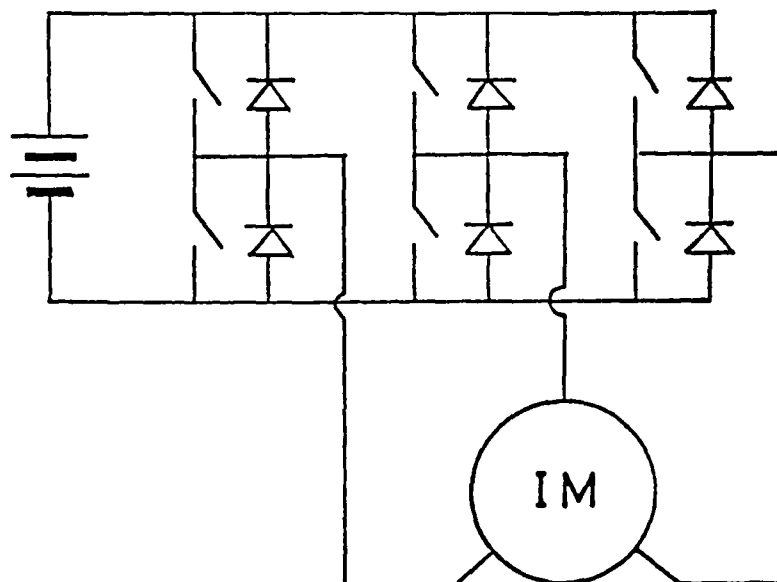


Fig. B-3 Three-phase bridge inverter driven induction motor

APPENDIX C**IDEALIZED COMPARISONS OF TWO-PHASE
AND THREE-PHASE INVERTERS**

The two-phase inverter circuit shown in Fig. 2 and the three-phase arrangement in Fig. B-3 are used for these comparisons.

Assuming Equal DC Power to a Resistive Load

Two-phase

For this situation, both the load current and load voltage are assumed to be square waves as shown in Fig. C1. This would be the case if the motor center-tapped windings in Fig. 2 were the primary windings of two ideal transformers with a purely resistive load on each secondary.

Let

$$\begin{aligned} V_{2\phi} &\triangleq \text{rms volts/phase on each half of center-tapped} \\ &\quad \text{winding} \\ &= V_{DC} \end{aligned}$$

and

$$I_{2\phi} \triangleq \text{rms current/phase through the resistive load}$$

Assuming that the ideal transformers each have unity turns ratio from half of the primary winding to the secondary,

$$I_{2\phi} = I_{DC}/2$$

The current I_{DC} is the dc source current. Since the two pairs of switches in Fig. 2 are operated with 90° phase displacement, the total dc source current is always equal to twice the current in one phase. Basically, I_{DC} divides equally at all instants, with $I_{DC}/2$ flowing through one half of each transformer primary.

Thus

$$V_{T,P} \triangleq \text{switch peak voltage}$$

$$= 2V_{DC}$$

and

$$I_{T,P} \triangleq \text{switch peak current}$$

$$= I_{DC}/2$$

and let

$$TR_{2\phi} \triangleq \text{total switch rating } V_{T,P} I_{T,P} \text{ for two-phase}$$

$$= (4) (2V_{DC}) (I_{DC}/2)$$

$$= 4V_{DC} I_{DC}$$

Three-phase

In this case, the circuit of Fig. B-3 is considered, except with the motor winding replaced with a wye connected balanced set of load resistors. With a current I_{DC} flowing from the dc source in Fig. B-3 the line-to-neutral load voltage and current are as shown in Fig. C-1. In this case

$$V_{T,P} = V_{DC}$$

$$I_{T,P} = I_{DC}$$

and let

$$TR_{3\phi} \triangleq \text{total switch rating } V_{T,P} I_{T,P} \text{ for three-phase}$$

$$= (6) (V_{DC}) (I_{DC})$$

$$= 6V_{DC} I_{DC}$$

Therefore, the total switch rating for two-phase is 2/3 of that for three-phase.

Note: This can be checked in another very simple manner as follows. If the power delivered to the resistive loads is the same for the two-phase and the three-phase circuits, then the power taken from the dc supply must be the same in each case.

$$P_{DC} = V_{DC} I_{DC}$$

Also

$$I_{T,P,2\phi} = I_{DC}/2$$

and

$$I_{T,P,3\phi} = I_{DC}$$

Therefore

$$TR_{2\phi} = (4) (2V_{DC}) (I_{DC}/2) = 4V_{DC} I_{DC}$$

$$TR_{3\phi} = (6) (V_{DC}) (I_{DC}) = 6V_{DC} I_{DC}$$

and

$$TR_{2\phi} = 2/3 TR_{3\phi}$$

Assuming Equal Fundamental Power to a Resistive Load

Two-phase

Let

$$V_{1,2\phi} \triangleq \text{amplitude of fundamental voltage/phase}$$

$$\begin{aligned}
 &= \frac{1}{\pi} \int_0^{2\pi} v_{2\phi} \sin \omega t d(\omega t) \\
 &= \frac{2V_{DC}}{\pi} \int_0^{\pi} \sin \omega t d(\omega t) \\
 &= \frac{4V_{DC}}{\pi}
 \end{aligned}$$

and similarly for the current

$$I_{1,2\phi} = \frac{4I_{T,P,2\phi}}{\pi}$$

Then

$P_{1,2\phi} \triangleq$ total fundamental power to load

$$\begin{aligned}
 &= (2) \left(\frac{4V_{DC}}{\pi\sqrt{2}} \right) \left(\frac{4I_{T,P,2\phi}}{\pi\sqrt{2}} \right) \\
 &= \frac{16}{\pi^2} V_{DC} I_{T,P,2\phi}
 \end{aligned}$$

Three-phase

Let

$v_{1,3\phi} \triangleq$ amplitude of fundamental voltage/phase

$$\begin{aligned}
 &= \frac{1}{\pi} \int_0^{2\pi} v_{3\phi} \sin \omega t d(\omega t) \\
 &= \frac{2V_{DC}}{\pi} \left[\int_0^{\pi/3} \frac{1}{3} \sin \omega t d(\omega t) + \int_{\pi/3}^{2\pi/3} \frac{2}{3} \sin \omega t d(\omega t) \right. \\
 &\quad \left. + \int_{2\pi/3}^{\pi} \frac{1}{3} \sin \omega t d(\omega t) \right] \\
 &= \frac{2V_{DC}}{\pi}
 \end{aligned}$$

and for the current

$$\begin{aligned}
 I_{1,3\phi} &\triangleq \frac{1}{\pi} \int_0^{2\pi} i_{3\phi} \sin \omega t d(\omega t) \\
 &= \frac{2I_{PT,3\phi}}{\pi} \left[\int_0^{\pi/3} \frac{1}{2} \sin \omega t d(\omega t) + \int_{\pi/3}^{2\pi/3} \sin \omega t d(\omega t) \right. \\
 &\quad \left. + \int_{2\pi/3}^{\pi} \frac{1}{2} \sin \omega t d(\omega t) \right] \\
 &= \frac{3I_{T,P,3\phi}}{\pi}
 \end{aligned}$$

Then

$$\begin{aligned}
 P_{1,3\phi} &\triangleq \text{total fundamental load power} \\
 &= (3) \left(\frac{2V_{DC}}{\pi\sqrt{2}} \right) \left(\frac{3I_{T,P,3\phi}}{\pi\sqrt{2}} \right) \\
 &= \frac{9V_{DC}I_{T,P,3\phi}}{\pi^2}
 \end{aligned}$$

For equal load power

$$P_{1,2\phi} = P_{1,3\phi}$$

$$\frac{16}{\pi^2} V_{DC} I_{T,P,2\phi} = \frac{9V_{DC}I_{T,P,3\phi}}{\pi^2}$$

or

$$I_{T,P,2\phi} = \frac{9}{16} I_{T,P,3\phi}$$

Finally, the total switch ratings $TR_{2\phi}$ and $TR_{3\phi}$ are

$$TR_{2\phi} = (4) (2V_{DC}) (I_{T,P,2\phi})$$

$$TR_{3\phi} = (6) (V_{DC}) (I_{T,P,3\phi})$$

Then

$$\begin{aligned} TR_{2\phi} &= (4) (2V_{DC}) \left(\frac{9}{16} I_{T,P,3\phi}\right) \\ &= \frac{9}{2} V_{DC} I_{T,P,3\phi} \end{aligned}$$

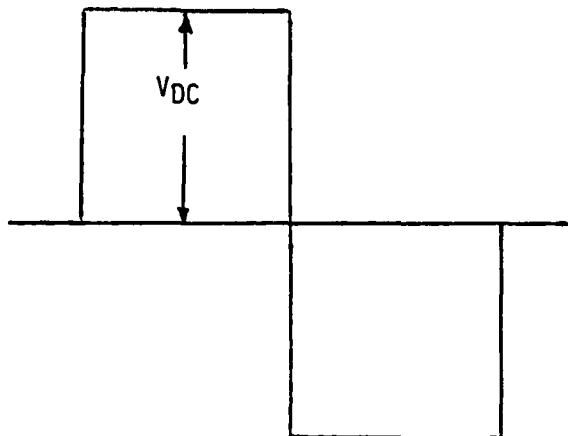
and

$$TR_{3\phi} = 6V_{DC} I_{T,P,3\phi}$$

Thus

$$TR_{2\phi} = \frac{3}{4} TR_{3\phi}$$

Two-phase load
voltage and
current



Three-phase line-to-neutral
load voltage and current

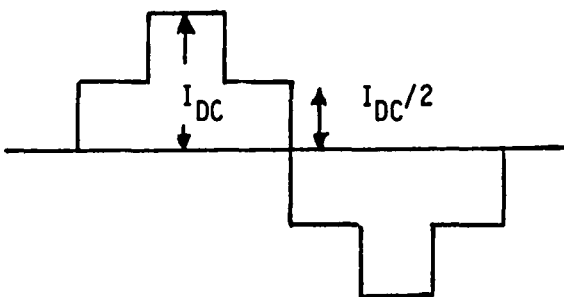
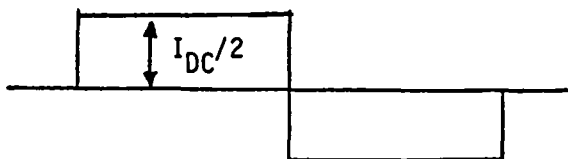
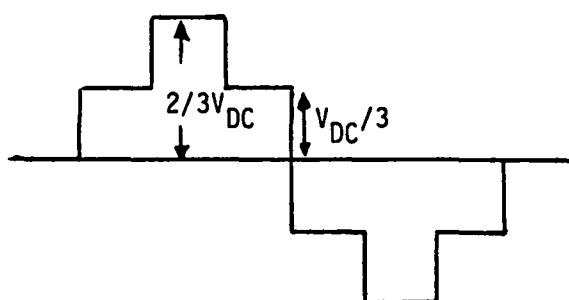


Fig. C-1 Load voltages and currents for Fig. 2 and Fig. B-3 respectively
with motors replaced by resistive load

Note: Two ideal transformers are used in Fig. 2, with unity turns ratio from each half of their primaries to their secondaries connected to resistive loads. A wye-connected set of balanced load resistors replaces the motor in Fig. B-3.

APPENDIX D**DETAILED DESIGN OF TWO-PHASE BIFILAR INDUCTION MACHINE**

MAIN DATA OF UMC TWO-PHASE BIFILAR INDUCTION MOTOR

| | |
|---|---|
| 1. Output | $P_m = 30 \text{ kW}$ |
| 2. Number of phases | $m = 2$ |
| 3. Frequency | $f = 80 \text{ Hz}$ |
| 4. Equivalent voltage of battery | $V_D = 189 \text{ V}$ |
| 5. Phase current | $I_{ph} = 110.2 \text{ A}$ |
| 6. Efficiency | $\eta = 0.91$ |
| 7. Power factor | $\cos \phi = 0.88$ |
| 8. Number of poles ($p \triangleq$ pole pairs) | $2p = 2$ |
| 9. External diameter of stator | $D_o = 29.21 \text{ cm (11.5 in)}$ |
| 10. Internal diameter of stator | $D = 14.6 \text{ cm (5.75 in)}$ |
| 11. Length of stack | $L = 16 \text{ cm (6.3 in)}$ |
| 12. Length of air gap | $l_g = 0.03 \text{ cm (0.0118 in)}$ |
| 13. Number of slots of stator | $Z_1 = 24$ |
| 14. Number of slots of rotor | $Z_2 = 20$ |
| 15. Turns per coil | $Z_{S1} = 11$ |
| 16. Number of coils | $n_c = 12$ |
| 17. Series turns per phase | $T_{ph} = 33$ |
| 18. Number of branches | $a_p = 2$ |
| 19. Resistance of stator | $R_s = 0.0274 \Omega$ |
| 20. Resistance of rotor | $R'_r = 0.0213 \Omega$ |
| 21. Leakage inductance of stator | $L_{1s} = 2.5 \times 10^{-4} \text{ H}$ |
| 22. Leakage inductance of rotor | $L_{1r} = 2.7 \times 10^{-4} \text{ H}$ |
| 23. Magnetizing inductance | $L_m = 13.86 \times 10^{-3} \text{ H}$ |

UMC TWO-PHASE BIFILAR MOTOR

1. Given data

$$P_m = 30 \text{ kW}$$

$m = 2$ (number of phases)

$f = 80 \text{ Hz}$ (basic frequency)

$P = 1$ (pair of poles)

$V_D = 189 \text{ V}$ (equivalent base battery voltage)

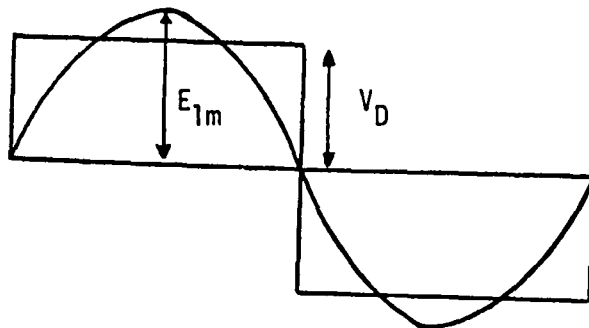


Fig. D-1

$$E_{1m} = \frac{4}{\pi} V_D = \frac{4}{\pi} \times 189 \text{ V} = 241 \text{ V}$$

$$E_1(\text{rms}) = \frac{4}{\sqrt{2}\pi} \times 189 \text{ V} = 170 \text{ V}$$

2. External diameter of stator D_o

choose $D_o = 29.21 \text{ cm} = 11.5 \text{ in}$

3. Internal diameter of stator D

let $D = 14.6 \text{ cm} = 5.75 \text{ in}$

4. Specific magnetic loading $\bar{B} = \frac{2P\phi_m}{\pi DL}$

assumed $\bar{B} = 0.45 \text{ wb/m}^2$

$\bar{B} = 0.3 - 0.6 \text{ wb/m}^2$ for common motor

5. Slots of stator $Z_1 = 24$

6. Slots of rotor Z_2

$$Z_2 = Z_1 + 4P = 20$$

7. Assumed Efficiency $\eta = 0.91$

Power factor $\cos \phi = 0.88$

8. The kVA rating S

$$S = \frac{P_m}{\cos \phi} = \frac{30}{0.91 \times 0.88} = 37.46 \text{ kVA}$$

9. The motor constant G

$$G = \frac{S}{D^2 L n} = 11 \text{ kw} \overline{B} \times ac \times 10^{-3} = 11 \times 0.9029 \times 0.45 \times 30,000 \times 10^{-3} = 134$$

where L is length of stack

k_w is winding factor

ac is specific electric loading

n is synchronous speed (rps)

$$k_w = k_p \times k_d \quad k_p = 1 \text{ (single layer winding)}$$

$$k_d = \frac{\sin (\pi/2m)}{n' \sin (\pi/2mn')} = \frac{\sin (\pi/2 \times 2)}{6 \times \sin (\pi/2 \times 2 \times 6)} = 0.9029$$

$$n = \frac{Z_1}{2pm} = \frac{24}{2 \times 2} = 6 \text{ (number of slots per phase per pole)}$$

$$n = \frac{f}{p} = \frac{80}{1} = 80 \text{ rps}$$

$$ac = 2m T_{ph} I_{ph} / D = 5000 \times 45,000 \text{ Amp-cond/m}$$

$$\text{Let } ac = 30,000$$

$$10. D^2 L = \frac{S}{Gn} = \frac{37.46}{134 \times 80} = 3.4944 \times 10^{-3} \text{ m}^3$$

$$L = \frac{D^2 L}{D^2} = \frac{3.4944 \times 10^{-3}}{0.146^2} = 0.164 \text{ m}$$

Let $L = 0.16 \text{ m} = 16 \text{ cm} = 6.3 \text{ in}$

11. The flux per pole ϕ_m

$$\phi_m = \bar{B} \times \frac{\pi D}{2P} \times L = 0.45 \times \frac{\pi \times 0.146}{2} \times 0.16 = 0.0165 \text{ wb}$$

12. The turns per phase (in series) T_{ph}

$$T_{ph} = \frac{E_1}{4.44 \text{ kw f}_m} = \frac{170}{4.44 \times 0.9029 \times 80 \times 0.0165} = 32.1$$

choose $T_{ph} = 33$

13. The real flux per pole ϕ_m

$$\phi_m = \frac{E_1}{4.44 \text{ kw f}_m T_{ph}} = \frac{170}{4.44 \times 0.9029 \times 80 \times 33} = 0.016 \text{ wb}$$

14. The number of coils n_c

$$n_c = \frac{Z_1}{2} = \frac{24}{2} = 12 \text{ (single layer)}$$

The number of branches a_p

$$a_p = 2$$

15. The coils per phase in series n_{ph}

$$n_{ph} = \frac{n_c}{a_p \times m} = \frac{12}{2 \times 2} = 3$$

16. The turns of coil Z_{s1}

$$Z_{s1} = \frac{T_{ph}}{n_{ph}} = \frac{33}{3} = 11$$

$$17. \bar{B} = \frac{\phi_m}{\frac{\pi D L}{2P}} = \frac{0.016}{\frac{\pi \times 0.146 \times 0.16}{2}} = 0.436 \text{ wb/m}^2$$

18. Phase current I_{ph}

$$I_{ph} = \frac{s \times 10^3}{m \times E_1} = \frac{37.46 \times 10^3}{2 \times 170} = 110.2 \text{ A}$$

$$ac = 2m T_{ph} \times I_{ph} / \pi D = 2 \times 2 \times 33 \times 110.2 / \pi \times 0.146 = 31714 \text{ Amp-cond/m}$$

19. The density of current of stator winding δ_1

$$\text{choose } \delta_1 = 5 \text{ A/mm}^2$$

20. The section of coil S_c

$$S_c = \frac{I_{ph}}{a_{p1}} = \frac{110.2}{2 \times 5} = 11.02 \text{ mm}^2$$

choose 3 x #13 wire and 2 x #15 wire

$$\#13 \text{ wire } d = 1.83 \text{ mm } A_d = 2.63 \text{ mm}^2$$

$$\text{insulated } d' = 1.83 + 0.18 = 2.01 \text{ mm}$$

$$\#15 \text{ wire } d = 1.45 \text{ mm } A_d = 1.65 \text{ mm}^2$$

$$d' = 1.63 \text{ mm}$$

$$S_c = 3 \times 2.63 + 2 \times 1.65 = 11.19 \text{ mm}^2$$

21. The number of wires in parallel n_p

$$n_p = 3 + 2 = 5$$

22. The total number of wires in a slot n_s

$$n_s = 2 \times n_p \times Z_{s1} = 2 \times 5 \times 11 = 110$$

The first number 2 on the right side represents the bifilar winding.

23. The real density of current δ_1

$$\delta_1 = \frac{I_{ph}}{a_p s_c} = \frac{110.2}{2 \times 11.19} = 4.92 \text{ A/mm}^2$$

24. Length of mean conductor

$$\begin{aligned} L_{mc} &= L + 1.1Y + 3 \text{ (cm)} \\ &= 16 + 1.1Y + 3 = 16 + 1.1 \times 22.93 + 3 = 44.2 \text{ cm} \end{aligned}$$

$$\text{where } Y = \frac{\pi D}{2P} = \frac{\pi \times 14.6}{2} = 22.93 \text{ cm}$$

We use concentric coils: 1-8

1-10 coil spans
1-12

25. Length per phase L_{ph}

$$L_{ph} = T_{ph} \times 2 \times L_{mc} = 33 \times 2 \times 0.442 = 29.17 \text{ m}$$

26. Resistance per phase R_s (75°C)

$$R_s = P_{75} \times L_{ph}/S_c \times a_p = 0.021 \times 29.17/11.19 \times 2 = 0.0274 \Omega$$

27. Reduced rotor current I'_2

$$I'_2 \approx I_{ph} \cos \phi = 110.2 \times 0.88 = 97 \text{ A}$$

28. The tooth pitch of rotor τ_{s2}

$$\tau_{s2} = \frac{\pi D_2}{Z_2} = \frac{\pi \times 14.54}{20} = 2.284 \text{ cm}$$

where diameter of rotor $D_2 = D - 2 \times l_g = 14.6 - 2 \times 0.03 = 14.54 \text{ cm}$

$l_g = 0.3 \text{ mm}$ (length of air gap)

29. Number of slots per pole S_2 (rotor)

$$S_2 = \frac{Z_2}{2p} = \frac{20}{2} = 10$$

30. The current of the bar I_b

$$I_b = \frac{2m k_w T_{ph}}{Z_2} I_2' = \frac{2 \times 2 \times 0.9029 \times 33}{20} \times 97 = 578 \text{ A}$$

31. The current of the end ring I_c

$$I_c = \frac{I_b S_2}{\pi} = 578 \times 10/\pi = 1840 \text{ A}$$

32. Casting aluminum alloy for rotor cage

$$PA1 (75^\circ\text{C}) = 0.04 \Omega \text{ mm}^2/\text{m}$$

(The value can be in negotiation with manufacturer)

33. Let $\delta_{2b} = 3.2 \text{ A/mm}^2$

34. The section of each bar a_2

$$a_2 = \frac{I_b}{\delta_{2b}} = \frac{578}{3.2} = 180.6 \text{ mm}^2$$

35. The resistance per bar λ_b

$$\lambda_b = P_{A1} \times L/a_2 = 0.04 \times 0.16/180.6 = 3.54 \times 10^{-5} \Omega$$

36. The section of end ring a_{2c}

Let $\delta_{2c} = 2.8 \text{ A/mm}^2$

$$a_{2c} = \frac{I_c}{\delta_{2c}} = \frac{1840}{2.8} = 657 \text{ mm}^2$$

37. The resistance of ring r_c

$$r_c = \rho_{A1} \times \pi \times D_r / a_{2c} = 0.04 \times \pi \times 0.126 / 657 = 2.41 \times 10^{-5} \Omega$$

where $D_r = 0.126$ m (the mean diameter of ring)

38. The reduced resistance of rotor r'_2

$$r'_2 = \frac{Z_2(r_b + 2r_c s_2^2 / \pi^2 Z_2) I_b^2}{m I'_2^2} = \frac{20 (3.54 + 2 \times 2.41 \times 10^2 / \pi^2 \times 20) \times 578^2 \times 10^{-5}}{2 \times 97^2}$$

$$= 0.02124 \Omega \approx 0.0213 \Omega$$

39. Carter's factor k_c

$$k_c = k_{c1} \cdot k_{c2}$$

$$k_{c1} = \frac{\tau_{S1}}{\tau_{S1} - b_0 + 2 l_g \times l_n [1 + \frac{b_0}{2 l_g}]}$$

$$= \frac{19.1}{19.1 - 3.5 + 2 \times 0.3 \times l_n [1 + \frac{3.5}{2 \times 0.3}]} = 1.14$$

$$\text{where } \tau_{S1} = \frac{\pi D}{Z_1} = \frac{\pi \times 146}{24} = 19.1 \text{ mm}$$

(tooth pitch of the stator)

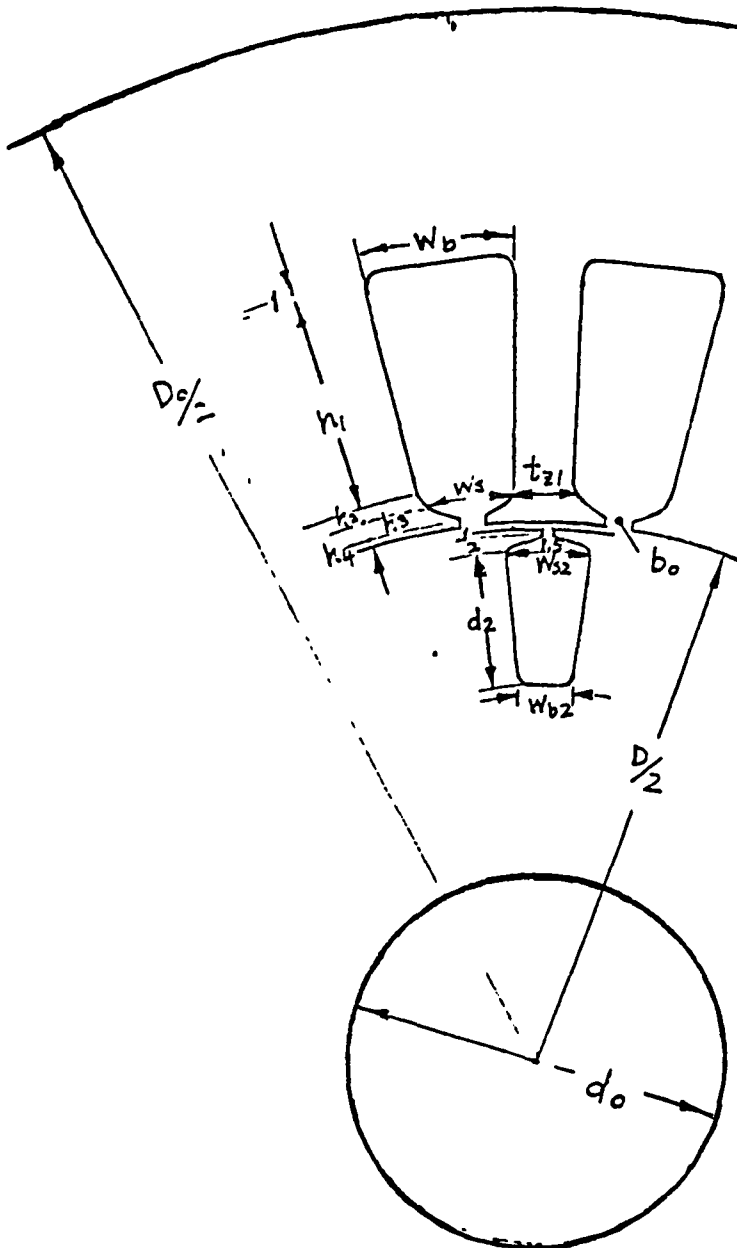
$b_0 = 3.5$ mm (width of slot opening - refer to Fig. 1)

$$k_{c2} = \frac{\tau_{S2}}{\tau_{S2} - b_{02} 2 l_g \times l_n [1 + \frac{b_{02}}{2 l_g}]}$$

$$= \frac{2.284 \times 10}{22.84 - 1.5 + 2 \times 0.3 \times l_n [1 + \frac{1.5}{2 \times 0.3}]} = 1.034$$

$$k_c = k_{c1} \cdot k_{c2} = 1.14 \times 1.034 = 1.18$$

Effective length of air gap l'_g



$$W_b = \frac{[D+2(h_1+h_2+h_3+h_4)+2]\pi}{Z_1} - t_{Z1} = \frac{(146+2 \times 36+2)\pi}{24} - 7.8 = 21 \text{ mm}$$

$$W_{S2} = \frac{[D - 2\{g - 2x_3\}] \pi}{Z_2} - t_{Z2} = \frac{(146 - 2 \times 0.3 - 6) \pi}{20} - 9.2 = 12.7 \text{ mm}$$

$$d_2 = 17 \text{ mm}$$

$$w_{b2} = \frac{(D - 21g - 2x3 - 2xd_2) \pi}{z_2} - t_{z2} = \frac{(146 - 2x0.3 - 6 - 2x17) \pi}{20} - 9.2 = 7.356 \text{ mm}$$

$$\begin{aligned}
 h_1 &= 31 \text{ mm} \\
 h_2 &= 2 \text{ mm} \\
 h_3 &= 2 \text{ mm} \\
 h_4 &= 1 \text{ mm} \\
 b_o &= 3.5 \text{ mm} \\
 t_{Z1} &= 7.8 \text{ mm} \\
 t_{Z2} &= 9.2 \text{ mm}
 \end{aligned}$$

$$W_S + t_{Z1} = \frac{[D+2(h_3+h_4)]\pi}{z_1}$$

$$= \frac{[146 + 2(2+1)]}{24}\pi$$

$$= 19.9 \text{ mm}$$

$$W_s = 19.9 - 7.8 = 12.1 \text{ mm}$$

Fig. D-2

$$l_g' = k_c l_g = 1.18 \times 0.3 = 0.354 \text{ mm}$$

40. The area of air gap A_g

$$A_g = \frac{\pi D}{2p} L = \frac{2 \times 0.146}{2} \times 0.16 = 0.0367 \text{ m}^2$$

41. Modified density of flux of air gap B_g

$$B_g = 1.36 \times \frac{\phi}{m} / A_g = 1.36 \times 0.016 / 0.0367 = 0.593 \text{ wb/m}^2$$

where 1.36 is for considering saturation in both teeth of stator and rotor

42. Area of teeth per pole of stator A_{z1}

$$\begin{aligned} A_{z1} &= t_{z1} \times L \times 0.92 \times S_1 = 0.78 \times 16 \times 0.92 \times 12 \\ &= 138 \text{ cm}^2 = 0.0138 \text{ m}^2 \end{aligned}$$

$$\text{where } S_1 = \frac{Z_1}{2p} = \frac{24}{2} = 12$$

43. Modified density of flux in teeth B_{z1}

$$B_{z1} = 1.36 \times \frac{\phi}{m} / A_{z1} = 1.36 \times 0.016 / 0.0138 = 1.577 \text{ wb/m}^2$$

44. Length of tooth l_{z1}

$$l_{z1} = k_1 + k_2 = 31 + 2 = 33 \text{ mm} = 0.033 \text{ m}$$

45. Height of core h_{c1} (stator)

$$\begin{aligned} h_{c1} &= \frac{D_o - [D + 2(h_1 + h_2 + h_3 + h_4)]}{2} \\ &= 29.21 - \frac{[14.6 + 2(3.1 + 0.2 + 0.2 + 0.1)]}{2} = 3.705 \text{ cm} \\ &= 0.03705 \text{ m} \end{aligned}$$

46. Area of core A_{c1} (stator)

$$A_{c1} = h_{c1} \times L \times 0.92 = 0.03705 \times 0.16 \times 0.92 = 0.005454 \text{ m}^2$$

47. Maximum density of flux through the core B_{c1}

$$B_{c1} = \frac{\phi_m}{2A_{c1}} = \frac{0.016}{2 \times 0.005454} = 1.4668 \text{ wb/m}^2$$

48. Length of core per half pole l_{c1}

$$l_{c1} = \frac{(D_0 - h_{c1})\pi}{4p} = \frac{(29.21 - 3.705)\pi}{4} = 20.03 \text{ cm}$$

49. Effective length of core l'_{c1}

$$l'_{c1} = \zeta l_{c1} = 0.38 \times 20.03 = 7.6 \text{ cm} = 0.076 \text{ m}$$

50. $\zeta = 0.38$ considering the densities of flux along the length of core are not equal

51. The fill coefficient of slot k_f

$$k_f = \frac{\frac{n_s d^2}{w_s + w_b} \times (h_1 + h_2)}{\frac{12.1 + 21}{2} \times (31 + 2)} = \frac{2 \times 11 \times (3 \times 2.01^2 + 2 \times 1.63^2)}{12.1 + 21 \times (31 + 2)} = 0.702$$

$k_f = 0.702 < 0.75$ (This means that bifilar winding can be inserted in slots without difficulty.)

52. Area of rotor teeth per pole A_{Z2}

$$A_{Z2} = t_{Z2} \times L \times 0.92 \times s_2 = 0.92 \times 16 \times 0.92 \times 10 = 135.4 \text{ cm} = 0.01354 \text{ m}^2$$

53. Modified density of flux in rotor teeth B_{Z2}

$$B_{Z2} = \frac{1.36\phi_m}{A_{Z2}} = \frac{1.36 \times 0.016}{0.01354} = 1.607 \text{ wb/m}^2$$

54. Length of rotor tooth l_{Z2}

$$l_{Z2} \approx d_2 = 17 \text{ mm} = 0.017 \text{ m}$$

55. The height of rotor core h_{c2}

$$\begin{aligned} h_{c2} &= \frac{D - 2 l_g - 2 d_2 - 2 \times 2 - d_o}{2} + \frac{1}{6} \times d_o \\ &= \frac{146 - 2 \times 0.3 - 2 \times 17 - 4 - 45}{2} + \frac{1}{6} \times 45 \\ &= 38.7 \text{ mm} \end{aligned}$$

where $d_o = 45 \text{ mm}$ (d_o is diameter of the shaft)

56. The maximum density of flux through the rotor core B_{c2}

$$B_{c2} = \frac{\phi_m}{2A_{c2}} = \frac{0.016}{2 \times 0.0057} = 1.404 \text{ wb/m}^2$$

57. Area of rotor core A_{c2}

$$A_{c2} = h_{c2} \times L \times 0.92 = 0.387 \times 0.16 \times 0.92 = 0.0057 \text{ m}^2$$

According to the B-H curve on Fig.D-3(Sec. 4-264, Fig. 4-31, Standard Handbook for Electrical Engineers, Tenth Ed., Donald G. Fink and John M. Carroll, McGraw-Hill), we get

$$B_{Z1} = 1.577 \text{ wb/m}^2 = 15770 \text{ gauss}$$

$$H_{Z1} = 32 \text{ oe} = 32 \times 79.577 = 2546 \text{ A/m}$$

$$B_{c1} = 1.4668 \text{ wb/m}^2 = 14668 \text{ gauss}$$

$$H_{c1} = 17 \text{ oe} = 17 \times 79.577 = 1352 \text{ A/m}$$

$$B_{Z2} = 1.607 \text{ wb/m}^2 = 16070 \text{ gauss}$$

$$H_{Z2} = 40 \text{ oe} = 40 \times 79.577 = 3183 \text{ A/m}$$

$$B_{c2} = 1.404 \text{ wb/m}^2 = 14040 \text{ gauss}$$

$$H_{c2} = 13 \text{ oe} = 13 \times 79.577 = 1034 \text{ A/m}$$

MAGNETIC MATERIALS

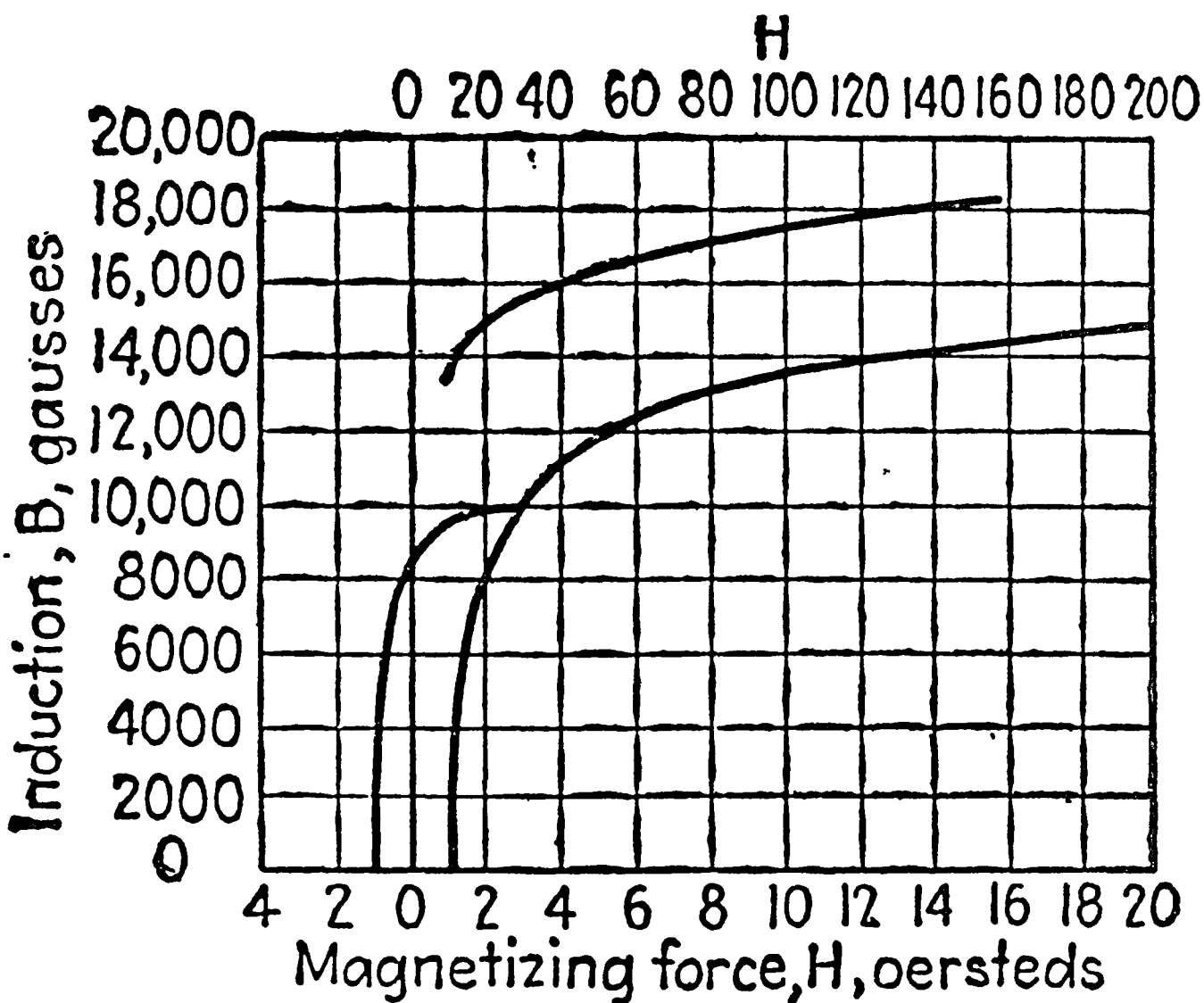


Fig. D-3 Normal-induction curve and hysteresis loop of electrical sheet, No. 22 gage.

58. Magnetizing force AT

$$AT = AT_g + AT_{Z1} + AT_{c1} + AT_{Z2} + AT_{c2}$$

59. Magnetizing force of air gap AT_g

$$AT_g = 8 \times 10^5 \times l_g' \times B_g = 8 \times 10^5 \times 0.000354 \times 0.593 = 168 \text{ A}$$

60. Magnetizing force of stator tooth AT_{Z1}

$$AT_{Z1} = H_{Z1} \times l_{Z1}' = 2546 \times 0.033 = 84 \text{ A}$$

61. Magnetizing force of stator core AT_{c1}

$$AT_{c1} = H_{c1} \times l_{c1}' = 1352 \times 0.076 = 102.7 \text{ A}$$

62. Magnetizing force of rotor tooth AT_{Z2}

$$AT_{Z2} = H_{Z2} \times l_{Z2}' = 3183 \times 0.017 = 54 \text{ A}$$

63. Magnetizing force of rotor core AT_{c2}

$$AT_{c2} = H_{c2} l_{c2}' = 1034 \times 0.0152 = 16 \text{ A}$$

where $l_{c2}' = \zeta l_{c2} = 0.38 \times 4 = 1.52 \text{ cm} = 0.0152 \text{ m}$

$$l_{c2}' = \frac{D - 2 l_g - 2 d_2 - 2 h_{c2}'}{4p} \approx 4 \text{ cm}$$

$$AT = 168 + 84 + 102.7 + 54 + 16 = 424.7 \text{ A}$$

64. Magnetizing current I_{or}

$$I_{or} = p \times 2AT / 1.17 \times kw \times T_{ph} = 2 \times 424.7 / 1.17 \times 0.9029 \times 33 = 24.4 \text{ A}$$

65. Magnetizing reactance X_m

$$X_m \approx \frac{E_1}{I_{\text{or}}} = \frac{17.0}{24.4} = 6.967 \Omega$$

66. Magnetizing inductance L_m

$$L_m = \frac{X_m}{2\pi f} = \frac{6.967}{2\pi \times 80} = 13.86 \times 10^{-3} \text{ H}$$

67. The specific slot permeance of stator λ_{s1}

$$\begin{aligned} \lambda_{s1} &= \frac{h_2}{w_2 - w_s} \ln \left(\frac{w_2}{w_s} \right) + \frac{h_3}{w_s - b_o} \ln \left(\frac{w_s}{b_o} \right) + \frac{h_4}{b_o} + \frac{h_1+1}{w_b} \left[\frac{\beta^2 - \frac{\beta^4}{4} - \ln \beta - \frac{3}{4}}{(1-\beta)(1-\beta^2)^2} \right] \\ &= \frac{2}{12.62-12.1} \ln \left(\frac{12.62}{12.1} \right) + \frac{2}{12.1-3.5} \ln \left(\frac{12.1}{3.5} \right) + \frac{1}{3.5} + \\ &\quad \frac{32}{21} \left[\frac{0.6^2 - \frac{0.6^4}{4} - \ln 0.6 - \frac{3}{4}}{(1-0.6)(1-0.6^2)^2} \right] = 0.162 + 0.288 + 0.286 + 0.822 = 1.558 \end{aligned}$$

$$\text{where } w_2 = \frac{[146 + 2(h_4 + h_3 + h_2)] \pi}{24} - 7.8 = 12.62 \text{ mm}$$

$$w_s = 12.1 \text{ mm}$$

$$h_2 = 2 \text{ mm}$$

$$h_3 = 2 \text{ mm}$$

$$h_4 = 1 \text{ mm}$$

$$b_o = 3.5 \text{ mm}$$

$$\beta = \frac{w_2}{w_b} = \frac{12.62}{21} = 0.6 \quad (\text{refer to Fig. 1})$$

68. The specific slot permeance of rotor λ_{s2}'

$$\lambda_{s2} = \frac{h_3'}{W_{s2}-1.5} \ln \left(\frac{W_{s2}}{1.5} \right) + \frac{1}{1.5} + \frac{d_2}{W_{b2}} \left[\frac{\beta^2 - \frac{\beta^4}{4} - \ln \beta - \frac{3}{4}}{(1-\beta)(1-\beta^2)^2} \right] = \frac{2}{12.7-1.5} \times$$

$$\ln \left(\frac{12.7}{1.5} \right) + \frac{1}{1.5} + \frac{17}{7.356} \left[\frac{1.726^2 - \frac{1.726^4}{4} - \ln 1.726 - \frac{3}{4}}{(1-1.726)(1-1.726^2)^2} \right] = 1.49$$

where $W_{s2} = 12.7 \text{ mm}$

$W_{b2} = 7.356 \text{ mm}$

$d_2 = 17 \text{ mm}$

$$\beta = \frac{W_{s2}}{W_{b2}} = 1.726$$

69. The reduced value λ'_{s2}

$$\lambda'_{s2} = \frac{k_w^2 z_1}{z_2} \lambda_{s2} = \frac{0.9029^2 \times 24}{20} \times 1.49 = 1.46$$

70. The slot leakage reactance of stator x_{s1}

$$x_{s1} = \frac{8f_m L T_{ph}^2}{10^7 z_1} \lambda_{s1} = \frac{8 \times 80 \times 2 \times 6.3 \times 33^2}{10^7 \times 24} \times 1.558 = 0.057 \Omega$$

where L is in inches

71. The slot leakage reactance of rotor x_{s2}

$$x_{s2} = \frac{8f_m L T_{ph}^2}{10^7 z_1} \lambda'_{s2} = \frac{8 \times 80 \times 2 \times 6.3 \times 33^2}{10^7 \times 24} \times 1.46 = 0.535 \Omega$$

72. The end leakage reactance x_e

$$x_e = \frac{4fm D T_{ph}^2}{10^7 (2p)^2} = \frac{4 \times 80 \times 2 \times 5.75 \times 33^2}{10^7 (2)^2} = 0.1 \Omega$$

where $D = 14.6 \text{ cm} = 5.75 \text{ in}$

73. Differential leakage reactance (sum of the zigzag and belt leakage reactance)

$$x_d = \frac{5}{6} x_m \left(\frac{\frac{6k_{c1}}{5} - 1 + \frac{5\sigma^2}{5}}{S_1^2} + \frac{\frac{\sigma k_{c2}}{5} - 1}{S_2^2} \right) = \frac{5}{6} \times 6.967 \times \left(\frac{\frac{6 \times 1.14}{5} - 1 + \frac{5(0.5)^2}{5}}{12^2} \right. \\ \left. + \frac{0.5 \times 1.034 - 1}{5 \times 10^2} \right) = 0.0516$$

$\sigma = 0.5$ is the angle of rotor slot skew, as a fraction of one stator slot pitch

74. The leakage reactance of stator x_1

$$x_1 = x_{s1} + \frac{z_2}{z_1 + z_2} (x_e + x_d) = 0.057 + \frac{20}{24 + 20} (0.1 + 0.0516) = 0.126 \Omega$$

75. The reduced leakage reactance of rotor x'_2

$$x'_2 = x_{s2} + \frac{z_1}{z_1 + z_2} (x_e + x_d) = 0.0535 + \frac{24}{24 + 20} (0.1 + 0.0516) = 0.136 \Omega$$

$$76. L_{1s} = \frac{x_1}{2\pi f} = \frac{0.126}{2 \times \pi \times 80} = 2.5 \times 10^{-4} \text{ H}$$

$$L_{1r} = \frac{x'_2}{2\pi f} = \frac{0.136}{2 \times \pi \times 80} = 2.7 \times 10^{-4} \text{ H}$$

$$f = 20 \text{ Hz} \quad V_D = 60 \text{ V}$$

$$R_s = 0.0274$$

$$R_r' = 0.0213$$

$$L_{1r} = 2.41 \times 10^{-4} \text{ H}$$

$$L_{1s} = 2.256 \times 10^{-4} \text{ H}$$

$$L_m = 6.51 \times 10^{-3} \text{ H}$$

$$I_{or} = 66 \text{ A} \\ (\text{rms})$$

$$I_{or} = \sqrt{2} \times 66 \\ (\text{peak}) \\ = 93 \text{ A}$$

$$f = 80 \text{ Hz} \quad V_D = 189 \text{ V}$$

$$R_s = 0.0274$$

$$R_r' = 0.0213$$

$$L_{1r} = 2.7 \times 10^{-4} \text{ H}$$

$$L_{1s} = 2.5 \times 10^{-4} \text{ H}$$

$$L_m = 13.86 \times 10^{-3} \text{ H}$$

$$I_{or} = 24.4 \text{ A} \\ (\text{rms})$$

$$I_{or} = \sqrt{2} \times 24 \\ (\text{peak}) \\ \simeq 34 \text{ A}$$

$$f = 160 \text{ Hz} \quad V_D = 240 \text{ V}$$

$$R_s = 0.0274$$

$$R_r' = 0.0213$$

$$L_{1r} = 3.23 \times 10^{-4} \text{ H}$$

$$L_{1s} = 2.94 \times 10^{-4} \text{ H}$$

$$L_m = 26.8 \times 10^{-3} \text{ H}$$

$$I_{or} = 8 \text{ A} \\ (\text{rms})$$

$$I_{or} = \sqrt{2} \times 8 \\ (\text{peak}) \\ \simeq 11 \text{ A}$$

Modified Parameters of the Motor Operating at

$$f = 20 \text{ Hz} \quad V_D = 60 \text{ V}$$

$$(1) \quad E_1(\text{rms}) = \frac{4}{\sqrt{2} \times \pi} \quad V_D = \frac{4}{\sqrt{2} \times \pi} \times 60 = 54 \text{ V}$$

$$(13) \quad \phi_m = \frac{E_1}{4.44 \text{ kw f T}_{ph}} = \frac{54}{4.44 \times 0.9029 \times 20 \times 33} \\ = 0.0204$$

Neglect the change of resistance, as the operation frequency is changed.

$$(26) \quad R_s = 0.0274 \Omega$$

$$(38) \quad R'_r = 0.0213 \Omega$$

$$(41) \quad B_g = 1.36 \phi_m / A_g = \frac{1.36 \times 0.0204}{0.0367} \\ = 0.756$$

$$(43) \quad B_{Z1} = 1.36 \phi_m / A_{Z1} = \frac{1.36 \times 0.0204}{0.0138} \\ = 2.01$$

$$(47) \quad B_{c1} = \phi_m / 2A_{c1} = \frac{0.0204}{2 \times 0.005454} = 1.87$$

Modified Parameters of the Motor Operating at

$$f = 160 \text{ Hz} \quad V_D = 240 \text{ V}$$

$$E_1(\text{rms}) = \frac{4}{\sqrt{2} \times \pi} \times 240 = 216 \text{ V}$$

$$\phi_m = \frac{216}{4.44 \times 0.9029 \times 160 \times 33} = 0.0102$$

$$R_s = 0.0274 \Omega$$

$$R'_r = 0.0213 \Omega$$

$$B_g = \frac{1.36 \times 0.0102}{0.0367} = 0.378$$

$$B_{Z1} = \frac{1.36 \times 0.0102}{0.0138} = 1.005$$

$$B_{c1} = \frac{0.0102}{2 \times 0.005454} = 0.935$$

$$(53) \quad B_{Z2} = \frac{1.36\phi_m}{A_{Z2}} = \frac{1.36 \times 0.0204}{0.01354} = 2.049$$

$$B_{Z2} = \frac{1.36 \times 0.0102}{0.01354} = 1.0245$$

$$(56) \quad B_{c2} = \frac{\phi_m}{2 \times A_{c2}} = \frac{0.0204}{2 \times 0.0057} = 1.79$$

$$B_{c2} = \frac{0.0102}{2 \times 0.0057} = 0.895$$

$$(57) \quad B_{Z1} = 2.01$$

$$B_{Z1} = 1.005$$

$$B'_{Z1} = 0.9 \times B_{Z1} = 1.809$$

(When teeth are over saturated, part of flux passes through slots.)

$$H_{Z1} = 130 \times 79.577 = 10345$$

$$H_{Z1} = 3 \times 79.577 = 239$$

$$B_{c1} = 1.87$$

$$B_{c1} = 0.935$$

$$B'_{c1} = 0.9 \times 1.87 = 1.683$$

(Part of flux spreads to housing.)

$$H_{c1} = 55 \times 79.577 = 4376$$

$$H_{c1} = 2.6 \times 79.577 = 207$$

$$B_{Z2} = 2.049$$

$$B_{Z2} = 1.0245$$

$$B'_{Z2} = 0.9 \times 1.84 = 1.656$$

$$H_{Z2} = 160 \times 79.577 = 12732$$

$$B_{c2} = 1.79$$

$$B'_{c2} = 0.9 \times 1.79 = 1.61$$

$$H_{c2} = 40 \times 79.577 = 3183$$

$$(59) \quad AT_g = 8 \times 10^5 \times I_g \times B_g = 8 \times 10^5 \times 0.000354 \times 0.756 \\ = 214$$

$$(60) \quad AT_{z1} = H_{z1} I_{z1} = 10345 \times 0.033 = 341$$

$$(61) \quad AT_{c1} = H_{c1} I_{c1} = 4376 \times 0.076 = 332$$

$$(62) \quad AT_{z2} = H_{z2} I_{z2} = 12732 \times 0.017 = 216$$

$$(63) \quad AT_{c2} = H_{c2} I_{c2} = 3183 \times 0.0152 = 48$$

$$AT = AT_g + AT_{z1} + AT_{c1} + AT_{z2} + AT_{c2} \\ = 214 + 341 + 332 + 216 + 48 = 1151$$

$$(64) \quad I_{or} = \frac{P \times 2 \times AT}{1.17 \times kw \times T_{ph}} = \frac{2 \times 1151}{1.17 \times 0.9029 \times 33} \\ = 66$$

$$(65) \quad x_m = \frac{E_1}{I_{or}} = \frac{54}{66} = 0.818$$

$$H_{Z2} = 3.2 \times 79.577 = 255$$

$$B_{c2} = 0.895$$

$$H_{c2} = 2.5 \times 79.577 = 199$$

$$AT_g = 8 \times 10^5 \times 0.000354 \times 0.378 \\ = 107$$

$$AT_{z1} = 239 \times 0.033 = 8$$

$$AT_{c1} = 207 \times 0.076 = 16$$

$$AT_{z2} = 255 \times 0.017 = 5$$

$$AT_{c2} = 199 \times 0.0152 = 3$$

$$AT = 107 + 8 + 16 + 5 + 3 = 139$$

$$I_{or} = \frac{2 \times 139}{1.17 \times 0.9029 \times 33} \approx 8$$

$$x_m = \frac{216}{8} = 27$$

$$(66) \quad L_m = \frac{x_m}{2\pi f} = \frac{0.818}{2 \times \pi \times 20} = 6.51 \times 10^{-3}$$

$$L_m = \frac{27}{2 \times 160} = 26.8 \times 10^{-3}$$

The overload current is around two times larger than rating, so slot leakage inductance still can be considered as a constant.

$$(70) \quad x_{s1} = \frac{8fm L T_{ph}^2}{10^7 z_1} \lambda_{s1}$$

$$= \frac{8 \times 20 \times 2 \times 6.3 \times 33^2}{10^7 \times 24} \times 1.558 = 0.01425$$

$$x_{s1} = \frac{8 \times 160 \times 2 \times 6.3 \times 33^2}{10^7 \times 24} \times 1.558$$

$$= 0.114$$

$$(71) \quad x_{s2} = \frac{8fm L T_{ph}^2}{10^7 \times z_1} = \lambda'_{s2}$$

$$= \frac{8 \times 20 \times 2 \times 6.3 \times 33^2}{10^7 \times 24} \times 1.46 = 0.1336$$

$$x_{s2} = \frac{8 \times 160 \times 2 \times 6.3 \times 33^2}{10^7 \times 24} \times 1.46$$

$$= 0.107$$

$$(72) \quad x_e = \frac{4fm D T_{ph}^2}{10^7 (2p)^2} = \frac{4 \times 20 \times 2 \times 5.75 \times 33^2}{10^7 (2)^2}$$

$$= 0.025$$

$$x_e = \frac{4 \times 160 \times 2 \times 5.75 \times 33^2}{10^7 (2)^2}$$

$$= 0.2$$

$$(73) \quad x_d = \frac{5}{6} x_m \left(\frac{6k_{c1} - 1 - 5\sigma^2}{5S_1^2} + \frac{\sigma k_{c2}}{5S_2^2} - 1 \right)$$

$$= \frac{5}{6} \times 0.818 \times \left(\frac{6 \times 1.14 - 1 - 5 \times 0.5^2}{5 \times 12^2} + \frac{0.5 \times 1.034 - 1}{5 \times 10^2} \right)$$

$$= 0.00605$$

$$x_d = \frac{5}{6} \times 27 \times \left(\frac{6 \times 1.14 - 1 + 5 \times 0.5^2}{5 \times 12^2} + \frac{0.5 \times 1.034 - 1}{5 \times 10^2} \right)$$

$$= 0.2$$

$$(74) \quad X_1 = X_{s1} + \frac{Z_2}{Z_1+Z_2} (X_e + X_d) = 0.01425$$

$$+ \frac{20}{20+24} (0.025 + 0.00605) = 0.02835$$

$$X_1 = 0.114 + \frac{20}{20+24} (0.2 + 0.2)$$

$$= 0.296$$

$$(75) \quad X'_2 = X_{s2} + \frac{Z_1}{Z_1+Z_2} (X_e + X_d)$$

$$= 0.01336 + \frac{24}{24+20} (0.025 + 0.00605)$$

$$= 0.0303 \Omega$$

$$X'_2 = 0.107 + \frac{24}{24+20} (0.2 + 0.2)$$

$$= 0.325$$

$$(76) \quad L_{1s} = \frac{X_1}{2\pi f} = \frac{0.02835}{2 \times \pi \times 20} = 2.256 \times 10^{-4}$$

$$L_{1s} = \frac{0.296}{2 \times \pi \times 160} = 2.94 \times 10^{-4}$$

$$L_{1r} = \frac{X'_2}{2\pi f} = \frac{0.0303}{2 \times \pi \times 20} = 2.41 \times 10^{-4}$$

$$L_{1r} = \frac{0.325}{2 \times \pi \times 160} = 3.23 \times 10^{-4}$$

$$R_s = 0.0274 \Omega$$

$$R_s = 0.0274 \Omega$$

$$R'_r = 0.0213 \Omega$$

$$R'_r = 0.0213 \Omega$$

$$L_m = 6.51 \times 10^{-3}$$

$$L_m = 26.8 \times 10^{-3}$$

APPENDIX E
MOTOR TRANSIENT TEMPERATURE RISE

Peak Momentary Motor Temperature Rise

The specifications require three motor operating points.

1. 100 per cent speed, 30 kW output for 1 hour
2. 10 per cent speed, 16 kW output for 3 min.
3. 80 per cent speed, 60 kW output for 3 min.

The first one is obviously no problem.

$$I_{ph} = \frac{170}{216} \times 110.2 = 86.7 \text{ A}$$

$$\delta_1 = \frac{86.7}{2 \times 11.19} = 3.87 \text{ A/mm}^2 \text{ (See Appendix D)}$$

The copper losses are small due to the low current, and the motor operates under saturation, so the core losses are also small. Although the mechanical losses are greatest at top speed, high speed creates very good heat dissipation conditions. One hour operation is expected to produce nearly steady state temperature rise.

The second one is worse than the third case for temperature rise because at this operating point there are maximum losses and worst case heat dissipation conditions.

The heat balance differential (1) can be applied to evaluate the transient temperature rise.

$$\frac{d\theta}{dt} + \theta \frac{S\lambda}{GC_p} = \frac{P}{GC_p} \quad (1)$$

where θ is temperature rise, °C

S is cooling surface of the hot body, m^2

G is weight of the hot body, kg

C_p is specific heat of the hot body, $\text{J/kg}\cdot^\circ\text{C}$

λ is specific heat dissipation or emissivity,

J per second per m^2 of surface per °C difference

between surface and ambient cooling medium

P is heat developed, J per second or W

During a short time we neglect the exchange between stator and rotor (the heat-resistance of air gap is very large), and even neglect the heat dissipation. This means that all the heat developed causes temperature rise, and of course, this is the most serious situation.

Then (1) becomes

$$\frac{d\theta}{dt} = \frac{P}{GC_p}$$

$$\theta = \int \frac{P}{GC_p} dt \quad (2)$$

If we assume P and C_p are constant, then

$$\theta = \frac{P}{GC_p} t \quad (3)$$

where t = 3 minutes = 180 s

$$\begin{aligned} G &= m \times 2 \times L_{ph} \times S_c \times a_p \times 10^{-3} \times g_c \\ &= 2 \times 2 \times 29.17 \times 11.19 \times 2 \times 10^{-3} \times 8.9 = 23.24 \\ g_c &= 8.9 \text{ kg/dm}^2 \text{ (specific gravity of copper)} \end{aligned}$$

The total weight G of the two-phase bifilar winding is greater because each single winding conducts for only a half cycle. Thus, the bifilar windings have an advantage for short time transient temperature rise - not significant for steady state.

The specific heat C_p of copper is

$$\begin{aligned} C_p &= 0.092 \text{ Btu/lbF} \\ &= 0.092 \times \frac{1055}{0.454 \times 5} = 384.8 \text{ J/kg}^\circ\text{C} \end{aligned}$$

P is stator winding losses

$$P = m \times r_s \times I_{rms}^2 = 2 \times 0.0274 \times 200.4^2$$

$$= 2201$$

(As shown in Appendix G, I_{rms} is 200.4 A)

From (3), we get

$$\theta = \frac{P}{GC_p} t = \frac{2201}{23.24 \times 384.8} \times 180$$

$$= 44.3^\circ\text{C}$$

We suggest the insulation class F. Specifications for the F class insulation are as follows:^{*}

The hot-spot temperature is 155°C.

The maximum permitting temperature rise for totally enclosed fan-cooled motors is 105°C, based on ambient temperature of 40°C, 3330 ft. altitude, and determined by the resistance method.

If we directly apply (1) for 30% duty

$$\frac{d\theta}{dt} + \frac{s\lambda}{GC_p} \theta = \frac{P}{GC_p}$$

$$\begin{aligned} \text{then } \theta &= \frac{P/GC_p}{S\lambda/GC_p} - \frac{P/GC_p}{S\lambda/GC_p} e^{-\frac{S\lambda}{GC_p} t} \\ &= \frac{P}{S\lambda} - \frac{P}{S\lambda} e^{-\frac{S\lambda}{GC_p} t} \end{aligned} \quad (4)$$

$$\text{where } \lambda = 1/c = 1/0.04 = 25 \text{ J/sec m}^2\text{°C}$$

(assume no cooling air)

$$\begin{aligned} S &= Z_1 \times L_{mc} \times L_{sp} = 24 \times 0.442 \times 0.091 \\ &= 1.05 \text{ m}^2 \end{aligned}$$

L_{sp} is the perimeter of stator slot

* Standard Handbook for Electrical Engineers, 11th Edition, McGraw-Hill, pp. 20-45.

$$\begin{aligned}
 L_{sp} &= 2(h_1 + h_2) + w_b + w_s \\
 &= 2(31 + 2) + 21 + 12.1 = 99.1 \text{ mm} \\
 &= 0.0991 \text{ m}
 \end{aligned}$$

For Z_1 , L_{mc} , h_1 , h_2 , w_b , and w_s refer to the design sheet of the motor in Appendix D.

From (4)

$$\theta = \frac{2201}{1.05 \times 25} - \frac{2201}{1.05 \times 25} e^{-\frac{1.05 \times 25}{23.24 \times 384.8} t}$$

$$= 83.85 - 83.85 e^{-0.00294t}$$

30% duty 3 minutes operation
7 minutes off

For the first operation

$$t = 3 \times 60 = 180 \text{ sec}$$

$$\begin{aligned}
 \theta_1 &= 83.85 - 83.85 e^{-0.00294 \times 180} \\
 &= 34.5^\circ\text{C}
 \end{aligned}$$

During the 7 minute off interval

$$\begin{aligned}
 \theta'_1 &= \theta_1 e^{-0.00294 \times t} \\
 &= 34.5 e^{-0.00294 \times 420} = 10^\circ\text{C}
 \end{aligned}$$

The second duty cycle

$$\theta_2 = \theta_1 + 10 = 44.5^\circ\text{C}$$

$$\theta'_2 = 44.5 e^{-0.00294 \times 420} = 13^\circ\text{C}$$

The third duty cycle

$$\theta_3 = \theta_1 + 13 = 47.5^\circ\text{C}$$

$$\theta'_3 = 47.5 \times e^{-0.00294 \times 420} = 13.8^\circ\text{C}$$

The fourth duty cycle

$$\theta_4 = \theta_1 + 13.8 = 48.3^\circ\text{C}$$

$$\theta'_4 = 48.3 \times e^{-0.00294 \times 420} = 14.05^\circ\text{C}$$

The fifth duty cycle

$$\theta_5 = \theta_1 + 14.05 = 48.55^\circ\text{C}$$

$$\theta'_5 = 48.55 \times e^{-0.00294 \times 420} = 14.12^\circ\text{C}$$

The sixth duty cycle

$$\theta_6 = \theta_1 + 14.12 = 48.62^\circ\text{C}$$

$$\theta'_6 = 48.62 \times e^{-0.00294 \times 420} = 14.14^\circ\text{C}$$

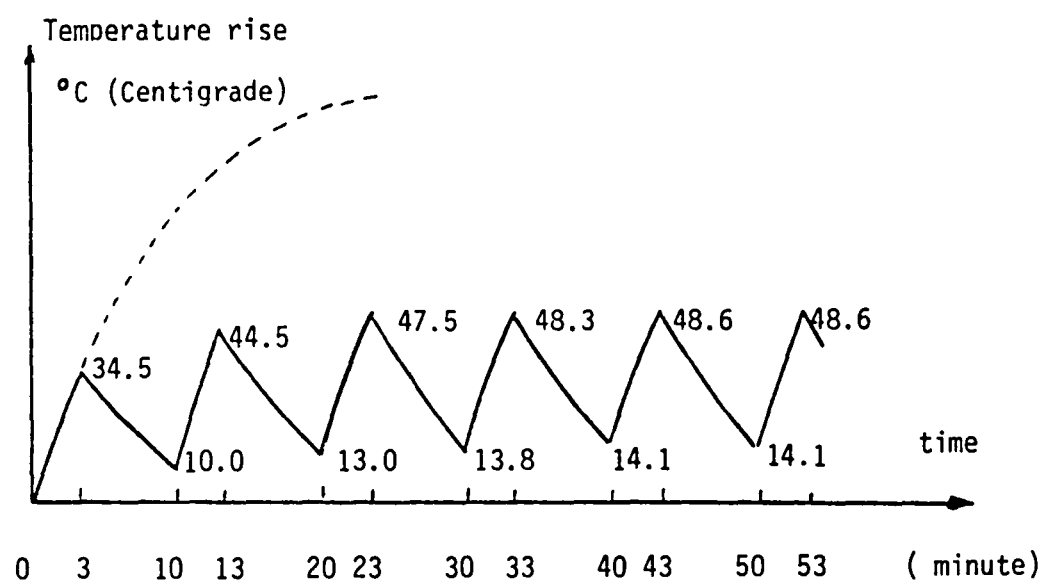


Fig. E-1 Transient Temperature Rise

APPENDIX F

DETAILED INVERTER DESIGN

F.1 INTRODUCTION

The complete system schematic diagram is shown in Fig. F-1. This is identical to Fig. 12 of section 4.4 in this report, but it is included again here for convenience. This appendix describes the detailed design of the two-phase inverter-bifilar induction motor system.

F.2 POWER CIRCUIT DESIGN

Fig. F-2 is the power circuit (same as Fig. 2). The most important aspect of the design of the power circuit is the determination of the rating requirements for the power switch devices. Analysis and simulation of the two-phase bifilar induction machine define the ideal switch voltage and current ratings to supply the power required at the specification operating points.

The power switch ratings (section 3.4.1), assuming ideal circuit conditions, are

$$\text{Peak Voltage} \quad V_p = 480V$$

$$\text{Peak Current} \quad I_p = 245A$$

$$\text{RMS Current} \quad I_{\text{RMS}} = 200A$$

$$\begin{array}{ll} \text{Maximum} & \\ \text{Switching} & f_{S,\text{MAX}} = 3.4\text{kHz at 245A peak} \\ \text{Frequency} & \end{array}$$

However, it is necessary to analyze the specific circuit configuration to determine the precise transient and steady state voltage and current requirements of the switching devices. One of the primary disadvantages of the circuit in Fig. F-2 is the existence of greater transient voltages. These are the result of leakage inductance due to imperfect coupling between the bifilar windings and motor lead inductance which is now in the commutation path where current switching occurs. The lead inductance does not produce voltage transients in the three-phase bridge system.

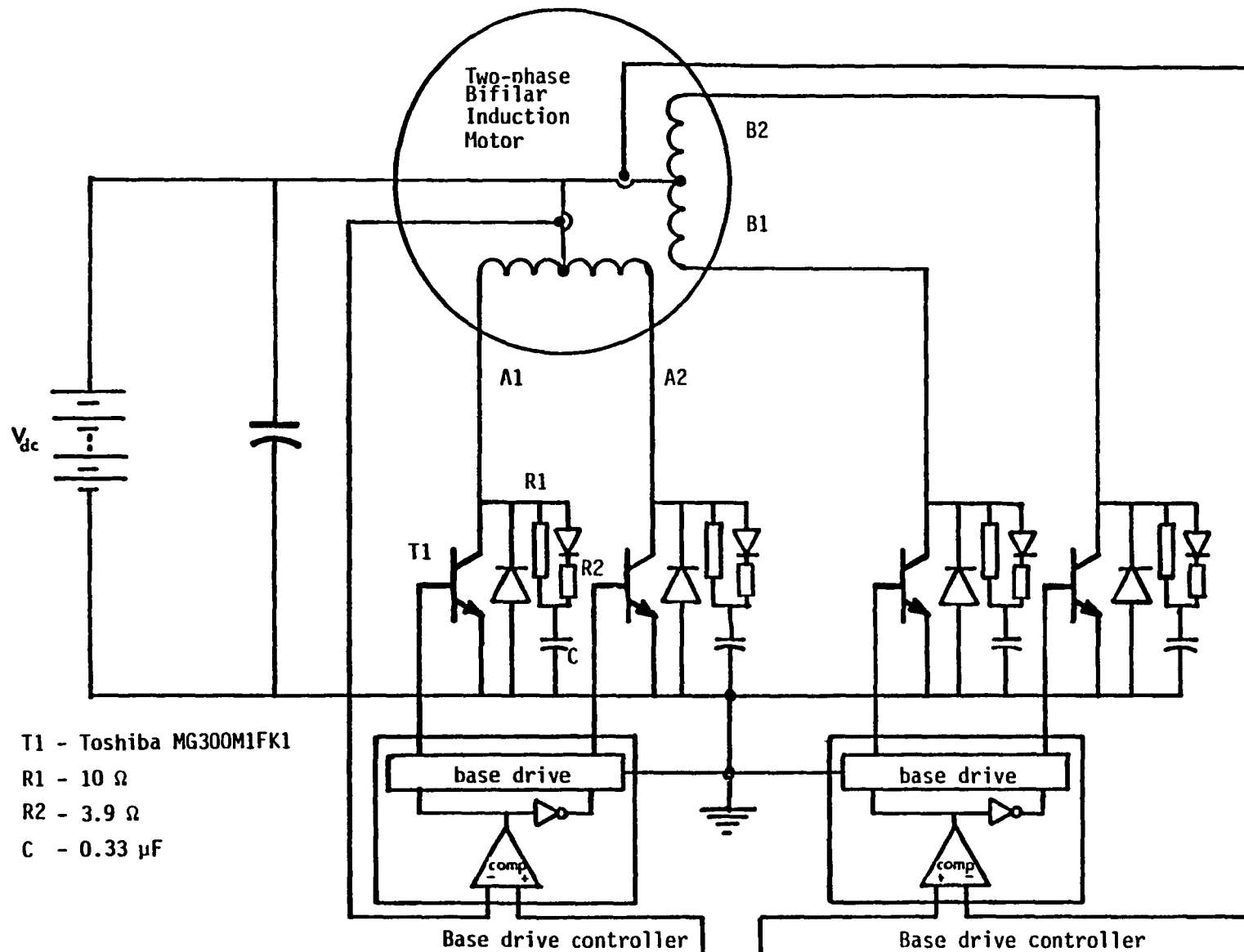
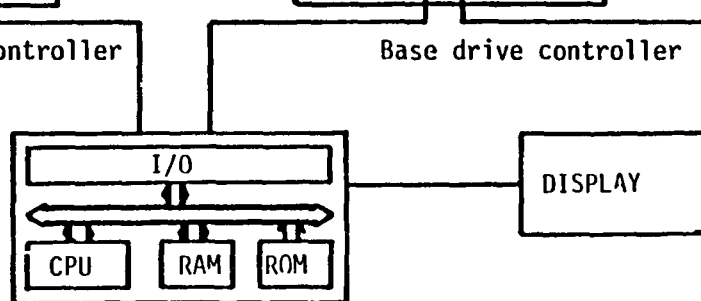


Fig. P-1 Complete System

Schematic Diagram

(same as Fig.12)



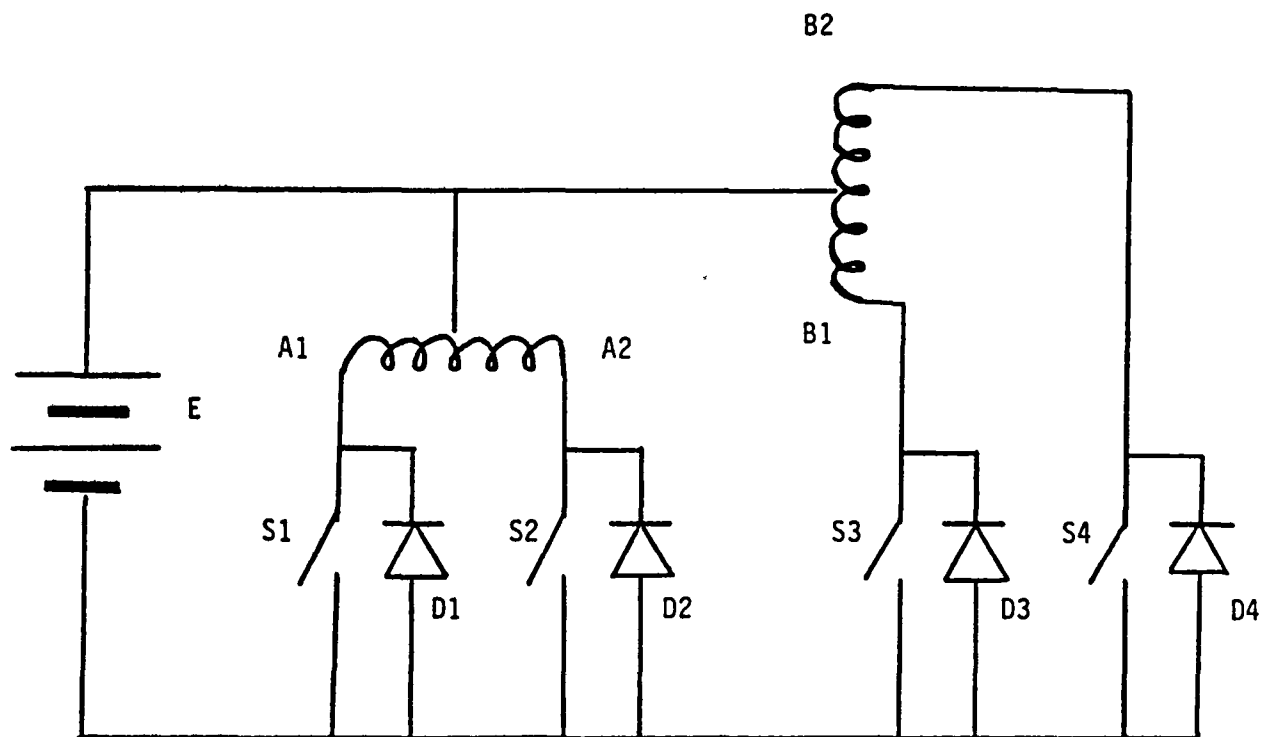


Fig. F-2 Two-phase Bifilar Induction Motor/Inverter

F.3 TRANSIENT VOLTAGE SPIKE ANALYSIS

Consider Fig. F-2 at the moment when switch S1 is opened to transfer its current to the S2-D2 branch. If the A1 and A2 bifilar windings are perfectly coupled, and if there is no lead inductance in the circuit including the dc source, motor leads and switch-diode branches, then the current commutation can occur instantly with no voltage transient. Unfortunately, the bifilar winding coupling is not perfect and lead inductances do exist. Therefore, voltage transients are generated proportional to the rate of change of current and the equivalent leakage inductances of the bifilar windings and the battery, motor and switch-diode wiring inductances. Thus, it is essential to minimize these inductances and determine accurate estimates of their maximum values.

Snubber Design

Fig. F-3 shows a simplified model of a single snubber circuit including a lumped inductance to represent bifilar winding leakage inductances and lead inductances.

The order of magnitude of the spike voltage is determined from assuming that all of the initial energy stored in the inductance is transferred to the capacitor, that is,

$$\frac{1}{2} L I_p^2 = \frac{1}{2} C V_p^2 \quad (1)$$

where

$I_p \triangleq$ peak current at instant switch opens

$V_p \triangleq$ peak voltage on capacitor

$L \triangleq$ equivalent total leakage and lead inductance

$C \triangleq$ snubber capacitance

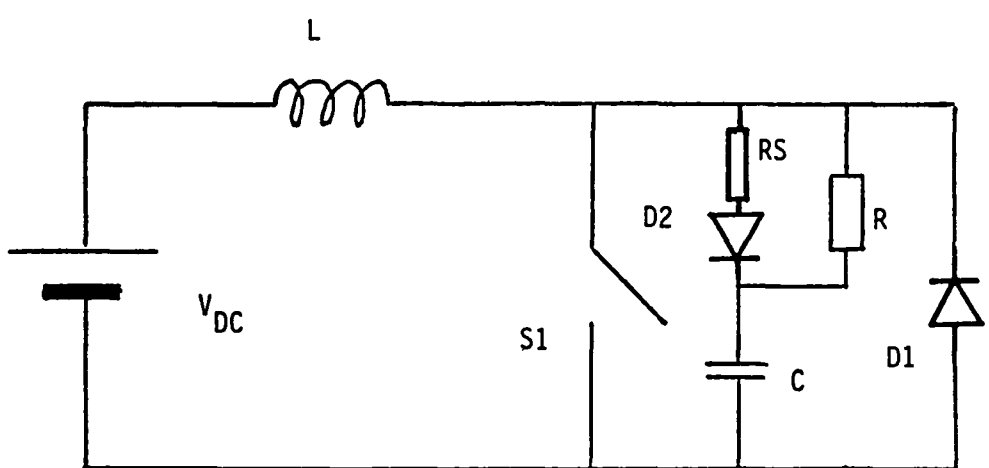


Fig. F-3 Simplified Switching Circuit

Thus

$$V_p = \sqrt{\frac{L}{C}} I_p \quad (2)$$

First, it is necessary to determine the maximum value of L. This inductance is primarily the leakage inductance due to imperfect coupling in the bifilar windings. Normally, the lead inductances are small, particularly if the inverter is mounted close to the motor and if a high quality capacitor is connected directly from the motor winding center-tap to the negative dc bus, which minimizes the effect of battery lead inductance and the inductance in the winding center-tap lead.

The normal total leakage reactance for a 10-100hp induction motor is 0.23 per unit (pu). Of this total, the stator leakage is about 0.1 pu. This stator leakage can be reduced to about 0.05 pu for high torque motors. Finally, the equivalent leakage inductance between two tightly coupled windings in one motor phase should be less than .005 pu. This results in an estimated maximum value of L equal to $15\mu\text{H}$. However, it is estimated that the leakage inductance between two bifilar motor windings could be reduced an order of magnitude below $15\mu\text{H}$ with special motor winding techniques. For the following calculations an L of $4\mu\text{H}$ is used. With $I_p = 245\text{A}$, from (2)

$$V_p = \sqrt{\frac{4\mu\text{H}}{C}} 245 = \frac{0.49}{\sqrt{C}} \quad (3)$$

If C is chosen equal to $0.33\mu\text{F}$,

$$V_p = \frac{0.49}{0.33\mu\text{F}} = 853\text{V} \quad (4)$$

This is a reasonable limit for V_p .

The snubber R is necessary to limit the peak snubber capacitor discharge current at the moment of turning on the power switch. If R is chosen equal to 10 ohms, then

$$I_p(0) = \frac{2V_{DC}}{R} = 48A \quad (5)$$

This is a reasonable $I_p(0)$ to allow for the device rating.

Voltage Spike Simulation

The snubber design carried out in the previous section is based on an approximate transient voltage estimation. The precise switching behavior can be determined by digital simulation including all non-linear effects, or by hardware experiments. Since no hardware construction was done, digital simulations were performed using SPICE to provide more accurate results than could be obtained from approximate analysis.

The switching transient is short relative to changes which occur in the rotor circuit of the induction motor. Thus, the steady state equivalent circuit model is used for the motor load, i.e., r_2/s where r_2 is rotor resistance and s is the slip. The equivalent stator circuit is derived using the three winding transformer input-output relations. Fig. F-4 shows the flux linkages of the transformer, which is equivalent to the bifilar wound induction motor with the assumptions that the switching transient is very fast and that all windings have equal turns. The #1 and #2 windings are the stator bifilar windings, and the #3 winding is the rotor winding. v_1 , v_2 , v_3 and i_1 , i_2 , i_3 are the terminal voltages and currents for each winding. ϕ_1 , ϕ_2 and ϕ_3 are defined as the total flux of #1, #2 and #3 windings, respectively. $\phi_{\ell 1}$, $\phi_{\ell 2}$, $\phi_{\ell 3}$ are the corresponding leakage flux for the #1, #2 and #3 windings, respectively. ϕ_M is the mutual flux between either stator winding and the rotor winding, and ϕ_B is the mutual flux between the two stator windings. The following relations are obtained.

$$\phi_1 = \phi_{\ell 1} + \phi_B + \phi_M \quad (6)$$

$$\phi_2 = \phi_{\ell 2} + \phi_B + \phi_M \quad (7)$$

$$\phi_3 = \phi_{\ell 3} + \phi_M \quad (8)$$

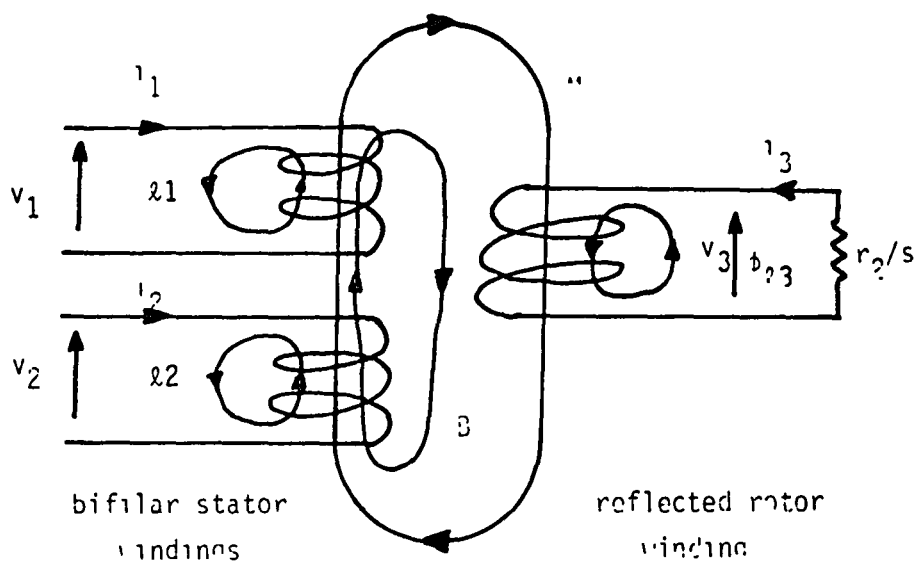


Fig. F-4 Flux linkage relations of three winding transformer

where $v_1 = \frac{d\phi_1}{dt}$, $v_2 = \frac{d\phi_2}{dt}$, and $v_3 = \frac{d\phi_3}{dt}$

Since the #1 and #2 windings are bifilar windings, they are very tightly coupled. Thus, all of the flux ϕ_M links the #3 winding as well as both the #1 and #2 windings.

Defining the mutual (or magnetizing) inductance L_M between the #1, #2 and #3 windings, the mutual flux ϕ_M is

$$\phi_M = L_M i_3 + L_M (i_1 + i_2) \quad (9)$$

Defining the mutual inductance L_{MB} between the #1 and #2 windings, the mutual flux ϕ_B is

$$\phi_B = L_{MB} i_1 + L_{MB} i_2 \quad (10)$$

Defining the leakage inductances $L_{\ell 1}$, $L_{\ell 2}$, and $L_{\ell 3}$ of the #1, #2 and #3 windings respectively, then $\phi_{\ell 1}$, $\phi_{\ell 2}$, and $\phi_{\ell 3}$ are

$$\phi_{\ell 1} = L_{\ell 1} i_1 \quad (11)$$

$$\phi_{\ell 2} = L_{\ell 2} i_2 \quad (12)$$

$$\phi_{\ell 3} = L_{\ell 3} i_3 \quad (13)$$

Combining (6) - (13)

$$\phi_1 = L_{\ell 1} i_1 + L_{MB} (i_1 + i_2) + L_M (i_1 + i_2 + i_3) \quad (14)$$

$$\phi_2 = L_{\ell 2} i_2 + L_{MB} (i_1 + i_2) + L_M (i_1 + i_2 + i_3) \quad (15)$$

$$\phi_3 = L_{\ell 3} i_3 + L_M (i_1 + i_2 + i_3) \quad (16)$$

These three equations provide the equivalent circuit shown in Fig. F-5, where the rotor load and stator resistance r_1 are added. v_1 and v_2 are controlled to be E, -E or 0. This equivalent circuit becomes the conventional equivalent circuit if one of the bifilar winding branches is removed.

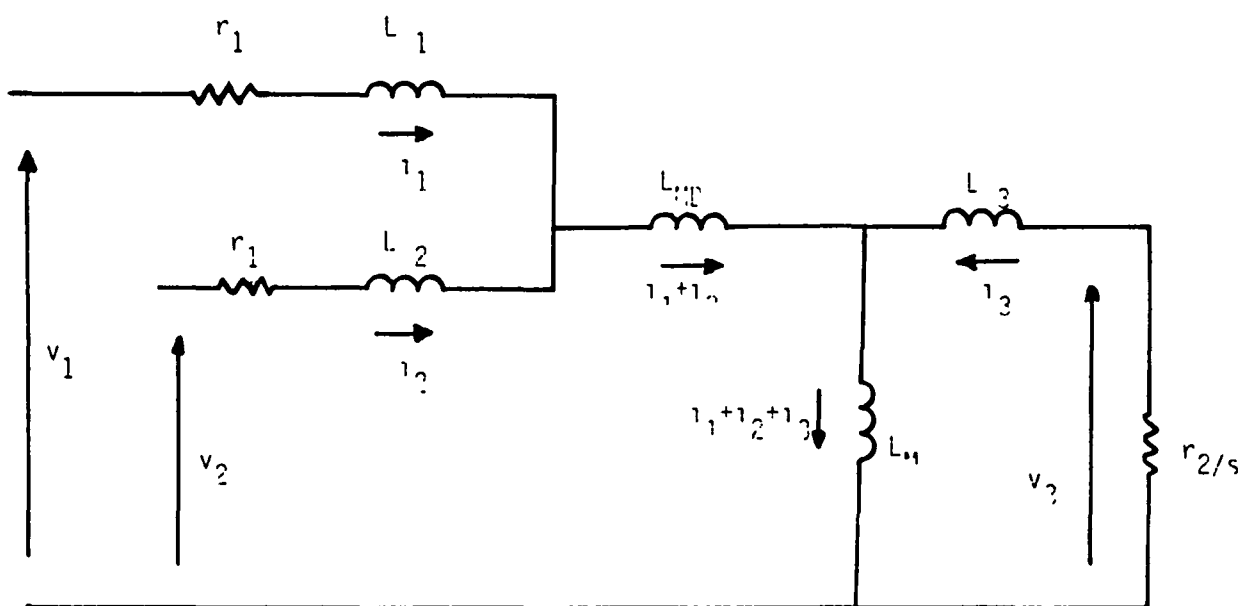


Fig. F-5 Equivalent Switching Circuit

SPICE is a general purpose circuit simulation program. Circuits may contain resistors, capacitors, inductors, mutual inductors, independent voltage and current sources, four types of dependent sources, transmission lines, and the most common semiconductor devices: diodes, BJTs, JFETs and MOSFETs.

Fig. F-6 shows the equivalent circuits used for simulation, including snubber circuits and base drive circuits. When one device is turned off, the base drive voltage source is changed linearly from 10 volts to zero for a 5 microsecond interval. After a 15 μ s delay, when the other is turned on, the base voltage is controlled linearly from zero to 10 volts for a 5 μ s interval. When one device is switched off, the current first flows through the feedback diode of the other device. Thus, the delay time in turn-on of the next device has no effect. The interval during which the base voltage source is linearly controlled is changed from 5 μ s to 2 μ s, but the transient voltage changes no more than 0.4% in its peak value. The lumped leakage inductances LLS1 and LLS2, shown in Fig. F-6, are chosen to be 4 μ H, while the sum of LLS1 and LMB is equal to the stator leakage inductance. LM and LLR are equal to the magnetizing and rotor leakage inductances respectively. RS1 and RS2 are the stator winding resistances, and RR2 is calculated from r_2/s where r_2 is the rotor resistance and s is the slip at the steady state operating point. The series resistances R11 and R22 help to suppress the transient voltage. By trial and error, 3.9 ohms are selected. A peak transient voltage of 943 volts across the transistors is obtained for the following operating conditions and system parameters:

10% speed, 16 kW output

Percent slip = 8.5%

Stator current = 245A

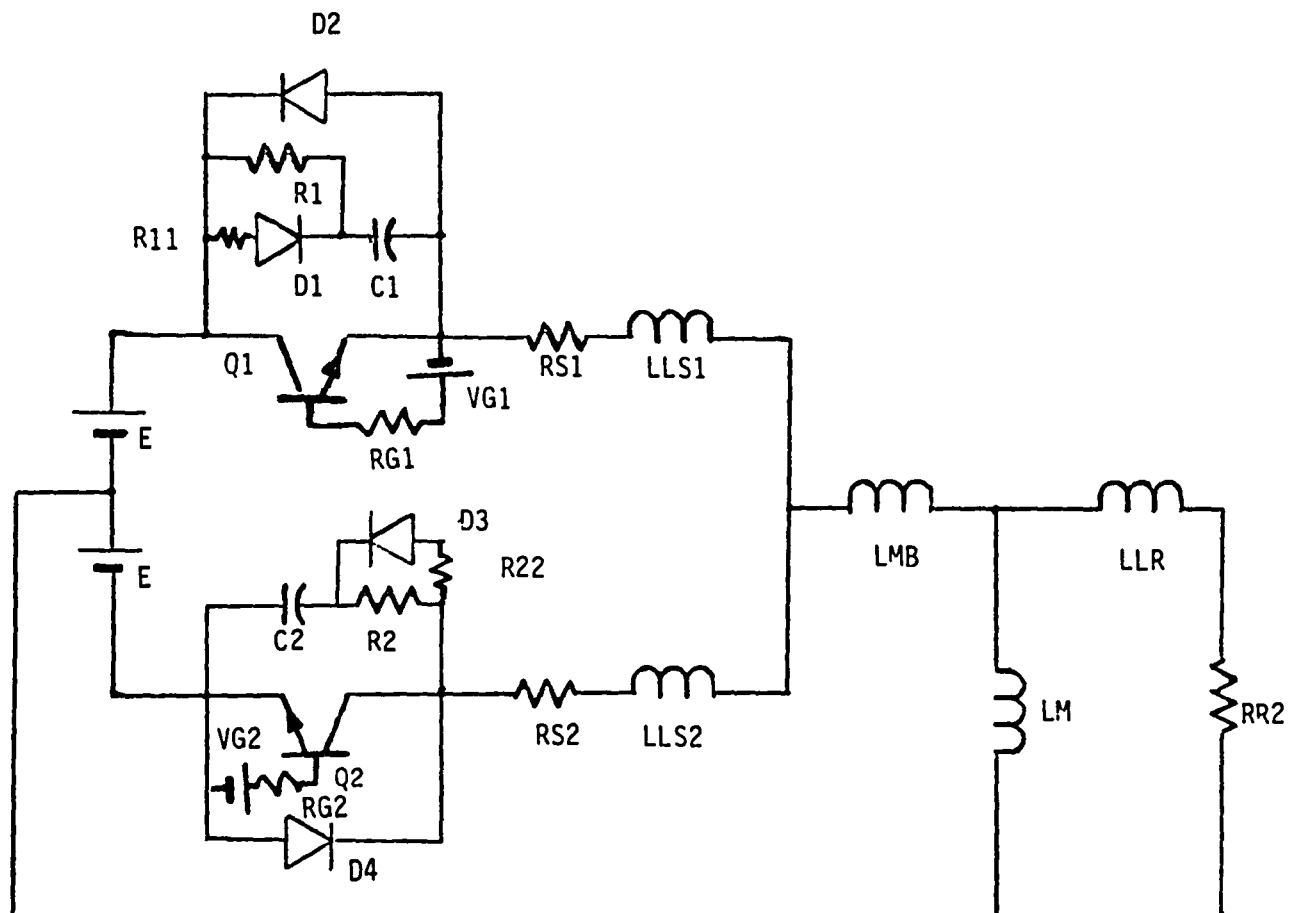


Fig. F-6 Equivalent circuit used for simulation

Note: $LLS1$ and $LLS2$ are equivalent leakage inductance.

Magnetizing current (through LM) = 93A

Rotor current = 142A

LM = 6.51mH; LLR = 241 μ H

LLS1 = LLS2 = 4 μ H; LMB = 221.6 μ H

RS1 = RS2 = 0.0274 Ω ; RR2 = 0.0213/0.085 = 0.251 Ω

R1 = R2 = 10 Ω ; R11 = R22 = 3.9 Ω

C1 = C2 = 0.33 μ F

The transient waveforms of the collector-emitter voltage and bifilar winding current (i_1 in Fig. F-6) are plotted in Fig. F-7, and the corresponding simulation source program is listed in Fig. F-8. Without R11 and R22, the transient voltage is about 1160 volts.

Next, the equivalent leakage inductances LLS1 and LLS2 are changed from zero to 10 μ H and the peak transient voltage is plotted in Fig. F-9. The operating condition of 80% speed, 60kW output is also simulated, and the transient voltage variation is shown in Fig. F-9 using the following parameters:

Stator current = 245A

Magnetizing current = 20A

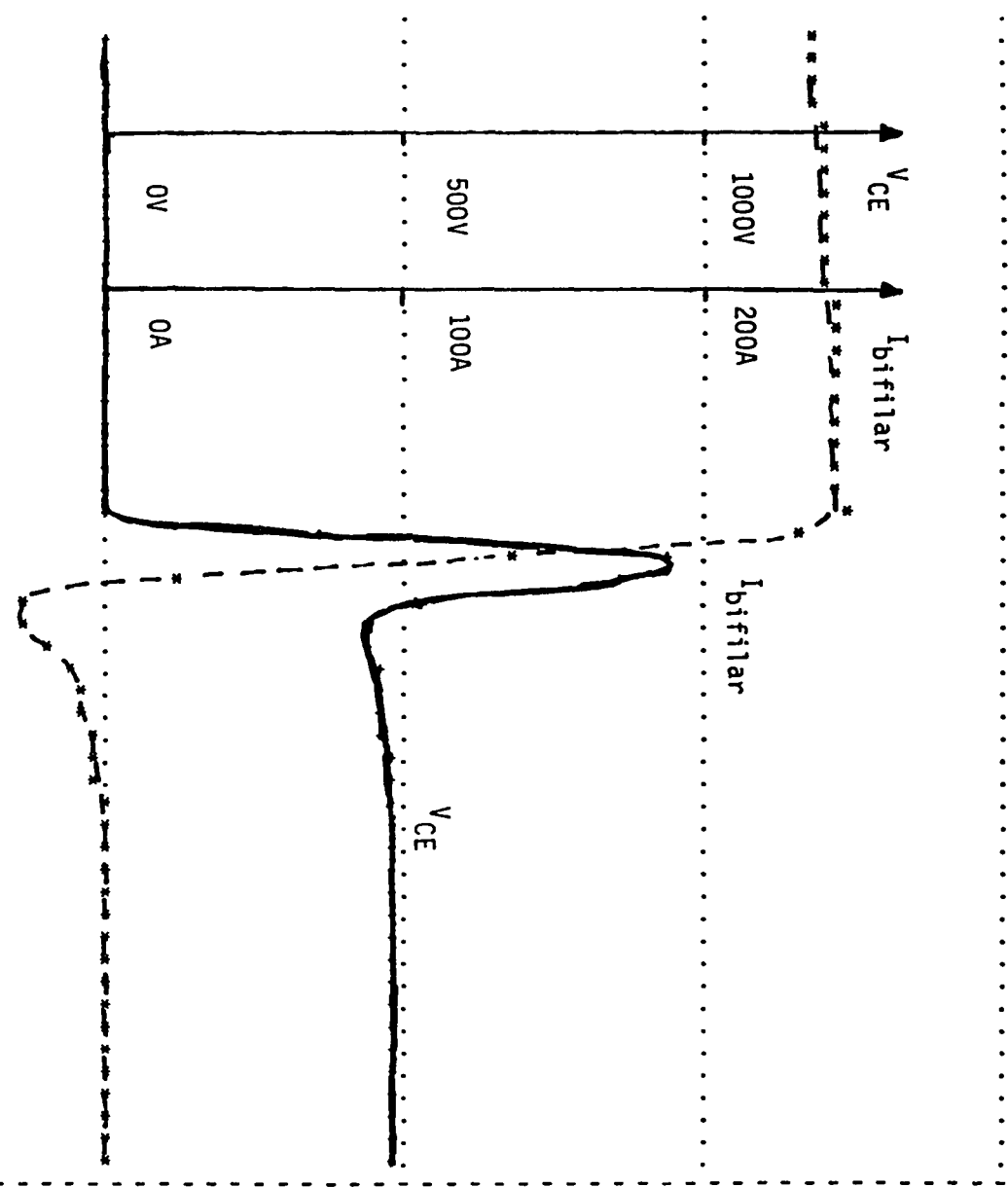
Rotor current = 225A

LM = 26.8mH; LLS1 + LMB = 294 μ H

RR2 = 0.0213/.02 = 1.07 Ω (2% slip)

Other parameters same as for 16kW, 10% speed condition

Fig. F-9 indicates that the spike voltage is somewhat less than 1000V if the equivalent leakage inductance is 4 μ H.



| time | V_{CE} |
|-----------|-----------|
| 8.000D-05 | 9.426D-02 |
| 8.100D-05 | 9.433D-02 |
| 8.200D-05 | 9.439D-02 |
| 8.300D-05 | 9.446D-02 |
| 8.400D-05 | 9.452D-02 |
| 8.500D-05 | 9.459D-02 |
| 8.600D-05 | 9.466D-02 |
| 8.700D-05 | 9.472D-02 |
| 8.800D-05 | 9.479D-02 |
| 8.900D-05 | 9.485D-02 |
| 9.000D-05 | 9.492D-02 |
| 9.100D-05 | 9.498D-02 |
| 9.200D-05 | 9.505D-02 |
| 9.300D-05 | 9.511D-02 |
| 9.400D-05 | 9.518D-02 |
| 9.500D-05 | 9.524D-02 |
| 9.600D-05 | 9.531D-02 |
| 9.700D-05 | 9.537D-02 |
| 9.800D-05 | 9.544D-02 |
| 9.900D-05 | 9.550D-02 |
| 1.000D-04 | 9.557D-02 |
| 1.010D-04 | 1.199D-01 |
| 1.020D-04 | 3.616D+02 |
| 1.030D-04 | 9.425D+02 |
| 1.040D-04 | 8.579D+02 |
| 1.050D-04 | 5.265D+02 |
| 1.060D-04 | 4.446D+02 |
| 1.070D-04 | 4.464D+02 |
| 1.080D-04 | 4.555D+02 |
| 1.090D-04 | 4.622D+02 |
| 1.100D-04 | 4.660D+02 |
| 1.110D-04 | 4.687D+02 |
| 1.120D-04 | 4.706D+02 |
| 1.130D-04 | 4.715D+02 |
| 1.140D-04 | 4.722D+02 |
| 1.150D-04 | 4.730D+02 |
| 1.160D-04 | 4.730D+02 |
| 1.170D-04 | 4.742D+02 |
| 1.180D-04 | 4.744D+02 |
| 1.190D-04 | 4.745D+02 |
| 1.200D-04 | 4.746D+02 |
| 1.210D-04 | 4.747D+02 |
| 1.220D-04 | 4.747D+02 |
| 1.230D-04 | 4.748D+02 |
| 1.240D-04 | 4.748D+02 |
| 1.250D-04 | 4.749D+02 |
| 1.260D-04 | 4.748D+02 |
| 1.270D-04 | 4.748D+02 |
| 1.280D-04 | 4.748D+02 |
| 1.290D-04 | 4.747D+02 |
| 1.300D-04 | 4.747D+02 |

Fig. F-7 Voltage spike simulation : 16kw, 10% speed, $I_p = 245A$,
 $C_1=C_2=0.33 \mu F$, $L_{S1}=L_{S2}=4 \mu H$, $R_{11}=R_{22}=3.9\Omega$, $R_1=R_2=10\Omega$ in Fig.F-6

***** 1/28/85***** SPICE 2E.2 (26SEP78) *****15445436*****

JPL PROJECT VOLTAGE SPIKE 12/18/84

SPI00060

INPUT LISTING

TEMPERATURE = 27.000 DEG C

```
*****
*** BIFILAR WINDING      3 TRANSFORMER MODEL          SPI00070
*** MAIN CIRCUIT          SPI00080
* CURRENT SENSE FOR COLLECTOR CURRENT VCOLLE
VDC1 1 0 240VOLT
Q1 9 2 3 QHNP
VCOLLE 1 9 1UV
***** ADJUST R11 *****
R11 1 8 3.9000HM
D1 8 4 DMOD
R1 1 4 10.00HM
* CHANGE C FOR SHUEBER //////
C1 4 3 0.33UF
D2 3 1 DMOD
RS1 3 5 0.0274
* CHANGE LLS1*****
LLS1 5 7 4.00UH IC=198A
* CURRENT SENSE FOR BIFILAR WINDING VBIFI          SPI00170
VBIFI 7 6 1UV
*
VDC2 0 11 240V
Q2 13 12 11 QHNP
***** ADJUST R22 *****
R22 13 16 3.9000HM
D3 16 14 DMOD
R2 13 14 10.00HM
* CHANGE C FOR SHUEBER //////
C2 14 11 0.33UF IC=450V
D4 11 13 DMOD
RS2 13 15 0.0274
* CHANGE LLS2*****
LLS2 15 6 4.00UF
* CHANGE LMB*****LMB+LLS1(LLS2)=225.6UH AT 20 HZ, 294UH AT 160HZ   SPI00280
* *****LM=6.51MH, LLR=241UH AT 20 HZ
* *****LM=26.8MH, LLR=323UH AT 160 HZ
LMB 6 21 221.6UH IC=198A
LM 21 0 6.51MH IC=85A
LLR 21 22 241UH IC=113A
RR2 22 0 0.251
*** GATE DRIVE          SPI00330
RG1 2 7 10HM
RG2 12 17 10HM
VG1 7 3 PWL (0 10V 100US 10V 105US -10 420US -10 425US 10V)
VG2 17 11 PWL(0 -10 120US -10 125US 10V 400US 10V 405US -10)
*** DEVISE MODEL          SPI00380
.MODEL QHNP NPN(VA=2000V,VB=2000V)
.MODEL DMOD D(BV=2000V)
*** OUTPUT                SPI00410
.PRINT TRAN V(9,3),I(VCOLLE),V(4,3),I(VBIFI),V(6)
.PLOT TRAN V(9,3),I(VBIFI)
.TRAN 1.0US 130US UIC
* .OPTIONS LIMPTS=201 LIST NODE
.END
```

Fig. F-8 Source listing of SPICE simulation program

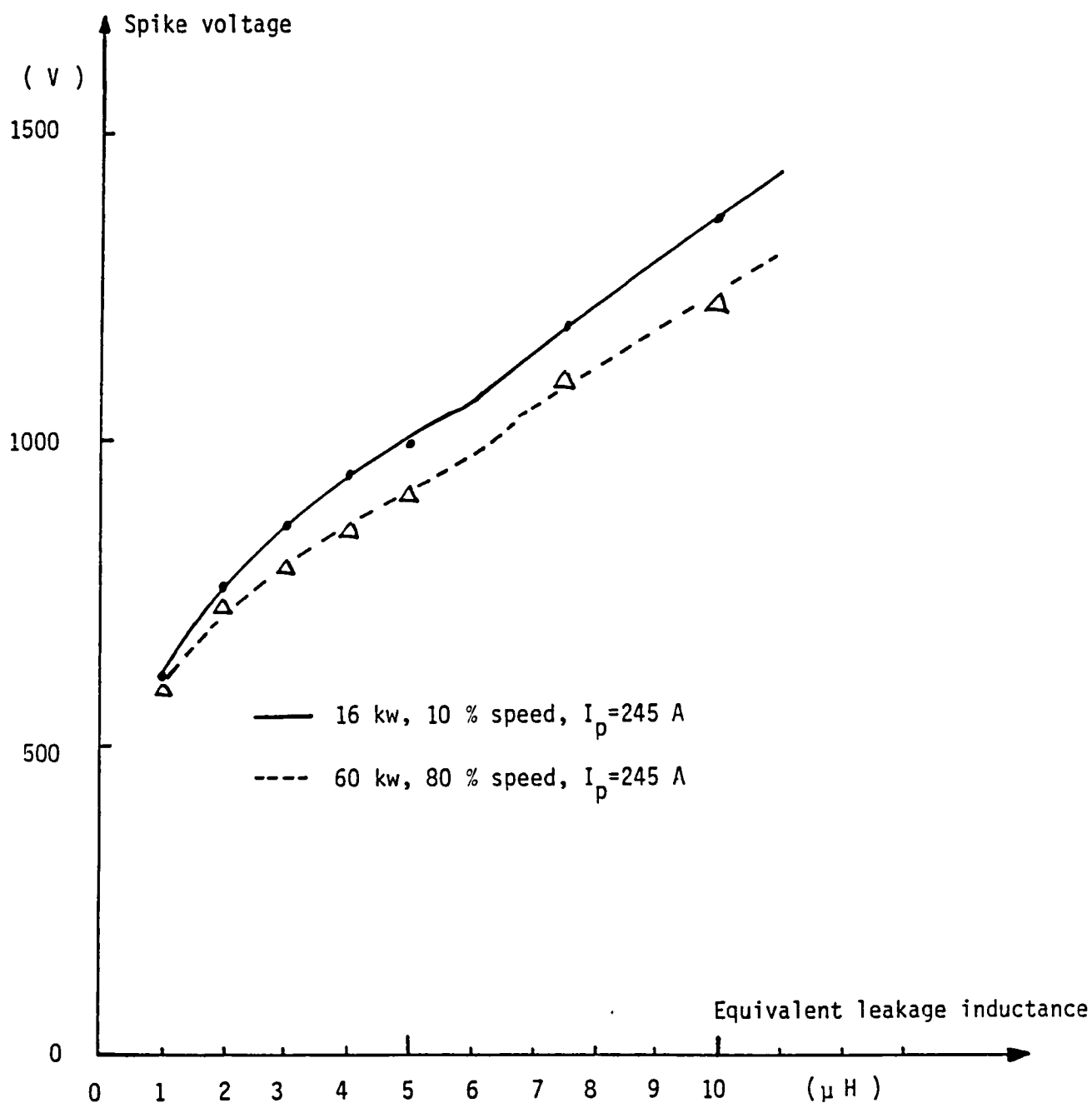


Fig. F-9 Spike voltage vs equivalent leakage inductance
(simulation results)

F.4 LOSS CALCULATION*

Switching Loss

There are four possible switching operations for which different loss calculations are required. Fig. F-10 shows the switching devices and the snubber circuit components only for the A phase. I_{A1} and I_{A2} stand for the stator currents for bifilar windings A1 and A2 respectively, and V_{C1} and V_{C2} are the voltages across capacitors C_1 and C_2 respectively. The following four cases are considered to calculate the switching loss only for switch S1.

(1) Turn-On of S1 When $I_{A2} > 0$: Initially, while switching device S1 is open, diode D4 conducts and capacitor voltage V_{C1} is charged up to $2V_{DC}$. The stored energy in this capacitor is

$$W_C = \frac{1}{2} C (2V_{DC})^2 = 2CV_{DC}^2 \quad (17)$$

Some of this energy will be dissipated in S1 during its turn-on and some will be dissipated in the snubber R1. Assuming an exponential drop of collector-emitter voltage v_{S1} as S1 turns on,

$$v_{S1} = 2V_{DC} e^{-t/\tau}$$

* "Analysis and Design of Optimized Snubber Circuits for dv/dt Protection in Power Thyristor Applications," S. J. Wu, GE 660.24, 2/71.

"Optimum Snubbers for Power Semiconductors," William McMurray, 1971 IAS Conference Record, pp. 885-893.

"Snubbers for Pulse-Width Modulated Bridge Converters with Power Transistors or GTOs," Tore M. Undeland, IPEC Tokyo '83 Conference Record, pp. 313-323.

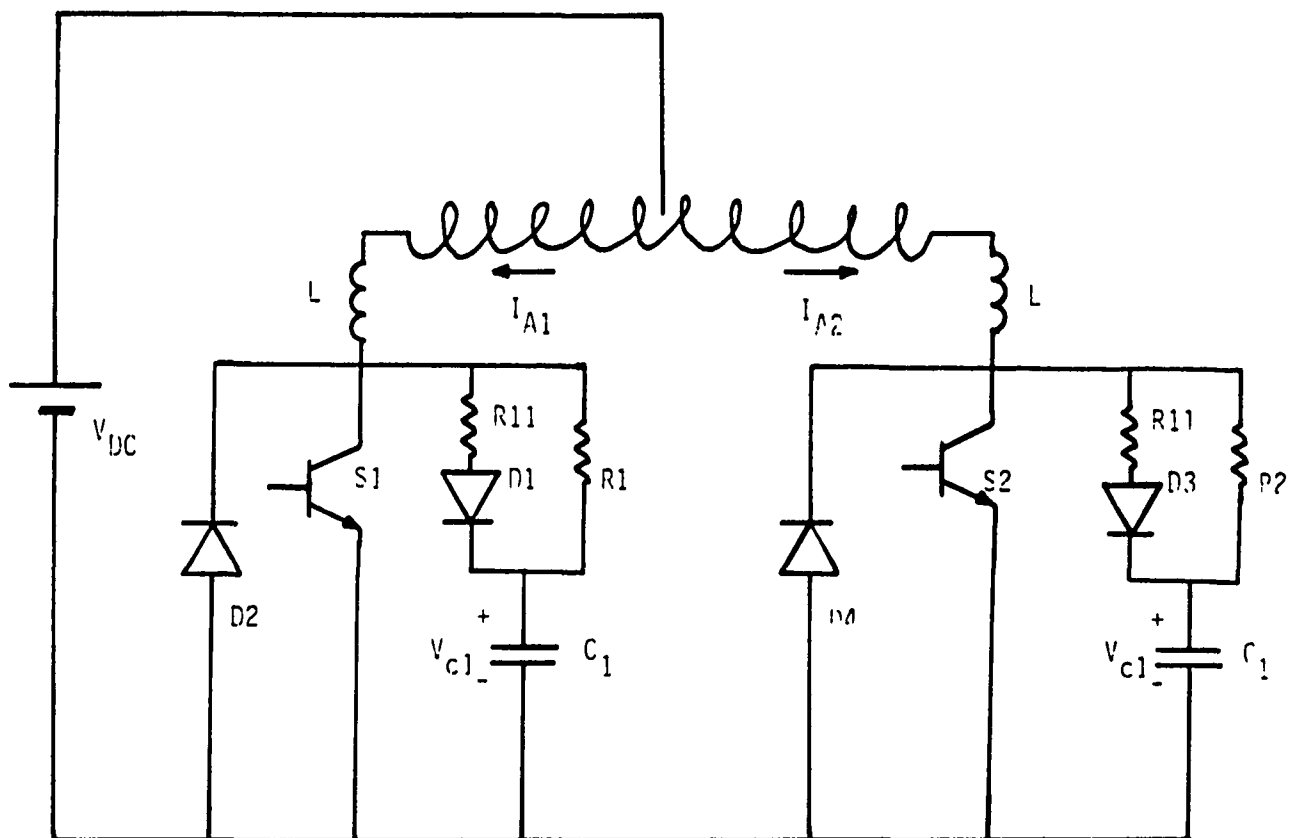


Fig. F-10 Switching devices and snubber circuits only for A phase

where τ is the exponential time constant. Then the discharging current i_S is

$$i_S = \frac{v_C - v_{S1}}{R} = \frac{2V_{DC}}{R} (e^{-t/\tau_S} - e^{-t/\tau}) \frac{\tau_S}{\tau_S - \tau} \quad (19)$$

where $\tau_S = RC$.

The energy dissipated in $S1$ is

$$W_{S1} \approx \int_0^{\infty} v_{S1} i_{S1} dt = \frac{2V_{DC}^2}{R} \frac{\tau \tau_S}{\tau_S + \tau} \quad (20)$$

Since all of the initial stored energy in the snubber capacitor must be dissipated, the total turn-on switching energy loss is given by

(2) Turn-Off of $S1$ when $I_{A1} > 0$: While switch $S1$ is on, I_{A1} flows through $S1$.

The energy initially stored in the equivalent leakage L is

$$W_L = \frac{1}{2} L i_L^2(0) \quad (21)$$

where $i_L(0)$ is the current I_{A1} at the instant $S1$ turns off.

The final energy stored in C after the switch is open is

$$W_C = \frac{1}{2} C (2V_{DC})^2 = 2CV_{DC}^2 \quad (22)$$

An amount of energy equal to that in (22) is dissipated in the equivalent charging resistance for capacitor $C1$. Some of the initial stored energy in L is returned to the dc source, but the worst case turn-off switching energy loss is

$$W_L - W_C = \frac{1}{2} L i_L^2(0) + 2CV_{DC}^2 \quad (23)$$

(3) Turn-On of S1 When $I_{A2} > 0$: While switch S2 is on, I_{A2} flows through S2 and capacitor C1 is charged up to $2V_{DC}$. Even though S2 is turned off and the base current is supplied to switch S1, S1 is still open. If $|I_{A1}|$ is less than 48A, first capacitor C1 discharges its stored energy, and after the capacitor voltage V_{C1} minus the voltage drop across R1 goes to zero, diode D2 conducts. If $|I_{A1}|$ is larger than 48A, then diode D2 conducts very quickly after switch S2 is turned off.

The worst case energy loss is estimated to be equal to the stored energy in the capacitor. Thus, the loss energy is

$$W_C = \frac{1}{2} C (2V_{DC})^2 = 2CV_{DC}^2 \quad (24)$$

(4) Turn-Off of S1 when $I_{A1} < 0$: While S2 is open, diode D2 is on, and capacitor voltage V_{C1} is zero. When S2 turns on, I_{A1} extinguishes and V_{C1} is charged up to $2V_{DC}$.

The loss calculation is very similar to case (2), and the total loss energy is

$$W_L + W_C = \frac{1}{2} L i_L^2(0) + 2CV_{DC}^2 \quad (25)$$

On-State Loss

The total on-state loss is the integral of the instantaneous power dissipated in the four switch branches, which is

$$P_{ON} = \frac{1}{T} \left[\int_0^{t_{ON,1}} V_{S1} i_{S1} dt + \int_{t_{ON,1}}^{t_{ON,1}+t_{OFF,1}} V_{D1} i_{D1} dt + \int_{t_{ON,1}+t_{OFF,1}}^{t_{ON,1}+t_{ON,2}+t_{OFF,1}} V_{S1} i_{S1} dt + \dots \dots \dots \right] \times 4$$

$$= [d(V_{S1} I_{S1}) + (1-d) V_{D1} I_{D1}] \times 4 \quad (26)$$

where $d \triangleq$ duty cycle of switching

$V_{S1} \triangleq$ on-state voltage drop across S1 (assumed constant)

$I_{S1} \triangleq$ average current through S1

$V_{D1} \triangleq$ diode drop (assumed constant)

$I_{D1} \triangleq$ average current through diode

and (26) assumes that the average currents over the cycle through the transistor and the diode are equal.

Summary

The total switching energy loss w_{SW} for one switching is given by adding the turn-on energy loss, (17), and the turn-off energy loss, (23) or (25).

$$w_{SW} = \frac{1}{2} L i_L^2(0) + 4CV_{DC}^2 \quad (27)$$

and the total switching loss over a period T is

$$\begin{aligned} P_{SW} &= \frac{1}{T} \sum_{n=0}^N \left[\frac{1}{2} L i_L^2(t_n) + 4CV_{DC}^2 \right] \times 4 \\ &\approx \left[\frac{1}{2} L I_{L,RMS}^2 f_S + 4CV_{DC}^2 f_S \right] \times 4 \end{aligned} \quad (28)$$

The total on-state loss is given by (26). Thus, the total inverter loss is the sum of (26) and (28)

$$P_T = \left[\frac{1}{2} L I_{L,RMS}^2 f_S + 4CV_{DC}^2 f_S + dV_{S1} I_{S1} - (1-d) V_{D1} I_{D1} \right] \times 4$$

Calculated Losses

13.1 kW output at 80% speed

$$I_{rms} = 53.2A; I_p = 103A; f_S = 1.6 \text{ kHz}$$

$$d = 0.72/2 = 0.36; V_{S1} = 1.8V; V_{D1} = 0.8V$$

$$I_{ave} = 48.8/2 = 24.4A/\text{device}$$

On-State Loss from (26)

$$P_{on} = [0.36 \times 1.2 \times 24.4 + 0.64 \times 0.8 \times 24.4] \times 4 = 113.2$$

Switching loss from (28)

$$P_{sw} = [0.5 \times 4 \times 10^{-6} \times 53.2^2 + 4 \times 0.33 \times 10^{-6} \times 240^2] \times 1.6 \times 10^3 \\ \times 4 = 522.8$$

Total: 636.0 W

Efficiency: 95.4%

16.4 kW output at 10% speed

$$I_{rms} = 200A; I_p = 245A; f_S = 3.4\text{kHz}$$

$$d = 0.6/2 = 0.3; V_{S1} = 1.8V; V_{D1} = 0.8V$$

$$I_{ave} = 197.4/2 = 98.7A/\text{device}$$

On-State Loss from (26)

$$P_{on} = [0.3 \times 1.8 \times 98.7 + 0.7 \times 0.8 \times 98.7] \times 4 = 434.3$$

Switching Loss from (28)

$$P_{sw} = [0.5 \times 4 \times 10^{-6} \times 200^2 + 4 \times 0.33 \times 10^{-6} \times 240^2] \times 3.4 \times 10^3 \\ \times 4 = 2,122.0$$

Total: 2,556.3 W

Efficiency: 86.5%

60.5 kW Output at 80% Speed

$$I_{rms} = 175A; I_p = 245A; f_S = 160Hz$$

$$d = 0.83/2 = 0.42; V_{S1} = 18V; V_{D1} = 0.8V$$

$$I_{ave} = 173/2 = 86.5A/\text{device}$$

On-State Loss from (26)

$$P_{on} = [0.42 \times 1.8 \times 86.5 + 0.58 \times 0.8 \times 86.5] \times 4 = 422.1$$

Switching Loss from (28)

$$P_{sw} = [0.5 \times 4 \times 10^{-6} \times 175^2 + 4 \times 0.33 \times 10^{-6} \times 240^2] \times 160 \times 4 = \\ 87.9$$

Total: 510.0 W

Efficiency: 99.2%

F.5 CONTROLLER

The microprocessor based controller system must generate the required driving signals for the power transistors to implement current controlled PWM. The hardware necessary for this controller is shown in Fig. F-11 which consists of the main CPU, ROM, RAM, I/O ports and other electronic components. The controller sets the output frequency of the inverter drive, in reference to the driving command, from 0-200Hz. In addition, the controller sets the amplitude and the envelope of the controlled current at any given load and speed to provide maximum efficiency with acceptable torque pulsations. The closed loop control diagram is shown in Fig. F-12.

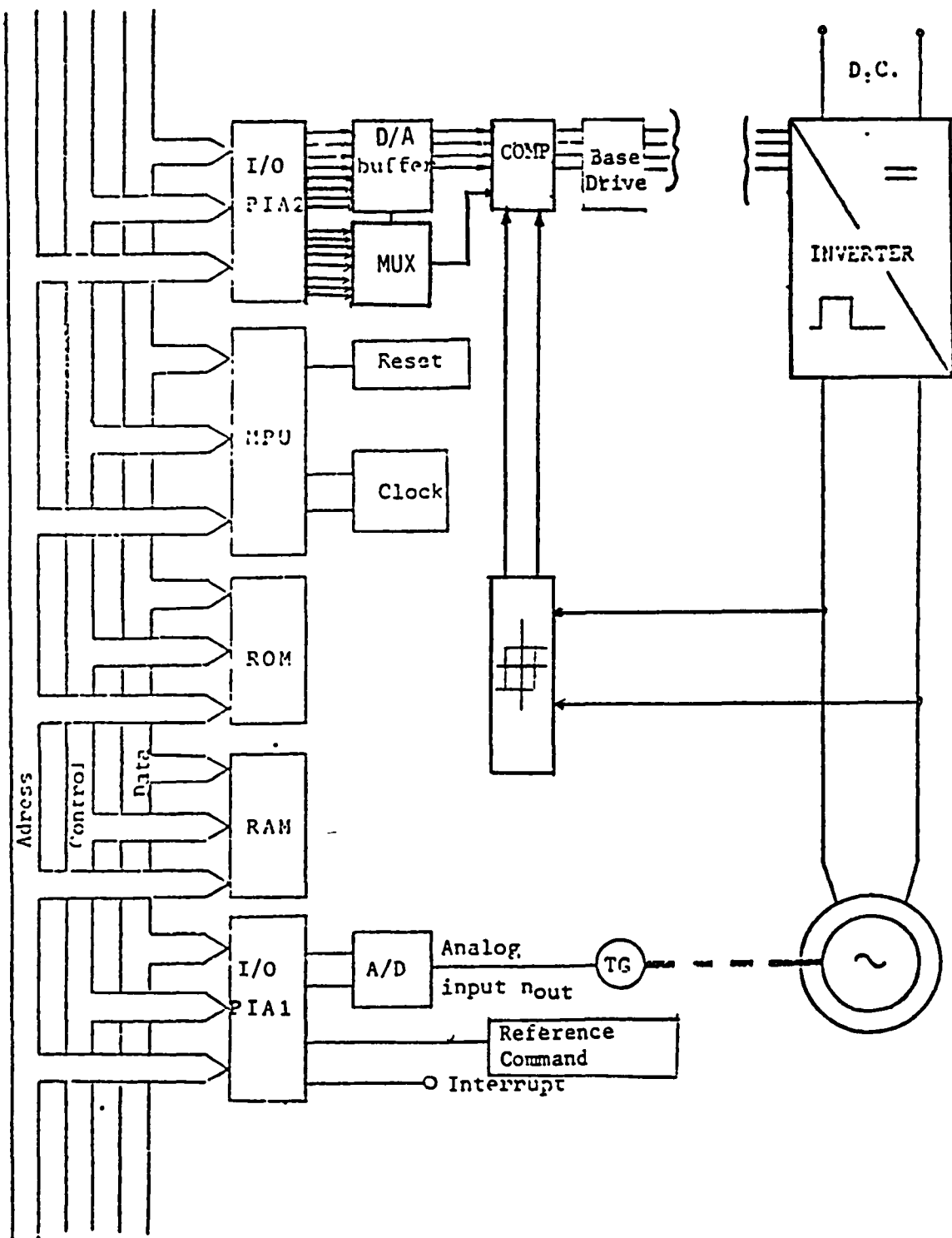


Fig. F-11 System hardware

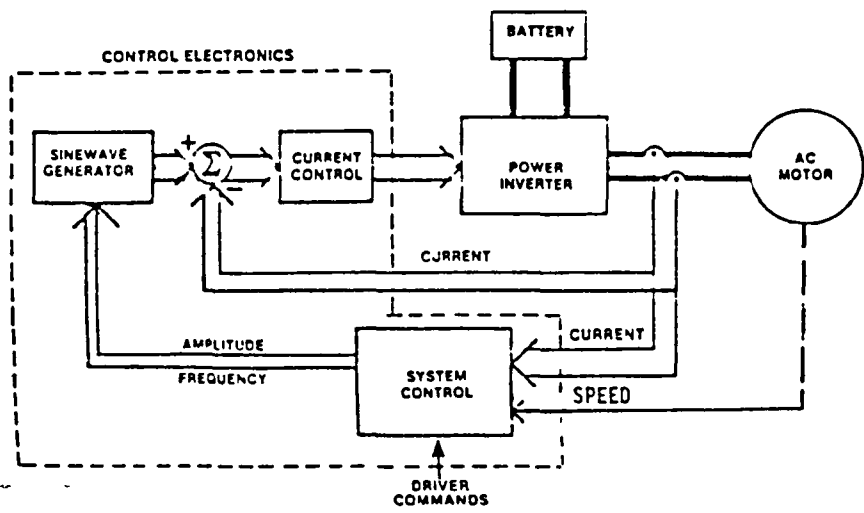


Fig. F-12 Closed loop control

APPENDIX G**SIMULATION RESULTS**

G.1 DERIVATION OF EQUATIONS FOR TWO-PHASE MACHINE

The circuit diagram of the two-phase inverter/bifilar induction motor is shown in Fig. 2, section 3.0 of this report. Fig. G-1 shows the expected phase voltage and current waveforms without PWM current control. The phase relationships between the stator and rotor windings are shown in Fig. G-2.

The derivation of the simulation model for the two-phase induction motor proceeds as follows:

$$\text{Let } L_{1SA} = L_{1SB} = L_{1S}, \quad L_{1rA} = L_{1rB} = L_{1r}$$

$$L_S = L_{1S} + L_m, \quad L_r = L_{1r} + L_m$$

L_m is the mutual inductance of A-phase or B-phase

i_{AS}, i_{BS} have the frequency of supply (ω)

i_{Ar}, i_{Br} have the frequency of the slip ($\omega - \omega_r$)

$$\begin{aligned} v_{AS} &= R_S i_{AS} + L_{1S} \frac{di_{AS}}{dt} + \frac{d}{dt} \lambda_{AS} \\ v_{BS} &= R_S i_{BS} + L_{1S} \frac{di_{BS}}{dt} + \frac{d}{dt} \lambda_{BS} \\ v_{Ar} &= R_r i_{Ar} + L_{1r} \frac{di_{Ar}}{dt} + \frac{d}{dt} \lambda_{Ar} \\ v_{Br} &= R_r i_{Br} + L_{1r} \frac{di_{Br}}{dt} + \frac{d}{dt} \lambda_{Br} \end{aligned} \tag{1}$$

$$\lambda_{AS} = L_m i_{AS} + L_m i_{Ar} \cos \theta - L_m i_{Br} \sin \theta$$

$$\lambda_{BS} = L_m i_{BS} + L_m i_{Ar} \sin \theta + L_m i_{Br} \cos \theta$$

$$\lambda_{Ar} = L_m i_{Ar} + L_m i_{AS} \cos \theta + L_m i_{BS} \sin \theta$$

$$\lambda_{Br} = L_m i_{Br} - L_m i_{AS} \sin \theta + L_m i_{BS} \cos \theta$$

(2)

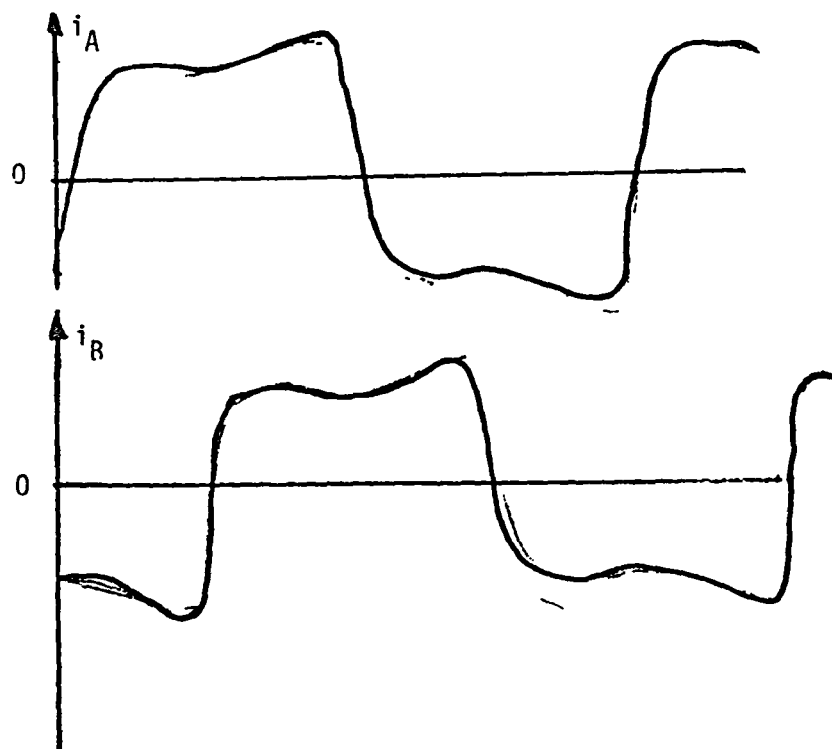
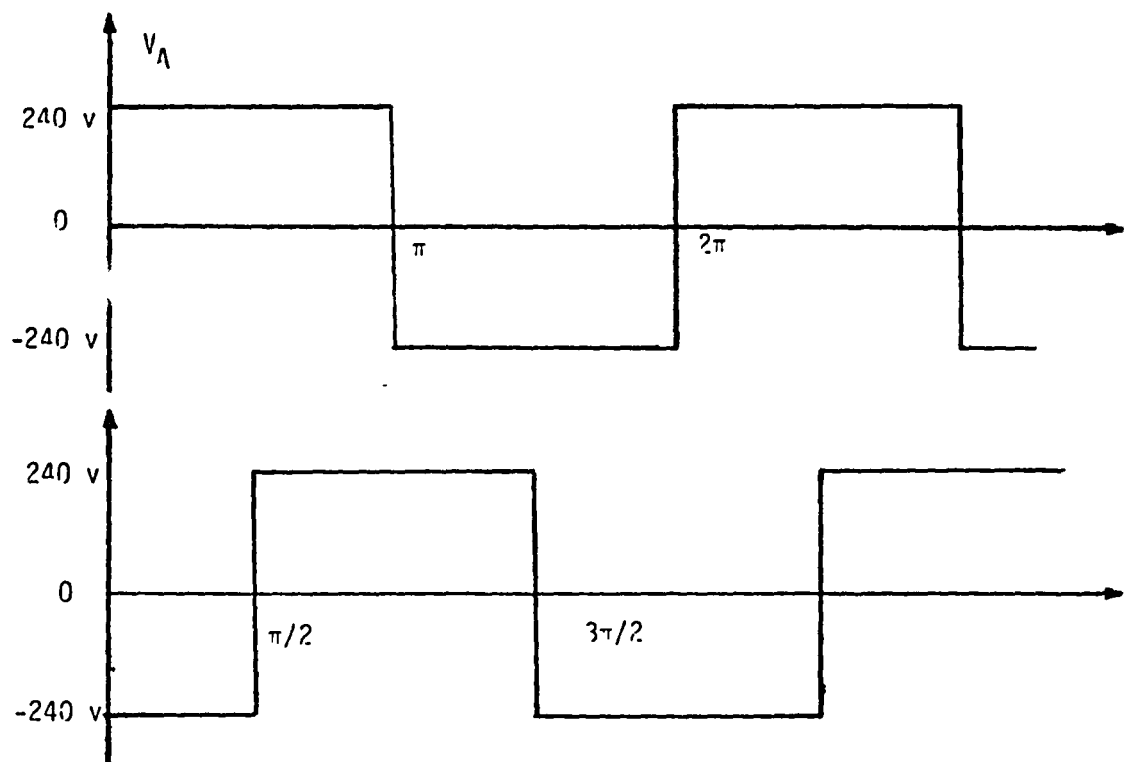


Fig. G-1 Expected Waveforms without peak current controller

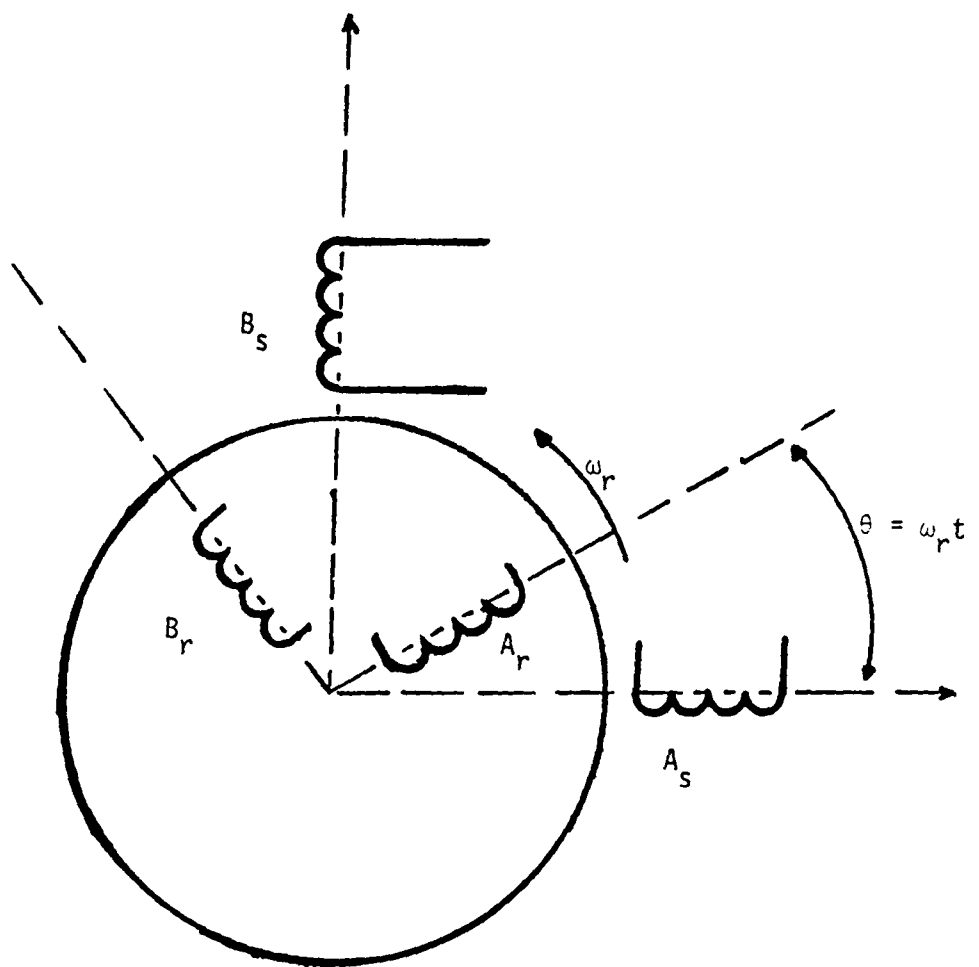


Fig. G-2 Phase relationship of stator and rotor

Equations (1) and (2) can be expressed in matrix form as follows:

$$\begin{vmatrix} \vec{v}_S \\ \vec{v}_r \end{vmatrix} = \begin{vmatrix} \bar{R}_S & 0 \\ 0 & \bar{R}_r \end{vmatrix} \begin{vmatrix} \vec{i}_S \\ \vec{i}_r \end{vmatrix} + \begin{vmatrix} L_{1s} & 0 \\ 0 & L_{1r} \end{vmatrix} \frac{d}{dt} \begin{vmatrix} \vec{i}_S \\ \vec{i}_r \end{vmatrix} + \frac{d}{dt} \begin{vmatrix} L_1 & L_2 \\ L_3 & L_4 \end{vmatrix} \begin{vmatrix} \vec{i}_S \\ \vec{i}_r \end{vmatrix} \quad (3)$$

where

$$\bar{R}_S \triangleq \begin{vmatrix} R_S & 0 \\ 0 & R_S \end{vmatrix} \quad \bar{R}_r \triangleq \begin{vmatrix} R_r & 0 \\ 0 & R_r \end{vmatrix}$$

$$L_{1s} \triangleq \begin{vmatrix} L_{1s} & 0 \\ 0 & L_{1s} \end{vmatrix} \quad L_{1r} \triangleq \begin{vmatrix} L_{1r} & 0 \\ 0 & L_{1r} \end{vmatrix}$$

$$\vec{v}_S \triangleq \begin{vmatrix} v_{AS} \\ v_{BS} \end{vmatrix} \quad \vec{v}_r \triangleq \begin{vmatrix} v_{Ar} \\ v_{Br} \end{vmatrix} \quad \vec{i}_S \triangleq \begin{vmatrix} i_{AS} \\ i_{BS} \end{vmatrix} \quad \vec{i}_r \triangleq \begin{vmatrix} i_{Ar} \\ i_{Br} \end{vmatrix}$$

$$L_1 \triangleq \begin{vmatrix} L_m & 0 \\ 0 & L_m \end{vmatrix} \quad L_2 \triangleq \begin{vmatrix} L_m \cos\theta & -L_m \sin\theta \\ L_m \sin\theta & L_m \cos\theta \end{vmatrix}$$

$$L_3 \triangleq \begin{vmatrix} L_m \cos\theta & L_m \sin\theta \\ -L_m \sin\theta & L_m \cos\theta \end{vmatrix} \quad L_4 \triangleq \begin{vmatrix} L_m & 0 \\ 0 & L_m \end{vmatrix}$$

$$\begin{vmatrix} \vec{v}_S \\ \vec{v}_r \end{vmatrix} = \begin{vmatrix} \bar{R}_S & 0 \\ 0 & \bar{R}_r \end{vmatrix} \begin{vmatrix} \vec{i}_S \\ \vec{i}_r \end{vmatrix} + \begin{vmatrix} L_{1s} & 0 \\ 0 & L_{1r} \end{vmatrix} \begin{vmatrix} \dot{\vec{i}}_S \\ \dot{\vec{i}}_r \end{vmatrix} + \frac{d}{dt} \begin{vmatrix} L_1 \vec{i}_S + L_2 \vec{i}_r \\ L_3 \vec{i}_S + L_4 \vec{i}_r \end{vmatrix}$$

$$\begin{aligned}
 &= \left| \frac{\bar{R}_S}{\bar{R}_r} - \frac{\dot{i}_S}{\dot{i}_r} \right| + \left| \frac{\bar{L}_1 S}{\bar{L}_1 r} - \frac{\dot{i}_S}{\dot{i}_r} \right| + \left| \frac{\dot{L}_1 \dot{i}_S + L_1 \dot{i}_S}{\dot{L}_3 \dot{i}_S + L_3 \dot{i}_S} - \frac{\dot{L}_2 \dot{i}_r + L_2 \dot{i}_r}{\dot{L}_4 \dot{i}_r + L_4 \dot{i}_r} \right| \\
 &= \left| \frac{\bar{R}_S + \dot{L}_1}{\dot{L}_3} \right| \left| \frac{\dot{L}_2}{\bar{R}_r + L_4} \right| \left| \frac{\dot{i}_S}{\dot{i}_r} \right| + \left| \frac{\bar{L}_1 S + L_1}{L_3} \right| \left| \frac{L_2}{\bar{L}_1 r + L_4} \right| \left| \frac{\dot{i}_S}{\dot{i}_r} \right| \quad (4)
 \end{aligned}$$

If i_{Ar} and i_{Br} are transformed to d-q coordinates which are fixed on the stator, that is, d-q axes rotating in the reverse direction relative to the rotor, then i_{Ar} and i_{Br} with angular velocity $(\omega - \omega_r)$ become i'_{Ar} and i'_{Br} with angular velocity (ω) .

$$\begin{aligned}
 \dot{i}'_r &\triangleq \begin{vmatrix} i'_{Ar} \\ i'_{Br} \end{vmatrix} & \dot{i}_r &\triangleq \bar{C} \dot{i}'_r \\
 \dot{i}'_r &\triangleq \bar{C}^{-1} \dot{i}_r & \dot{i}_r &= \dot{\bar{C}} \dot{i}'_r + \bar{C} \dot{i}_r
 \end{aligned} \quad (5)$$

$$\dot{i}'_r \triangleq \bar{C}^{-1} \dot{i}_r \quad \dot{i}_r = \dot{\bar{C}} \dot{i}'_r + \bar{C} \dot{i}_r$$

$$\bar{C} = \begin{vmatrix} \cos(-\theta) & -\sin(-\theta) \\ \sin(-\theta) & \cos(-\theta) \end{vmatrix} = \begin{vmatrix} \cos\theta & \sin\theta \\ -\sin\theta & \cos\theta \end{vmatrix}$$

$$\bar{C}^{-1} = \begin{vmatrix} \cos\theta & -\sin\theta \\ \sin\theta & \cos\theta \end{vmatrix} \quad \dot{\bar{C}} = \begin{vmatrix} -\omega_r \sin\theta & -\omega_r \cos\theta \\ \omega_r \cos\theta & -\omega_r \sin\theta \end{vmatrix}$$

$$\theta \triangleq \omega_r t$$

From (4) and (5),

$$\left| \frac{\dot{V}_S}{\bar{C}^{-1} \dot{V}_r} \right| = \left| \frac{\bar{R}_S + \dot{L}_1}{\bar{C}^{-1} \dot{L}_3} \right| \left| \frac{\dot{L}_2}{\bar{C}^{-1} (\bar{R}_r + L_4)} \right| \left| \frac{\dot{i}_S}{\dot{i}_r} \right| +$$

$$\begin{vmatrix} \dot{L}_1 S + L_1 & -L_2 \\ \bar{C}^{-1} L_3 & \bar{C}^{-1} (\bar{L}_{1r} + L_4) \end{vmatrix} \begin{vmatrix} \dot{i}_S \\ \bar{C} i_r + \bar{C} \dot{i}_r \end{vmatrix}$$

$$= \begin{vmatrix} \dot{\bar{R}}_S + \dot{L}_1 & \dot{L}_2 \bar{C} + L_2 \dot{\bar{C}} \\ \bar{C}^{-1} L_3 & \bar{C}^{-1} (\bar{R}_r + \dot{L}_4) \bar{C} \\ \end{vmatrix} \begin{vmatrix} \dot{i}_S \\ \dot{i}_r \end{vmatrix}$$

$$\begin{vmatrix} \dot{L}_1 S + L_1 & -L_2 \bar{C} \\ \bar{C}^{-1} L_3 & \bar{C}^{-1} (\bar{L}_{1r} + L_4) \bar{C} \end{vmatrix} \begin{vmatrix} \dot{i}_S \\ \dot{i}_r \end{vmatrix}$$

(6)

$$\textcircled{1} \quad \dot{\bar{R}}_S + \dot{L}_1 = \begin{vmatrix} R_S & 0 \\ 0 & R_S \end{vmatrix} \quad \text{Therefore, } \dot{L}_1 = \begin{vmatrix} 0 & 0 \\ 0 & 0 \end{vmatrix}$$

$$\textcircled{2} \quad \dot{L}_2 \bar{C} + \dot{L}_2 \bar{C} = \begin{vmatrix} -\omega_r L_m \sin\theta & -\omega_r L_m \cos\theta \\ \omega_r L_m \cos\theta & -\omega_r L_m \sin\theta \end{vmatrix} \begin{vmatrix} \cos\theta & \sin\theta \\ -\sin\theta & \cos\theta \end{vmatrix}$$

$$+ \begin{vmatrix} L_m \cos\theta & -L_m \sin\theta \\ L_m \sin\theta & L_m \cos\theta \end{vmatrix} \begin{vmatrix} -\omega_r \sin\theta & -\omega_r \cos\theta \\ \omega_r \cos\theta & -\omega_r \sin\theta \end{vmatrix} = |0|$$

$$\textcircled{3} \quad \bar{C}^{-1} \dot{L}_3 = \begin{vmatrix} \cos\theta & -\sin\theta \\ \sin\theta & \cos\theta \end{vmatrix} \begin{vmatrix} -\omega_r L_m \sin\theta & \omega_r L_m \cos\theta \\ -\omega_r L_m \cos\theta & -\omega_r L_m \sin\theta \end{vmatrix} = \begin{vmatrix} 0 & \omega_r L_m \\ -\omega_r L_m & 0 \end{vmatrix}$$

$$\textcircled{4} \quad \bar{C}^{-1}(\bar{R}_r + \dot{\bar{L}}_4) \bar{C} + \bar{C}^{-1}(\bar{L}_{1r} + \bar{L}_4) \dot{\bar{C}}$$

$$= \begin{vmatrix} R_r & 0 \\ 0 & R_r \end{vmatrix} + \begin{vmatrix} \cos\theta & -\sin\theta \\ \sin\theta & \cos\theta \end{vmatrix} \begin{vmatrix} L_r & 0 \\ 0 & L_r \end{vmatrix} = \begin{vmatrix} -\omega_r \sin\theta & \omega_r \cos\theta \\ -\omega_r \cos\theta & -\omega_r \sin\theta \end{vmatrix}$$

$$= \begin{vmatrix} R_r & 0 \\ 0 & R_r \end{vmatrix} + \begin{vmatrix} 0 & \omega_r L_r \\ -\omega_r L_r & 0 \end{vmatrix} = \begin{vmatrix} R_r & \omega_r L_r \\ -\omega_r L_r & R_r \end{vmatrix}$$

$$\textcircled{5} \quad \bar{L}_{1s} + L_1 = \begin{vmatrix} L_{1s} & 0 \\ 0 & L_{1s} \end{vmatrix} + \begin{vmatrix} L_m & 0 \\ 0 & L_m \end{vmatrix} = \begin{vmatrix} L_s & 0 \\ 0 & L_s \end{vmatrix}$$

$$\textcircled{6} \quad L_2 \bar{C} = \begin{vmatrix} L_m \cos\theta & -L_m \sin\theta \\ L_m \sin\theta & L_m \cos\theta \end{vmatrix} \begin{vmatrix} \cos\theta & \sin\theta \\ -\sin\theta & \cos\theta \end{vmatrix} = \begin{vmatrix} L_m & 0 \\ 0 & L_m \end{vmatrix}$$

$$\textcircled{7} \quad \bar{C}^{-1} L_3 = \begin{vmatrix} \cos\theta & -\sin\theta \\ \sin\theta & \cos\theta \end{vmatrix} \begin{vmatrix} L_m \cos\theta & L_m \sin\theta \\ -L_m \sin\theta & L_m \cos\theta \end{vmatrix} = \begin{vmatrix} L_m & 0 \\ 0 & L_m \end{vmatrix}$$

$$\textcircled{8} \quad \bar{C}^{-1}(\bar{L}_{1r} + \bar{L}_4) \bar{C} = \begin{vmatrix} L_r & 0 \\ 0 & L_r \end{vmatrix}$$

So equation $\textcircled{6}$ becomes

$$\begin{vmatrix} \dot{\bar{V}}_s \\ \bar{C}^{-1} \dot{\bar{V}}_r \end{vmatrix} = \begin{vmatrix} R_s & 0 & | & 0 \\ 0 & -\frac{R_s}{\omega_r L_m} & | & -\frac{R_r}{\omega_r L_r} \\ -\omega_r L_m & 0 & | & -\omega_r L_r & R_r \end{vmatrix} \begin{vmatrix} \dot{\bar{V}}_s \\ \dot{\bar{V}}_r \end{vmatrix} +$$

$$\begin{array}{c}
 \left| \begin{array}{cc|cc} L_S & 0 & L_m & 0 \\ 0 & L_S & 0 & L_m \\ \hline L_m & 0 & L_r & 0 \\ 0 & L_m & 0 & L_r \end{array} \right| \quad \left| \begin{array}{c} \dot{i}_S \\ -\dot{i}_r \end{array} \right| \\
 \dot{i}_S = \left| \begin{array}{c} \dot{i}_{AS} \\ \cdot \\ \dot{i}_{BS} \end{array} \right| \quad \dot{i}_r = \left| \begin{array}{c} \dot{i}_{Ar} \\ \cdot \\ \dot{i}_{Br} \end{array} \right| \quad \dot{i}_{AS} \triangleq \frac{di_{AS}}{dt} = pi_{AS} \dots
 \end{array} \quad (7)$$

If the machine has a squirrel-cage rotor, then

$$\bar{C}^{-1} \dot{v}_r = \begin{pmatrix} 0 \\ 0 \end{pmatrix}$$

Therefore

$$\begin{array}{c}
 \left| \begin{array}{c} v_{AS} \\ v_{BS} \\ 0 \\ 0 \end{array} \right| = \left| \begin{array}{cccc} R_S + L_S p & 0 & L_m p & 0 \\ 0 & R_S + L_S p & 0 & L_m p \\ L_m p & \omega_r L_m & R_r + L_r p & \omega_r L_r \\ -\omega_r L_m & L_m p & -\omega_r L_r & R_r + L_r p \end{array} \right| \quad \left| \begin{array}{c} i_{AS} \\ i_{BS} \\ i'_{Ar} \\ i'_{Br} \end{array} \right| \\
 (8)
 \end{array}$$

The commonly used torque equation is

$$T = pL_m (i_{BS} i'_{Ar} - i_{AS} i'_{Br}) \quad (9)$$

Equations (8) and (9) are the mathematical model for simulation of the two-phase machine. Equation (8) can be changed to the form

$$\begin{array}{c}
 \left| \begin{array}{c} v_{AS} \\ v_{BS} \\ 0 \\ 0 \end{array} \right| = \left| \begin{array}{cccc} R_S & 0 & 0 & 0 \\ 0 & R_S & 0 & 0 \\ 0 & 0 & R_r & 0 \\ 0 & 0 & 0 & R_r \end{array} \right| \quad \left| \begin{array}{c} i_{AS} \\ i_{BS} \\ i'_{Ar} \\ i'_{Br} \end{array} \right| + \left| \begin{array}{cccc} L_{1S} + L_m & 0 & L_m & 0 \\ 0 & L_{1S} + L_m & 0 & L_m \\ L_m & 0 & L_{1r} + L_m & 0 \\ 0 & L_m & 0 & L_{1r} + L_m \end{array} \right| \quad \left| \begin{array}{c} \cdot \\ i_{AS} \\ i_{BS} \\ i'_{Ar} \\ i'_{Br} \end{array} \right|
 \end{array}$$

$$+ \begin{vmatrix} 0 & 0 & 0 & 0 \\ 0 & 0 & 0 & 0 \\ 0 & \omega_r L_m & 0 & \omega_r (L_{1r} + L_m) \\ -\omega_r L_m & 0 & -\omega_r (L_{1r} + L_m) & 0 \end{vmatrix} \begin{vmatrix} i_{AS} \\ i_{BS} \\ i'_{Ar} \\ i'_{Br} \end{vmatrix} \quad (10)$$

where

$$\begin{vmatrix} L_S & 0 & L_m & 0 \\ 0 & L_S & 0 & L_m \\ L_m & 0 & L_r & 0 \\ 0 & L_m & 0 & L_r \end{vmatrix}^{-1} \triangleq \frac{1}{L_S L_r - L_m^2} \begin{vmatrix} L_r & 0 & -L_m & 0 \\ 0 & L_r & 0 & -L_m \\ -L_m & 0 & L_S & 0 \\ 0 & -L_m & 0 & L_S \end{vmatrix}$$

$$L_S \triangleq L_{1S} + L_m$$

$$L_r \triangleq L_{1r} + L_m$$

Then, (10) may be written

$$\begin{vmatrix} i_{AS} \\ i_{BS} \\ i'_{Ar} \\ i'_{Br} \end{vmatrix} = \frac{1}{L_S L_r - L_m^2} \begin{vmatrix} L_r & 0 & -L_m & 0 \\ 0 & L_r & 0 & -L_m \\ -L_m & 0 & L_S & 0 \\ 0 & -L_m & 0 & L_S \end{vmatrix} \begin{vmatrix} v_{AS} \\ v_{BS} \\ v'_{Ar}(0) \\ v'_{Br}(0) \end{vmatrix}$$

$$- \frac{1}{L_S L_r - L_m^2} \begin{vmatrix} L_r R_s & -L_m^2 \omega_r & -L_m R_r & -L_m L_r \omega_r \\ \omega_r L_m^2 & L_r R_s & L_m L_r \omega_r & -L_m R_r \\ -L_m R_s & L_s L_m \omega_r & L_s R_r & L_s L_r \omega_r \\ -L_s L_m \omega_r & -L_m R_s & -L_s L_r \omega_r & L_s R_r \end{vmatrix} \begin{vmatrix} i_{AS} \\ i_{BS} \\ i'_{Ar} \\ i'_{Br} \end{vmatrix} \quad (11)$$

or

$$\dot{i}_{AS} = \frac{1}{L_S L_r - L_m^2} (L_r V_{AS} - L_r R_S i_{AS} + L_m^2 \omega_r i_{BS} + L_m R_r i_{Ar} + L_m L_r \omega_r i_{Br})$$

$$\dot{i}_{BS} = \frac{1}{L_S L_r - L_m^2} (L_r V_{BS} - \omega_r L_m^2 i_{AS} - L_r R_S i_{BS} - L_m L_r \omega_r i_{Ar} + L_m R_r i_{Br})$$

$$\dot{i}_{Ar} = \frac{1}{L_S L_r - L_m^2} (-L_m V_{AS} + L_m R_S i_{AS} - L_S L_m \omega_r i_{BS} - L_S R_r i_{Ar} - L_S L_r \omega_r i_{Br})$$

$$\dot{i}_{Br} = \frac{1}{L_S L_r - L_m^2} (-L_m V_{BS} + L_S L_m \omega_r i_{AS} + L_m R_S i_{BS} + L_S L_r \omega_r i_{Ar} - L_S R_r i_{Br})$$

Let

$$A_{22} \triangleq L_S / A_{50}$$

$$A_{41} = (A_{31} i_{BS} + A_{26} i_{Br}') \times \omega_r$$

$$A_{26} = 2\pi L_r$$

$$A_{42} = (A_{31} i_{AS} + A_{26} i_{Ar}') \times \omega_r$$

$$A_{31} = 2\pi L_m$$

$$A_{47} = A_{42} - R_r i_{Br}'$$

$$A_{36} = L_r / A_{50}$$

$$A_{50} = L_S L_r - L_m^2$$

$$A_{38} = L_m / A_{50}$$

$$A_{53} = V_{BS} - R_S i_{BS}$$

$$A_{39} = P \times A_{31} / 2\pi$$

$$A_{61} = -A_{41} - R_r i_{Ar}'$$

$$A_{40} = V_{AS} - R_S i_{AS}$$

Therefore

$$\dot{i}_{AS} = A_{40} \times A_{36} - A_{61} \times A_{38} \triangleq x (1)$$

$$\dot{i}_{BS} = A_{53} \times A_{36} - A_{47} \times A_{38} \triangleq x (4)$$

$$\dot{i}_{Ar} = A_{61} \times A_{22} - A_{40} \times A_{38} \triangleq x (2)$$

$$\dot{i}_{Br} = A_{47} \times A_{22} - A_{53} \times A_{38} \triangleq x (3)$$

(12)

$$T = PL_m (i_{BS} i_{Ar}' - i_{AS} i_{Br}') = A_{39} (i_{BS} i_{Ar}' - i_{AS} i_{Br}') = A_{83}$$

The simulation diagram for (12) is shown in Fig. G-3.

The following sections of this appendix include simulation programs and results for different operating points, using the mathematical model of (12).

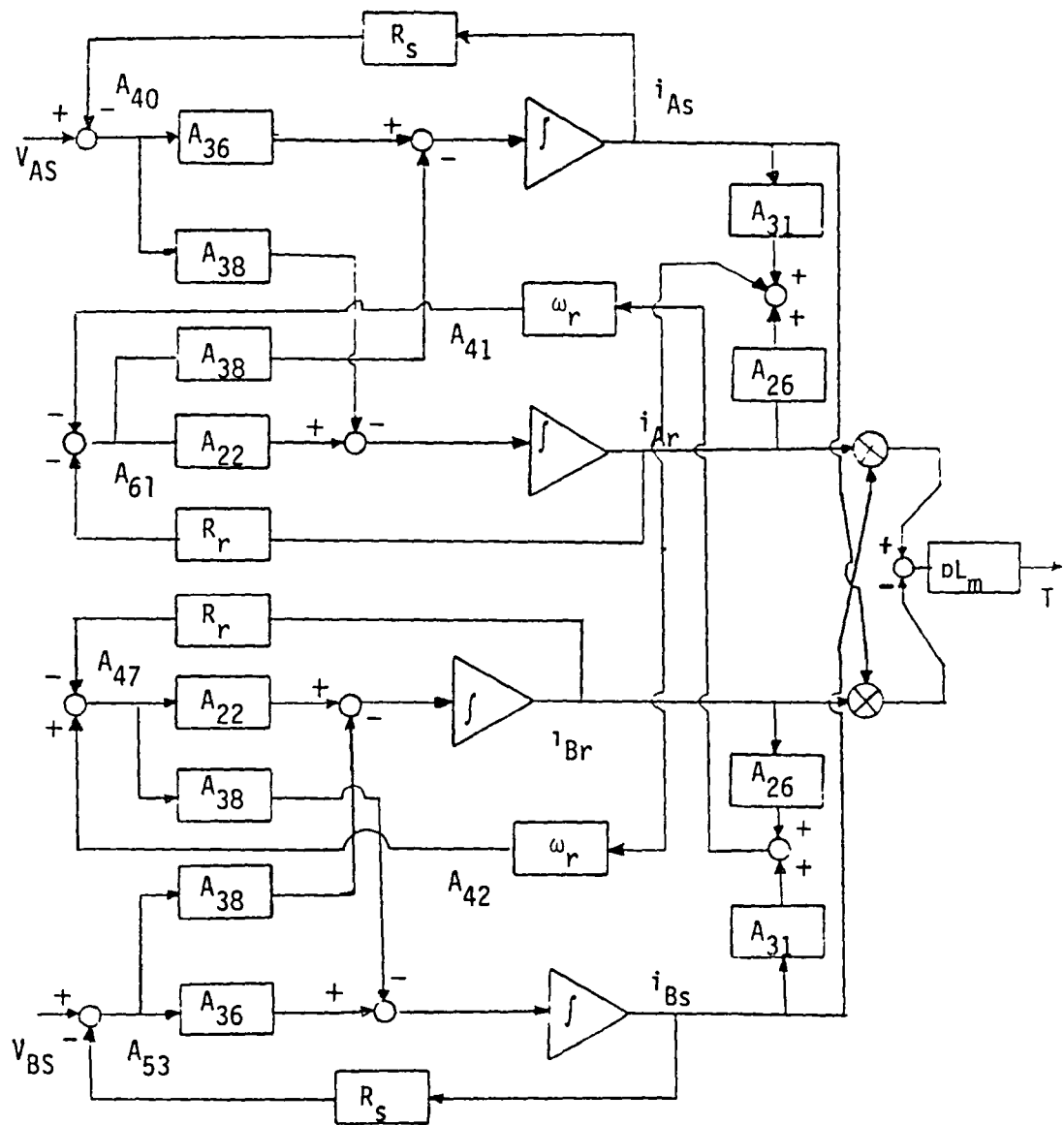


Fig. G-3 Simulation diagram of two-phase
induction motor

G.2 TWO-PHASE SIMULATION RESULTS FOR 10% SPEED, 16 KW

Source Program

Plots

 Stator Voltage

 Stator Current

 Output Power

 Current Spectrum

 Power Spectrum

Partial Listing of Plot Data

FILE: LS WATFIV A UNIVERSITY OF MISSOURI COMPUTER NETWORK

PAGE 001

```

//LS      JOB (XXXXLH),'GOODARZI',
// PASSWORD=XXXX
/*JOBPARM   T=5,L=6
//ROUTE PRINT UVMVMA.R12
// EXEC WATFIV
//GO.SYSIN DD *
$JOB           ,NOLIST,T=(5,0)
C*****                                                 *
C          10% SPEED,16KW JPL PROJECT                 *
C*****                                                 *
C*****                                                 *
DIMENSION AR1(800),AR2(800),AR3(800),Y(20),X(20),GA(20),PE(20),
1      XX(4,20),H(9),ZZ1(20),ZZ2(20),ZZ3(20),IFL(7),AR4(800),
2      AR5(800),AR6(800),AR7(800),AR8(800)
LOGICAL*1 LR1(800),LR2(800),LR3(800),LR4(800),LR5(800),LR6(800),
1      LR7(800),LR8(800)
REAL LOS,LOR,LM,IAS,IBS,ICS,IAR,IBR,ICR,IDS,IQS,IDR,IQR,LMDQ,INS,
1      POUT,IAREF,IBREF,L1,L2,M,IMAX,IMAGD,IMAGQ,IBU,
2      MAG1(512),MAG2(512)
COMPLEX F1(512),F2(512)
C      WRITE16,50)
C 50 FORMAT(/,3X,'TIME',8X,'VDS',8X,'IDS',8X,'VQS',8X,'IQS',8X,
C 4      'IDR',9X,'POUT')
      IMAX=205.
      SLIP=.085
      E=240.
      DI=40
      NRUN=1
      ISTOP=0
      KEEP=1
      IFL(1)=-1
      NINT=7
      IPNT1=0
      IPNT2=0
      IPNT3=0
      IPNT4=0
      IPNT5=0
      IPNT6=0
      IPNT7=0
C *****
C      PARAMETERS FOR TWOPHASE INDUCTION MOTOR
C *****
      LOS=.2256E-03
      LOR=.2410E-03
      LM=6.5100E-03
      RS=.0274
      RR=.0213
      PAI=3.141593
      P=1.
      FREQ=20.
      OMEGA=2*PAI*FREQ
      OMEGR=OMEGA*(1.-SLIP)
      L1=LOS+LM
      L2=LOR+LM

```

FILE: LS MATFIV A UNIVERSITY OF MISSOURI COMPUTER NETWORK

PAGE 002

```
M=LM
FACT=1./(L1*L2-M*M)
FACT1=L2*FACT
FACT2=L2*RS*FACT
FACT22=L1*RR*FACT
FACT3=M*M*OMEGR*FACT
FACT4=M*L2*OMEGR*FACT
FACT44=M*L1*OMEGR*FACT
FACT5=M*RR*FACT
FACT55=M*RS*FACT
FACT6=M*FACT
FACT7=L1*L2*OMEGR*FACT
1 IFL(2)=-1
2 CALL RKFOUR(NINT,Y,X,GA,PE,XX,H,ZZ1,ZZ2,ZZ3,TIME,PNTS,KEEP,IFL)
IF(IFL(4))3,4,5
3 INIT=1
TIME1=-1
NC=1
NCC=1
TIME=0.
FINTIM=2.0500
PTMAX=800.
Y(1)=0.
Y(2)=0.
Y(3)=0.
Y(4)=0.
Y(5)=0.0
Y(6)=0.0
Y(7)=0.0
AREAIN=0.0
ARADOUT=0.0
H(1)=0.2000E-04
C H(7)=-1
VDS=0.0
VQS=0.0
IN=0
SUM=0.
SUM1=0.
NUMBER=0.
SW=0.0
SWITCH=0.0
PSW=0.0
TOTSW=0.0
IAE=-1
IBE=-1
DO 33 I=1,512
F1(I)=(0.0,0.0)
F2(I)=(0.0,0.0)
33 CONTINUE
C
4 IF(TIME-TIME1)7,8,7
7 TIME1=TIME
C
DEG=FREQ*TIME
IDEG=DEG
```

FILE: LS WATFIV A UNIVERSITY OF MISSOURI COMPUTER NETWORK

PAGE 003

```

DEG=(DEG-IDEG)*360.
C
IAREF=IMAX*SIN(OMEGA*TIME)
IBREF=IMAX*SIN(OMEGA*TIME-PAI/2.)
C
IF(IAREF.GT.0.0) IAREF=IMAX
IF(IAREF.LT.0.00) IAREF=-IMAX
IF(IBREF.GT.0.0) IBREF=IMAX
IF(IBREF.LT.0.00) IBREF=-IMAX
C
DIA=Y(1)-IAREF
DIB=Y(2)-IBREF
C
VDS=E
VQS=E
IF(IAREF.LT.0) VDS=-E
IF(IBREF.LT.0) VQS=-E
C
IF(TIME.LT.0.35000) GOTO 8
IF(DIA.GT.DI.AND.IAREF.GT.0.0)      GOTO 24
IF(DIA.GT.DI)          IAE=1
GOTO 27
24   IAE=1
IF(TIME.LT.2.0000) GOTO 27
SW=SW+1
PSW=ABS((240.*Y(1)*5.5E-06)/(6*0.050000))+PSW
27   IF(DIA.LT.(-DI)) IAE=0
IF(VDS.GT.0.0.AND.IAE.EQ.1) GOTO 18
IF(VDS.LT.0.0.AND.IAE.EQ.0) GOTO 18
GOTO 22
18   VDS=-VDS
IF(TIME.LT.2.0000) GOTO 22
SWITCH=SWITCH+1.
22   IF(DIB.GT.DI)      IBE=1
IF(DIB.LT.(-DI))      IBE=0
IF(VQS.GT.0.0.AND.IBE.EQ.1) GOTO 19
IF(VQS.LT.0.0.AND.IBE.EQ.0) GOTO 19
GOTO 23
19   VQS=-VQS
23   IF(TIME.GT.1.90000.AND.TIME.LT.1.9001) AREAIN=Y(6)
IF(TIME.GT.1.90000.AND.TIME.LT.1.9001) ARAOUT=Y(5)
IF(TIME.GT.1.90000.AND.TIME.LT.1.9001) ARMS=Y(7)
C
IF(TIME.LT.2.0000) GOTO 8
TOTSW=TOTSW+1.
C
8 CONTINUE
C
X(1)=FACT1*VDS-FACT2*Y(1)+FACT3*Y(2)+FACT4*Y(4)+FACT5*Y(3)
X(2)=FACT1*VQS-FACT2*Y(2)-FACT3*Y(1)-FACT4*Y(3)+FACT5*Y(4)
X(3)=-FACT6*VDS+FACT55*Y(1)-FACT44*Y(2)-FACT7*Y(4)-FACT22*Y(3)
X(4)=-FACT6*VQS+FACT55*Y(2)+FACT44*Y(1)+FACT7*Y(3)-FACT22*Y(4)
X(5)=LM*(Y(2)*Y(3)-Y(1)*Y(4))*OMEGR/.15
X(6)=(Y(1)*VDS+Y(2)*VQS)/.15
X(7)=Y(1)*Y(1)/.15

```

FILE: LS WATFIV A UNIVERSITY OF MISSOURI COMPUTER NETWORK

PAGE 004

```

C      GOTO 2
5 IPR=0
NC=NC-1
IF(NC)9,9,10
9 NC=NCC
IPR=1
10 IF(TIME.GE.FINTIM) ISTOP=1
IF((IPR+ISTOP).EQ.0) GOTO 11
C      IF(TIME.LT.2.0000)GOTO 11
IDS=Y(1)
IQS=Y(2)
IDR=Y(3)
IQR=Y(4)
C      IMAGD=IDS+IDR
IMAGQ=IQS+IQR
C      TQ=LM*(IQS*IDR-IDS*IQR)
POUT=TQ*OMEGR
C      PIN=IDS*VDS+IQS*VQS
C      SUM1=SUM1+PIN
C      SUM=SUM+POUT
C      NUMBER=NUMBER+1.
IF(TIME.LT.2.00) GOTO 38
IN=IN+1
C      F1(IN)=CMPLX(Y(1),0.0)
C      F2(IN)=CMPLX(POUT,0.0)
38 CONTINUE
WRITE(6,250)DEG,IDS,VDS,POUT
IF(TIME.LT.2.00035) POUT=0.0
CALL FPLOT(800,IPNT1,AR1,LR1,ISTOP,1,1,TIME,IDS)
CALL FPLOT(800,IPNT2,AR2,LR2,ISTOP,1,1,TIME,VDS)
C      CALL FPLOT(800,IPNT4,AR4,LR4,ISTOP,1,2,TIME,IQS)
C      CALL FPLOT(800,IPNT4,AR4,LR4,ISTOP,2,2,TIME,VQS)
CALL FPLOT(800,IPNT3,AR3,LR3,ISTOP,1,2,TIME,IMAGD)
C      CALL FPLOT(800,IPNT3,AR3,LR3,ISTOP,2,2,TIME,IDR)
CALL FPLOT(800,IPNT3,AR3,LR3,ISTOP,1,1,TIME,POUT)
C
11 INIT=0
IF(ISTOP)1,1,6
6 CONTINUE
250 FORMAT(' ',1X,F6.1,3(F9.1,2X))
C      AVER=SUM/NUMBER
C      AVER1=SUM1/NUMBER
C      EFF=AVER/AVER1
PIN=Y(6)-AREAIN
POUT=Y(5)-ARAOUT
RMS=(Y(7)-ARMS)**0.5
C      ****
C      NOTE .7 IS THE VOLTAGE DROP ACROSS THE DIODE
C      1.85 IS THE CE VOLTAGE OF THE TRANSISTOR
C      SWITCH IS THE # OF INTERVAL OF THE SWITCHING (DIODE CONDUCTION)
C      TOTSW IS TOTAL # OF INTEGRATION INTERVALS

```

FILE: LS HATFIV A UNIVERSITY OF MISSOURI COMPUTER NETWORK

PAGE 005

```

C PDIODE IS THE LOSS OF DIODE DURING CONDUCTION
C PTPANS IS THE ON TIME LOSS OF THE TRANSISTOR
C PSW IS THE SWITCHING LOSS OF EACH TRANSISTOR (E*I*TSW/T)
C TOTSL IS THE TOTAL LOSS OF THE SWITCH
C ****
C PDIODE=(SWITCH/TOTSW)*0.7*IMAX/PAI
C PTRANS=(1-SWITCH/TOTSW)*1.85*IMAX/PAI
C TOTSL=PDIODE+PTRANS+PSW
C TOT4SL=4*TOTSL
C DTRIO=SWITCH/TOTSW
C EFFIO=POUT/(TOT4SL+PIN)
C
C WRITE(6,702)POUT,EFFIO,SLIP,IMAX,DTRIO,RMS
C WRITE(6,703)SW,PSW,PTRANS,PDIODE,TOT4SL,IN
702 FORMAT(//,' POWER OUT=',F8.1,2X,'EFFIO=',F5.3,2X,'SLIP=',
1F7.5,2X,'IMAX=',F6.1,2X,'DTRIO=',F7.1,2X,'I(RMS)=',F6.2,///)
703 FORMAT(/,'#SW/CYC=',F5.1,8X,'PSW=',F6.1,3X,'PTRANS=',F5.1,
1 2X,'PDIODE=',F4.1,2X,'TOT4SL=',F6.1,5X,'IN=',I5,/////)
C WRITE(6,705)
705 FORMAT('1',3X,'Z',9X,'I HARMONIC ',9X,'P HARMONIC',//)
C706 FORMAT(2X,F5.1,5X,F12.8,5X,F15.8)
C ISTOP=0.0
CC CALL FFT(F1,9)
CC CALL FFT(F2,9)
CC DO 401 I=1,150
CC MAG1(I)=CABS(F1(I))/512.
CC MAG2(I)=CABS(F2(I))/512.
CC Z=FLOAT(I-1)
CC IF (I.EQ.1) MAG1(2)=270.
CC AMP1=MAG1(I)/MAG1(2)
CC AMP2=MAG2(I)/MAG2(1)
C WRITE(6,706) Z,AMP1,AMP2
CC IF(I.EQ.150) ISTOP=1
C
C CALL FPLOT(800,IPNT5,AR5,LR5,ISTOP,1,1,Z,AMP1)
C CALL FPLOT(800,IPNT6,AR6,LR6,ISTOP,1,1,Z,AMP2)
CC401 CONTINUE
STOP
END
SUBROUTINE FFT(X,M)
COMPLEX X(512),U,W,T
N=2**M
NV2=N/2
NM1=N-1
J=1
DO 7 I=1,NM1
IF(I.GT.J) GOTO 5
T=X(J)
X(J)=X(I)
X(I)=T
5 K=NV2
6 IF(K.GE.J)GO TO 7
J=J-K
K=K/2
GO TO 6

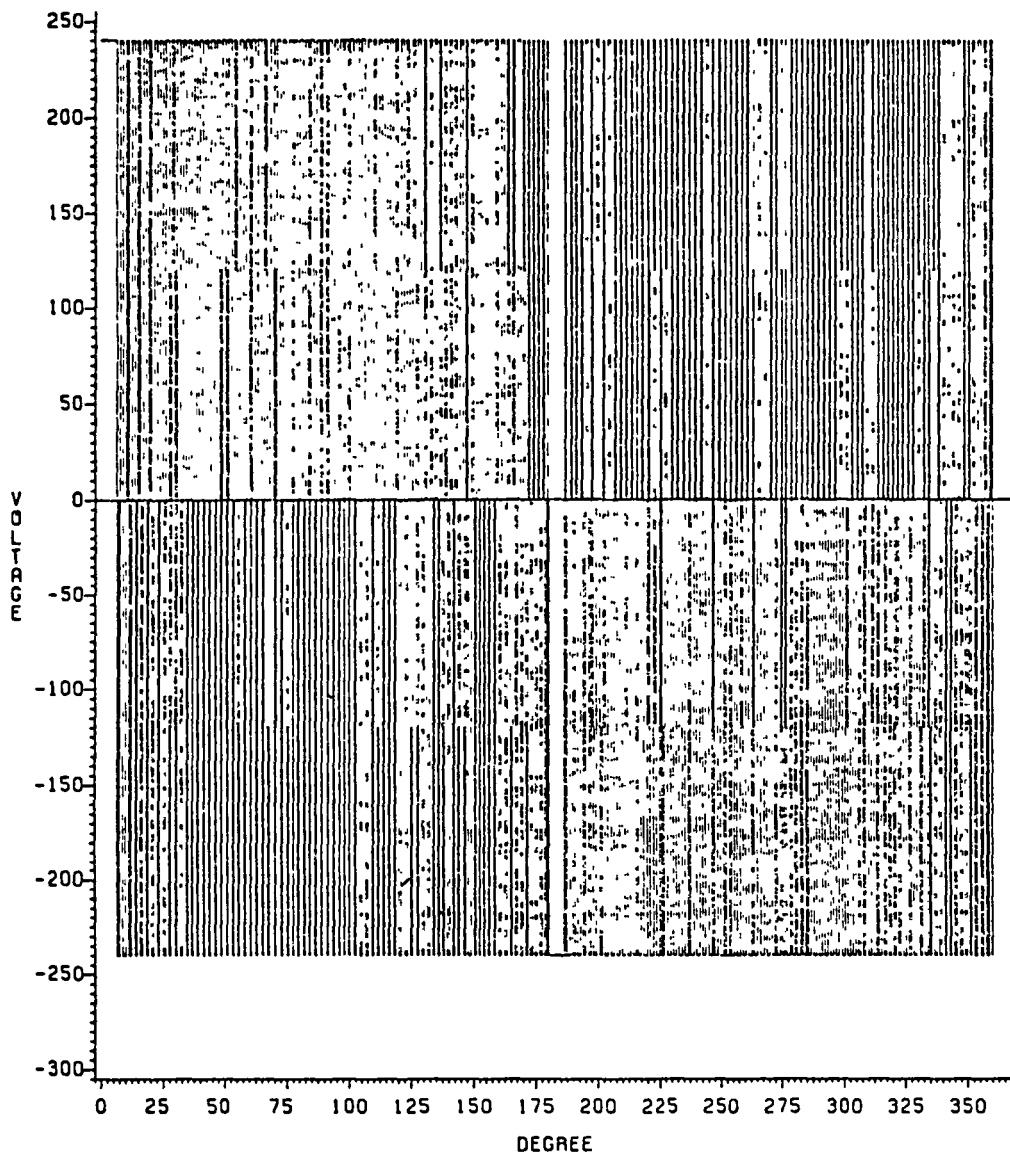
```

FILE: LS WATFIV A UNIVERSITY OF MISSOURI COMPUTER NETWORK

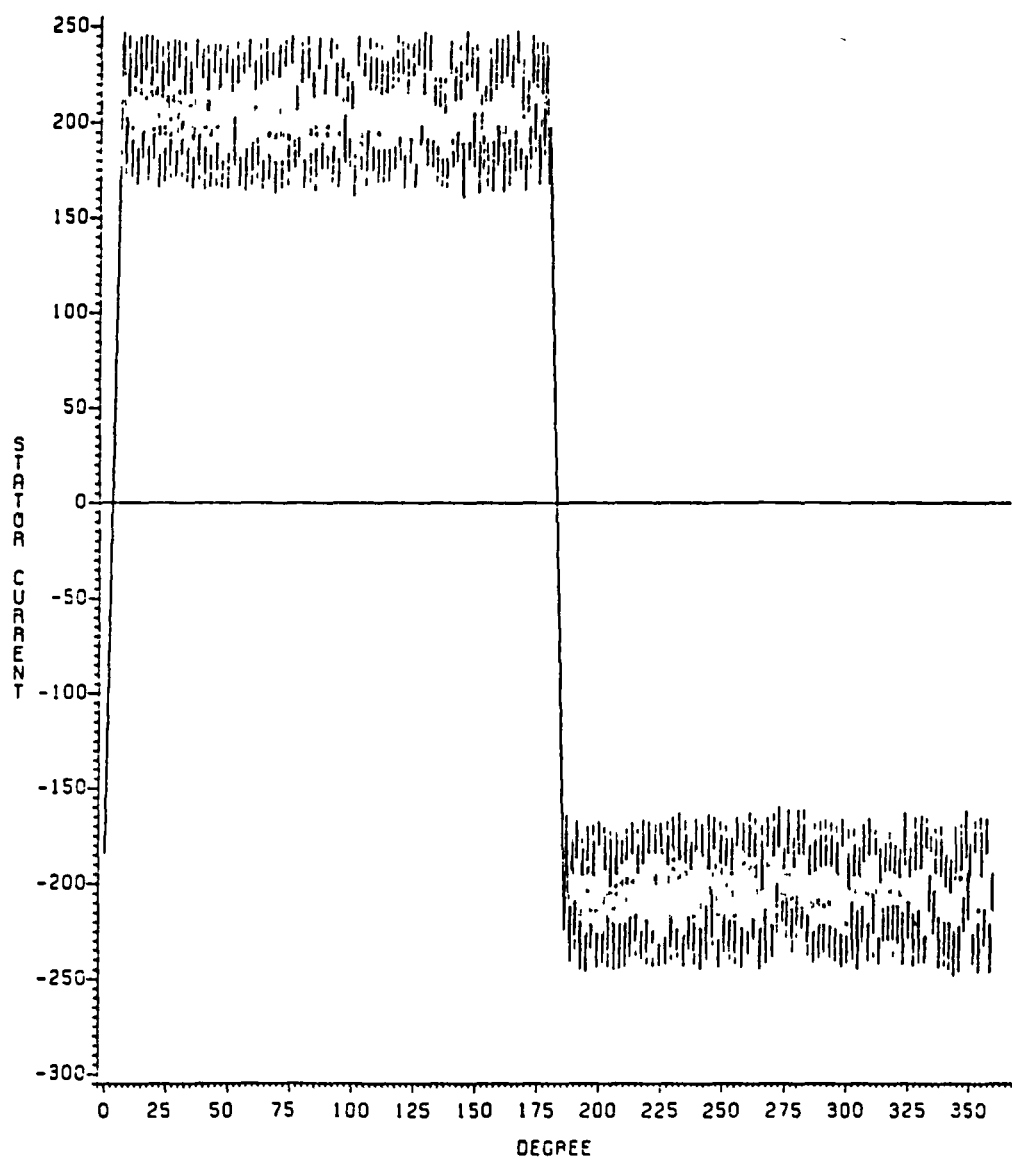
PAGE 006

```
7 J=J+K
PI=3.14159265358979
DO 20 L=1,M
LE=2**L
LE1=LE/2
U=(1.0,0.0)
Z=COS(PI/FLOAT(LE1))
Y=-SIN(PI/FLOAT(LE1))
W=CMPLX(Z,Y)
DO 20 J=1,LE1
DO 10 I=J,N,LE
IP=I+LE1
T=X(IP)*U
X(IP)=X(I)-T
10 X(I)=X(I)+T
20 U=U*W
RETURN
END
$ENTRY
1 I  CURRENT OF PHASE A STATOR
1 V  VOLTAGE OF PHASE A
1 P  POWER VS TIME
1 I  CURRENT FREQUENCY SPECTRUM
1 P  POWER FREQUENCY SPECTRUM
$STOP
/*
//
```

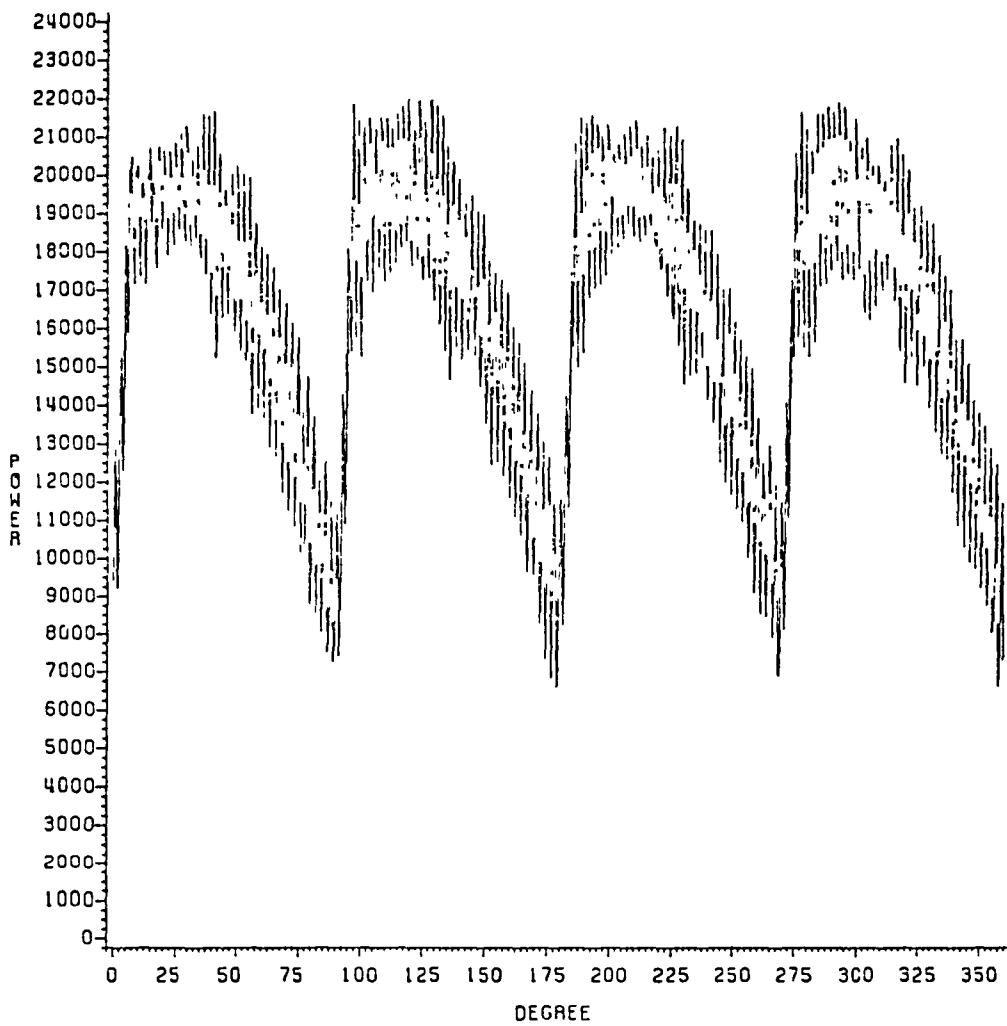
STATOR VOLTAGE (10% SPEED,16KW)



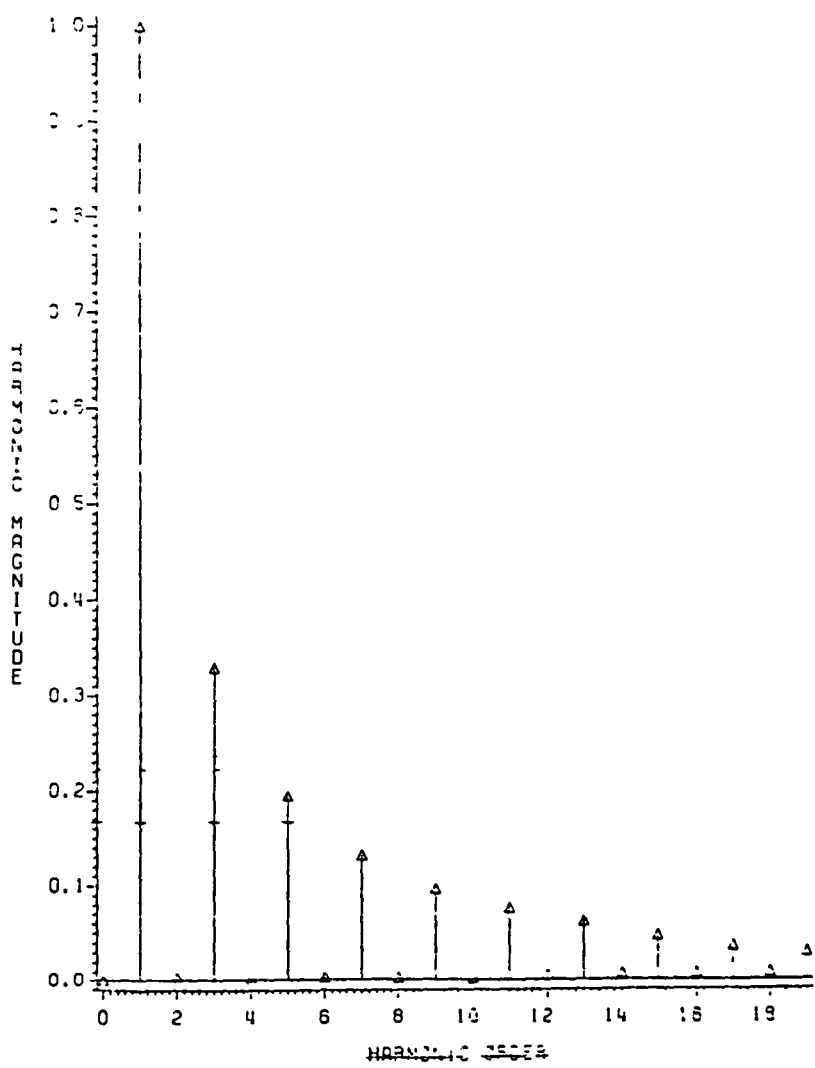
STATOR CURRENT (10% SPEED, 16 KW)



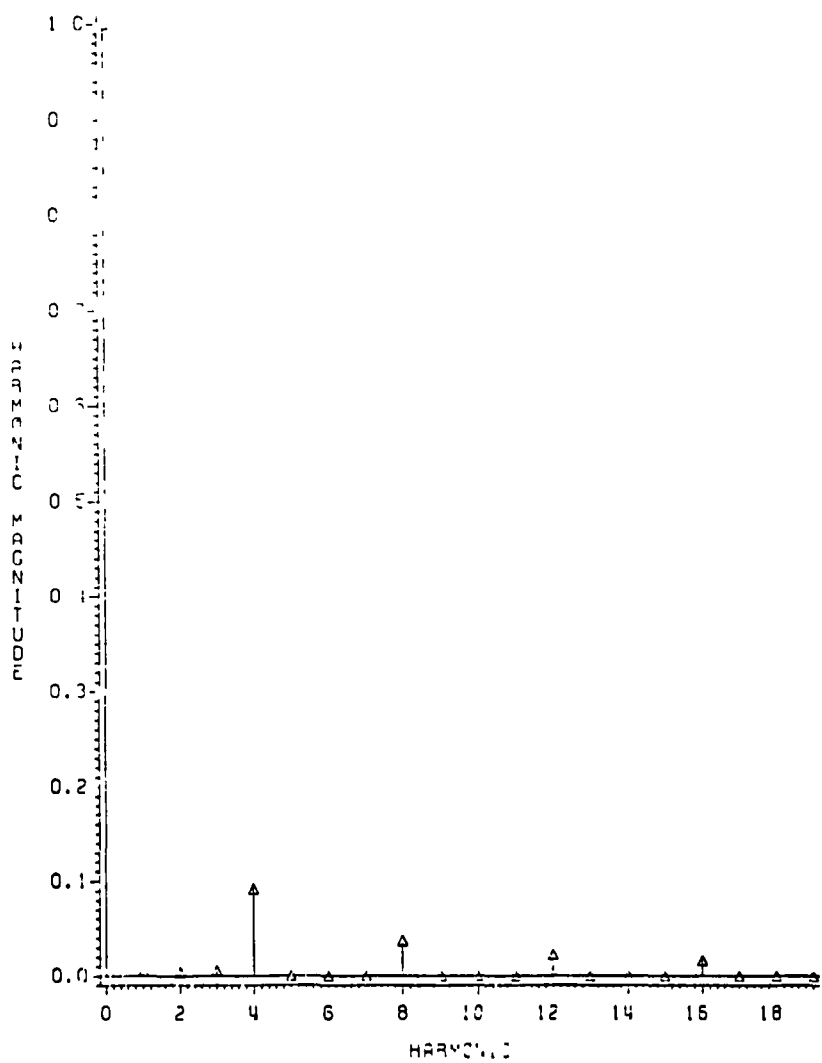
OUTPUT POWER (10% SPEED, 16KW)



CURRENT SPECTRUM (10% SPEED, 16 KW)



POWER SPECTRUM (10% SPEED, 16KW)



FILE: LSPPLOT WATFIV A UNIVERSITY OF MISSOURI COMPUTER NETWORK

PAGE 001

```
//PLOTLS JOB (XXXXLH),'GOODARZI',
// PASSWORD=XXXX
//JOBPARM R=900,B=99000
// EXEC PLOTSAS
//SYSIN DD *
*****
*          10% SPEED 16KW JPL PROJECT
*          PLOT   DATA
* DEGREE   CURRENT    VOLTAGE    POWER
*****
GOPTIONS DEVICE=VARIAN;
DATA ONE;
INPUT X Y1-Y3;
CARDS;
 0.1   -184.3     240.0    9429.2
 0.4   -164.8     240.0   10725.8
 0.6   -145.3     240.0   12025.3
 0.9   -126.0     240.0   12876.4
 1.2   -106.7     240.0   11486.5
 1.5   -87.6      240.0   10119.5
 1.8   -68.5      240.0    9224.4
 2.0   -49.6      240.0   10584.4
 2.3   -30.8      240.0   11946.4
 2.6   -12.1      240.0   13310.3
 3.0    14.2      240.0   15241.9
 3.3    32.7      240.0   14390.6
 3.6    51.0      240.0   13116.9
 3.9    69.3      240.0   12308.7
 4.1    87.5      240.0   13723.0
 4.4   105.5      240.0   15138.2
 4.7   123.5      240.0   16553.9
 5.1   148.7      240.0   18556.9
 5.4   166.4      240.0   17790.5
 5.7   184.0      240.0   16608.7
 5.9   201.6      240.0   15884.9
 6.2   219.0      240.0   17345.3
 6.5   236.3      240.0   18805.1
 6.8   246.6     -240.0   20059.5
 7.1   221.9     -240.0   20278.0
 7.4   197.4     -240.0   20476.7
 7.6   172.9     -240.0   20227.3
 7.9   183.4     240.0   18895.5
 8.2   200.7     240.0   17797.6
 8.5   217.9     240.0   17147.4
 8.8   235.0     240.0   18629.2
 9.0   245.1     -240.0   19888.2
 9.3   220.3     -240.0   20028.4
 9.6   195.5     -240.0   20148.9
 9.9   170.9     -240.0   20249.9
10.2   181.1     240.0   19392.7
10.5   198.2     240.0   18367.0
10.7   215.3     240.0   17363.8
11.0   232.2     240.0   18449.1
11.3   242.1     -240.0   19709.7
```

FILE: LSPPLOT WATFIV A UNIVERSITY OF MISSOURI COMPUTER NETWORK

PAGE 002

| | | | |
|------|-------|--------|---------|
| 11.6 | 217.1 | -240.0 | 19770.4 |
| 11.9 | 192.1 | -240.0 | 19811.7 |
| 12.1 | 167.3 | -240.0 | 19833.7 |
| 12.4 | 177.4 | 240.0 | 19028.3 |
| 12.7 | 194.3 | 240.0 | 18080.2 |
| 13.0 | 211.2 | 240.0 | 17154.6 |
| 13.3 | 227.9 | 240.0 | 18265.2 |
| 13.6 | 244.6 | 240.0 | 19777.7 |
| 13.8 | 226.3 | -240.0 | 20012.9 |
| 14.1 | 201.2 | -240.0 | 19975.6 |
| 14.4 | 176.1 | -240.0 | 19919.0 |
| 14.7 | 185.9 | 240.0 | 20750.0 |
| 15.0 | 202.7 | 240.0 | 19869.6 |
| 15.2 | 219.3 | 240.0 | 19011.5 |
| 15.5 | 235.8 | 240.0 | 18567.9 |
| 15.8 | 245.3 | -240.0 | 19823.9 |
| 16.1 | 219.9 | -240.0 | 19724.2 |
| 16.4 | 194.6 | -240.0 | 19605.5 |
| 16.6 | 169.4 | -240.0 | 19467.9 |
| 16.9 | 179.0 | 240.0 | 18766.9 |
| 17.2 | 195.6 | 240.0 | 17975.6 |
| 17.5 | 212.1 | 240.0 | 17588.6 |
| 17.8 | 228.5 | 240.0 | 19119.3 |
| 18.1 | 244.8 | 240.0 | 20645.3 |
| 18.3 | 226.1 | -240.0 | 20742.3 |
| 18.6 | 200.6 | -240.0 | 20536.9 |
| 18.9 | 175.2 | -240.0 | 20312.8 |
| 19.2 | 184.7 | 240.0 | 19658.1 |
| 19.5 | 201.0 | 240.0 | 18939.4 |
| 19.7 | 217.3 | 240.0 | 18242.4 |
| 20.0 | 233.5 | 240.0 | 19408.4 |
| 20.3 | 242.6 | -240.0 | 20641.3 |
| 20.6 | 216.9 | -240.0 | 20371.6 |
| 20.9 | 191.2 | -240.0 | 20083.4 |
| 21.2 | 165.6 | -240.0 | 19776.9 |
| 21.4 | 175.0 | 240.0 | 19173.0 |
| 21.7 | 191.2 | 240.0 | 18531.4 |
| 22.0 | 207.3 | 240.0 | 17911.2 |
| 22.3 | 223.4 | 240.0 | 19091.0 |
| 22.6 | 239.4 | 240.0 | 20622.7 |
| 22.8 | 220.4 | -240.0 | 20582.2 |
| 23.1 | 194.6 | -240.0 | 20211.5 |
| 23.4 | 168.8 | -240.0 | 19822.9 |
| 23.7 | 178.0 | 240.0 | 19269.9 |
| 24.0 | 194.0 | 240.0 | 18705.7 |
| 24.3 | 210.0 | 240.0 | 18162.5 |
| 24.5 | 225.9 | 240.0 | 19353.9 |
| 24.8 | 241.7 | 240.0 | 20883.5 |
| 25.1 | 222.5 | -240.0 | 20772.9 |
| 25.4 | 196.5 | -240.0 | 20319.0 |
| 25.7 | 170.6 | -240.0 | 19847.5 |
| 25.9 | 179.6 | 240.0 | 19345.0 |
| 26.2 | 195.5 | 240.0 | 18857.4 |
| 26.5 | 211.3 | 240.0 | 18390.6 |
| 26.8 | 227.0 | 240.0 | 19590.5 |

FILE: LSPPLOT MATFIV A UNIVERSITY OF MISSOURI COMPUTER NETWORK

PAGE 003

| | | | |
|------|-------|--------|---------|
| 27.1 | 242.6 | 240.0 | 21114.3 |
| 27.3 | 223.3 | -240.0 | 20932.6 |
| 27.6 | 197.2 | -240.0 | 20395.0 |
| 27.9 | 171.1 | -240.0 | 19517.4 |
| 28.2 | 179.9 | 240.0 | 18747.8 |
| 28.5 | 195.7 | 240.0 | 18342.1 |
| 28.8 | 211.3 | 240.0 | 18274.2 |
| 29.0 | 226.9 | 240.0 | 19796.9 |
| 29.3 | 242.3 | 240.0 | 21311.4 |
| 29.6 | 222.9 | -240.0 | 21057.7 |
| 29.9 | 196.6 | -240.0 | 20436.0 |
| 30.2 | 170.4 | -240.0 | 19488.9 |
| 30.4 | 179.0 | 240.0 | 18782.5 |
| 30.7 | 194.6 | 240.0 | 18451.9 |
| 31.0 | 210.1 | 240.0 | 18141.3 |
| 31.3 | 225.6 | 240.0 | 19354.8 |
| 31.6 | 240.9 | 240.0 | 20862.5 |
| 31.8 | 221.3 | -240.0 | 20541.9 |
| 32.1 | 194.9 | -240.0 | 19841.8 |
| 32.4 | 168.5 | -240.0 | 19125.3 |
| 32.7 | 177.1 | 240.0 | 18775.6 |
| 33.0 | 192.5 | 240.0 | 18519.2 |
| 33.3 | 207.9 | 240.0 | 18282.4 |
| 33.5 | 223.2 | 240.0 | 19495.2 |
| 33.8 | 238.4 | 240.0 | 20986.8 |
| 34.1 | 218.7 | -240.0 | 20592.9 |
| 34.4 | 192.1 | -240.0 | 19808.4 |
| 34.7 | 165.6 | -240.0 | 18729.2 |
| 34.9 | 174.1 | 240.0 | 18154.0 |
| 35.2 | 189.4 | 240.0 | 17976.7 |
| 35.5 | 204.6 | 240.0 | 17818.6 |
| 35.8 | 219.8 | 240.0 | 19033.6 |
| 36.1 | 234.9 | 240.0 | 20511.6 |
| 36.4 | 243.0 | -240.0 | 21592.9 |
| 36.6 | 216.1 | -240.0 | 20728.4 |
| 36.9 | 189.4 | -240.0 | 19585.0 |
| 37.2 | 169.8 | 240.0 | 17517.2 |
| 37.5 | 185.0 | 240.0 | 17418.1 |
| 37.8 | 200.1 | 240.0 | 17595.1 |
| 38.0 | 215.2 | 240.0 | 19061.1 |
| 38.3 | 230.2 | 240.0 | 20516.4 |
| 38.6 | 238.2 | -240.0 | 21564.1 |
| 38.9 | 211.2 | -240.0 | 20615.2 |
| 39.2 | 184.4 | -240.0 | 18415.1 |
| 39.5 | 164.7 | 240.0 | 16380.2 |
| 39.7 | 179.8 | 240.0 | 16363.8 |
| 40.0 | 194.9 | 240.0 | 17572.0 |
| 40.3 | 209.8 | 240.0 | 19012.7 |
| 40.6 | 224.7 | 240.0 | 20442.1 |
| 40.9 | 239.6 | 240.0 | 21860.2 |
| 41.1 | 219.5 | -240.0 | 20066.5 |
| 41.4 | 192.5 | -240.0 | 17645.8 |
| 41.7 | 165.6 | -240.0 | 15240.1 |
| 42.0 | 173.7 | 240.0 | 16036.4 |
| 42.3 | 188.7 | 240.0 | 17460.4 |

FILE: LSPPLOT WATFIV A UNIVERSITY OF MISSOURI COMPUTER NETWORK

PAGE 004

| | | | |
|------|-------|--------|---------|
| 42.6 | 203.6 | 240.0 | 18872.6 |
| 42.8 | 218.4 | 240.0 | 20273.1 |
| 43.1 | 233.1 | 240.0 | 20567.1 |
| 43.4 | 240.8 | -240.0 | 20240.8 |
| 43.7 | 213.7 | -240.0 | 18064.5 |
| 44.0 | 186.6 | -240.0 | 16961.5 |
| 44.2 | 166.6 | 240.0 | 16264.5 |
| 44.5 | 181.5 | 240.0 | 17652.0 |
| 44.8 | 196.3 | 240.0 | 19027.3 |
| 45.1 | 211.1 | 240.0 | 19368.4 |
| 45.4 | 225.8 | 240.0 | 19519.8 |
| 45.6 | 240.4 | 240.0 | 19688.1 |
| 45.9 | 220.1 | -240.0 | 18738.5 |
| 46.2 | 192.9 | -240.0 | 17551.2 |
| 46.5 | 165.8 | -240.0 | 16350.9 |
| 46.8 | 173.6 | 240.0 | 17277.2 |
| 47.1 | 188.4 | 240.0 | 17670.4 |
| 47.3 | 203.1 | 240.0 | 17888.2 |
| 47.6 | 217.7 | 240.0 | 18122.4 |
| 47.9 | 232.3 | 240.0 | 19289.0 |
| 48.2 | 239.8 | -240.0 | 20194.6 |
| 48.5 | 212.4 | -240.0 | 18921.6 |
| 48.7 | 185.2 | -240.0 | 17636.0 |
| 49.0 | 165.0 | 240.0 | 15900.9 |
| 49.3 | 179.7 | 240.0 | 16184.6 |
| 49.6 | 194.3 | 240.0 | 16484.1 |
| 49.9 | 208.9 | 240.0 | 17640.4 |
| 50.2 | 223.4 | 240.0 | 18953.6 |
| 50.4 | 237.8 | 240.0 | 20253.1 |
| 50.7 | 217.4 | -240.0 | 19337.1 |
| 51.0 | 190.0 | -240.0 | 17171.5 |
| 51.3 | 169.7 | 240.0 | 15304.2 |
| 51.6 | 184.4 | 240.0 | 15666.2 |
| 51.8 | 198.9 | 240.0 | 16196.5 |
| 52.1 | 213.4 | 240.0 | 17490.5 |
| 52.4 | 227.8 | 240.0 | 18770.3 |
| 52.7 | 242.1 | 240.0 | 20035.9 |
| 53.0 | 221.6 | -240.0 | 19054.5 |
| 53.2 | 194.1 | -240.0 | 17473.1 |
| 53.5 | 166.8 | -240.0 | 15187.1 |
| 53.8 | 174.4 | 240.0 | 15162.9 |
| 54.1 | 188.9 | 240.0 | 15602.2 |
| 54.4 | 203.4 | 240.0 | 16721.9 |
| 54.7 | 217.7 | 240.0 | 17962.5 |
| 54.9 | 232.1 | 240.0 | 19188.5 |
| 55.2 | 239.3 | -240.0 | 19946.9 |
| 55.5 | 211.8 | -240.0 | 17808.1 |
| 55.8 | 184.3 | -240.0 | 15561.1 |
| 56.1 | 163.9 | 240.0 | 13787.5 |
| 56.3 | 178.4 | 240.0 | 14420.9 |
| 56.6 | 192.8 | 240.0 | 15639.9 |
| 56.9 | 207.2 | 240.0 | 16843.9 |
| 57.2 | 221.5 | 240.0 | 18032.8 |
| 57.5 | 235.8 | 240.0 | 18663.3 |
| 57.7 | 242.9 | -240.0 | 18738.1 |

FILE: LSPPLOT WATFIV A UNIVERSITY OF MISSOURI COMPUTER NETWORK

PAGE 005

| | | | |
|------|-------|--------|---------|
| 58.0 | 215.3 | -240.0 | 16643.1 |
| 58.3 | 187.8 | -240.0 | 15071.4 |
| 58.6 | 167.3 | 240.0 | 13950.0 |
| 58.9 | 181.7 | 240.0 | 15114.6 |
| 59.2 | 196.1 | 240.0 | 16263.9 |
| 59.4 | 210.4 | 240.0 | 16933.3 |
| 59.7 | 224.6 | 240.0 | 17520.7 |
| 60.0 | 238.8 | 240.0 | 18121.2 |
| 60.3 | 218.1 | -240.0 | 16509.8 |
| 60.6 | 190.5 | -240.0 | 14869.4 |
| 60.8 | 170.0 | 240.0 | 13684.0 |
| 61.1 | 184.3 | 240.0 | 14804.2 |
| 61.4 | 198.7 | 240.0 | 15908.6 |
| 61.7 | 212.9 | 240.0 | 16623.4 |
| 62.0 | 227.1 | 240.0 | 17273.6 |
| 62.3 | 241.2 | 240.0 | 17936.3 |
| 62.5 | 220.4 | -240.0 | 16351.2 |
| 62.8 | 192.8 | -240.0 | 14643.3 |
| 63.1 | 165.3 | -240.0 | 12927.2 |
| 63.4 | 172.7 | 240.0 | 13536.2 |
| 63.7 | 187.0 | 240.0 | 14596.3 |
| 63.9 | 201.3 | 240.0 | 15357.6 |
| 64.2 | 215.5 | 240.0 | 16071.8 |
| 64.5 | 229.6 | 240.0 | 16797.7 |
| 64.8 | 243.7 | 240.0 | 17584.9 |
| 65.1 | 222.9 | -240.0 | 16272.8 |
| 65.4 | 195.2 | -240.0 | 14483.9 |
| 65.6 | 167.6 | -240.0 | 12687.6 |
| 65.9 | 175.0 | 240.0 | 13190.5 |
| 66.2 | 189.3 | 240.0 | 13960.5 |
| 66.5 | 203.5 | 240.0 | 14741.6 |
| 66.8 | 217.7 | 240.0 | 15533.6 |
| 67.0 | 231.8 | 240.0 | 16493.3 |
| 67.3 | 238.9 | -240.0 | 16998.4 |
| 67.6 | 211.1 | -240.0 | 15136.6 |
| 67.9 | 183.5 | -240.0 | 13243.6 |
| 68.2 | 162.9 | 240.0 | 11709.8 |
| 68.5 | 177.2 | 240.0 | 12549.6 |
| 68.7 | 191.5 | 240.0 | 13399.8 |
| 69.0 | 205.7 | 240.0 | 14336.7 |
| 69.3 | 219.9 | 240.0 | 15274.1 |
| 69.6 | 233.9 | 240.0 | 16194.4 |
| 69.9 | 241.0 | -240.0 | 16616.5 |
| 70.1 | 213.2 | -240.0 | 14638.9 |
| 70.4 | 185.5 | -240.0 | 12682.5 |
| 70.7 | 165.0 | 240.0 | 11220.4 |
| 71.0 | 179.3 | 240.0 | 12133.1 |
| 71.3 | 193.5 | 240.0 | 13030.0 |
| 71.5 | 207.7 | 240.0 | 13909.7 |
| 71.8 | 221.9 | 240.0 | 14779.9 |
| 72.1 | 235.9 | 240.0 | 15687.0 |
| 72.4 | 243.0 | -240.0 | 16130.0 |
| 72.7 | 215.2 | -240.0 | 14223.4 |
| 73.0 | 187.5 | -240.0 | 12321.3 |
| 73.2 | 166.9 | 240.0 | 10813.7 |

FILE: LSPPLOT WATFIV A UNIVERSITY OF MISSOURI COMPUTER NETWORK

PAGE 006

| | | | |
|------|-------|--------|---------|
| 73.5 | 181.2 | 240.0 | 11659.6 |
| 73.8 | 195.5 | 240.0 | 12488.1 |
| 74.1 | 209.7 | 240.0 | 13325.2 |
| 74.4 | 223.8 | 240.0 | 14290.8 |
| 74.6 | 237.9 | 240.0 | 15265.0 |
| 74.9 | 244.9 | -240.0 | 15774.6 |
| 75.2 | 217.2 | -240.0 | 13759.3 |
| 75.5 | 189.5 | -240.0 | 11706.8 |
| 75.8 | 168.9 | 240.0 | 10123.0 |
| 76.1 | 183.2 | 240.0 | 10932.5 |
| 76.3 | 197.5 | 240.0 | 11950.6 |
| 76.6 | 211.7 | 240.0 | 12976.6 |
| 76.9 | 225.8 | 240.0 | 14010.3 |
| 77.2 | 205.1 | -240.0 | 12438.5 |
| 77.5 | 177.5 | -240.0 | 10341.8 |
| 77.7 | 184.8 | 240.0 | 10596.5 |
| 78.0 | 199.1 | 240.0 | 11596.1 |
| 78.3 | 213.3 | 240.0 | 12659.1 |
| 78.6 | 227.5 | 240.0 | 13729.3 |
| 78.9 | 241.6 | 240.0 | 14741.3 |
| 79.1 | 220.8 | -240.0 | 13070.5 |
| 79.4 | 193.1 | -240.0 | 10926.0 |
| 79.7 | 165.6 | -240.0 | 8778.8 |
| 80.0 | 173.0 | 240.0 | 9049.0 |
| 80.3 | 187.4 | 240.0 | 10157.1 |
| 80.6 | 201.7 | 240.0 | 11271.8 |
| 80.8 | 215.9 | 240.0 | 12392.8 |
| 81.1 | 230.1 | 240.0 | 13104.1 |
| 81.4 | 244.2 | 240.0 | 13716.0 |
| 81.7 | 223.5 | -240.0 | 11973.1 |
| 82.0 | 195.8 | -240.0 | 10210.1 |
| 82.2 | 168.3 | -240.0 | 8557.5 |
| 82.5 | 175.8 | 240.0 | 9258.8 |
| 82.8 | 190.2 | 240.0 | 10336.2 |
| 83.1 | 204.5 | 240.0 | 10920.4 |
| 83.4 | 218.8 | 240.0 | 11486.3 |
| 83.6 | 233.0 | 240.0 | 12033.9 |
| 83.9 | 212.3 | -240.0 | 10770.6 |
| 84.2 | 184.8 | -240.0 | 9168.2 |
| 84.5 | 164.4 | 240.0 | 8052.6 |
| 84.8 | 178.8 | 240.0 | 9157.0 |
| 85.1 | 193.2 | 240.0 | 9689.1 |
| 85.3 | 207.6 | 240.0 | 10202.8 |
| 85.6 | 221.9 | 240.0 | 10698.1 |
| 85.9 | 236.2 | 240.0 | 11782.5 |
| 86.2 | 243.4 | -240.0 | 12529.6 |
| 86.5 | 215.8 | -240.0 | 10985.4 |
| 86.7 | 188.3 | -240.0 | 9335.4 |
| 87.0 | 167.9 | 240.0 | 7512.7 |
| 87.3 | 182.4 | 240.0 | 7977.9 |
| 87.6 | 196.9 | 240.0 | 8424.7 |
| 87.9 | 211.3 | 240.0 | 8990.4 |
| 88.2 | 225.7 | 240.0 | 10237.1 |
| 88.4 | 240.0 | 240.0 | 11487.9 |
| 88.7 | 219.4 | -240.0 | 10463.3 |

G.3 TWO-PHASE SIMULATION RESULTS FOR 80% SPEED, 60 KW

Source Program

Plots

 Stator Voltage and Current

 Output Power

 Current Spectrum

 Power Spectrum

Listing of Plot Data

FILE: OPTIM WATFIV A UNIVERSITY OF MISSOURI COMPUTER NETWORK

PAGE 001

```

//OPTIM    JOB (XXXXXLH),'GOODARZI',
// PASSWORD=?????
/*JOBPARM      T=4,L=6
/**ROUTE PRINT UVMVA.EEPR1
// EXEC WATFIV
//GO.SYSIN DD *
$JOB
C*****#
C          80% SPEED 60KHZ JPL PROJECT
C*****#
C*****#
DIMENSION AR1(800),AR2(800),AR3(800),Y(20),X(20),GA(20),PE(20),
1        XX(4,20),H(9),ZZ1(20),ZZ2(20),ZZ3(20),IFL(7),AR4(800),
2        AR5(800),AR6(800),AR7(800),AR8(800)
LOGICAL#1 LR1(800),LR2(800),LR3(800),LR4(800),LR5(800),LR6(800),
1        LR7(800),LR8(800)
COMPLEX F1(512),F2(512)
REAL LOS,LOR,LN,IAS,IBS,ICS,IAR,IBR,ICR,IDS,IQS,IDR,IQR,LMDQ,INS,
1        POUT,IAREF,IBREF,L1,L2,M,IMAX,IMAGD,IMAGQ,IBU,
2        MAG1(256),MAG2(256)
IMAX=245
DI=15.0
SLIP=0.02
C   WRITE(6,50)
C 50 FORMAT(/,3X,'TIME',8X,'VDS',8X,'IDS',8X,'VQS',8X,'IQS',8X,
C 4           'IDR',9X,'POUT')
NRUN=1
ISTOP=0
KEEP=1
IFL(1)=-1
NINT=7
IPNT1=0
IPNT2=0
IPNT3=0
IPNT4=0
IPNT5=0
IPNT6=0
IPNT7=0
E=240.
C *****#
C     PARAMETERS FOR TWOPHASE INDUCTION MOTOR
C *****#
LOS=.2940E-03
LOR=.3230E-03
LN=26.800E-03
RS=.0274
RR=.0213
PAI=3.141593
P=1.
FREQ=160.
OMEGA=2.0*PAI*FREQ
OMEGR=OMEGA*(1.-SLIP)
L1=LOS+LN
L2=LOR+LN

```

FILE: OPTIM MATFIV A UNIVERSITY OF MISSOURI COMPUTER NETWORK

PAGE 002

```
M=LM
FACT=1./(L1*L2-MMM)
FACT1=L2*FACT
FACT2=L2*RS*FACT
FACT22=L1*RR*FACT
FACT3=M*MM*OMEGR*FACT
FACT4=M*L2*OMEGR*FACT
FACT44=M*L1*OMEGR*FACT
FACT5=M*RR*FACT
FACT55=M*RS*FACT
FACT6=M*FACT
FACT7=L1*L2*OMEGR*FACT
1 IF(L2)=-1
2 CALL RKFOUR(NINT,Y,X,GA,PE,XX,H,ZZ1,ZZ2,ZZ3,TIME,PNTS,KEEP,IFL)
IF(IFL(4))3,4,5
3 INIT=1
TIME1=-1
NC=1
NCC=1
TIME=0.
FINTIM=0.2500
PTMAX=800.
Y(1)=0.
Y(2)=0.
Y(3)=0.
Y(4)=0.
Y(5)=0.0
Y(6)=0.0
C Y(7)=0.0
AREAIN=0.0
ARAOUT=0.0
H(1)=.050E-04
C H(7)=-1
VDS=0.0
VQS=0.0
SUM=0.
IN=0
SUM1=0.
NUMBER=0.
SW=0.0
DI1=DI
SWITCH=0.0
PSW=0.0
TOTSW=0.0
IAE=-1
IBE=-1
DO 61 I=1,256
F1(I)=(0.0,0.0)
F2(I)=(0.0,0.0)
61 CONTINUE
C
4 IF(TIME-TIME1)7,8,7
7 TIME1=TIME
C
DEG=FREQ*TIME
```

FILE: OPTIM HATFIV A UNIVERSITY OF MISSOURI COMPUTER NETWORK

PAGE 003

```

IDEG=DEG
DEG=(DEG-IDEGL)*360.

C
IAREF=IMAX*SIN(OMEGA*TIME)
IBREF=IMAX*SIN(OMEGA*TIME-PAI/2.)
C
IF(IAREF.GT.0.0) IAREF=IMAX
IF(IAREF.LT.0.00) IAREF=-IMAX
IF(IBREF.GT.0.0) IBREF=IMAX
IF(IBREF.LT.0.00) IBREF=-IMAX
C
DIA=Y(1)-IAREF
DIB=Y(2)-IBREF
C
VDS=E
VQS=E
IF(IAREF.LT.0) VDS=-E
IF(IBREF.LT.0) VQS=-E
C
IF(TIME.LT.0.02000) GOTO 8
IF(TIME.GT.0.00000) GOTO 23
ISW=0
IF(DIA.LT.DI1)ISW=1
IF(DIA.GT.DI) DI1=DIA
IF(DIA.GT.DI.AND.IAREF.GT.0.0.AND.ISW.EQ.0)      GOTO 24
IF(DIA.GT.DI)      IAE=1
GOTO 27
24   IAE=1
IF(TIME.LT.0.24375) GOTO 27
SW=SH+1
PSW=ABS((240.*Y(1)*5.5E-06)/(6*6.25E-03))+PSW
27   IF(DIA.LT.(-DI)) IAE=0
IF(VDS.GT.0.0.AND.IAE.EQ.1) GOTO 18
IF(VDS.LT.0.0.AND.IAE.EQ.0) GOTO 18
GOTO 22
18   VDS=-VDS
IF(TIME.LT.0.24375) GOTO 22
SWITCH=SWITCH+1.
22   IF(DIB.GT.DI)      IBE=1
IF(DIB.LT.(-DI)) IBE=0
IF(VQS.GT.0.0.AND.IBE.EQ.1) GOTO 19
IF(VQS.LT.0.0.AND.IBE.EQ.0) GOTO 19
GOTO 23
19   VQS=-VQS
23   IF(TIME.GT.0.23125.AND.TIME.LT.0.2312612)AREAIN=Y(6)
IF(TIME.GT.0.23125.AND.TIME.LT.0.2312612)ARAOUT=Y(5)
IF(TIME.GT.0.23125.AND.TIME.LT.0.2312612)ARMS=Y(7)
C
IF(TIME.LT.0.24375) GOTO 8
TOTSW=TOTSW+1.
C
8   CONTINUE
C
X(1)=FACT1*VDS-FACT2*Y(1)+FACT3*Y(2)+FACT4*Y(4)+FACT5*Y(3)
X(2)=FACT1*VQS-FACT2*Y(2)-FACT3*Y(1)-FACT4*Y(3)+FACT5*Y(4)

```

FILE: OPTIM WATFIV A UNIVERSITY OF MISSOURI COMPUTER NETWORK

PAGE 004

```

X(3)=-FACT6*VDS+FACT55*Y(1)-FACT44*Y(2)-FACT7*Y(4)-FACT22*Y(3)
X(4)=-FACT6*VQS+FACT55*Y(2)+FACT44*Y(1)+FACT7*Y(3)-FACT22*Y(4)
X(5)=LM*(Y(2)*Y(3)-Y(1)*Y(4))*OMEGR/.01875
X(6)=(Y(1)*VDS+Y(2)*VQS)/.01875
X(7)=Y(1)*Y(1)/.01875
C
      GOTO 2
  5 IPR=0
  NC=NC-1
  IF(NC)9,9,10
  9 NC=NCC
  IPR=1
 10 IF(TIME.GE.FINTIM) ISTOP=1
  IF((IPR+ISTOP).EQ.0) GOTO 11
C
  IF(TIME.LT.0.23125) GOTO 11
  IDS=Y(1)
  IQS=Y(2)
  IDR=Y(3)
  IQR=Y(4)
C
  IMAGD=IDS+IDR
  IMAGQ=IQS+IQR
C
  TQ=LM*(IQS*IDR-IDS*IQR)
  POUT=TQ*OMEGR
C
  PIN=IDS*VDS+IQS*VQS
C
  SUM1=SUM1+PIN
C
  SUM=SUM1+POUT
C
  NUMBER=NUMBER+1.
  IF(TIME.LT.0.24375) GOTO 31
  IN=IN+1
CC
  F1(IN)=CMPLX(Y(1),0.0)
CC
  F2(IN)=CMPLX(POUT,0.0)
  31
  CONTINUE
  WRITE(6,250)DEG,IDS,VDS,POUT
C
  IF(TIME.LT.0.19250) POUT=0.0
  CALL FPLOT(800,IPNT1,AR1,LR1,ISTOP,1,1,TIME,IDS)
  CALL FPLOT(800,IPNT2,AR2,LR2,ISTOP,1,1,TIME,VDS)
C
  CALL FPLOT(800,IPNT4,AR4,LR4,ISTOP,1,2,TIME,IQS)
C
  CALL FPLOT(800,IPNT4,AR4,LR4,ISTOP,2,2,TIME,VQS)
C
  CALL FPLOT(800,IPNT3,AR3,LR3,ISTOP,1,2,TIME,IMAGD)
C
  CALL FPLOT(800,IPNT3,AR3,LR3,ISTOP,2,2,TIME,IDR)
  CALL FPLOT(800,IPNT5,AR5,LR5,ISTOP,1,1,TIME,POUT)
C
  11 INIT=0
  IF(ISTOP)1,1,6
  6
  CONTINUE
  250 FORMAT(' ',F6.1,3(F9.2,2X))
C
  AVER=SUM/NUMBER
C
  AVERI=SUM1/NUMBER
C
  EFF=AVER/AVERI
  PIN=Y(6)-AREAIN
  POUT=Y(5)-ARAOUT
  RMS=(Y(7)-ARMS)**0.5

```

FILE: OPTIM MATFIV A UNIVERSITY OF MISSOURI COMPUTER NETWORK

PAGE 001

```

C ****
C NOTE .7 IS THE VOLTAGE DROP ACROSS THE DIODE
C 1.85 IS THE CE VOLTAGE OF THE TRANSISTOR
C SWITCH IS THE # OF INTERVAL OF THE SWITCHING (DIODE CONDUCTION)
C TOTSW IS TOTAL # OF INTEGRATION INTERVALS
C PDIODE IS THE LOSS OF DIODE DURING CONDUCTION
C PTRANS IS THE ON TIME LOSS OF THE TRANSISTOR
C PSW IS THE SWITCHING LOSS OF EACH TRANSISTOR (E*I*TSW/T)
C TOTSL IS THE TOTAL LOSS OF THE SWITCH
C ****
C PDIODE=(SWITCH/TOTSW)*0.7*IMAX/PAI
C PTRANS=(1-SWITCH/TOTSW)*1.85*IMAX/PAI
C TOTSL=PDIODE+PTRANS+PSW
C TOT4SL=4*TOTSL
C DTRIO=SWITCH/TOTSW
C EFFIO=POUT/(TOT4SL+PIN)
C EFFIO=POUT/PIN
C SW=SW+SW
C
C WRITE(6,702)POUT,EFFIO,SLIP,IMAX,DTRIO,RMS
C WRITE(6,703)SH,PSW,PTRANS,PDIODE,TOT4SL,IN
C 702 FORMAT(//,' POWER OUT=',F8.1,2X,'EFFIO=',F5.3,2X,'SLIP=',
C 1F7.5,2X,'IMAX=',F6.1,2X,'DTRIO=',F7.1,2X,'I(RMS)=',F7.1,/)
C 703 FORMAT(//,'#SW/CYC=',F5.1,8X,'PSW=',F6.1,3X,'PTRANS=',F5.1,
C 1,2X,'PDIODE=',F4.1,2X,'TOT4SL=',F6.1,5X,'IN=',I5,//////)
C WRITE(6,705)
C 705 FORMAT(IX,'Z',11X,'I HARMONIC ',15X,'P HARMONIC',//)
C 706 FORMAT(1X,F5.1,5X,F12.8,5X,F15.8)
C ISTOP=0.0
CC CALL FFT(F1,8)
CC CALL FFT(F2,8)
CC DO 401 I=1,128
CC MAG1(I)=CABS(F1(I))/256.
CC MAG2(I)=CABS(F2(I))/256.
CC Z=FLOAT(I-1)
CC IF (I.EQ.1) MAG1(2)=275.
CC AMP1=MAG1(I)/MAG1(2)
CC AMP2=MAG2(I)/MAG2(1)
C WRITE(6,706) Z,AMP1,AMP2
CC IF(I.EQ.128) ISTOP=1
C IF(AMP2.GT.300) AMP2=0.0
C
C CALL FPLOT(800,IPNT4,AR4,LR4,ISTOP,1,1,Z,AMP1)
C CALL FPLOT(800,IPNT3,AR3,LR3,ISTOP,1,1,Z,AMP2)
C 401 CONTINUE
STOP
END
SUBROUTINE FFT(X,M)
COMPLEX X(256),U,M,T
N=2*M
NV2=N/2
NM1=N-1
J=1
DO 7 I=1,NM1
IF(I.GT.J) GOTO 5

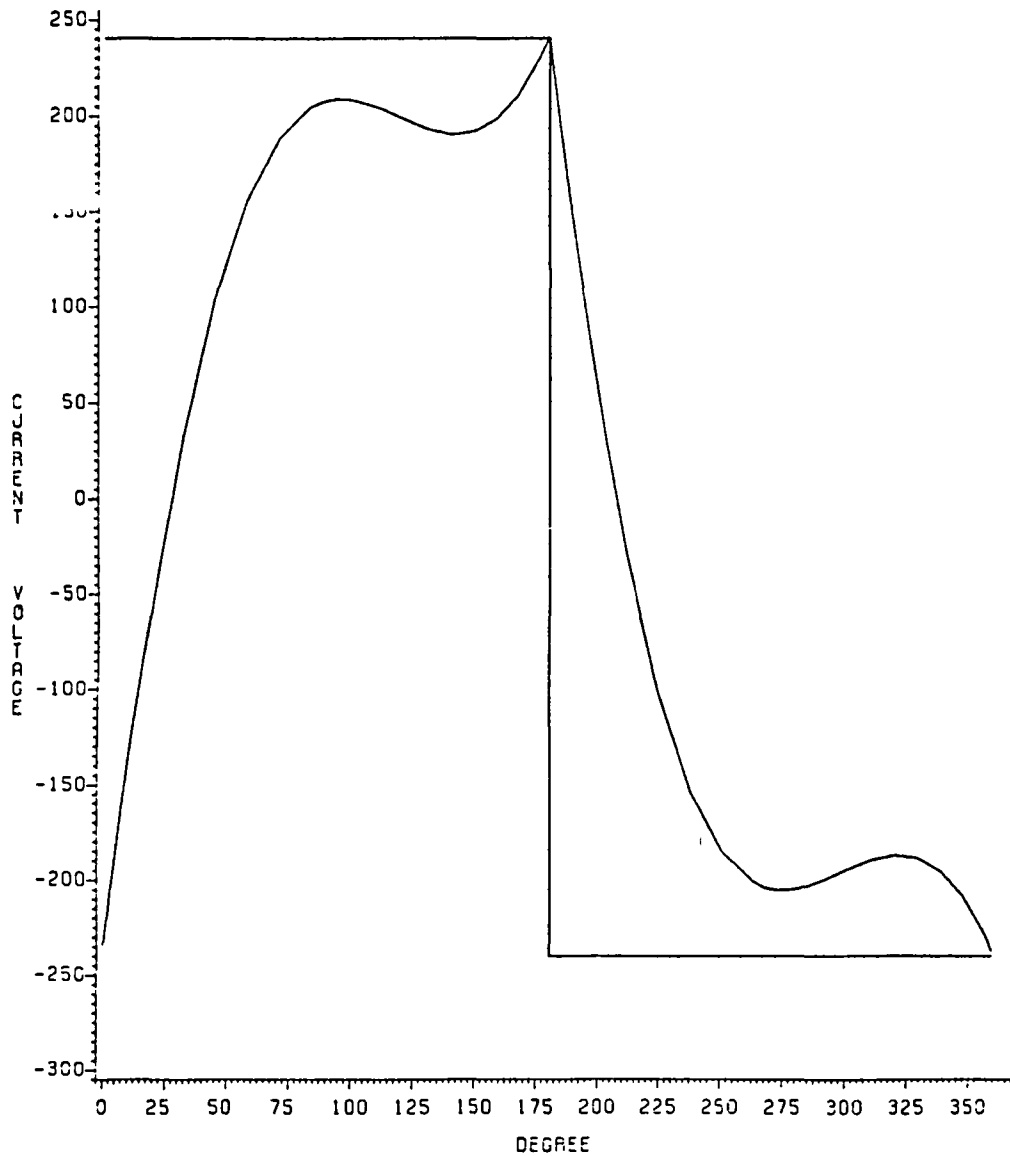
```

FILE: OPTIM NATFIV A UNIVERSITY OF MISSOURI COMPUTER NETWORK

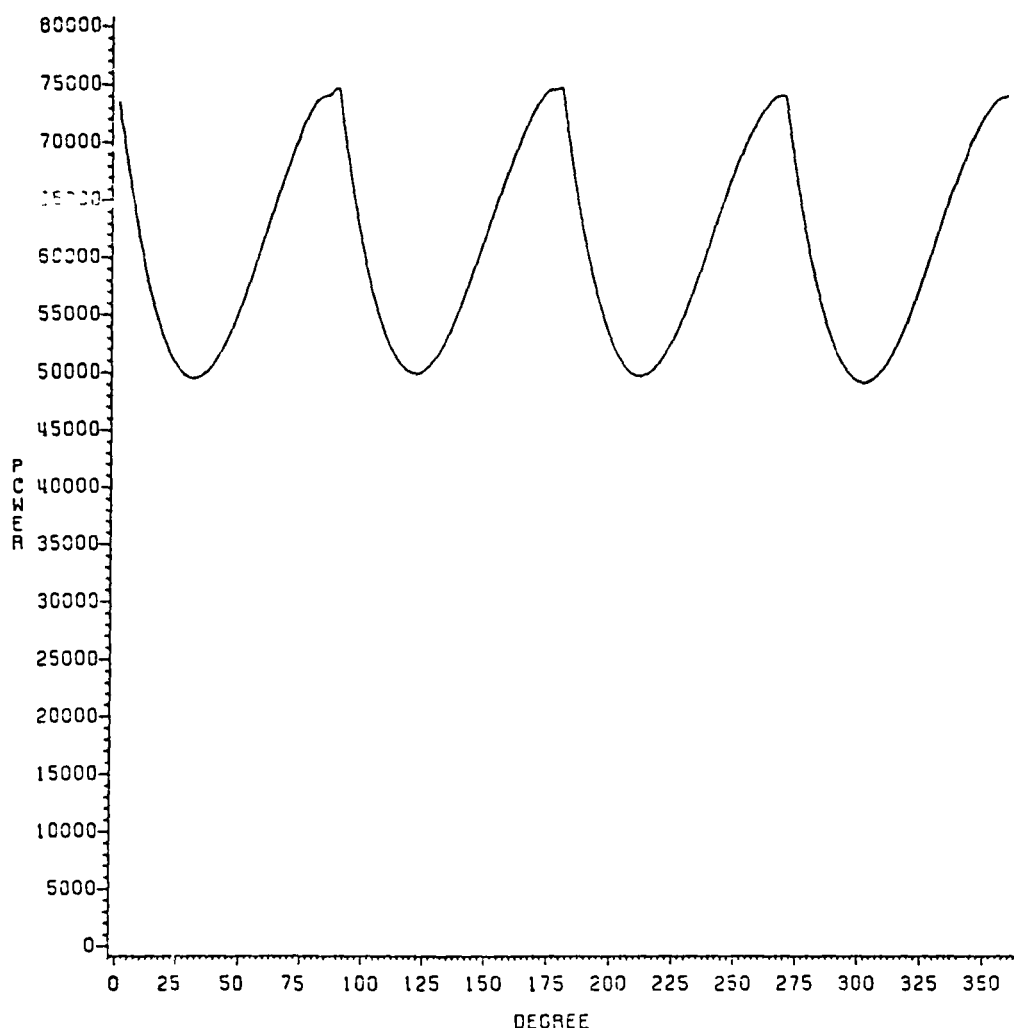
PAGE 006

```
T=X(J)
X(J)=X(I)
X(I)=T
5 K=NV2
6 IF(K.GE.J)GO TO 7
J=J-K
K=K/2
GO TO 6
7 J=J+K
PI=3.14159265358979
DO 20 L=1,M
LE=2**L
LE1=LE/2
U=(1.0,0.0)
Z=COS(PI/FLOAT(LE1))
Y=-SIN(PI/FLOAT(LE1))
W=CMPLX(Z,Y)
DO 20 J=1,LE1
DO 10 I=J,N,LE
IP=I+LE1
T=X(IP)*U
X(IP)=X(I)-T
X(I)=X(I)+T
10 X(I)=X(I)+T
20 U=U*W
RETURN
END
$ENTRY
1      A  CURRENT OF PHASE A OF STATOR
1      V  VOLTAGE OF PHASE A OF STATOR
1      P  POWER VS TIME
1      I  CURRENT HARMONIC MAGNITUDE VS HARMONIC ORDER
1      P  POWER HARMONIC MAGNITUDE VS HARMONIC ORDER
$STOP
/*
//
```

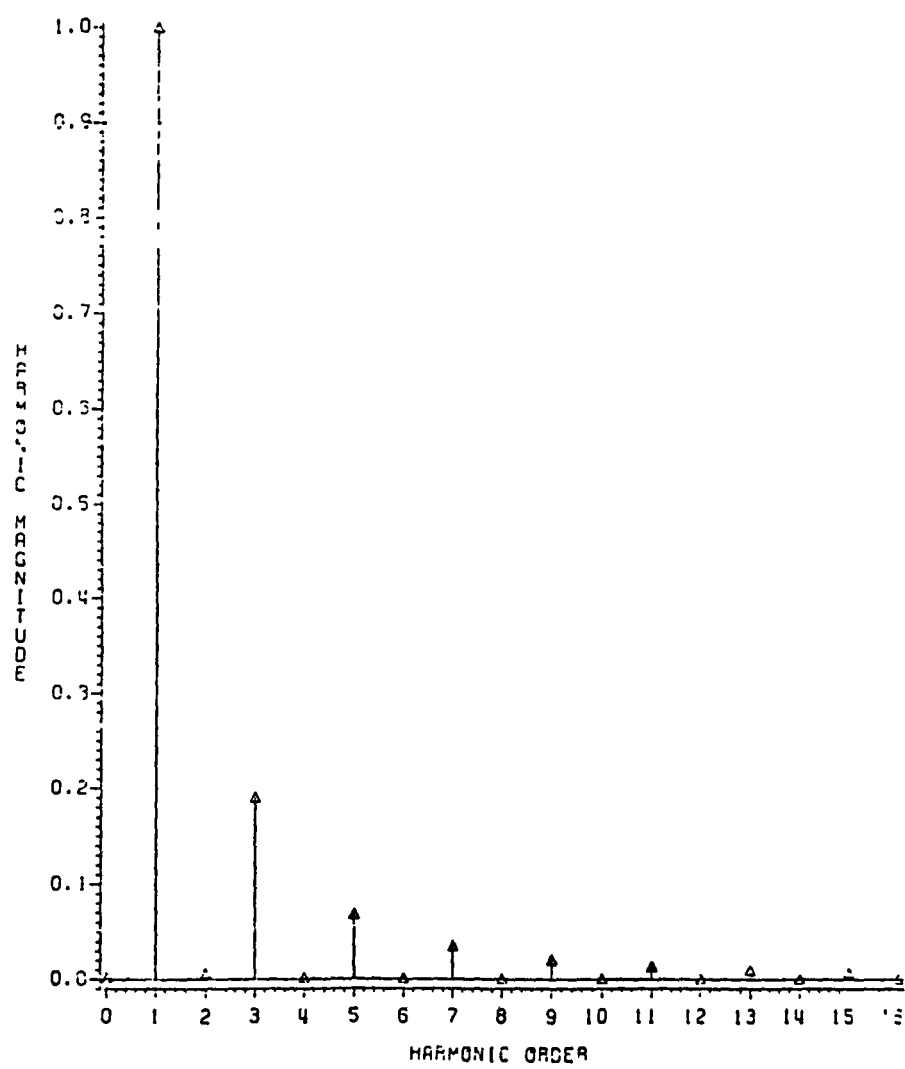
VOLTAGE & CURRENT (80% S,60KW,MOTOR OPERATION)



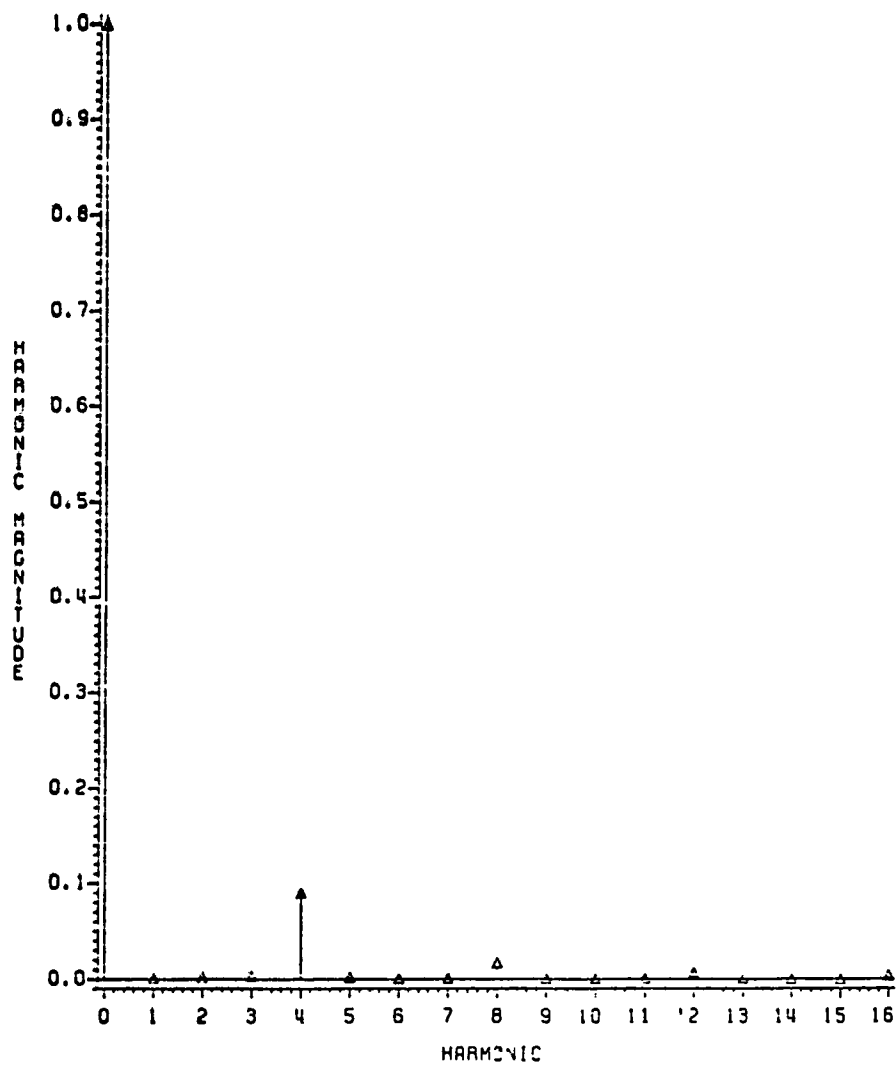
OUTPUT POWER (80% S,60KW, MOTOR OPERATION)



CURRENT SPECTRUM (80% SPEED, 60 KW)



POWER SPECTRUM (80% SPEED, 60KW)



FILE: MOTOR PLOT A UNIVERSITY OF MISSOURI COMPUTER NETWORK

PAGE 001

```

//MOTORP JOB (XXXXLH),'GOODARZI',
// PASSWORD=XXXX
/*JOBPARM R=900,B=99000
// EXEC PLOTSAS
//SYSIN DD *
      OPTIONS DEVICE=VARIAN;
      DATA ONE;
      INPUT X Y1-Y3;
*****
*          80% SPEED,60KW JPL PROJECT
*          PLOT DATA
* DEGREE |CURRENT |VOLTAGE |POWER
*****|*****|*****|*****
CARDS;
 0 4 -233.96    240.00   73530 25
 0.9 -227.92    240.00   72584.00
 1.5 -221.93    240.00   71657.56
 2.1 -215.98    240.00   70751.13
 2.9 -207.63    240.00   69503.44
 4.1 -195.96    240.00   67807 31
 5.7 -179.75    240.00   65544.56
 8.0 -157.41    240.00   62615.67
11.2 -126.97    240.00   59009 33
15.8 -86.28     240.00   54955.57
22.4 -33.54     240.00   51216.40
31.6  31.40     240.00   49532.14
44.6  104.19    240.00   52894.97
57.6  155.75    240.00   60361.47
70.6  188.23    240.00   68587.13
83.7  204.60    240.00   74058.00
88.3  207.21    240.00   74693.56
89.9  207.80    240.00   74708.81
90.3  207.92    240.00   74138.25
90.7  208.03    240.00   73465.38
91.1  208.13    240.00   72802.44
91.5  208.22    240.00   72149.25
92.1  208.33    240.00   71242.75
92.9  208.45    240.00   69995.00
94.1  208.57    240.00   68298.13
95.7  208.61    240.00   66034.44
98.0  208.44    240.00   63103.30
101.2 207.81    240.00   59492.22
105.8 206.24    240.00   55429.19
112.4 203.07    240.00   51671.75
121.6 197.75    240.00   49950.17
130.8 192.98    240.00   51714.76
140.0 190.43    240.00   55985.92
149.2 191.68    240.00   61636.06
158.4 198.18    240.00   67448.50
167.6 211.24    240.00   72177.50
176.8 231.96    240.00   74603.25
179.1 238.45    240.00   74714.19
179.9 240.87    240.00   74698.63

```

FILE: MOTOR PLOT A UNIVERSITY OF MISSOURI COMPUTER NETWORK

PAGE 002

| | | | |
|-------|---------|---------|----------|
| 180.5 | 236.11 | -240.00 | 73889.38 |
| 181.1 | 230.08 | -240.00 | 72941.25 |
| 181.7 | 224.10 | -240.00 | 72012.88 |
| 182.2 | 218.16 | -240.00 | 71104.63 |
| 183.1 | 209.82 | -240.00 | 69854.19 |
| 184.2 | 198.17 | -240.00 | 68153.75 |
| 185.8 | 181.99 | -240.00 | 65884.75 |
| 188.1 | 159.68 | -240.00 | 62946.13 |
| 191.4 | 129.29 | -240.00 | 59323.89 |
| 196.0 | 88.69 | -240.00 | 55243.95 |
| 202.5 | 36.05 | -240.00 | 51460.83 |
| 211.7 | -28.73 | -240.00 | 49697.88 |
| 224.7 | -101.31 | -240.00 | 52920.96 |
| 237.8 | -152.69 | -240.00 | 60219.04 |
| 250.8 | -185.00 | -240.00 | 68248.75 |
| 263.8 | -201.25 | -240.00 | 73508.50 |
| 268.4 | -203.82 | -240.00 | 74067.63 |
| 269.6 | -204.24 | -240.00 | 74071.44 |
| 270.0 | -204.37 | -240.00 | 74058.94 |
| 270.4 | -204.49 | -240.00 | 73484.50 |
| 270.8 | -204.60 | -240.00 | 72807.69 |
| 271.2 | -204.70 | -240.00 | 72140.88 |
| 271.6 | -204.79 | -240.00 | 71484.19 |
| 272.2 | -204.90 | -240.00 | 70572.56 |
| 273.0 | -205.02 | -240.00 | 69317.56 |
| 274.1 | -205.13 | -240.00 | 67611.13 |
| 275.8 | -205.17 | -240.00 | 65333.88 |
| 278.1 | -205.00 | -240.00 | 62384.63 |
| 281.3 | -204.37 | -240.00 | 58749.62 |
| 285.9 | -202.80 | -240.00 | 54655.75 |
| 292.4 | -199.63 | -240.00 | 50861.50 |
| 301.6 | -194.33 | -240.00 | 49102.36 |
| 310.9 | -189.59 | -240.00 | 50845.82 |
| 320.1 | -187.09 | -240.00 | 55110.38 |
| 329.3 | -188.39 | -240.00 | 60769.29 |
| 338.5 | -194.96 | -240.00 | 66604.94 |
| 347.7 | -208.09 | -240.00 | 71369.31 |
| 356.9 | -228.90 | -240.00 | 73842.38 |
| 359.2 | -235.41 | -240.00 | 73966.63 |
| 359.8 | -237.12 | -240.00 | 73962.13 |

```

1
PROC GPLOT;
PLOT Y1*X Y2*X /OVERLAY ;
SYMBOL1 I=JOIN L=1;
SYMBOL2 I=JOIN L=13;
LABEL X=DEGREE
      Y1=CURRENT VOLTAGE;
TITLE VOLTAGE & CURRENT (80% S,60KW,MOTOR OPERATION);
PROC GPLOT;
PLOT Y3*X /XAXIS=0 TO 80000 BY 5000;
SYMBOL1 I=SPLINE;
LABEL X=DEGREE
      Y3= POWER ;
TITLE OUTPUT POWER (80% S,60KW, MOTOR OPERATION);
/*

```

G.4 TWO-PHASE SIMULATION RESULTS FOR 80% SPEED, 12 KW

Source Program

Plots

 Stator Voltage

 Stator Current

 Output Power

 Current Spectrum

 Power Spectrum

Partial Listing of Plot Data

FILE: OPTIM WATFIV A UNIVERSITY OF MISSOURI COMPUTER NETWORK

PAGE 001

```

//OPTIM   JOB (XXXXLH),'JPL PROJ',
//  PASSWORD=XXXX
/*JOBPARM      T=2,L=4
//**ROUTE PRINT UMVMA.EEPR3
//    EXEC  WATFIV
//GO.SYSIN DD *
$JOB
      DIMENSION AR1(800),AR2(800),AR3(800),Y(20),X(20),GA(20),PE(20),
1        XX(4,20),H(9),ZZ1(20),ZZZ(20),ZZ3(20),IFL(7),AR4(800),
2        AR5(800),AR6(800),AR7(800),AR8(800)
      LOGICAL*I LR1(800),LR2(800),LR3(800),LR4(800),LR5(800),LR6(800),
1        LR7(800),LR8(800)
      COMPLEX F1(512),F2(512)
      REAL LOS,LOP,LH,IAS,IBS,ICS,IAR,IBR,ICR,IDS,IQS,IDR,IQR,LMDQ,INS,
1        POUT,IAREF,IBREF,L1,L2,M,IMAX,IMAGD,IMAGQ,IBU,
2        MAG1(256),MAG2(256)
      IMAX=65.0
      DI=38.0
      SLIP=0.00725
*****
C          *                                *
C          80% SPEED,12KW      JPL PROJECT      *
C          *                                *
*****WRITE(6,50)
C  50 FORMAT(/,3X,'TIME',8X,'VDS',8X,'IDS',8X,'VQS',8X,'IQS',8X,
C  4       'IDR',9X,'POUT')
      NRUN=1
      ISTOP=0
      KEEP=1
      IFL(1)=-1
      NINT=7
      IPNT1=0
      IPNT2=0
      IPNT3=0
      IPNT4=0
      IPNT5=0
      IPNT6=0
      IPNT7=0
      E=240.
*****
C          *                                *
C          PARAMETERS FOR TWOPHASE INDUCTION MOTOR
C          *                                *
*****LOS=.2940E-03
      LOR=.3230E-03
      LM=26.800E-03
      RS=.0274
      RR=.0213
      PAI=3.141593
      P=1.
      FREQ=160.
      OMEGA=2.0*PAI*FREQ
      OMEGR=OMEGA*(1.-SLIP)
      L1=LOS+LM
      L2=LOR+LM

```

FILE: OPTIM WATFIV A UNIVERSITY OF MISSOURI COMPUTER NETWORK

PAGE 002

```

M=LM
FACT=1./(L1*L2-M*M)
FACT1=L2*FACT
FACT2=L2*RS*FACT
FACT22=L1*RR*FACT
FACT3=M*M*OMEGR*FACT
FACT4=M*L2*OMEGR*FACT
FACT44=M*L1*OMEGR*FACT
FACT5=M*RR*FACT
FACT55=M*RS*FACT
FACT6=M*FACT
FACT7=L1*L2*OMEGR*FACT
1 IFL(2)=-1
2 CALL RKFOUR(NINT,Y,X,GA,PE,XX,H,ZZ1,ZZ2,ZZ3,TIME,PNTS,KEEP,IFL)
 IF(IFL(4))3,4,5
3 INIT=1
 TIME1=-1
 NC=1
 NCC=1
 TIME=0.
 FINTIM=0.2500
 PTMAX=800.
 Y(1)=0.
 Y(2)=0.
 Y(3)=0.
 Y(4)=0.
 Y(5)=0.0
 Y(6)=0.0
 C Y(7)=0.0
 AREAIN=0.0
 ARAOUT=0.0
 H(1)=.050E-04
 C H(7)=-1
 VDS=0.0
 VQS=0.0
 SUM=0.
 SUMI=0.
 IN=0
 SUMI=0.
 NUMBER=0.
 SW=0.0
 DI1=DI
 SWITCH=0.0
 PSW=0.0
 TOTSW=0.0
 TAE=-1
 IBE=-1
 DO 61 I=1,256
 F1(I)=(0.0,0.0)
 F2(I)=(0.0,0.0)
 61 CONTINUE
 C
 4 IF(TIME-TIME1)7,8,7
 7 TIME1=TIME
 C

```

FILE: OPTIM WATFIV A UNIVERSITY OF MISSOURI COMPUTER NETWORK

PAGE 003

```

DEG=FREQ*TIME
IDEF=DEG
DFG=(DEG-JDEG)*360.

C      IAREF=IMAX*SIN(OMEGA*TIME)
C      IBREF=IMAX*SIN(OMEGA*TIME-PAI/2.)
C
C      IF(IAREF.GT.0.0) IAREF=IMAX
C      IF(IAREF.LT.0.00) IAREF=-IMAX
C      IF(IBREF.GT.0.0) IBREF=IMAX
C      IF(IBREF.LT.0.00) IBREF=-IMAX
C
C      DIA=Y(1)-IAREF
C      DIB=Y(2)-IBREF
C
C      VDS=E
C      VQS=E
C      IF(IAREF.LT.0)    VDS=-E
C      IF(IBREF.LT.0)    VQS=-E
C
C      IF(TIME.LT.0.02000) GOTO 8
C      IF(TIME.GT.0.00000) GOTO 23
C      ISW=0
C      IF(DIA.LT.DI1)ISW=1
C      IF(DIA.GT.DI) DI1=DIA
C      IF(DIA.GT.DI.AND.IAREF.GT.0.0.AND.ISW.EQ.0)      GOTO 24
C      IF(DIA.GT.DI)      IAE=1
C      GOTO 27
24    IAE=1
C      IF(TIME.LT.0.24375) GOTO 27
C      SW=SW+1
C      PSW=ABS((240.*Y(1)*5.5E-06)/(6*6.25E-03))+PSW
27    IF(DIA.LT.(-DI))  IAE=0
C      IF(VDS.GT.0.0.AND.IAE.EQ.1)  GOTO 18
C      IF(VDS.LT.0.0.AND.IAE.EQ.0)  GOTO 18
C      GOTO 22
18    VDS=-VDS
C      IF(TIME.LT.0.24375) GOTO 22
C      SWITCH=SWITCH+1.
22    IF(DIB GT.DI)      IBE=1
C      IF(DIB.LT.(-DI))  IBE=0
C      IF(VQS.GT.0.0.AND.IBE.EQ.1)  GOTO 19
C      IF(VQS.LT.0.0.AND.IBE.EQ.0)  GOTO 19
C      GOTO 23
19    VQS=-VQS
23    IF(TIME.GT.0.23125.AND.TIME.LT.0.2316612)AREAIN=Y(6)
C      IF(TIME.GT.0.23125.AND.TIME.LT.0.2316612)ARAOUT=Y(5)
C      IF(TIME.GT.0.23125.AND.TIME.LT.0.2316612)ARMS=Y(7)
C
C      IF(TIME.LT.0.24375) GOTO 8
C      TOTSW=TOTSW+1.

C
8     CONTINUE
C
X(1)=FACT1*VDS-FACT2*Y(1)+FACT3*Y(2)+FACT4*Y(4)+FACT5*Y(3)

```

FILE: OPTIM WATFIV A UNIVERSITY OF MISSOURI COMPUTER NETWORK

PAGE 004

```

X(2)=FACT1*VQS-FACT2*Y(2)-FACT3*Y(1)-FACT4*Y(3)+FACT5*Y(4)
X(3)=-FACT6*VDS+FACT55*Y(1)-FACT44*Y(2)-FACT7*Y(4)-FACT22*Y(3)
X(4)=-FACT6*VGS+FACT55*Y(2)+FACT44*Y(1)+FACT7*Y(3)-FACT22*Y(4)
X(5)=LM*(Y(2)*Y(3)-Y(1)*Y(4))*OMEGR/.01875
X(6)=(Y(1)*VDS+Y(2)*VQS)/.01875
X(7)=Y(1)*Y(1)/.01875
C
      GOTO 2
5 IPR=0
NC=NC-1
IF(NC)9,9,10
9 NC=NCC
IPR=1
10 IF(TIME.GE.FINTIM) ISTOP=1
IFI(IPR+ISTOP).EQ.0) GOTO 11
C
      IF(TIME.LT.0.24375) GOTO 11
IDS=Y(1)
IQS=Y(2)
IDR=Y(3)
IQR=Y(4)
C
      IMAGD=IDS+IDR
IMAGG=IQS+IQR
C
      TQ=LM*(IQS*IDR-IDS*IQR)
POUT=TQ*OMEGR
C
      PIN=IDS*VDS+IQS*VQS
SUM1=SUM1+PIN
C
      SUM=SUM+POUT
C
      NUMBER=NUMBER+1.
IFI(TIME.LT.0.24375) GOTO 31
IFI(DEG.GT.180.) GOTO 41
SUMI=SUMI+Y(1)
41 IN=IN+1
F1(IN)=CMPLX(Y(1),0.0)
F2(IN)=CMPLX(POUT,0.0)
31 CONTINUE
WRITE(6,250)DEG,IDS,VDS,POUT
C
IFI(TIME.LT.0.24400) POUT=0.0
CALL FPLOT(800,IPNT1,AR1,LR1,ISTOP,1,1,TIME,IDS)
CALL FPLOT(800,IPNT2,AR2,LR2,ISTOP,1,1,TIME,VDS)
CALL FPLOT(800,IPNT4,AR4,LR4,ISTOP,1,2,TIME,IQS)
CALL FPLOT(800,IPNT4,AR4,LR4,ISTOP,2,2,TIME,VGS)
CALL FPLOT(800,IPNT3,AR3,LR3,ISTOP,1,2,TIME,IMAGD)
CALL FPLOT(800,IPNT3,AR3,LR3,ISTOP,2,2,TIME,IDR)
CALL FPLOT(800,IPNT5,AR5,LR5,ISTOP,1,1,TIME,POUT)
C
      11 INIT=0
IFI(ISTOP)1,1,6
6 CONTINUE
250 FORMAT(' ',F6.1,3(F9.2,2X))
C
      AVER=SUM/NUMBER
AVERI=2*SUMI/IN
EFF=AVER/AVERI
  
```

FILE: OPTIM WATFIV A UNIVERSITY OF MISSOURI COMPUTER NETWORK

PAGE 005

```

PIN=Y(6)-AREAIN
POUT=Y(5)-ARAOUT
RMS=(Y(7)-ARMS)**0.5
C *****
C NOTE .7 IS THE VOLTAGE DROP ACROSS THE DIODE
C 1.85 IS THE CE VOLTAGE OF THE TRANSISTOR
C SWITCH IS THE # OF INTERVAL OF THE SWITCHING (DIODE CONDUCTION)
C TOTSW IS TOTAL # OF INTEGRATION INTERVALS
C PDIODE IS THE LOSS OF DIODE DURING CONDUCTION
C PTRANS IS THE ON TIME LOSS OF THE TRANSISTOR
C PSW IS THE SWITCHING LOSS OF EACH TRANSISTOR (E*I*TSW/T)
C TOTSL IS THE TOTAL LOSS OF THE SWITCH
C *****
PDIODE=(SWITCH/TOTSW)*0.7*IMAX/PAI
PTRANS=(1-SWITCH/TOTSW)*1.85*IMAX/PAI
TOTSL=PDIODE+PTRANS+PSW
TOT4SL=4*TOTSL
DTRIO=1-(SWITCH/TOTSW)
C EFFIO=POUT/(TOT4SL+PIN)
EFFIO=POUT/PIN
SW=SW+SW
C
WRITE(6,702)POUT,EFFIO,SLIP,IMAX,DI,RMS,AVERI,DTRIO
WRITE(6,703)SW,PSW,PTRANS,PDIODE,TOT4SL,IN
702 FORMAT(//,' POWER OUT=' ,F6.0,4X,'EFFIO=' ,F5.3,2X,'SLIP=' ,
1F7.5,2X,'IMAX=' ,F4.0,2X,'DI=' ,F3.0,4X,
2'I(RMS)' ,F5.1,3X,'I(AVE)' ,F5.1,3X,'DTRIO=' ,F5.3,////)
703 FORMAT(//,'#SW/CYC=' ,F5.1,8X,'PSW=' ,F6.1,3X,'PTRANS=' ,F5.1,
1 2X,'PDIODE=' ,F4.1,2X,'TOT4SL=' ,F6.1,5X,'IN=' ,I5,////////)
CC WRITE(6,705)
C705 FORMAT(IX,'Z',11X,'I HARMONIC ',15X,'P HARMONIC',//)
C706 FORMAT(1X,F5.1,5X,F12.8,5X,F15.8)
CC ISTOP=0.0
CC CALL FFT(F1,8)
CC CALL FFT(F2,8)
CC DO 401 I=1,128
CC MAG1(I)=CABS(F1(I))/256.
CC MAG2(I)=CABS(F2(I))/256.
CC Z=FLOAT(I-1)
CC IF (I.EQ.1) MAG1(2)=200.
CC AMP1=MAG1(I)/MAG1(2)
CC AMP2=MAG2(I)/MAG2(1)
CC WRITE(6,706) Z,AMP1,AMP2
CC IF(I.EQ.128) ISTOP=1
C IF(AMP2.GT.300) AMP2=0.0
C
CC CALL FPLOT(800,IPNT4,AR4,LR4,ISTOP,1,1,Z,AMP1)
CC CALL FPLOT(800,IPNT3,AR3,LR3,ISTOP,1,1,Z,AMP2)
C401 CONTINUE
STOP
END
SUBROUTINE FFT(X,M)
COMPLEX X(256),U,W,T
N=2**M
NV2=N/2

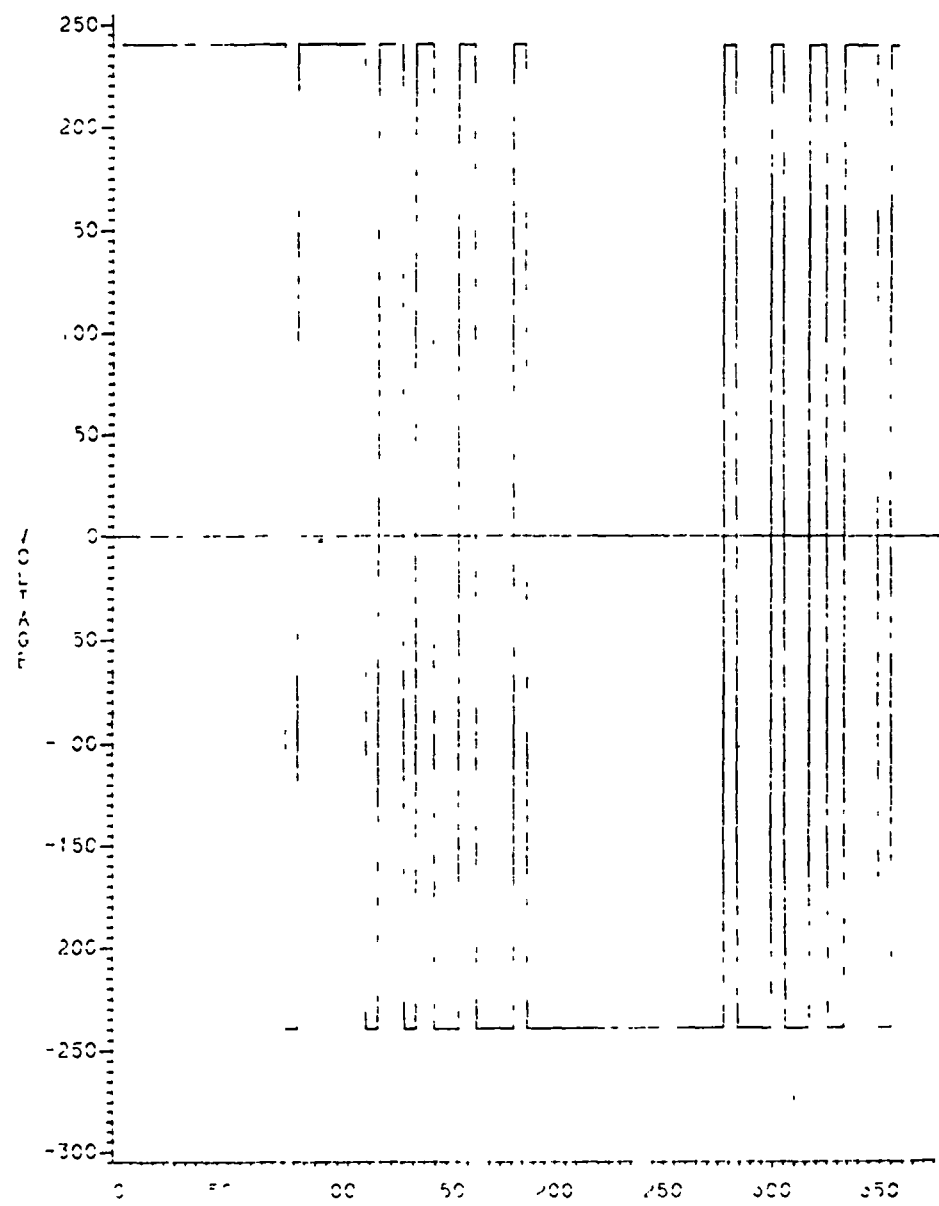
```

FILE: OPTIM WATFIV A UNIVERSITY OF MISSOURI COMPUTER NETWORK

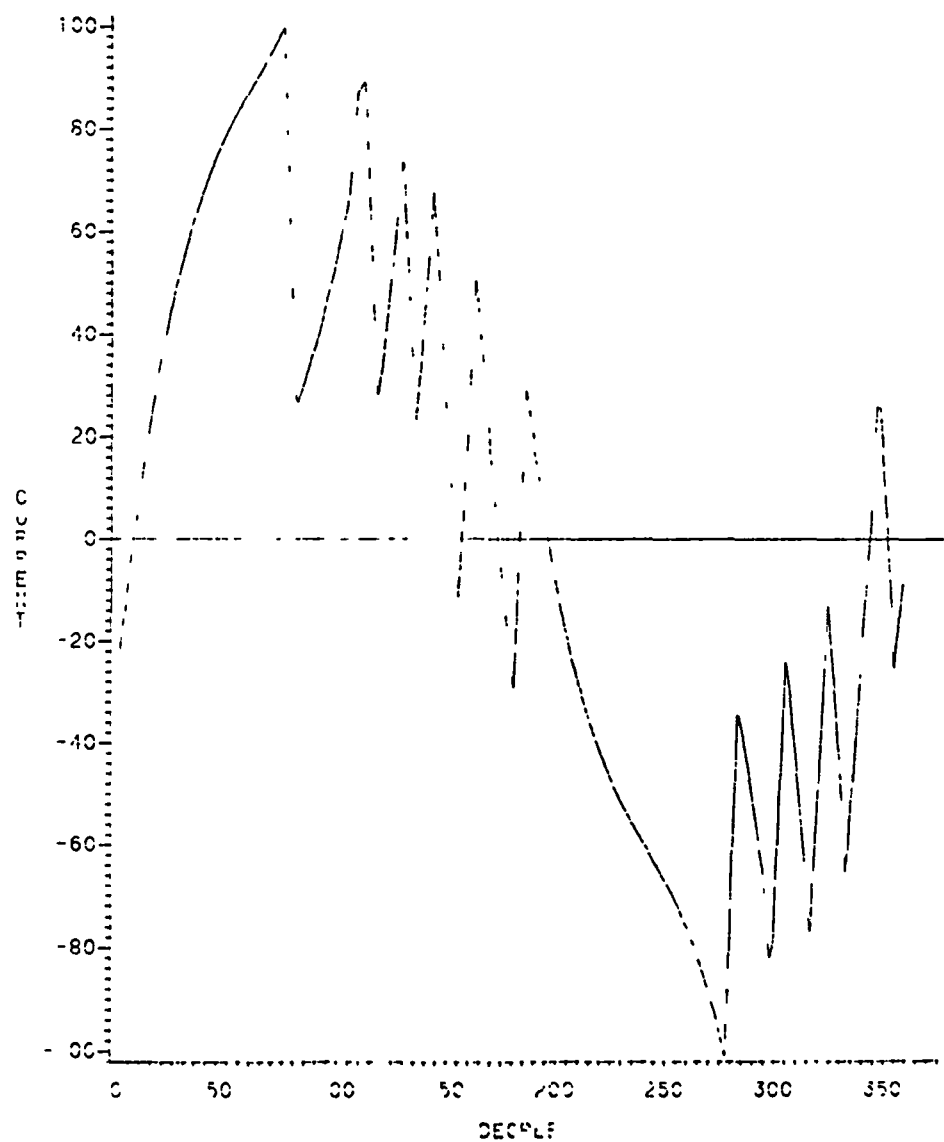
PAGE 006

```
NM1=N-1
J=1
DO 7 I=1,NM1
IF(I.GT.J) GOTO 5
T=X(J)
X(J)=X(I)
X(I)=T
5 K=NM2
6 IF(K.GE.J)GO TO 7
J=J-K
K=K/2
GO TO 6
7 J=J+K
PI=3.14159265358979
DO 20 L=1,M
LE=2**L
LE1=LE/2
U=(1.0,0.0)
Z=COS(PI/FLOAT(LE1))
Y=-SIN(PI/FLOAT(LE1))
W=CMPLX(Z,Y)
DO 20 J=1,LE1
DO 10 I=J,N,LE
IP=I+LE1
T=X(IP)*U
X(IP)=X(I)-T
10 X(I)=X(I)+T
20 U=U*W
RETURN
END
$ENTRY
1      A    CURRENT OF PHASE A OF STATOR
1      P    POWER VS TIME
1      I    CURRENT HARMONIC MAGNITUDE VS HARMONIC ORDER
1      P    POWER HARMONIC MAGNITUDE VS HARMONIC ORDER
1      V    VOLTAGE OF PHASE A OF STATOR
$STOP
/*
//
```

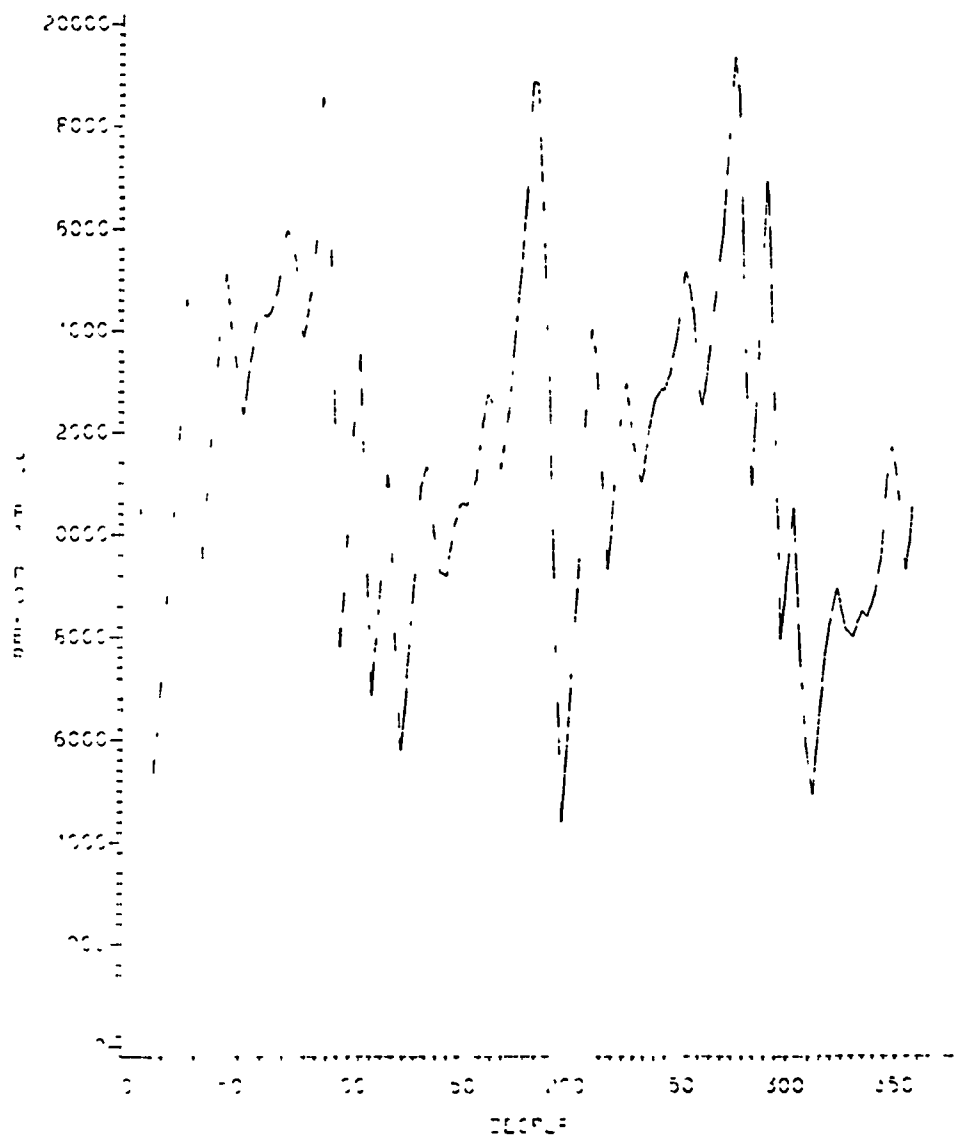
STATOR VOLTAGE (80% SPEED, 12 KW)



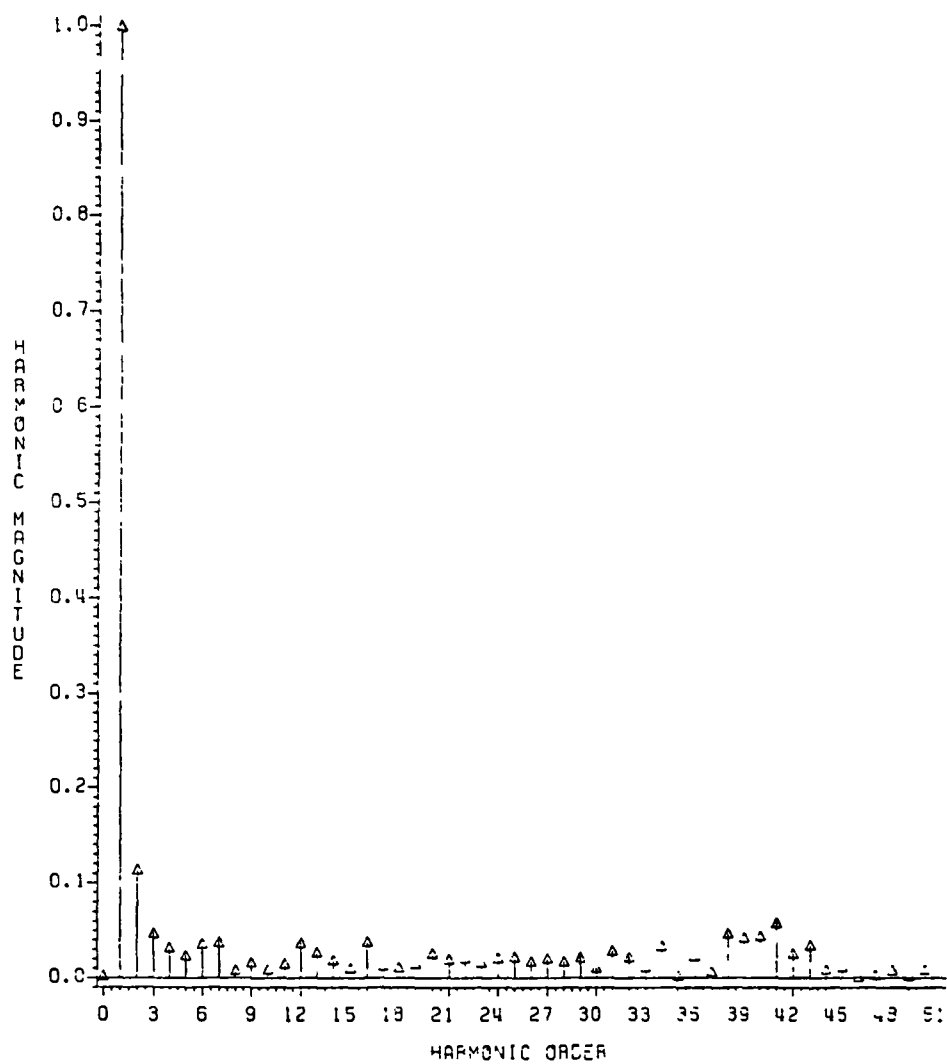
STATOR CURRENT (80% SPEED, 12 KW)



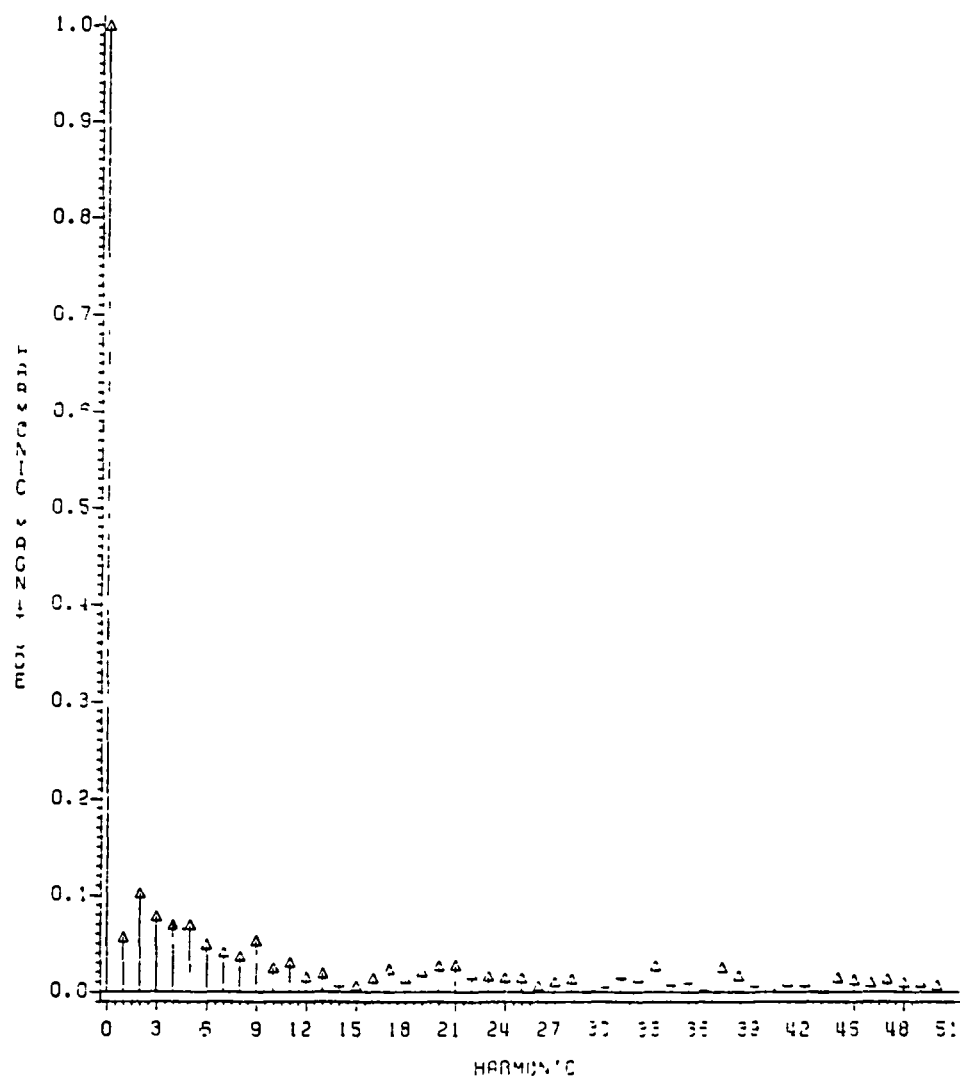
OUTPUT POWER (80% SPEED, 12KW)



CURRENT SPECTRUM (80% SPEED, 12 KW)



POWER SPECTRUM (80% SPEED, 12KW)



FILE: PLOTP160.WATFIV A UNIVERSITY OF MISSOURI COMPUTER NETWORK

PAGE 001

```

//PLOTS JOB (XXXXLH),'JPL PROJ',
// PASSWORD=
/*JOBPARM R=900,B=99000
// EXEC PLOTSAS
//SYSIN DD *
      OPTIONS DEVICE=CAL1077;
      DATA ONE;
      INPUT X Y1-Y3;
CARDS;
=====

```

DATA FOR 80% SPEED 60 KW OPERATION

| DEGREE | CURRENT | VOLTAGE | POWER |
|--------|---------|---------|----------|
| 1.1 | -22.81 | 240.00 | 5920.99 |
| 1.6 | -20.59 | 240.00 | 6231.94 |
| 2.2 | -18.39 | 240.00 | 6548.00 |
| 2.8 | -16.23 | 240.00 | 6868.89 |
| 3.6 | -13.22 | 240.00 | 7330.49 |
| 4.7 | -9.07 | 240.00 | 7997.52 |
| 6.4 | -3.40 | 240.00 | 8965.61 |
| 8.7 | 4.21 | 240.00 | 10373.63 |
| 11.9 | 14.19 | 240.00 | 12412.63 |
| 16.5 | 26.83 | 240.00 | 15305.36 |
| 23.0 | 41.97 | 240.00 | 19177.87 |
| 23.4 | 42.81 | 240.00 | 18808.73 |
| 23.8 | 43.65 | 240.00 | 18330.34 |
| 24.2 | 44.48 | 240.00 | 17862.74 |
| 24.6 | 45.29 | 240.00 | 17405.93 |
| 25.2 | 46.42 | 240.00 | 16778.39 |
| 26.0 | 47.99 | 240.00 | 15927.89 |
| 27.1 | 50.13 | 240.00 | 14799.00 |
| 28.8 | 53.03 | 240.00 | 13350.31 |
| 29.2 | 53.73 | 240.00 | 13531.00 |
| 29.6 | 54.42 | 240.00 | 13812.66 |
| 30.0 | 55.10 | 240.00 | 14090.93 |
| 30.4 | 55.77 | 240.00 | 14365.63 |
| 30.9 | 56.71 | 240.00 | 14747.93 |
| 31.8 | 58.00 | 240.00 | 15275.69 |
| 32.9 | 59.76 | 240.00 | 15995.06 |
| 34.5 | 62.14 | 240.00 | 16954.89 |
| 36.8 | 65.29 | 240.00 | 18187.43 |
| 40.1 | 69.33 | 240.00 | 19653.47 |
| 40.5 | 69.81 | 240.00 | 19466.14 |
| 40.9 | 70.28 | 240.00 | 19217.89 |
| 41.3 | 70.74 | 240.00 | 18979.47 |
| 41.7 | 71.20 | 240.00 | 18750.66 |
| 42.3 | 71.83 | 240.00 | 18443.44 |
| 43.1 | 72.71 | 240.00 | 18042.04 |
| 44.2 | 73.91 | 240.00 | 17539.42 |
| 45.8 | 75.54 | 240.00 | 16957.45 |
| 48.1 | 77.71 | 240.00 | 16387.70 |

FILE: PLOTP160.WATFIV A UNIVERSITY OF MISSOURI COMPUTER NETWORK

PAGE 002

| | | | |
|------|-------|---------|----------|
| 48.5 | 78.08 | 240.00 | 16533.59 |
| 48.9 | 78.45 | 240.00 | 16717.02 |
| 49.3 | 78.81 | 240.00 | 16893.27 |
| 49.8 | 79.17 | 240.00 | 17062.34 |
| 50.3 | 79.67 | 240.00 | 17288.99 |
| 51.1 | 80.36 | 240.00 | 17584.35 |
| 52.3 | 81.33 | 240.00 | 17950.66 |
| 53.9 | 82.65 | 240.00 | 18363.02 |
| 56.2 | 84.45 | 240.00 | 18727.66 |
| 56.6 | 84.76 | 240.00 | 18682.68 |
| 57.0 | 85.07 | 240.00 | 18627.90 |
| 57.4 | 85.38 | 240.00 | 18581.06 |
| 57.8 | 85.69 | 240.00 | 18542.06 |
| 58.4 | 86.12 | 240.00 | 18500.16 |
| 59.2 | 86.73 | 240.00 | 18467.24 |
| 60.3 | 87.58 | 240.00 | 18472.39 |
| 62.0 | 88.78 | 240.00 | 18590.52 |
| 64.3 | 90.48 | 240.00 | 18928.00 |
| 64.7 | 90.79 | 240.00 | 18958.41 |
| 65.1 | 91.09 | 240.00 | 18969.84 |
| 65.5 | 91.39 | 240.00 | 18971.66 |
| 65.9 | 91.70 | 240.00 | 18963.81 |
| 66.5 | 92.13 | 240.00 | 18936.08 |
| 67.3 | 92.75 | 240.00 | 18863.47 |
| 68.4 | 93.63 | 240.00 | 18693.46 |
| 70.0 | 94.91 | 240.00 | 18316.52 |
| 70.4 | 95.23 | 240.00 | 18347.82 |
| 70.8 | 95.56 | 240.00 | 18413.83 |
| 71.2 | 95.89 | 240.00 | 18485.64 |
| 71.7 | 96.22 | 240.00 | 18563.12 |
| 72.2 | 96.69 | 240.00 | 18682.33 |
| 73.0 | 97.38 | 240.00 | 18869.82 |
| 74.2 | 98.36 | 240.00 | 19171.70 |
| 75.8 | 99.80 | 240.00 | 19668.84 |
| 76.4 | 93.83 | -240.00 | 18545.96 |
| 76.9 | 86.57 | -240.00 | 17178.11 |
| 77.5 | 79.32 | -240.00 | 15829.75 |
| 78.1 | 72.09 | -240.00 | 14501.10 |
| 78.9 | 61.89 | -240.00 | 12656.22 |
| 80.1 | 47.51 | -240.00 | 10116.46 |
| 81.7 | 27.30 | -240.00 | 6666.26 |
| 82.2 | 26.69 | 240.00 | 6761.41 |
| 82.8 | 27.39 | 240.00 | 7121.00 |
| 83.4 | 28.10 | 240.00 | 7468.83 |
| 84.0 | 28.83 | 240.00 | 7864.62 |
| 84.8 | 29.87 | 240.00 | 8409.14 |
| 85.2 | 30.41 | 240.00 | 8298.47 |
| 85.6 | 30.95 | 240.00 | 8100.25 |
| 86.0 | 31.49 | 240.00 | 7890.95 |
| 86.4 | 32.04 | 240.00 | 7670.58 |
| 87.0 | 32.84 | 240.00 | 7339.98 |
| 87.8 | 33.98 | 240.00 | 6834.56 |
| 88.9 | 35.65 | 240.00 | 6043.88 |
| 90.5 | 38.12 | 240.00 | 4773.80 |
| 91.0 | 38.76 | 240.00 | 4903.55 |

FILE: PLOTP160 WATFIV A UNIVERSITY OF MISSOURI COMPUTER NETWORK

PAGE 003

| | | | |
|-------|--------|---------|----------|
| 91.4 | 39.40 | 240.00 | 5129.91 |
| 91.8 | 40.05 | 240.00 | 5358.91 |
| 92.2 | 40.71 | 240.00 | 5590.45 |
| 92.7 | 41.54 | 240.00 | 5922.09 |
| 93.6 | 43.03 | 240.00 | 6398.95 |
| 94.7 | 45.03 | 240.00 | 7087.78 |
| 96.3 | 47.97 | 240.00 | 8087.09 |
| 98.6 | 52.39 | 240.00 | 9539.93 |
| 101.9 | 59.18 | 240.00 | 11643.59 |
| 106.4 | 69.95 | 240.00 | 14630.51 |
| 112.9 | 87.72 | 240.00 | 18636.06 |
| 113.5 | 82.94 | -240.00 | 18127.67 |
| 114.1 | 76.89 | -240.00 | 17470.94 |
| 114.7 | 70.88 | -240.00 | 16835.94 |
| 115.2 | 64.89 | -240.00 | 16222.70 |
| 116.0 | 56.49 | -240.00 | 15392.52 |
| 117.2 | 44.71 | -240.00 | 14292.68 |
| 118.8 | 28.28 | -240.00 | 12885.57 |
| 119.4 | 29.04 | 240.00 | 13154.08 |
| 120.0 | 31.12 | 240.00 | 13562.98 |
| 120.5 | 33.23 | 240.00 | 13964.82 |
| 121.1 | 35.37 | 240.00 | 14359.29 |
| 121.9 | 38.44 | 240.00 | 14904.15 |
| 123.1 | 42.88 | 240.00 | 15647.38 |
| 124.7 | 49.35 | 240.00 | 16640.20 |
| 127.0 | 58.90 | 240.00 | 17917.97 |
| 130.2 | 73.20 | 240.00 | 19445.14 |
| 130.8 | 69.33 | -240.00 | 19197.31 |
| 131.4 | 64.19 | -240.00 | 18870.05 |
| 131.9 | 59.09 | -240.00 | 18562.40 |
| 132.5 | 54.02 | -240.00 | 18273.94 |
| 133.3 | 46.92 | -240.00 | 17898.85 |
| 134.5 | 37.00 | -240.00 | 17433.36 |
| 136.1 | 23.22 | -240.00 | 16903.72 |
| 136.7 | 24.93 | 240.00 | 17099.50 |
| 137.2 | 27.96 | 240.00 | 17353.89 |
| 137.8 | 31.02 | 240.00 | 17594.44 |
| 138.4 | 34.11 | 240.00 | 17321.02 |
| 139.2 | 38.54 | 240.00 | 18117.16 |
| 140.3 | 44.90 | 240.00 | 18486.34 |
| 142.0 | 54.12 | 240.00 | 18906.48 |
| 144.3 | 67.58 | 240.00 | 19289.04 |
| 144.8 | 64.52 | -240.00 | 19189.06 |
| 145.4 | 60.20 | -240.00 | 19071.40 |
| 146.0 | 55.92 | -240.00 | 18969.96 |
| 146.5 | 51.68 | -240.00 | 18384.70 |
| 147.4 | 45.74 | -240.00 | 18791.24 |
| 148.5 | 37.46 | -240.00 | 18712.46 |
| 150.1 | 26.02 | -240.00 | 18705.63 |
| 152.4 | 10.35 | -240.00 | 18893.12 |
| 155.7 | -10.80 | -240.00 | 19553.66 |
| 156.2 | -7.91 | 240.00 | 19597.46 |
| 156.8 | -3.69 | 240.00 | 19600.96 |
| 157.4 | 0.55 | 240.00 | 19584.65 |
| 158.0 | 4.83 | 240.00 | 19548.38 |

G.5 TWO-PHASE SIMULATION RESULTS FOR POWER REGENERATION AT 80% SPEED

Plots

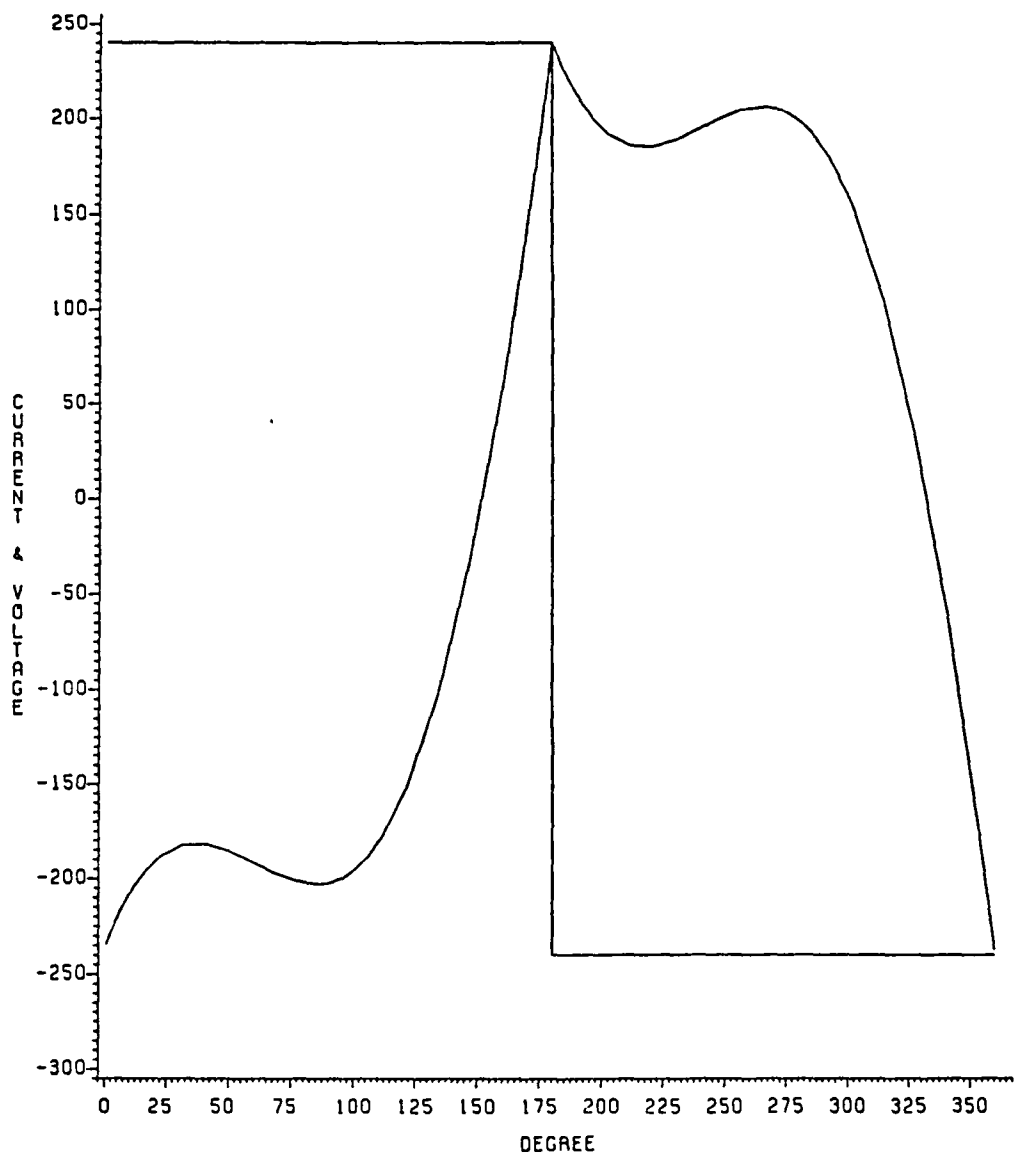
 Stator Voltage and Current

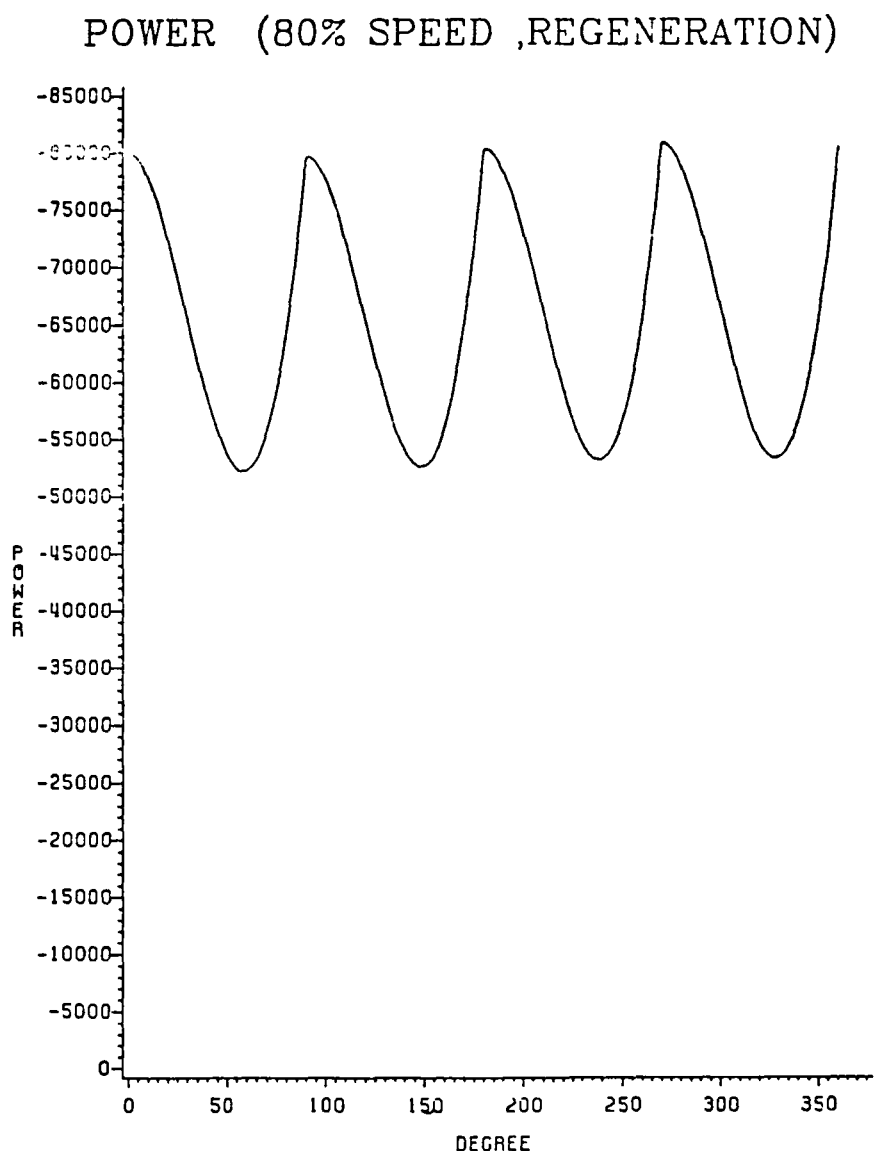
 Output Power

Listing of Plot Data

Comment: Source Program is the same as for G.3 except the slip frequency
is negative.

VOLTAGE & CURRENT (80% SPEED,REGENERATIVE)





FILE: REG PLOT A UNIVERSITY OF MISSOURI COMPUTER NETWORK

PAGE 001

```

//REGP      JOB (XXXXLH),'GOODARZI',
// PASSWORD=XXXX
/*JOBPARM R=900,B=99000
// EXEC PLOTSAS
//SYSIN DD *
      GOPTIONS DEVICE=VARIAN;
      DATA ONE;
      INPUT X Y1-Y3;
*****
*          REGENERATION MODE @ 80% SPEED   JPL PROJECT
*          PLOT DATA
*          |           |           |
* DEGREE |VOLTAGE | CURRENT |POWER
*****|*****|*****|*****|
CARDS;
 0.5 -234.49    240.00 -79927.88
 1.1 -232.59    240.00 -79913.88
 1.6 -230.73    240.00 -79883.56
 2.2 -228.91    240.00 -79837.13
 3.0 -226.41    240.00 -79744.81
 4.2 -223.00    240.00 -79562.31
 5.8 -218.45    240.00 -79205.38
 8.1 -212.52    240.00 -78515.63
11.3 -205.15    240.00 -77208.75
16.0 -196.63    240.00 -74807.44
22.5 -188.09    240.00 -70622.75
31.7 -182.09    240.00 -64028.68
40.9 -181.74    240.00 -57917.55
50.1 -185.33    240.00 -53617.25
59.3 -191.03    240.00 -52301.88
68.5 -197.03    240.00 -54937.41
77.7 -201.52    240.00 -62237.88
86.9 -202.77    240.00 -74629.75
89.2 -202.38    240.00 -78543.88
89.8 -202.24    240.00 -79573.25
90.2 -202.12    240.00 -79703.56
90.6 -201.99    240.00 -79704.81
91.0 -201.85    240.00 -79698.00
91.4 -201.71    240.00 -79682.94
92.0 -201.48    240.00 -79647.94
92.8 -201.11    240.00 -79571.56
94.0 -200.52    240.00 -79411.38
95.6 -199.52    240.00 -79085.44
97.9 -197.77    240.00 -78438.06
101.2 -194.58    240.00 -77188.06
105.8 -188.51    240.00 -74862.19
112.3 -176.55    240.00 -70770.81
121.5 -152.17    240.00 -64283.78
134.5 -101.16    240.00 -56195.74
147.5 -29.33     240.00 -52653.23
160.6  63.87     240.00 -56617.87
173.6  177.76    240.00 -70080.00
178.2  222.68    240.00 -77304.44
179.8  239.11    240.00 -80170.49

```

FILE: REG PLOT A UNIVERSITY OF MISSOURI COMPUTER NETWORK

PAGE 002

| 180.4 | 238.47 | -240.00 | -80355.13 | |
|-------|---------|---------|-----------|--|
| 181.0 | 236.56 | -240.00 | -80352.50 | |
| 181.5 | 234.69 | -240.00 | -80333.38 | |
| 182.1 | 232.87 | -240.00 | -80298.25 | |
| 182.9 | 230.35 | -240.00 | -80221.63 | |
| 184.1 | 226.93 | -240.00 | -80061.06 | |
| 185.7 | 222.35 | -240.00 | -79734.38 | |
| 188.0 | 216.40 | -240.00 | -79086.13 | |
| 191.3 | 208.99 | -240.00 | -77834.75 | |
| 195.9 | 200.42 | -240.00 | -75505.56 | |
| 202.4 | 191.81 | -240.00 | -71410.00 | |
| 211.6 | 185.73 | -240.00 | -64915.04 | |
| 220.8 | 185.32 | -240.00 | -58869.37 | |
| 230.0 | 188.85 | -240.00 | -54598.85 | |
| 239.2 | 194.52 | -240.00 | -53279.17 | |
| 248.4 | 200.51 | -240.00 | -55878.30 | |
| 257.6 | 205.00 | -240.00 | -63112.98 | |
| 266.9 | 206.26 | -240.00 | -75411.81 | |
| 269.2 | 205.88 | -240.00 | -79299.13 | |
| 270.0 | 205.67 | -240.00 | -80751.25 | |
| 270.4 | 205.55 | -240.00 | -80879.50 | |
| 270.8 | 205.42 | -240.00 | -80878.31 | |
| 271.2 | 205.27 | -240.00 | -80868.75 | |
| 271.6 | 205.12 | -240.00 | -80851.06 | |
| 272.2 | 204.88 | -240.00 | -80812.31 | |
| 273.0 | 204.51 | -240.00 | -80730.44 | |
| 274.1 | 203.90 | -240.00 | -80562.56 | |
| 275.8 | 202.88 | -240.00 | -80225.38 | |
| 278.1 | 201.10 | -240.00 | -79561.69 | |
| 281.3 | 197.86 | -240.00 | -78288.13 | |
| 285.9 | 191.72 | -240.00 | -75926.63 | |
| 292.4 | 179.65 | -240.00 | -71782.19 | |
| 301.6 | 155.10 | -240.00 | -65216.10 | |
| 314.7 | 103.83 | -240.00 | -57010.73 | |
| 327.7 | 31.73 | -240.00 | -53344.49 | |
| 340.7 | -61.74 | -240.00 | -57181.73 | |
| 353.7 | -175.89 | -240.00 | -70511.56 | |
| 358.3 | -220.89 | -240.00 | -77688.31 | |
| 360.0 | -237.35 | -240.00 | -80537.50 | |

```

;
PROC GPLOT;
PLOT Y1*X Y2*X /OVERLAY;
SYMBOL1 I=JOIN L=1;
SYMBOL2 I=JOIN L=13;
LABEL X=DEGREE
      Y1=CURRENT & VOLTAGE ;
TITLE VOLTAGE & CURRENT (80% SPEED,REGENERATIVE);

PROC GPLOT;
PLOT Y3*X /VAXIS=0 TO -85000 BY -5000;
SYMBOL1 I=SPLINE;
LABEL X=DEGREE
      Y3= POWER ;
TITLE REGENERATIVE POWER (80% SPEED );

```

G.6 THREE-PHASE SIMULATION RESULTS

Source Program

Plots

 Stator Voltage and Current

 Output Power

Listing of Plot Data

FILE: JPL330 WATFIV A UNIVERSITY OF MISSOURI COMPUTER NETWORK

PAGE 001

```

//B6330 JOB (XXXXEE),'ABBAS GOODARZI',CLASS=A,MSGLEVEL=(0,0),          JPL00010
// PASSWORD=XXXX                      JPL00020
/*JOBPARM T=2 ,L=2                  JPL00030
/*ROUTE PRINT UMMVMA.EEPR3          JPL00040
// EXEC WATFIV                      JPL00050
//GO.SYSIN DD *                      JPL00060
$JOB                                JPL00070
      DIMENSION AR1(800),AR2(800),AR3(800),Y(20),X(20),GA(20),PE(20),    JPL00080
      1XX(4,20),H(9),ZZ1(20),ZZ2(20),ZZ3(20),IFL(7),AR4(800)           JPL00090
      LOGICAL*1 LR1(800),LR2(800),LR3(800),LR4(800)                   JPL00100
      REAL L(6,6),LR(6,6),D(6,6),LI(6,6), WKAREA(54),LOS,LOR,LN,THETA,C,JPL00110
      1IAS,IBS,ICS,IAR,IBR,ICR,IER,RS,RR,DD,EE,FF,TQ,AA,BB,CC,E,OMEGR,   JPL00120
      2DL(6,6),IAREF,IBREF,ICREF,IMAX                           JPL00130
C/ PASSWORD=XXXX,MSGCLASS=S          JPL00140
C*JOBPARM T=3 ,L=3                  JPL00150
C*ROUTE PRINT UMMVSA.R0             JPL00160
C 50 FORMAT(/,2X,'TIME',8X,'VA',8X,'IAS',8X,'IBS',8X,'ICS',8X,       JPL00170
C 1     'IAR',8X,'IBR',8X,'ICR',5X,'POWER',7X,'ANGLE')            JPL00180
      IMAX=100.                         JPL00190
      SLIP=0.0125                      JPL00200
      DI=10.                          JPL00210
      E=240.                          JPL00220
      NRUN=1                           JPL00230
      ISTOP=0                          JPL00240
      KEEP=1                           JPL00250
      IFL(1)=-1                        JPL00260
      NINT=9                           JPL00270
      IPNT1=0                          JPL00280
      IPNT2=0                          JPL00290
      IPNT3=0                          JPL00300
      IPNT4=0                          JPL00310
*****                                JPL00320
C          MOTOR PARAMETERS          JPL00330
C          FOR BRIDGE INVERTER (JPL) DATA SIMPLIFIED MODEL        JPL00340
*****                                JPL00350
      LOS=75.360E-06                  JPL00360
      LOR=150.E-06                    JPL00370
      LM=4200.E-06                   JPL00380
      RS=0.007345                    JPL00390
      RR=0.004813                    JPL00400
      PAI=3.14159                     JPL00410
      PI2=2.*PAI/3.                  JPL00420
      THETA=0.                        JPL00430
      FREQ=330.                       JPL00440
      OMEGA=2*PAI*FREQ               JPL00450
      OMEGR=OMEGA*(1.-SLIP)          JPL00460
      WRITE(6,64)                      JPL00470
      WRITE(6,66)LOS,LOR              JPL00480
      WRITE(6,69)RS,RR                JPL00490
      WRITE(6,68)LM                   JPL00500
      WRITE(6,71)SLIP                 JPL00510
      WRITE(6,72)FREQ                 JPL00520
      WRITE(6,64)                      JPL00530
C      WRITE(6,50)                  JPL00540
64      FORMAT(' ',//,20X,'*****MOTOR PARAMETERS*****',//)        JPL00550

```

FILE: JPL330 WATFIV A UNIVERSITY OF MISSOURI COMPUTER NETWORK

PAGE 002

```

66  FORMAT(' ',20X,'LOS=',F9.7,5X,'LOR=',F9.7)          JPL00560
68  FORMAT(' ',20X,'LM=',F9.7)                         JPL00570
69  FORMAT(' ',20X,'RS=',F8.6,5X,'RR=',F8.6)           JPL00580
71  FORMAT(' ',20X,'SLIP=',F6.4)                        JPL00590
72  FORMAT(' ',20X,'FREQUENCY=',F6.1)                   JPL00600
WS=LM+LOS
WR=LM+LOR
T=SQRT(3. )/2.*OMEGR*LM
Z=-0.5*LM
U=SQRT(3. )/3.*OMEGR*(3./2.*LM+LOR)
DO 100 I=1,6
DO 100 J=1,6
L(I,J)=Z
LR(I,J)=0.
D(I,J)=0.
100 CONTINUE
DO 200 I=1,3
L(I,I)=WS
LR(I,I)=RS
200 CONTINUE
DO 201 I=4,6
L(I,I)=WR
LR(I,I)=RR
201 CONTINUE
L(1,4)=LM
L(2,5)=LM
L(3,6)=LM
L(4,1)=LM
L(5,2)=LM
L(6,3)=LM
LR(4,2)=T
LR(4,3)=-T
LR(4,5)=U
LR(4,6)=-U
LR(5,1)=-T
LR(5,3)=T
LR(5,4)=-U
LR(5,6)=U
LR(6,1)=T
LR(6,2)=-T
LR(6,4)=U
LR(6,5)=-U
DO 400 I=1,6
DO 400 J=1,6
400 L(I,J)=L(I,J)
CALL INVERS (LI,6)
CALL MATMUL (LI,LR,6,6,6,D)
1 IF(L(2)=-1
2 CALL RKFOUR(NINT,Y,X,GA,PE,XX,H,ZZ1,ZZ2,ZZ3,TIME,PNTS,KEEP,IFL)
IF(IFL(4))3,4,5
3 INIT=1
TIME1=-1
NC=1
NCC=3
TIME=0.

```

FILE: JPL330 WATFIV A UNIVERSITY OF MISSOURI COMPUTER NETWORK

PAGE 003

```

FINTIM=0.060505          JPL01110
Y(1)=0.                   JPL01120
Y(2)=0.                   JPL01130
Y(3)=0.                   JPL01140
Y(4)=0.                   JPL01150
Y(5)=0.                   JPL01160
Y(6)=0.                   JPL01170
Y(7)=0.0                 JPL01180
Y(8)=0.0                 JPL01190
Y(9)=0.0                 JPL01200
H(1)=0.1E-4               JPL01210
E2=E/2.                   JPL01220
IAE=-1                   JPL01230
IBE=-1                   JPL01240
ICE=-1                   JPL01250
UPIN=0.0                 JPL01260
UPOUT=0.0                JPL01270
UPLOSS=0.0               JPL01280
POWER=0.0                JPL01290
C SUM=0.0                 JPL01300
C PIN=0.0                 JPL01310
C RMS1=0.0                JPL01320
C RMS2=0.0                JPL01330
C COUNT=0.0               JPL01340
C SW=0.0                  JPL01350
C PSW=0.0                 JPL01360
C PERIOD=1./FREQ          JPL01370
C TF=FINTIM-PERIOD       JPL01380
4 IF(TIME-TIME1)7,8,7
7 TIME1=TIME              JPL01390
JPL01400
C*****                         JPL01410
C*****                         JPL01420
C                               JPL01430
C                               JPL01440
C REFFERENCE SIGNAL FOR GENERATING INPUT VOLTAGE   JPL01450
C AND THE CURENT CONTROLER REFRENCE SIGNAL        JPL01460
C                               JPL01470
C*****                         JPL01480
C*****                         JPL01490
C DEG=FREQ*TIME             JPL01500
C IDEG=DEG                 JPL01510
C DEG=(DEG-IDEG)*360.       JPL01520
C                               JPL01530
C VA=160.*SIN(OMEGA*TIME)  JPL01540
C VB=160.*SIN(OMEGA*TIME-PI2) JPL01550
C VC=160.*SIN(OMEGA*TIME+PI2) JPL01560
C IF(TIME.LT.2.8890909) GOTO 88
C VA0=E2                   JPL01570
C VB0=E2                   JPL01580
C VC0=E2                   JPL01590
C IAREF=IMAX*SIN(OMEGA*TIME)
C IBREF=IMAX*SIN(OMEGA*TIME-PI2)
C ICREF=IMAX*SIN(OMEGA*TIME+PI2)
C                               JPL01600
C                               JPL01610

```

FILE: JPL330 WATFIV A UNIVERSITY OF MISSOURI COMPUTER NETWORK

PAGE 004

```

IF(IAREF.LT.0.0) VA0=-E2          JPL01620
IF(IBREF.LT.0.0) VB0=-E2          JPL01630
IF(ICREF.LT.0.0) VC0=-E2          JPL01640
IF(TIME.LT.2.8890909) GOTO 87    JPL01650
C
12   DIA=Y(1)-IAREF               JPL01660
     DIB=Y(2)-IBREF               JPL01670
     DIC=Y(3)-ICREF               JPL01680
C
13   IF(DIA.GT.DI)     IAE=1        JPL01690
     IF(TIME.LT.TF.AND.DIA.GT.DI) GOTO 13    JPL01700
     SW=SW+1.
     PSW=ABS((240.*Y(1)*5.5E-06)/(6*PERIOD))+PSW
13   IF(DIA.LT.(-DI))  IAE=0        JPL01710
     IF(VA0.GT.0.0.AND.IAE.EQ.1) VA0=-VA0      JPL01720
     IF(VA0.LT.0.0.AND.IAE.EQ.0) VA0=-VA0      JPL01730
C
13   IF(DIB.GT.DI)     IBE=1        JPL01740
     IF(DIB.LT.(-DI))  IBE=0        JPL01750
     IF(VB0.GT.0.0.AND.IBE.EQ.1) VB0=-VB0      JPL01760
     IF(VB0.LT.0.0.AND.IBE.EQ.0) VB0=-VB0      JPL01770
C
13   IF(DIC.GT.DI)     ICE=1        JPL01780
     IF(DIC.LT.(-DI))  ICE=0        JPL01790
     IF(VC0.GT.0.0.AND.ICE.EQ.1) VC0=-VC0      JPL01800
     IF(VC0.LT.0.0.AND.ICE.EQ.0) VC0=-VC0      JPL01810
C
13   IF(VN=(VA0+VB0+VC0)/3.        JPL01820
     VA=VA0-VN                   JPL01830
     VB=VB0-VN                   JPL01840
     VC=VC0-VN                   JPL01850
C
87   VN=(VA0+VB0+VC0)/3.          JPL01860
     VA=VA0-VN                   JPL01870
     VB=VB0-VN                   JPL01880
     VC=VC0-VN                   JPL01890
C
88   CONTINUE
     IF(TIME.GT.0.03318.AND.TIME.LT.0.03323) UPIN=Y(7)  JPL01900
     IF(TIME.GT.0.03318.AND.TIME.LT.0.03323) UPOUT=Y(8)  JPL01910
     IF(TIME.GT.0.03318.AND.TIME.LT.0.03323) ULOSS=Y(9)  JPL01920
C
88   CONTINUE
     THETA=OMEGR*TIME            JPL01930
     DD=SIN(THETA)               JPL01940
     EE=SIN(THETA+2.*PAI/3.)     JPL01950
     FF=SIN(THETA-2.*PAI/3.)     JPL01960
C
88   IAR=2./3.*((COS(THETA)+0.5)*Y(4)+(COS(THETA-2.*PAI/3. )+0.5)*Y(5)  JPL01970
     . 1+(COS(THETA+2.*PAI/3. )+0.5)*Y(6))
C
88   CONTINUE
C
X(1)=-D(1,1)*Y(1)-D(1,2)*Y(2)-D(1,3)*Y(3)-D(1,4)*Y(4)-D(1,5)*Y(5) JPL02080
1   -D(1,6)*Y(6)+LI(1,1)*VA+LI(1,2)*VB+LI(1,3)*VC JPL02090
X(2)=-D(2,1)*Y(1)-D(2,2)*Y(2)-D(2,3)*Y(3)-D(2,4)*Y(4)-D(2,5)*Y(5) JPL02100
1   -D(2,6)*Y(6)+LI(2,1)*VA+LI(2,2)*VB+LI(2,3)*VC JPL02110
X(3)=-D(3,1)*Y(1)-D(3,2)*Y(2)-D(3,3)*Y(3)-D(3,4)*Y(4)-D(3,5)*Y(5) JPL02120
1   -D(3,6)*Y(6)+LI(3,1)*VA+LI(3,2)*VB+LI(3,3)*VC JPL02130
X(4)=-D(4,1)*Y(1)-D(4,2)*Y(2)-D(4,3)*Y(3)-D(4,4)*Y(4)-D(4,5)*Y(5) JPL02140
1   -D(4,6)*Y(6)+LI(4,1)*VA+LI(4,2)*VB+LI(4,3)*VC JPL02150
X(5)=-D(5,1)*Y(1)-D(5,2)*Y(2)-D(5,3)*Y(3)-D(5,4)*Y(4)-D(5,5)*Y(5) JPL02160

```

FILE: JPL330 HATFIV A UNIVERSITY OF MISSOURI COMPUTER NETWORK

PAGE 005

```

1 -D(5,6)*Y(6)+LI(5,1)*VA+LI(5,2)*VB+LI(5,3)*VC JPL02170
X(6)=-D(6,1)*Y(1)-D(6,2)*Y(2)-D(6,3)*Y(3)-D(6,4)*Y(4)-D(6,5)*Y(5) JPL02180
1 -D(6,6)*Y(6)+LI(6,1)*VA+LI(6,2)*VB+LI(6,3)*VC JPL02190
X(7)=(VA*Y(1)+VB*Y(2)+VC*Y(3))/.02632 JPL02200
X(8)=POWER/.02632 JPL02210
X(9)=3.*((Y(1)*RS+IAR*IAR*RR)/.02632 JPL02220
JPL02230
C GOTO 2 JPL02240
5 IPR=0 JPL02250
NC=NC-1 JPL02260
IF(NC)9,9,10 JPL02270
9 NC=NCC JPL02280
IPR=1 JPL02290
10 IF(TIME.GE.FINTIM)ISTOP=1 JPL02300
IF((IPR+ISTOP).EQ.0) GOTO 11 JPL02310
C C
IAR=2./3.*((COS(THETA)+0.5)*Y(4)+(COS(THETA-2.*PAI/3.)*0.5)*Y(5)) JPL02330
1+(COS(THETA+2.*PAI/3.)*0.5)*Y(6)) JPL02340
IBR=2./3.*((COS(THETA+2.*PAI/3.)*0.5)*Y(4)+(COS(THETA)+0.5)*Y(5)) JPL02350
1+(COS(THETA-2.*PAI/3.)*0.5)*Y(6)) JPL02360
ICR=2./3.*((COS(THETA-2.*PAI/3.)*0.5)*Y(4)+(COS(THETA+2.*PAI/3.)*0.5)*Y(5)+ (COS(THETA)+0.5)*Y(6)) JPL02370
TQ=(DD*Y(1)*IAR+FF*Y(2)*IAR+EE*Y(3)*IAR+EE*Y(1)*IBR JPL02380
1 +DD*Y(2)*IBR+FF*Y(3)*IBR+FF*Y(1)*ICR+EE*Y(2)*ICR JPL02390
1 +DD*Y(3)*ICR)*(-LM) JPL02400
POWER=TQ*OMEGR JPL02410
IF(TIME.LT.0.05756) GOTO 11 JPL02420
IAS=Y(1) JPL02430
IBS=Y(2) JPL02440
ICS=Y(3) JPL02450
IAR=Y(4) JPL02460
IBR=Y(5) JPL02470
ICR=Y(6) JPL02480
WRITE(6,250)TIME,VA,Y(1),Y(2),Y(3),Y(4),Y(5),Y(6),POWER,DEG JPL02490
PIN=(VA*IAS+VB*IBS+VC*ICS)+PIN JPL02500
SUM=SUM+POWER JPL02510
RMS1=RMS1+(IAS*IAS) JPL02520
RMS2=RMS2+(IAR*IAR) JPL02530
COUNT=COUNT+1. JPL02540
IF( TIME.LT.0.057597) POWER=0.0 JPL02550
CALL FPLOT(800,IPNT1,AR1,LR1,ISTOP,1,2,DEG,IAS) JPL02560
CALL FPLOT(800,IPNT1,AR1,LR1,ISTOP,2,2,DEG,VA) JPL02570
CALL FPLOT(800,IPNT2,AR2,LR2,ISTOP,1,2,DEG,IBS) JPL02580
CALL FPLOT(800,IPNT2,AR2,LR2,ISTOP,2,2,DEG,VB) JPL02590
CALL FPLOT(800,IPNT3,AR3,LR3,ISTOP,1,2,DEG,ICS) JPL02600
CALL FPLOT(800,IPNT3,AR3,LR3,ISTOP,2,2,DEG,VC) JPL02610
CALL FPLOT(800,IPNT4,AR4,LR4,ISTOP,1,1,DEG,POWER) JPL02620
11 INIT=0 JPL02630
IF(ISTOP)1,1,6 JPL02640
6 CONTINUE JPL02650
250 FORMAT(F8.6,8(F8.0,3X),F5.1) JPL02660
C 12 FORMAT(' ',A20,/,6(F12.6,3X)) JPL02670
POWERI=Y(7)-UPIN JPL02680
POWERO=Y(8)-UOUT JPL02690
JPL02700
JPL02710

```

FILE: JPL330 MATFIV A UNIVERSITY OF MISSOURI COMPUTER NETWORK

PAGE 006

```

PLOSS=Y(9)-UPLOSS                                JPL02720
EFFIO=POWER0/POWERI                               JPL02730
C      AVER=SUM/COUNT                            JPL02740
C      PIN=PIN/COUNT                            JPL02750
C      RMS1=(RMS1/COUNT)**.5                      JPL02760
C      RMS2=(RMS2/COUNT)**.5                      JPL02770
C      PLOSS=(RMS1*RMS1)*RS+(RMS2*RMS2)*RR       JPL02780
C      EFF=AVER/PIN                             JPL02790
C      EFFL=(POWERI-PLOSS)/POWERI                  JPL02800
C      EFFPSW=(POWERI-PLOSS)/(POWERI+PSW*3)        JPL02810
C      WRITE(6,266)POWERI,POWER0,EFFIO,SLIP,IMAX,EFFL JPL02820
266    FORMAT(' ',//,',POWER IN=',F8.1,4X,'POWER OUT=',F8.1,4X,
1     'EFF(IO)=',F5.3,4X,'SLIP=',F7.5,4X,'IMAX='
1,F5.1,3X,F5.3,'1')
      WRITE(6,267)SW,PSW,EFFPSW                  JPL02830
267    FORMAT(' ',SW=',F6.1,'PSW/LEG=',F8.1,'EFFPSW=',F8.4,///) JPL02840
C      STOP                                     JPL02850
C      END                                       JPL02860
C
SUBROUTINE INVERS(ZZBUS,N)
DOUBLE PRECISION ZBUS(6,6)
DIMENSION ZZBUS(6,6)
DO 1001 I=1,N
DO 1001 J=1,N
ZBUS(I,J)=ZZBUS(I,J)
1001 CONTINUE
DO 1070 I=1,N
TRY=ZBUS(I,I)
IF(ABS(TRY)>1000,1090,1000
1000 DO 1040 J=1,N
IF(I-J)>1010,1040,1010
1010 DO 1030 K=1,N
IF(I-K)>1020,1030,1020
1020 ZBUS(J,K)=ZBUS(J,K)-ZBUS(J,I)*ZBUS(I,K)/ZBUS(I,I)
1030 CONTINUE
1040 CONTINUE
DO 1060 K=1,N
IF(K-I)>1050,1060,1050
1050 ZBUS(K,I)=ZBUS(K,I)/ZBUS(I,I)
ZBUS(I,K)=ZBUS(I,K)/ZBUS(I,I)
1060 CONTINUE
ZBUS(I,I)=-1.0/ZBUS(I,I)
1070 CONTINUE
DO 1080 I=1,N
DO 1080 J=1,N
ZBUS(I,J)=-ZBUS(I,J)
1080 CONTINUE
DO 1002 I=1,N
DO 1002 J=1,N
ZZBUS(I,J)=ZBUS(I,J)
1002 CONTINUE
RETURN
1090 WRITE(6,1100)
1100 FORMAT('ERROR IN MATRIX INVERSE')

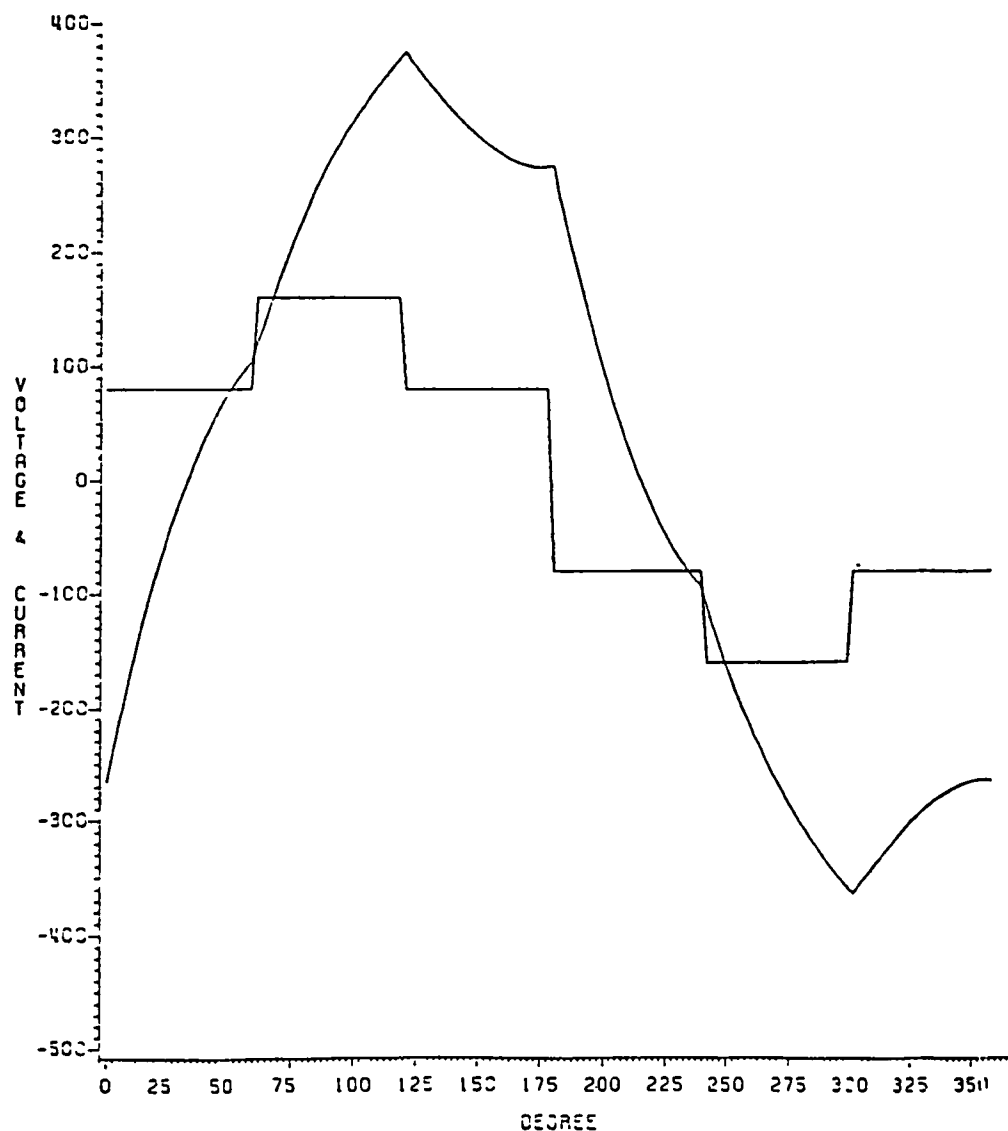
```

FILE: JPL330 MATFIV A UNIVERSITY OF MISSOURI COMPUTER NETWORK

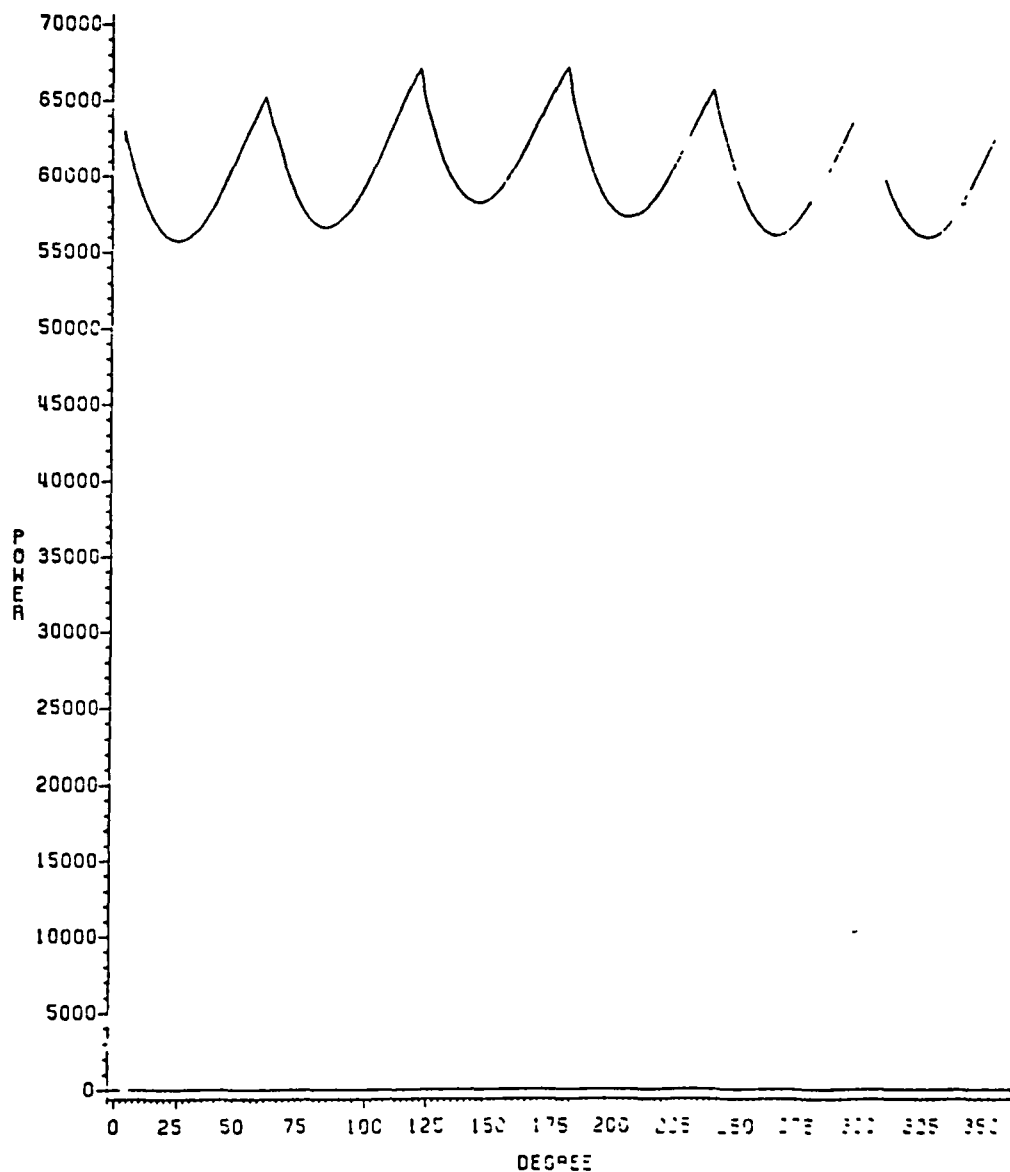
PAGE 007

```
      RETURN                               JPL03270
      END                                JPL03280
C
      SUBROUTINE MATMUL (A,B,M,L,N,C)    JPL03290
      DIMENSION A(M,L),B(L,N),C(M,N)    JPL03300
      DO 100 I=1,M                      JPL03310
      DO 100 J=1,N                      JPL03320
      C(I,J)=0.                         JPL03330
      DO 100 K=1,L                      JPL03340
100   C(I,J)=C(I,J)+A(I,K)*B(K,J)  JPL03350
      RETURN                               JPL03360
      END                                JPL03370
$ENTRY
1       AV  IAS & VA VS. TIME        JPL03380
1       P   POWER OF THE MOTOR      JPL03390
$STOP
/*                                     JPL03400
//                                     JPL03410
                           JPL03420
                           JPL03430
                           JPL03440
```

VOLTAGE & CURRENT (80% SPEED,MOTOR OPERATION)



OUTPUT POWER (80% SPEED MOTOR OPERATION)



FILE: THREE PLOT A UNIVERSITY OF MISSOURI COMPUTER NETWORK

PAGE 001

```
//THREEP JOB (XXXXLH),'GOODARZI',
// PASSWORD:XXXX
/*JOBPARM R=900,B=99000
// EXEC PLOTSAS
//SYSIN DD *
```

```
      GOPTIONS DEVICE=VARIAN;
      DATA ONE;
      INPUT X Y1-Y3;
```

```
*****
*      THREE PHASE PLOT DATA  JPL PROJECT
*      *
*      *
*****
```

CARDS:

| | | | |
|------|--------|-------|---------|
| 2 4 | -238.1 | 80 0 | 62992 7 |
| 4 8 | -215.4 | 80 0 | 61387 7 |
| 7 2 | -193 3 | 80.0 | 59997 3 |
| 9.5 | -172 0 | 80 0 | 58817.8 |
| 11.9 | -151.4 | 80 0 | 57843 1 |
| 14.3 | -131.4 | 80 0 | 57066.1 |
| 16.6 | -112.2 | 80.0 | 56478.4 |
| 19.0 | -93.8 | 80.0 | 56071 7 |
| 21.4 | -76.1 | 80.0 | 55836 0 |
| 23.8 | -59.1 | 80 0 | 55761.7 |
| 26.1 | -42.9 | 80.0 | 55837.9 |
| 28.5 | -27.5 | 80.0 | 56052.8 |
| 30.9 | -12 8 | 80.0 | 56394.6 |
| 33.2 | 1.1 | 80 0 | 56850.5 |
| 35.6 | 14.2 | 80.0 | 57407.2 |
| 38.0 | 26.5 | 80.0 | 58051.1 |
| 40.4 | 38.1 | 80.0 | 58768.1 |
| 42.7 | 48.9 | 80.0 | 59543.6 |
| 45.1 | 59.0 | 80.0 | 60362.7 |
| 47.5 | 68.3 | 80.0 | 61210.5 |
| 49.8 | 76.8 | 80.0 | 62070.9 |
| 52.2 | 84.6 | 80.0 | 62929.0 |
| 54.6 | 91.6 | 80.0 | 63768.9 |
| 56.9 | 97.9 | 80 0 | 64574.7 |
| 59.3 | 103.5 | 80 0 | 65330.1 |
| 61.7 | 120.9 | 160.0 | 63515.1 |
| 64.1 | 135.4 | 160.0 | 62315.5 |
| 66.4 | 151.3 | 160.0 | 60915.1 |
| 68.8 | 166.6 | 160.0 | 59724.7 |
| 71.2 | 181.2 | 160.0 | 58741.3 |
| 73.5 | 195.1 | 160.0 | 57956.0 |
| 75.9 | 208.5 | 160.0 | 57359.9 |
| 78.3 | 221.2 | 160.0 | 56947.8 |
| 80.7 | 233.4 | 160.0 | 56707.7 |
| 83.0 | 244.9 | 160.0 | 56629 4 |
| 85.4 | 256.0 | 160.0 | 56705.8 |
| 87.8 | 266.5 | 160.0 | 56921.1 |
| 90.1 | 276.6 | 160.0 | 57265.6 |
| 92.5 | 286.2 | 160.0 | 57726.8 |
| 94.9 | 295.3 | 160.0 | 58291.0 |

FILE: THREE LOT A UNIVERSITY OF MISSOURI COMPUTER NETWORK

PAGE 002

| | | | |
|-------|-------|-------|---------|
| 97.3 | 304.1 | 160.0 | 58944.8 |
| 99.6 | 312.4 | 160.0 | 59674.0 |
| 102.0 | 320.5 | 160.0 | 60464.4 |
| 104.4 | 328.1 | 160.0 | 61300.7 |
| 106.7 | 335.5 | 160.0 | 62168.1 |
| 109.1 | 342.7 | 160.0 | 63051.2 |
| 111.5 | 349.6 | 160.0 | 63934.3 |
| 113.8 | 356.2 | 160.0 | 64802.2 |
| 116.2 | 362.7 | 160.0 | 65638.1 |
| 118.6 | 369.1 | 160.0 | 66426.8 |
| 121.0 | 375.3 | 80.0 | 67152.6 |
| 123.3 | 367.0 | 80.0 | 65000.2 |
| 125.7 | 360.7 | 80.0 | 63487.0 |
| 128.1 | 354.4 | 80.0 | 62183.1 |
| 130.4 | 348.1 | 80.0 | 61083.0 |
| 132.8 | 341.9 | 80.0 | 60180.0 |
| 135.2 | 335.7 | 80.0 | 59467.0 |
| 137.5 | 329.7 | 80.0 | 58935.5 |
| 139.9 | 323.9 | 80.0 | 58577.0 |
| 142.3 | 318.2 | 80.0 | 58381.4 |
| 144.7 | 312.7 | 80.0 | 58338.2 |
| 147.0 | 307.5 | 80.0 | 58437.0 |
| 149.4 | 302.6 | 80.0 | 58665.8 |
| 151.8 | 297.9 | 80.0 | 59012.7 |
| 154.1 | 293.6 | 80.0 | 59464.2 |
| 156.5 | 289.6 | 80.0 | 60007.5 |
| 158.9 | 286.1 | 80.0 | 60627.9 |
| 161.3 | 282.9 | 80.0 | 61312.5 |
| 163.6 | 280.2 | 80.0 | 62046.2 |
| 166.0 | 277.9 | 80.0 | 62814.4 |
| 168.4 | 276.1 | 80.0 | 63602.2 |
| 170.7 | 274.8 | 80.0 | 64393.3 |
| 173.1 | 274.0 | 80.0 | 65172.8 |
| 175.5 | 273.8 | 80.0 | 65923.1 |
| 177.9 | 274.2 | 80.0 | 66630.7 |
| 180.2 | 275.1 | -80.0 | 67280.4 |
| 182.6 | 247.6 | -80.0 | 65003.4 |
| 185.0 | 225.0 | -80.0 | 63374.9 |
| 187.3 | 203.0 | -80.0 | 61957.1 |
| 189.7 | 181.7 | -80.0 | 60747.6 |
| 192.1 | 161.1 | -80.0 | 59738.1 |
| 194.4 | 141.2 | -80.0 | 58922.0 |
| 196.8 | 122.0 | -80.0 | 58291.2 |
| 199.2 | 103.6 | -80.0 | 57837.4 |
| 201.6 | 85.9 | -80.0 | 57551.2 |
| 203.9 | 69.0 | -80.0 | 57422.9 |
| 206.3 | 52.9 | -80.0 | 57441.2 |
| 208.7 | 37.5 | -80.0 | 57594.9 |
| 211.0 | 22.9 | -80.0 | 57871.9 |
| 213.4 | 9.0 | -80.0 | 58259.6 |
| 215.8 | -4.1 | -80.0 | 58744.8 |
| 218.2 | -16.4 | -80.0 | 59314.1 |
| 220.5 | -27.9 | -80.0 | 59953.4 |
| 222.9 | -38.7 | -80.0 | 60648.3 |
| 225.3 | -48.7 | -80.0 | 61384.1 |

FILE: THREE PLOT A UNIVERSITY OF MISSOURI COMPUTER NETWORK

PAGE 003

| | | | |
|-------|--------|--------|---------|
| 227.6 | -57.9 | -80.0 | 62145.7 |
| 230.0 | -66.4 | -80.0 | 62918.1 |
| 232.4 | -74.1 | -80.0 | 63685.0 |
| 234.8 | -81.2 | -80.0 | 64431.7 |
| 237.1 | -87.4 | -80.0 | 65142.2 |
| 239.5 | -93.0 | -80.0 | 65801.0 |
| 241.9 | -110.3 | -160 0 | 63900.4 |
| 244.2 | -124.8 | -160 0 | 62610.4 |
| 246.6 | -140.7 | -160 0 | 61121.6 |
| 249.0 | -155.9 | -160 0 | 59842 6 |
| 251.3 | -170.5 | -160 0 | 58768.7 |
| 253.7 | -184.4 | -160 0 | 57891.7 |
| 256.1 | -197.7 | -160 0 | 57205 8 |
| 258.5 | -210.4 | -160 0 | 56703 2 |
| 260.8 | -222.6 | -160 0 | 56370.8 |
| 263.2 | -234.1 | -160 0 | 56202.0 |
| 265.6 | -245.1 | -160 0 | 56186 1 |
| 267.9 | -255.7 | -160 0 | 56310.3 |
| 270.3 | -265.7 | -160 0 | 56563.8 |
| 272.7 | -275.3 | -160 0 | 56934 4 |
| 275.1 | -284.4 | -160 0 | 57409.3 |
| 277.4 | -293.2 | -160 0 | 57973.1 |
| 279.8 | -301.5 | -160 0 | 58615.2 |
| 282.2 | -309.5 | -160 0 | 59318 3 |
| 284.5 | -317.2 | -160 0 | 60068 8 |
| 286.9 | -324.6 | -160 0 | 60851.5 |
| 289.3 | -331.7 | -160 0 | 61651 4 |
| 291.6 | -338.6 | -160 0 | 62452 3 |
| 294.0 | -345.3 | -160 0 | 63240 0 |
| 296.4 | -351.8 | -160 0 | 63997 6 |
| 298.8 | -358.2 | -160 0 | 64710.0 |
| 301.1 | -364.4 | -80.0 | 65360.8 |
| 303.5 | -356.1 | -80.0 | 63149 2 |
| 305.9 | -349.8 | -80.0 | 61577.4 |
| 308.2 | -343.5 | -80.0 | 60218 0 |
| 310.6 | -337.2 | -80 0 | 59065.0 |
| 313.0 | -331.0 | -80 0 | 58112 4 |
| 315.4 | -324.9 | -80 0 | 57352.7 |
| 317.7 | -318.9 | -80 0 | 56777.5 |
| 320.1 | -313.1 | -80 0 | 56377.9 |
| 322.5 | -307.4 | -80 0 | 56145.2 |
| 324.8 | -302.0 | -80 0 | 56068.4 |
| 327.2 | -296.8 | -80 0 | 56135.7 |
| 329.6 | -291.9 | -80 0 | 56336.4 |
| 331.9 | -287.3 | -80 0 | 56657.9 |
| 334.3 | -283.0 | -80 0 | 57088.6 |
| 336.7 | -279.1 | -80 0 | 57613 4 |
| 339.1 | -275.5 | -80 0 | 58219.1 |
| 341.4 | -272.4 | -80 0 | 58892.3 |
| 343.8 | -269.7 | -80 0 | 59617.1 |
| 346.2 | -267.5 | -80 0 | 60378.2 |
| 348.5 | -265.7 | -80 0 | 61162.9 |
| 350.9 | -264.5 | -80 0 | 61956 4 |
| 353.3 | -263.8 | -80 0 | 62739.2 |
| 355.7 | -263.6 | -80 0 | 63499.7 |

FILE: THREE PLOT A UNIVERSITY OF MISSOURI COMPUTER NETWORK

PAGE 004

```
358.0 -264.0 -80.0 64218.1
;
PROC GPLOT;
PLOT Y1*X Y2*X /OVERLAY;
SYMBOL1 I=JOIN L=1;
SYMBOL2 I=JOIN L=13;
LABEL X=DEGREE
      Y1=VOLTAGE & CURRENT ;
TITLE VOLTAGE & CURRENT (80% SPEED,MOTOR OPERATION);
PROC GPLOT;
PLOT Y3*X/VREF=0;
SYMBOL1 I=SPLINE;
LABEL X=DEGREE
      Y3= POWER ;
TITLE OUTPUT POWER (80% SPEED MOTOR OPERATION),
/*
//
```

APPENDIX H

DERIVATION OF INDUCTION MOTOR d-q EQUATIONS
IN STATIONARY REFERENCE FRAME

DERIVATION OF INDUCTION MOTOR d-q EQUATIONS
IN STATIONARY REFERENCE FRAME

EE400 Research Problem Report
(4) Credit Hours

by

Hadi Tehrani
MSEE Candidate

February 21, 1984

for

Department of Electrical and Computer Engineering
University of Missouri-Columbia
Supervisor: Dr. R. G. Hoft, Professor of Electrical Engineering

TABLE OF CONTENTS

| | |
|--|----|
| 1.0 OBJECT | 1 |
| 2.0 INDUCTION MOTOR EQUATIONS IN THREE PHASE VARIABLES | 1 |
| 3.0 TRANSFORMATION TO STATIONARY d-q REFERENCE FRAME | 11 |
| 3.1 Definition of d-q Stationary Reference Frame | 11 |
| 3.2 Definition of D-Q Rotating Reference Frame | 11 |
| 3.3 Induction Motor d-q-0 Variables | 13 |
| 4.0 RESULTS | 22 |
| APPENDIX I | 23 |
| APPENDIX II | 26 |

1.0 OBJECT

For the majority of practical ac machines, including ideal induction machines, a great simplification is obtained by expressing the equations in a new reference frame and introducing certain currents and voltages which are different from, but are related to, the actual ones. The currents can have a physical meaning in that they can be considered to flow in windings acting along two axes at right angles, called the direct and quadrature axes. In this paper a two-axis d-q theory of the induction motor in a stationary reference frame is developed.

2.0 INDUCTION MOTOR EQUATIONS IN THREE PHASE VARIABLES

It is assumed that the induction motor is ideal and symmetrical, which means:

1. Uniform air gap
2. Linear magnetic circuit
3. Identical stator windings which produce a sinusoidal MMF wave in space
4. No changes in resistances due to temperature and frequency changes

The stator circuits are oriented along the a_s , b_s and c_s axes which are 120° apart. The rotor circuits are along the a_r , b_r and c_r axes which are also 120° apart. They rotate relative to the stationary stator axes with an angular velocity $\omega_r = \frac{d\theta}{dt}$, which is the motor shaft velocity, and the angle θ is the angle between the stator and rotor.

The basic KVL equations for the three phase induction motor are - for the stator

$$V_{as} = \left[R_{as} i_{as} + L_{1as} \frac{di_{as}}{dt} + \frac{d\lambda_{as}}{dt} \right] \quad (2.1)$$

$$V_{bs} = \left[R_{bs} i_{bs} + L_{1bs} \frac{di_{bs}}{dt} + \frac{d\lambda_{bs}}{dt} \right] \quad (2.2)$$

$$V_{cs} = \left[R_{cs} i_{cs} + L_{1cs} \frac{di_{cs}}{dt} + \frac{d\lambda_{cs}}{dt} \right] \quad (2.3)$$

and for the rotor

$$V_{ar} = R_{ar} i_{ar} + L_{1ar} \frac{di_{ar}}{dt} + \frac{d\lambda_{ar}}{dt} \quad (2.4)$$

$$V_{br} = R_{br} i_{br} + L_{1br} \frac{di_{br}}{dt} + \frac{d\lambda_{br}}{dt} \quad (2.5)$$

$$V_{cr} = R_{cr} i_{cr} + L_{1cr} \frac{di_{cr}}{dt} + \frac{d\lambda_{cr}}{dt} \quad (2.6)$$

where

$V_{as} \triangleq$ instantaneous line to neutral voltage of stator Phase a

$V_{bs} \triangleq$ " " " " " " " " Phase b

$V_{cs} \triangleq$ " " " " " " " " Phase c

$V_{ar} \triangleq$ " " " " " " " " rotor Phase a

$V_{br} \triangleq$ " " " " " " " " Phase b

$V_{cr} \triangleq$ " " " " " " " " Phase c

$R_{as} \triangleq$ line to neutral resistance of stator Phase a

$R_{bs} \triangleq$ " " " " " " " " Phase b

$R_{cs} \triangleq$ " " " " " " " " Phase c

$R_{ar} \triangleq$ line to neutral resistance of rotor Phase a

$R_{br} \triangleq$ " " " " " " Phase b

$R_{cr} \triangleq$ " " " " " " Phase c

$i_{as} \triangleq$ instantaneous phase or line current in stator Phase a

$i_{bs} \triangleq$ " " " " " " Phase b

$i_{cs} \triangleq$ " " " " " " Phase c

$i_{ar} \triangleq$ " " " " " " rotor Phase a

$i_{br} \triangleq$ " " " " " " Phase b

$i_{cr} \triangleq$ " " " " " " Phase c

$\lambda_{as} \triangleq$ instantaneous flux linkage of stator Phase a with air gap magnetic field

$\lambda_{bs} \triangleq$ " " " " " " Phase b " " " " "

$\lambda_{cs} \triangleq$ " " " " " " Phase c " " " " "

$\lambda_{ar} \triangleq$ " " " " " " rotor Phase a " " " " "

$\lambda_{br} \triangleq$ " " " " " " Phase b " " " " "

$\lambda_{cr} \triangleq$ " " " " " " Phase c " " " " "

$L_{1as} \triangleq$ leakage inductance of stator Phase a

$L_{1bs} \triangleq$ " " " " " " Phase b

$L_{1cs} \triangleq$ " " " " " " Phase c

$L_{1ar} \triangleq$ " " " " " " Phase a

$L_{1br} \triangleq$ " " " " " " Phase b

$L_{1cr} \triangleq$ " " " " " " Phase c

Fig. 2.1 shows the three phase axes of the stator and rotor.

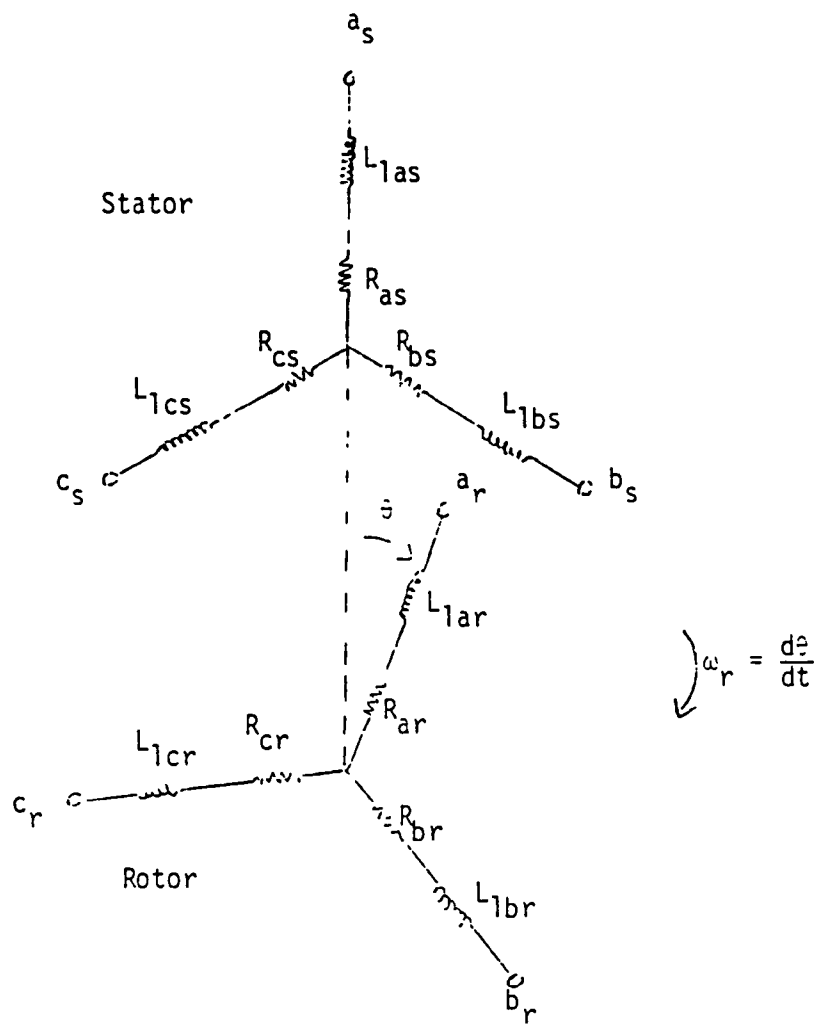


Fig. 2.1

Because of the symmetrical and balanced windings:

$$R_{as} = R_{bs} = R_{cs} = R_s \quad (\text{stator resistance/phase})$$

$$R_{ar} = R_{br} = R_{cr} = R_r \quad (\text{rotor resistance/phase})$$

$$L_{1as} = L_{1bs} = L_{1cs} = L_{1s} \quad (\text{stator leakage inductance/phase})$$

$$L_{1ar} = L_{1br} = L_{1cr} = L_{1r} \quad (\text{rotor leakage inductance/phase})$$

The basic equations can be shown in matrix form as

$$\begin{matrix}
 \begin{array}{c|c}
 v_{as} & \lambda_{as} \\
 v_{bs} & \lambda_{bs} \\
 v_{cs} & \lambda_{cs} \\
 v_{ar} & \lambda_{ar} \\
 v_{br} & \lambda_{br} \\
 v_{cr} & \lambda_{cr}
 \end{array}
 \\[10pt]
 = \begin{array}{c|c}
 R_s & \begin{array}{ccccc}
 0 & 0 & 0 & 0 & 0 \\
 0 & R_s & 0 & 0 & 0 \\
 0 & 0 & R_s & 0 & 0 \\
 0 & 0 & 0 & R_r & 0 \\
 0 & 0 & 0 & 0 & R_r
 \end{array} \\
 \hline
 \begin{array}{c|c}
 i_{as} & L_{1s} \\
 i_{bs} & L_{1s} \\
 i_{cs} & 0 \\
 i_{ar} & 0 \\
 i_{br} & 0 \\
 i_{cr} & 0
 \end{array}
 \end{array}
 \\[10pt]
 + \begin{array}{c|c}
 L_{1s} & 0 \\
 L_{1s} & 0 \\
 0 & L_{1s} \\
 0 & 0 \\
 0 & 0 \\
 0 & 0
 \end{array}
 + \frac{d}{dt} \begin{array}{c|c}
 i_{as} & i_{bs} \\
 i_{cs} & i_{ar} \\
 i_{ar} & i_{br} \\
 i_{br} & i_{cr}
 \end{array}
 \end{matrix}$$

(2.7)

where the variables written in vector form are

$$\begin{aligned} \vec{v}_s &= \begin{vmatrix} v_{as} \\ v_{bs} \\ v_{cs} \end{vmatrix} \quad (2.9a) & \vec{v}_r &= \begin{vmatrix} v_{ar} \\ v_{br} \\ v_{cr} \end{vmatrix} \quad (2.8a) \end{aligned}$$

$$\begin{aligned} \vec{i}_s &= \begin{vmatrix} i_{as} \\ i_{bs} \\ i_{cs} \end{vmatrix} \quad (2.9b) & \vec{i}_r &= \begin{vmatrix} i_{ar} \\ i_{br} \\ i_{cr} \end{vmatrix} \quad (2.8b) \end{aligned}$$

$$\begin{aligned} \vec{\lambda}_s &= \begin{vmatrix} \lambda_{as} \\ \lambda_{bs} \\ \lambda_{cs} \end{vmatrix} \quad (2.9c) & \vec{\lambda}_r &= \begin{vmatrix} \lambda_{ar} \\ \lambda_{br} \\ \lambda_{cr} \end{vmatrix} \quad (2.8c) \end{aligned}$$

Next, the equation for the total flux linkage for each stator and rotor phase and the air gap magnetic field is written as follows

$$\vec{\lambda} = \vec{L} \vec{i} \quad (2.10)$$

where

$$\begin{aligned} \lambda_{as} &= L_{ms} i_{as} + L_{ms} i_{bs} \cos(2\pi/3) + L_{ms} i_{cs} \cos(-2\pi/3) \\ &\quad + L_{mr} i_{ar} \cos \theta + L_{mr} i_{br} \cos(\theta+2\pi/3) + L_{mr} i_{cr} \cos(\theta-2\pi/3) \end{aligned} \quad (2.11)$$

$$\begin{aligned} \lambda_{bs} &= L_{ms} i_{as} \cos(-2\pi/3) + L_{ms} i_{bs} + L_{ms} i_{cs} \cos(2\pi/3) \\ &\quad + L_{mr} i_{ar} \cos(\theta-2\pi/3) + L_{mr} i_{br} \cos \theta + L_{mr} i_{cr} \cos(\theta+2\pi/3) \end{aligned} \quad (2.12)$$

$$\begin{aligned}\lambda_{cs} &= L_{ms} i_{as} \cos(2\pi/3) + L_{ms} i_{bs} \cos(-2\pi/3) + L_{ms} i_{cs} \\ &\quad L_{mr} i_{ar} \cos(\theta+2\pi/3) + L_{mr} i_{br} \cos(\theta-2\pi/3) + L_{mr} i_{cr} \cos\theta\end{aligned}\quad (2.13)$$

$$\begin{aligned}\lambda_{ar} &= L_{ms} i_{as} \cos\theta + L_{ms} i_{bs} \cos(\theta-2\pi/3) + L_{ms} i_{cs} \cos(\theta+2\pi/3) \\ &\quad L_{mr} i_{ar} + L_{mr} i_{br} \cos(-2\pi/3) + L_{mr} i_{cr} \cos(-2\pi/3)\end{aligned}\quad (2.14)$$

$$\begin{aligned}\lambda_{br} &= L_{ms} i_{as} (\theta+2\pi/3) + L_{ms} i_{bs} \cos\theta + L_{ms} i_{cs} \cos(\theta-2\pi/3) \\ &\quad L_{mr} i_{ar} \cos(2\pi/3) + L_{mr} i_{br} + L_{mr} i_{cr} \cos(-2\pi/3)\end{aligned}\quad (2.15)$$

$$\begin{aligned}\lambda_{cr} &= L_{ms} i_{as} \cos(\theta-2\pi/3) + L_{ms} i_{bs} \cos(\theta+2\pi/3) + L_{ms} i_{cs} \cos\theta \\ &\quad L_{mr} i_{ar} \cos(-2\pi/3) + L_{mr} i_{br} \cos(2\pi/3) + L_{mr} i_{ar}\end{aligned}\quad (2.16)$$

and

L_{ms} $\hat{=}$ magnetizing inductance/stator phase of air gap magnetic field
 L_{mr} $\hat{=}$ magnetizing inductance/rotor phase of air gap magnetic field

Equations (2.11)-(2.16) can be written in the matrix equation form of (2.17).

For simplicity, (2.17) can be divided into four 3X3 as follows

$$|L_1| = \begin{vmatrix} L_{ms} & -1/2L_{ms} & -1/2L_{ms} \\ -1/2L_{ms} & L_{ms} & -1/2L_{ms} \\ -1/2L_{ms} & -1/2L_{ms} & L_{ms} \end{vmatrix} \quad (2.18a)$$

$$|L_2| = \begin{vmatrix} L_{mr} \cos\theta & L_{mr} \cos(\theta+2\pi/3) & L_{ms} \cos(\theta+2\pi/3) \\ L_{mr} \cos(\theta-2\pi/3) & L_{mr} \cos\theta & L_{mr} \cos(\theta+2\pi/3) \\ L_{mr} \cos(\theta+2\pi/3) & L_{mr} \cos(\theta-2\pi/3) & L_{mr} \cos\theta \end{vmatrix} \quad (2.18b)$$

$$|L_3| = \begin{vmatrix} L_{ms} \cos\theta & L_{ms} \cos(\theta-2\pi/3) & L_{ms} \cos(\theta+2\pi/3) \\ L_{ms} \cos(\theta+2\pi/3) & L_{ms} \cos\theta & L_{ms} \cos(\theta-2\pi/3) \\ L_{ms} \cos(\theta-2\pi/3) & L_{ms} \cos(\theta+2\pi/3) & L_{ms} \cos\theta \end{vmatrix} \quad (2.18c)$$

| | | | | | | | |
|----------------|-----------------------------|-----------------------------|-----------------------------|-----------------------------|-----------------------------|-----------------------------|----------|
| λ_{as} | L_{ms} | $-1/2L_{ms}$ | $-1/2L_{ms}$ | $L_{mr}\cos\theta$ | $L_{mr}\cos(\theta+2\pi/3)$ | $L_{mr}\cos(\theta-2\pi/3)$ | i_{as} |
| λ_{bs} | $-1/2L_{ms}$ | L_{ms} | $-1/2L_{ms}$ | $L_{mr}\cos(\theta-2\pi/3)$ | $L_{mr}\cos\theta$ | $L_{mr}\cos(\theta+2\pi/3)$ | i_{bs} |
| λ_{cs} | $-1/2L_{ms}$ | $-1/2L_{ms}$ | L_{ms} | $L_{mr}\cos(\theta+2\pi/3)$ | $L_{mr}\cos(\theta-2\pi/3)$ | $L_{mr}\cos\theta$ | i_{cs} |
| λ_{ar} | $L_{ms}\cos\theta$ | $L_{ms}\cos(\theta-2\pi/3)$ | $L_{ms}\cos(\theta+2\pi/3)$ | L_{mr} | $-1/2L_{mr}$ | $-1/2L_{mr}$ | i_{ar} |
| λ_{br} | $L_{ms}\cos(\theta+2\pi/3)$ | $L_{ms}\cos\theta$ | $L_{ms}\cos(\theta-2\pi/3)$ | $-1/2L_{mr}$ | L_{mr} | $-1/2L_{mr}$ | i_{br} |
| λ_{cr} | $L_{ms}\cos(\theta-2\pi/3)$ | $L_{ms}\cos(\theta+2\pi/3)$ | $L_{ms}\cos\theta$ | $-1/2L_{mr}$ | $-1/2L_{mr}$ | L_{mr} | i_{cr} |

(2.17)

$$\left| L_4 \right| = \begin{vmatrix} L_{mr} & -1/2L_{mr} & -1/2L_{mr} \\ -1/2L_{mr} & L_{mr} & -1/2L_{mr} \\ -1/2L_{mr} & -1/2L_{mr} & L_{mr} \end{vmatrix} \quad (2.18d)$$

Then (2.17) can be written

$$\begin{pmatrix} \vec{\lambda}_s \\ \vec{\lambda}_r \end{pmatrix} = \begin{vmatrix} L_1 & L_2 \\ L_3 & L_4 \end{vmatrix} \begin{pmatrix} \vec{i}_s \\ \vec{i}_r \end{pmatrix} \quad (2.19)$$

Since this induction motor has no neutral connection

$$i_{as} + i_{bs} + i_{cs} = 0 \quad (2.20a)$$

$$i_{ar} + i_{br} + i_{cr} = 0 \quad (2.20b)$$

Therefore

$$i_{as} = -i_{bs} - i_{cs} \quad (2.21a)$$

$$i_{ar} = -i_{br} - i_{cr} \quad (2.21b)$$

If these equations are substituted into (2.17), matrixes L_1 and L_4 become

$$\left| L_1 \right| = \begin{vmatrix} 3/2L_{ms} & 0 & 0 \\ 0 & 3/2L_{ms} & 0 \\ 0 & 0 & 3/2L_{ms} \end{vmatrix} \quad (2.22)$$

$$\left| L_4 \right| = \begin{vmatrix} 3/2L_{mr} & 0 & 0 \\ 0 & 3/2L_{mr} & 0 \\ 0 & 0 & 3/2L_{mr} \end{vmatrix} \quad (2.23)$$

It is more convenient to write the resistance matrix and the leakage inductance matrix of (2.7) as follows

$$[R] = \begin{vmatrix} R_s & 0 \\ 0 & R_r \end{vmatrix} \quad (2.24)$$

$$[L_1] = \begin{vmatrix} L_{1s} & 0 \\ 0 & L_{1r} \end{vmatrix} \quad (2.25)$$

where

$$\begin{vmatrix} R_s & 0 & 0 \\ 0 & R_s & 0 \\ 0 & 0 & R_s \end{vmatrix} \quad (2.24a)$$

$$\begin{vmatrix} L_{1s} & 0 & 0 \\ 0 & L_{1s} & 0 \\ 0 & 0 & L_{1s} \end{vmatrix} \quad (2.25a)$$

$$\begin{vmatrix} R_r & 0 & 0 \\ 0 & R_r & 0 \\ 0 & 0 & R_r \end{vmatrix} \quad (2.24b)$$

$$\begin{vmatrix} L_{1r} & 0 & 0 \\ 0 & L_{1r} & 0 \\ 0 & 0 & L_{1r} \end{vmatrix} \quad (2.25b)$$

By substituting (2.19), (2.24) and (2.25) into equation (2.7), the induction motor equations can be written

$$[\vec{V}_s] = [R_s] [\vec{i}_s] + [L_1] d/dt [\vec{i}_s] + d/dt [L_2] [\vec{i}_r] + [L_{1s}] d/dt [\vec{i}_s] \quad (2.26)$$

$$[\vec{V}_r] = [R_r] [\vec{i}_r] + d/dt [L_3] [\vec{i}_s] + [L_4] d/dt [\vec{i}_r] + [L_{1r}] d/dt [\vec{i}_r] \quad (2.27)$$

Equations (2.26) and (2.27) can be written in matrix form

$$\begin{vmatrix} \vec{V}_s \\ \vec{V}_r \end{vmatrix} = \begin{vmatrix} [R_s] & \vec{i}_s \\ [R_r] & \vec{i}_r \end{vmatrix} + \begin{vmatrix} [L_{1s}] \\ [L_{1r}] \end{vmatrix} P \begin{vmatrix} \vec{i}_s \\ \vec{i}_r \end{vmatrix} + P \begin{vmatrix} [L_1] & [L_2] \\ [L_3] & [L_4] \end{vmatrix} \begin{vmatrix} \vec{i}_s \\ \vec{i}_r \end{vmatrix} \quad (2.28)$$

where

$$P = d/dt$$

3.0 TRANSFORMATION TO STATIONARY d-q REFERENCE FRAME

In this report, the following symbols are used:

d-q => stationary reference frame (fixed with respect to the stator)

D-Q => rotating reference frame (rotating at rotor speed - fixed with respect to the rotor)

3.1 Definition of d-q Stationary Reference Frame

For the d-q stationary reference frame, the d-axis is in line with the a-axis of the stator as shown in Fig. 3.1. Then,

$$v_d = v_{as} + v_{bs} \cos (120^\circ) + v_{cs} \cos (-120^\circ)$$

$$v_q = v_b \sin (120^\circ) + v_c \sin (-120^\circ)$$

or

$$\begin{vmatrix} v_d \\ v_q \end{vmatrix} = \begin{vmatrix} 1 & -1/2 & -1/2 \\ 0 & \sqrt{3}/2 & -\sqrt{3}/2 \end{vmatrix} \begin{vmatrix} v_{as} \\ v_{bs} \\ v_{cs} \end{vmatrix} \quad (3.1)$$

3.2 Definition of D-Q Rotating Reference Frame

The D-Q reference frame rotates relative to the d-q stationary reference frame, where θ is the angle between the d-axis and the D-axis and

$$\theta = \int \omega_r dt; \quad \omega_r = \frac{d\theta}{dt}$$

where ω_r is the rotor speed in radians/second. This is shown in Fig. 3.2.

$$\begin{vmatrix} v_d \\ v_q \end{vmatrix} = \begin{vmatrix} \cos \theta & -\sin \theta \\ \sin \theta & \cos \theta \end{vmatrix} \begin{vmatrix} v_D \\ v_Q \end{vmatrix} \quad (3.2a)$$

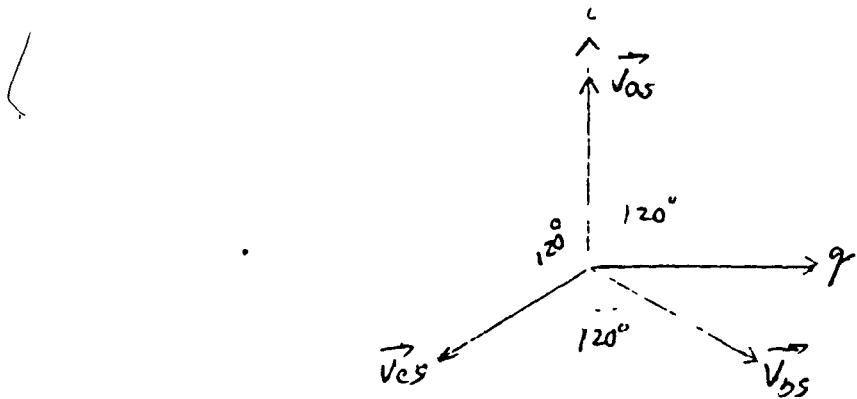


Fig. 3.1

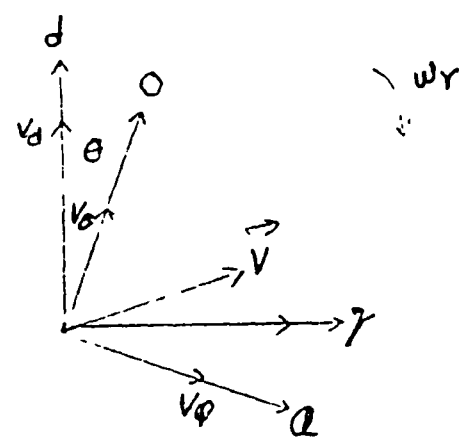


Fig. 3.2

$$\begin{vmatrix} v_D \\ v_Q \end{vmatrix} = \begin{vmatrix} \cos \theta & \sin \theta \\ -\sin \theta & \cos \theta \end{vmatrix} \begin{vmatrix} v_d \\ v_q \end{vmatrix} \quad (3.2b)$$

The \vec{v} is rotating clockwise at angular velocity ω_r .

3.3 Induction Motor d-q-0 Variables

For simplicity in the definitions of the d-q and D-Q reference frames, only two axes were considered. In general, it is desirable to consider three coordinate axes for two reasons. Matrix transformation methods can be used to transform variables from one reference frame to another, but only if the transformation matrices are square and nonsingular matrices. Thus, for three phase situations with three phase variables, it is necessary to consider transformations to coordinate axes where three variables exist. For balanced and symmetrical cases, it is often sufficient to consider only d-q variables. However, the three d-q-0 variables are necessary in the most general situations.

In the remainder of this report we are concerned with the d-q-0 reference frame. Again, this is a reference frame fixed with respect to the stator. The 0-variables will not only make it possible to use matrix transformation techniques, but they also will have important physical significance in many cases.

For this report, the d-q-0 transformation from stator three phase voltages or currents is defined as follows

$$\begin{vmatrix} v_{ds} \\ v_{qs} \\ v_{0s} \end{vmatrix} \triangleq \frac{2}{3} \begin{vmatrix} 1 & \cos 2\pi/3 & \cos (-2\pi/3) \\ 0 & \sin 2\pi/3 & \sin (-2\pi/3) \\ 1/2 & 1/2 & 1/2 \end{vmatrix} \begin{vmatrix} v_{as} \\ v_{bs} \\ v_{cs} \end{vmatrix} \quad (3.3a)$$

$$\begin{vmatrix} i_{ds} \\ i_{qs} \\ i_{0s} \end{vmatrix} \triangleq \frac{2}{3} \begin{vmatrix} 1 & \cos 2\pi/3 & \cos(-2\pi/3) \\ 0 & \sin 2\pi/3 & \sin(-2\pi/3) \\ 1/2 & 1/2 & 1/2 \end{vmatrix} \begin{vmatrix} i_{as} \\ i_{bs} \\ i_{cs} \end{vmatrix} \quad (3.3b)$$

Equations (3.3a) and (3.3b) transform the three phase stator line-to-neutral voltages or line currents to d-q-0 coordinate voltages or currents. It should be noted that

$$i_{0s} = 1/3 (i_{as} + i_{bs} + i_{cs}) \quad (3.4a)$$

and thus i_{0s} is zero for all three wire machines where no neutral is present. This is a consequence of Kirchoff's current law. However,

$$v_{0s} = 1/3 (v_{as} + v_{bs} + v_{cs}) \quad (3.4b)$$

is zero when balanced and symmetrical three phase line-to-neutral voltages are involved, but it is not zero in general.

Equations (3.3a) or (3.3b) apply to the transformation of stator three phase to d-q-0 quantities for all circuit variables including flux linkages as well as the voltages and currents.

The d-q-0 transformation for rotor quantities is defined as follows

$$\begin{vmatrix} v_{dr} \\ v_{qr} \\ v_{0r} \end{vmatrix} \triangleq \frac{2}{3} \begin{vmatrix} \cos \theta & \cos(\theta + 2\pi/3) & \cos(\theta - 2\pi/3) \\ \sin \theta & \sin(\theta + 2\pi/3) & \sin(\theta - 2\pi/3) \\ 1/2 & 1/2 & 1/2 \end{vmatrix} \begin{vmatrix} v_{ar} \\ v_{br} \\ v_{cr} \end{vmatrix} \quad (3.5)$$

Equation (3.5) transforms the rotor quantities, which are given in a three phase coordinate frame rotating with angular velocity ω_r , to the d-q-0 reference frame fixed with respect to the stator. The same transformation as in (3.5) is used to transform currents and flux linkages. Fig. 3.3 illus-

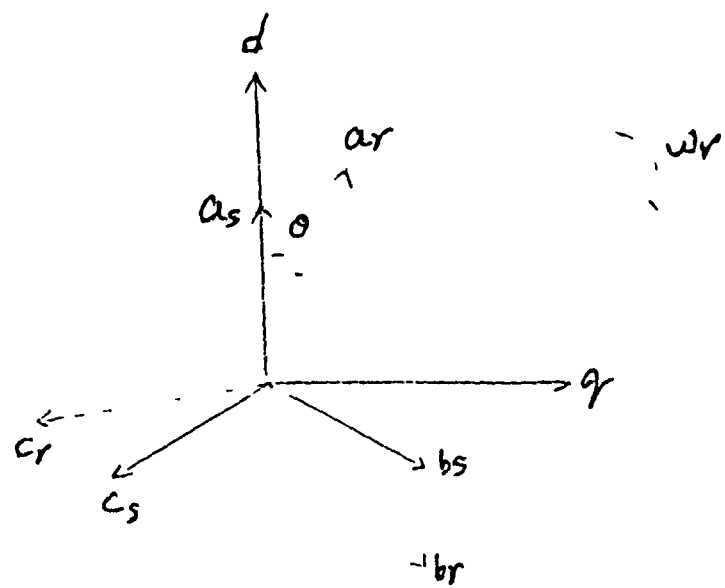


Fig. 3.3

trates this relationship. The 0-axis is orthogonal to the d and q-axes, and it may be considered directed into the paper.

A number of additional transformation relations are given as follows

for stator variables

$$\vec{v}_s = |A_s|^{-1} \vec{v}_{dq0}^s \quad (3.6a)$$

$$\vec{i}_s = |A_s|^{-1} \vec{i}_{dq0}^s \quad (3.6b)$$

$$\vec{\lambda}_s = |A_s|^{-1} \vec{\lambda}_{dq0}^s \quad (3.6c)$$

and for rotor variables

$$\vec{v}_r = |A_r|^{-1} \vec{v}_{dq0}^r \quad (3.7a)$$

$$\vec{i}_r = |A_r|^{-1} \vec{i}_{dq0}^r \quad (3.7b)$$

$$\vec{\lambda}_r = |A_r|^{-1} \vec{\lambda}_{dq0}^r \quad (3.7c)$$

where

$$|A_s| = \frac{2}{3} \begin{vmatrix} 1 & -1/2 & -1/2 \\ 0 & \sqrt{3}/2 & -\sqrt{3}/2 \\ 1/2 & 1/2 & 1/2 \end{vmatrix} \quad (3.8)$$

$$|A_s|^{-1} = \begin{vmatrix} 1 & 0 & 1 \\ -1/2 & \sqrt{3}/2 & 1 \\ -1/2 & -\sqrt{3}/2 & 1 \end{vmatrix} \quad (3.9)$$

$$|A_r| = \frac{2}{3} \begin{vmatrix} \cos \theta & \cos(\theta + 2\pi/3) & \cos(\theta - 2\pi/3) \\ \sin \theta & \sin(\theta + 2\pi/3) & \sin(\theta - 2\pi/3) \\ 1/2 & 1/2 & 1/2 \end{vmatrix} \quad (3.10)$$

$$|A_r|^{-1} = \begin{vmatrix} \cos \theta & \sin \theta & 1 \\ \cos(\theta + 2\pi/3) & \sin(\theta + 2\pi/3) & 1 \\ \cos(\theta - 2\pi/3) & \sin(\theta - 2\pi/3) & 1 \end{vmatrix} \quad (3.11)$$

From (2.7), the motor voltage equations are

$$|\vec{v}_s| = R_s |\vec{i}_s| + P L_{1s} |\vec{i}_s| + P |\vec{\lambda}_s| \quad (3.12)$$

$$|\vec{v}_r| = R_r |\vec{i}_r| + P L_{1r} |\vec{i}_r| + P |\vec{\lambda}_r| \quad (3.13)$$

Substituting (3.6) and (3.7) into (3.12) and (3.13) respectively gives

$$|A_s|^{-1} |v_{dq0}^s| = R_s |A_s|^{-1} |i_{dq0}^s| + L_{1s} P |A_s|^{-1} |i_{dq0}^s| + P |A_s|^{-1} |\lambda_{dq0}^s| \quad (3.14)$$

$$|A_r|^{-1} |v_{dq0}^r| = R_r |A_r|^{-1} |i_{dq0}^r| + L_{1r} P |A_r|^{-1} |i_{dq0}^r| + P |A_r|^{-1} |\lambda_{dq0}^r| \quad (3.15)$$

Equation (3.15) can be expanded as

$$\begin{aligned} |A_r|^{-1} |v_{dq0}^r| = & R_r |A_r|^{-1} |i_{dq0}^r| + L_{1r} P |A_r|^{-1} |\lambda_{dq0}^r| + \\ & L_{1r} |A_r|^{-1} P \{ |\lambda_{dq0}^r| \} + \{ P |A_r|^{-1} \} |\lambda_{dq0}^r| \\ & + |A_r|^{-1} \{ P |\lambda_{dq0}^r| \} \end{aligned} \quad (3.16)$$

Equation (3.14) need not be expanded because the matrix $|A_s|^{-1}$ is constant.

It can be shown that [1]

$$\{P|A_r|^{-1} = -|A_r|^{-1} \{P|A_r|\} |A_r|^{-1} \quad (3.17)$$

Substituting (3.17) into (3.16) gives

$$\begin{aligned} |A_r|^{-1} |v_{dq0}^r| &= R_r |A_r|^{-1} |i_{dq0}^r| + L_{1r} \{-|A_r|^{-1} \{P|A_r|\} |A_r|^{-1}\} |i_{dq0}^r| \\ &\quad + L_{1r} |A_r|^{-1} |P| |i_{dq0}^r| + \{-|A_r|^{-1} \{P|A_r|\} |A_r|^{-1}\} |x_{dq0}^r| \\ &\quad + |A_r|^{-1} \{P|x_{dq0}^r\} \end{aligned} \quad (3.18)$$

Multiplying both sides of (3.14) and (3.18) by $|A_s|$ and $|A_r|$ respectively gives

$$|v_{dq0}^s| = R_s |i_{dq0}^s| + L_{1s} P |i_{dq0}^s| + P |\lambda_{dq0}^s| \quad (3.19)$$

$$\begin{aligned} |v_{dq0}^r| &= R_r |i_{dq0}^r| + L_{1r} P |i_{dq0}^r| - L_{1r} \{P|A_r|\} |A_r|^{-1} |i_{dq0}^r| \\ &\quad + P |x_{dq0}^r| - \{P|A_r|\} |A_r|^{-1} |x_{dq0}^r| \end{aligned} \quad (3.20)$$

The expressions $\{P|A_r|\}$; $|A_r|^{-1}$ in (3.20) can be evaluated using matrix algebra, which is shown in Appendix I. The result is

$$\{P|A_r|\} |A_r|^{-1} = \begin{vmatrix} 0 & -1 & 0 \\ 1 & 0 & 0 \\ 0 & 0 & 0 \end{vmatrix} \frac{d\theta}{dt} \quad (3.21)$$

where

$$\frac{d\theta}{dt} \triangleq \omega_r$$

and

$$|H| \triangleq \begin{vmatrix} 0 & 1 & 0 \\ -1 & 0 & 0 \\ 0 & 0 & 0 \end{vmatrix} \quad (3.22)$$

Substituting (3.21) into (3.20) gives

$$\begin{aligned} |v_{dq0}^r| = & R_r |i_{dq0}^r| + L_{1r} P |i_{dq0}^r| + L_{1r} \omega_r |H| |i_{dq0}^r| \\ & + P |\lambda_{dq0}^r| + \omega_r |H| |\lambda_{dq0}^r| \end{aligned} \quad (3.23)$$

Equations (3.19) and (3.23) are the motor voltage equations in the d-q-0 frame.

Now, the flux linkage equations are expressed in terms of d-q-0 current as follows. Matrix (2.19) can be written

$$\vec{\lambda}_s = [L_1] \vec{i}_s + [L_2] \vec{i}_r \quad (3.24)$$

$$\vec{\lambda}_r = [L_3] \vec{i}_s + [L_4] \vec{i}_r \quad (3.25)$$

Substituting (3.6c) and (3.6b) into (3.24) and (3.7c) and (3.7b) into (3.25) gives

$$[A_s]^{-1} |\lambda_{dq0}^s| = [L_1] [A_s]^{-1} |i_{dq0}^s| + [L_2] [A_r]^{-1} |i_{dq0}^r| \quad (3.26)$$

$$[A_r]^{-1} |\lambda_{dq0}^r| = [L_3] [A_s]^{-1} |i_{dq0}^s| + [L_4] [A_r]^{-1} |i_{dq0}^r| \quad (3.27)$$

Multiplying both sides of (3.26) by A_s and (3.27) by A_r gives

$$|\lambda_{dq0}^s| = [A_s] [L_1] [A_s]^{-1} |i_{dq0}^s| + [A_s] [L_2] [A_r]^{-1} |i_{dq0}^r| \quad (3.28)$$

$$|\lambda_{dq0}^r| = [A_r] [L_3] [A_s]^{-1} |i_{dq0}^s| + [A_r] [L_4] [A_r]^{-1} |i_{dq0}^r| \quad (3.29)$$

where

$$|A_s| |L_2| |A_r|^{-1} = 3/2 L_{mr} \begin{vmatrix} 1 & 0 & 0 \\ 0 & 1 & 0 \\ 0 & 0 & 0 \end{vmatrix} \quad (3.30a)$$

$$|A_r| |L_3| |A_s|^{-1} = 3/2 L_{ms} \begin{vmatrix} 1 & 0 & 0 \\ 0 & 1 & 0 \\ 0 & 0 & 0 \end{vmatrix} \quad (3.30b)$$

$$|A_s| |L_1| |A_s|^{-1} = 3/2 L_{ms} \begin{vmatrix} 1 & 0 & 0 \\ 0 & 1 & 0 \\ 0 & 0 & 0 \end{vmatrix} \quad (3.31a)$$

$$|A_r| |L_4| |A_r|^{-1} = 3/2 L_{mr} \begin{vmatrix} 1 & 0 & 0 \\ 0 & 1 & 0 \\ 0 & 0 & 0 \end{vmatrix} \quad (3.31b)$$

as shown in Appendix II. Substituting (3.30) and (3.31) into (3.28) and (3.29), respectively, gives

$$|\lambda_{dq0}^s| = 3/2 L_{ms} |E| |i_{dq0}^s| + 3/2 L_{mr} |E| |i_{dq0}^r| \quad (3.32)$$

$$|\lambda_{dq0}^r| = 3/2 L_{ms} |E| |i_{dq0}^s| + 3/2 L_{mr} |E| |i_{dq0}^r| \quad (3.33)$$

where

$$|E| = \begin{vmatrix} 1 & 0 & 0 \\ 0 & 1 & 0 \\ 0 & 0 & 0 \end{vmatrix} \quad (3.34)$$

Equations (3.32) and (3.33) can be written in matrix form using (3.34)

$$\begin{array}{|c|c|c|c|c|c|c|c|} \hline \lambda_{ds} & L_{ms} & 0 & 0 & L_{mr} & 0 & 0 & i_{ds} \\ \hline \lambda_{qs} & 0 & L_{ms} & 0 & 0 & L_{mr} & 0 & i_{qs} \\ \hline \lambda_{os} & 0 & 0 & 0 & 0 & 0 & 0 & i_{os} \\ \hline \lambda_{dr} = 3/2 & L_{ms} & 0 & 0 & L_{mr} & 0 & 0 & i_{dr} \\ \hline \lambda_{qr} & 0 & L_{ms} & 0 & 0 & L_{mr} & 0 & i_{qr} \\ \hline \lambda_{or} & 0 & 0 & 0 & 0 & 0 & 0 & i_{or} \\ \hline \end{array} \quad (3.35)$$

Equations (3.32) and (3.33) can be substituted into (3.19) and (3.23) yielding

$$\begin{aligned} \langle v_{dq0}^s \rangle &= R_s \langle i_{dq0}^s \rangle + L_{1s} P \langle i_{dq0}^s \rangle + 3/2 P L_{ms} \langle E \rangle \langle i_{dq0}^s \rangle \\ &\quad + 3/2 P L_{mr} \langle E \rangle \langle i_{dq0}^r \rangle \end{aligned} \quad (3.36)$$

$$\begin{aligned} \dot{\psi}_{dq0}^r &= R_r \dot{i}_{dq0}^r + L_{1r} P \dot{i}_{dq0}^r + L_{1r} \omega_r [H] i_{dq0}^r \\ &+ 3/2 P L_{ms} [E] i_{dq0}^s + 3/2 P L_{mr} [E] i_{dq0}^r \\ &+ 3/2 \omega_r [H] L_{ms} [E] i_{dq0}^s + 3/2 \omega_r [H] L_{mr} \\ &[E] i_{dq0}^r \end{aligned} \quad (3.37)$$

where the motor equations are written in terms of d-q-0 currents. The final matrix in d-q-0 coordinates is found by writing (3.36) and (3.37) in matrix form

$$\begin{array}{|c||cccccc|c|} \hline & R_s + PL_s & 0 & 0 & \frac{3}{2}PL_{mr} & 0 & 0 & i_{ds} \\ \hline v_{ds} & 0 & R_s + PL_s & 0 & 0 & \frac{3}{2}PL_{mr} & 0 & i_{qs} \\ \hline v_{qs} & 0 & 0 & R_s + PL_{ls} & 0 & 0 & & i_{os} \\ \hline v_{os} & = & \frac{3}{2}PL_{ms} & \frac{3}{2}\omega_r L_{Lms} & 0 & R_r + PL_r & \omega_r L_r & i_{dr} \\ \hline v_{dr} & -\frac{3}{2}\omega_r L_{ms} & \frac{3}{2}PL_{ms} & 0 & -\omega_r L_r & R_r + PL_r & 0 & i_{qr} \\ \hline v_{qr} & 0 & 0 & 0 & 0 & 0 & R_r + PL_{lr} & i_{or} \\ \hline \end{array} \quad (3.38)$$

where

$$L_s = L_{1s} + 3/2 L_{ms}$$

$$L_r = L_{1r} + 3/2 L_{mr}$$

For the symmetrical three phase induction machine with wye-connected windings having no neutral connections, the 0-components disappear so that d-q-0 coordinates become d-q coordinates, reducing (3.32) to

$$\begin{bmatrix} v_{ds} \\ v_{qs} \\ v_{dr} \\ v_{qr} \end{bmatrix} = \begin{bmatrix} R_s + PL_s & 0 & \frac{3}{2}PL_{mr} & 0 \\ 0 & R_s + PL_s & 0 & \frac{3}{2}PL_{mr} \\ \frac{3}{2}PL_{ms} & \frac{3}{2}\omega_r L_{ms} & R_r + PL_s & \omega_r L_r \\ -\frac{3}{2}\omega_r L_{ms} & \frac{3}{2}PL_{ms} & -\omega_r L_r & R_r + PL_s \end{bmatrix} \begin{bmatrix} i_{ds} \\ i_{qs} \\ i_{dr} \\ i_{qr} \end{bmatrix} \quad (3.39)$$

4.0 RESULTS

Matrix methods have been used to derive the d-q equations for the induction machine. The resulting matrix equation (3.39) is much simpler than the conventional three phase representation. Only four voltage and current variables are involved instead of six. Also, the representation of (3.39) is very useful in control analysis using state variable methods and optimization techniques.

APPENDIX I

Equation (3.21) is derived as follows.

From (3.10),

$$P \begin{vmatrix} A_r \end{vmatrix} = 2/3 \begin{vmatrix} -\sin \theta & -\sin(\theta + 2\pi/3) & -\sin(\theta - 2\pi/3) \\ \cos \theta & \cos(\theta + 2\pi/3) & \cos(\theta - 2\pi/3) \\ 0 & 0 & 0 \end{vmatrix} \frac{d\theta}{dt}$$

Therefore, $(P \begin{vmatrix} A_r \end{vmatrix})^{-1} \begin{vmatrix} A_r \end{vmatrix}^{-1}$ can be expressed

$$(P \begin{vmatrix} A_r \end{vmatrix})^{-1} \begin{vmatrix} A_r \end{vmatrix}^{-1} = 2/3 \begin{vmatrix} -\sin \theta & -\sin(\theta + 2\pi/3) & -\sin(\theta - 2\pi/3) \\ \cos \theta & \cos(\theta + 2\pi/3) & \cos(\theta - 2\pi/3) \\ 0 & 0 & 0 \end{vmatrix} : \frac{d\theta}{dt} \times \begin{vmatrix} \cos \theta & \sin \theta & 1 \\ \cos(\theta + 2\pi/3) & \sin(\theta + 2\pi/3) & 1 \\ \cos(\theta - 2\pi/3) & \sin(\theta - 2\pi/3) & 1 \end{vmatrix}$$

Multiplying the first row of $P \begin{vmatrix} A_r \end{vmatrix}$ by the first column of $\begin{vmatrix} A_r \end{vmatrix}^{-1}$ yields

$$\begin{aligned} & -\sin \theta \cdot \cos \theta - \sin(\theta + 2\pi/3) \cos(\theta + 2\pi/3) - \sin(\theta - 2\pi/3) \cos(\theta - 2\pi/3) \\ &= - [1/2 \sin 2\theta + 1/2 \sin 2(\theta - 2\pi/3) + 1/2 \sin 2(\theta + 2\pi/3)] \\ &= - 1/2 [\sin 2\theta + \sin(2\theta + 2\pi/3) + \sin(2\theta - 2\pi/3)] \\ &= - 1/2 [\sin 2\theta + 2 \sin 2\theta (\cos 2\pi/3)] \\ &= - 1/2 [\sin 2\theta - \sin 2\theta] = 0 \end{aligned}$$

Next, multiplying the first row of $P \begin{vmatrix} A_r \end{vmatrix}$ by the second column of $\begin{vmatrix} A_r \end{vmatrix}^{-1}$ gives

$$\begin{aligned} & -\sin^2 \theta - \sin^2(\theta + 2\pi/3) - \sin^2(\theta - 2\pi/3) \\ &= - [1/2 - 1/2 \cos 2\theta + 1/2 - 1/2 \cos 2(\theta + 2\pi/3) + 1/2 - 1/2 \cos 2(\theta - 2\pi/3)] \\ &= - 3/2 + 1/2 [\cos 2\theta + \cos(2\theta + 2\pi/3) + \cos(2\theta - 2\pi/3)] \\ &= - 3/2 + 1/2 [\cos 2\theta + 2(\cos 2\theta)(\cos 2\pi/3)] \\ &= - 3/2 + 1/2 [\cos 2\theta - \cos 2\theta] = - 3/2 \end{aligned}$$

Finally, the first row of $P |A_r|$ is multiplied by the third column of $|A_r|^{-1}$ which yields

$$-\sin \theta - \sin(\theta + 2\pi/3) - \sin(\theta - 2\pi/3) = 0$$

Thus, the first row of (3.21) has been derived. The second and third rows of (3.21) are derived in a similar manner.

APPENDIX II

Equation (3.30) is derived as follows, using $|A_s|$ from (3.8), $|L_2|$ from (2.18b) and A_r from (3.10).

$$|A_s| |L_2| |A_r| =$$

$$= \frac{2}{3} \begin{vmatrix} 1 & -1/2 & -1/2 \\ 0 & \sqrt{3}/2 & -\sqrt{3}/2 \\ 1/2 & 1/2 & 1/2 \end{vmatrix} L_{mr} \begin{vmatrix} \cos \theta & \cos(\theta+2\pi/3) & \cos(\theta-2\pi/3) \\ \cos(\theta-2\pi/3) & \cos \theta & \cos(\theta+2\pi/3) \\ \cos(\theta+2\pi/3) & \cos(\theta-2\pi/3) & \cos \theta \end{vmatrix}$$

$$\times \begin{vmatrix} \cos \theta & \sin \theta & 1 \\ \cos(\theta+2\pi/3) & \sin(\theta+2\pi/3) & 1 \\ \cos(\theta-2\pi/3) & \sin(\theta-2\pi/3) & 1 \end{vmatrix}$$

First, $|A_s| |L_2|$ is determined. Multiplying the first row of $|A_s|$ by the first, second and third columns of $|L_2|$

$$\begin{aligned} \cos \theta - 1/2 \cos(\theta-2\pi/3) - 1/2 \cos(\theta+2\pi/3) \\ \cos \theta - 1/4 \cos \theta - \sqrt{3}/4 \sin \theta + 1/4 \cos \theta + \sqrt{3}/4 \sin \theta \\ (1 + 1/4 + 1/4) \cos \theta = 3/2 \cos \theta \end{aligned} \quad (1)$$

$$\begin{aligned} \cos(\theta+2\pi/3) - 1/2 \cos \theta - 1/2 \cos(\theta-2\pi/3) \\ - 1/2 \cos \theta - 3/2 \sin \theta - 1/2 \cos \theta + 1/4 \cos \theta - \sqrt{3}/4 \sin \theta \\ (-1/2 - 1/2 + 1/4) \cos \theta - 3(\sqrt{3}/4) \sin \theta = -3/4 \cos \theta - 3(\sqrt{3}/4) \sin \theta \end{aligned} \quad (2)$$

$$\begin{aligned} \cos(-2\pi/3) - 1/2 \cos(+2\pi/3) - 1/2 \cos \\ \cos(\theta-2\pi/3) - 1/2 \cos(\theta+2\pi/3) - 1/2 \cos \theta \\ - 1/2 \cos \theta + \sqrt{3}/2 \sin \theta + 1/4 \cos \theta + \sqrt{3}/4 \sin \theta - 1/2 \cos \theta \\ (-1/2 - 1/2 + 1/4) \cos \theta + 3(\sqrt{3}/4) \sin \theta = -3/4 \cos \theta + 3(\sqrt{3}/4) \sin \theta \end{aligned} \quad (3)$$

Multiplying the second row of $|A_s|$ by the first, second and third columns of $|L_2|$ gives

$$\begin{aligned} 3/2 \cos(\theta-2\pi/3) - \sqrt{3}/2 \cos(\theta+2\pi/3) \\ - \sqrt{3}/4 \cos \theta + 3/4 \sin \theta + \sqrt{3}/4 \cos \theta + 3/4 \sin \theta \\ = 3/2 \sin \theta \end{aligned} \quad (4)$$

$$\begin{aligned}
 & \sqrt{3}/2\cos\theta - \sqrt{3}/2(-1/2 \cos\theta + \sqrt{3}/2 \sin\theta) \\
 & \sqrt{3}/2\cos\theta + \sqrt{3}/4 \cos\theta - 3/4 \sin\theta \\
 & = 3(\sqrt{3}/4) \cos\theta - 3/4 \sin\theta
 \end{aligned} \tag{5}$$

$$\begin{aligned}
 & \sqrt{3}/2 \cos(\theta+2\pi/3) - \sqrt{3}/2\cos\theta \\
 & - 3/4 \cos\theta - 3/4 \sin\theta - \sqrt{3}/2\cos\theta \\
 & = -3(\sqrt{3}/4) \cos\theta - 3/4 \sin\theta
 \end{aligned} \tag{6}$$

Multiplying the third row of $|A_s|$ by the first, second and third column of $|L_2|$ gives

$$\begin{aligned}
 & 1/2 \cos\theta + \cos(\theta-2\pi/3) + \cos(\theta+2\pi/3) \\
 & 1/2 \cos\theta - 1/2\cos\theta + \sqrt{3}/2 \sin\theta - 1/2\cos\theta - \sqrt{3}/2 \sin\theta \\
 & 1 - 1/2 - 1/2 = 0
 \end{aligned} \tag{7}$$

$$1/2 | \quad | = 0 \tag{8}$$

$$1/2 | \quad | = 0 \tag{9}$$

The resulting $A_s | L_2$ is now multiplied by A_r^{-1} :

$$\begin{array}{c}
 2/3 L_{mr} \left| \begin{array}{ccc} 3/2\cos & -3/4\cos - 3(3/4)\sin & -3/4\cos + 3(3/4)\sin \\ 3/2\sin & 3(3/4)\cos - 3/4\sin & -3(3/4)\cos - 3/4\sin \\ 0 & 0 & 0 \end{array} \right| \\
 \times \left| \begin{array}{ccc} \cos\theta & \sin\theta & 1 \\ \cos(\theta+2\pi/3) & \sin(\theta+2\pi/3) & 1 \\ \cos(\theta-2\pi/3) & \sin(\theta-2\pi/3) & 1 \end{array} \right|
 \end{array} \tag{10}$$

The first row of $|A_s| |L_2|$ is now multiplied by the first, second and third columns of $|A_r|^{-1}$

$$\begin{aligned}
& 3/2\cos^2\theta + (-3/4\cos\theta - 3(\sqrt{3}/4)\sin\theta)(-1/2\cos\theta - \sqrt{3}/2\sin\theta) \\
& + (-3/4\cos\theta + 3(\sqrt{3}/4)\sin\theta)(-1/2\cos\theta + \sqrt{3}/2\sin\theta) \\
& 3/2\cos^2\theta + \sqrt{3}/8\cos^2\theta + 3(\sqrt{3}/8)\sin\theta\cos\theta + 3(\sqrt{3}/8)\sin\theta\cos\theta + 9/8\sin^2\theta \\
& + \sqrt{3}/8\cos^2\theta - 3(\sqrt{3}/8)\sin\theta\cos\theta - 3(\sqrt{3}/8)\sin\theta\cos\theta - 9/8\sin^2\theta \\
& 3/2\cos^2\theta + 3/8\cos^2\theta + 3(\sqrt{3}/8)\sin\theta\cos\theta + 3(\sqrt{3}/8)\sin\theta\cos\theta + 9/8\sin^2\theta \\
& + 3/8\cos^2\theta - 3(\sqrt{3}/8)\sin\theta\cos\theta + 3(\sqrt{3}/8)\sin\theta\cos\theta + 9/8\sin^2\theta \\
& 3/2 + 3/8 + 3/8 = 9/4\cos^2\theta + 9/4\sin^2\theta = 9/4
\end{aligned} \tag{11}$$

$$\begin{aligned}
& 3/2\sin\theta\cos\theta + (-3/4\cos\theta - 3(\sqrt{3}/4)\sin\theta)(-1/2\sin\theta + \sqrt{3}/2\cos\theta) \\
& + (-3/4\cos\theta + 3(\sqrt{3}/4)\sin\theta)(-1/2\sin\theta - \sqrt{3}/2\cos\theta) \\
& 3/2\sin\theta\cos\theta + 3/8\cos\theta\sin\theta - 3(\sqrt{3}/8)\cos^2\theta + 3(\sqrt{3}/8)\sin^2\theta \\
& - 9/8\sin\theta\cos\theta + 3/8\cos\theta\sin\theta + 3(\sqrt{3}/8)\cos^2\theta - 3(\sqrt{3}/8)\sin^2\theta \\
& - 9/8\sin\theta\cos\theta = 0
\end{aligned} \tag{12}$$

$$= 0 \tag{13}$$

The second row of $|A_s| |L_2|$ is now multiplied by the first, second and third columns of $|A_r|^{-1}$

$$\begin{aligned}
& 3/2\sin\theta\cos\theta + ((3\sqrt{3}/4)\cos\theta - 3/4\sin\theta)(-1/2\cos\theta - 3/2\sin\theta) \\
& + (-3(\sqrt{3}/4)\cos\theta - 3/4\sin\theta)(-1/2\cos\theta + \sqrt{3}/2\sin\theta) \\
& 3/2\sin\theta\cos\theta + -3(\sqrt{3}/8)\cos^2\theta - 9/8\sin\theta\cos\theta + 3/8\sin\theta\cos\theta \\
& + 3(\sqrt{3}/8)\sin^2\theta + 3(\sqrt{3}/8)\cos^2\theta - 9/8\sin\theta\cos\theta + 3/8\sin\theta\cos\theta - \\
& 3(\sqrt{3}/8)\sin^2\theta \\
& 3/2\sin\theta\cos\theta - 3(\sqrt{3}/8)\cos^2\theta - 9/8\sin\theta\cos\theta + 3/8\sin\theta\cos\theta \\
& + 3(\sqrt{3}/8)\sin^2\theta + 3(\sqrt{3}/8)\cos^2\theta - 9/8\sin\theta\cos\theta + 3/8\sin\theta\cos\theta - 3(\sqrt{3}/8)\sin^2\theta \\
& = 0
\end{aligned} \tag{14}$$

$$\begin{aligned}
& 3/2\sin^2\theta + (3(\sqrt{3}/4)\cos\theta - 3/4\sin\theta)(-1/2\sin\theta + \sqrt{3}/2\cos\theta) \\
& + (-3(\sqrt{3}/4)\cos\theta - 3/4\sin\theta)(-1/2\sin\theta - \sqrt{3}/2\cos\theta)
\end{aligned}$$

$$\begin{aligned}
 & 3/2\sin^2\theta + (3(\sqrt{3}/8)\sin\theta\cos\theta + 9/8\cos^2\theta + 3/8\sin^2\theta - \\
 & 3(\sqrt{3}/8)\sin\theta\cos\theta + 3(\sqrt{3}/8)\sin\theta\cos\theta + 9/8\cos^2\theta + 3/8\sin^2\theta + 3(\sqrt{3}/8)\sin\theta\cos\theta \\
 & 3/2\sin^2\theta - 3(\sqrt{3}/8)\sin\theta\cos\theta - 9/8\cos^2\theta + 3/8\sin^2\theta - 3(\sqrt{3}/8)\sin\theta\cos\theta \\
 & + 3(\sqrt{3}/8)\sin\theta\cos\theta + 9/8\cos^2\theta + 3/8\sin^2\theta + 3(\sqrt{3}/8)\sin\theta\cos\theta \\
 & (9/4\sin^2\theta + 9/4\cos^2\theta) = 9/4
 \end{aligned}$$

The third row of $|A_s| |L_2| |A_r|$, multiplied by the first, second and third columns of $|A_r|^{-1}$, gives zero in each case.

Therefore,

$$|A_s| |L_2| |A_r|^{-1} = \begin{vmatrix} 3/2L_{mr} & 0 & 0 \\ 0 & 3/2L_{mr} & 0 \\ 0 & 0 & 0 \end{vmatrix}$$

Equation (3.31) can be derived in the same manner.

End of Document